Atmospheric reactions of ethers and ketones

Peter McLoughlin B.Sc. (Hons.)

A thesis presented at Dublin City University

for the degree of Doctor in Philosophy

School of Chemical Sciences

Ollscoil Chathair Bhaile Átha Cliath

DUBLIN 9, IRELAND.

Telephone : 7045000. Facsimile : 360830. Telex : 30690.

September 1992

To the kindness , patience , and understanding of Helen .

Acknowledgements

I would like to express my gratitude to my supervisor Dr. Imelda Shanahan for her support and encouragement throughout this work .

I wish to thank my fellow post graduate students for their encouragement and help during the many days of endless Nhea . In particular I would like to thank Mick (Boots) Lyons , and the Gypsies in A115 , Redzer (A great player) Curley , Fintan (Smirnoff) O'Donnell , Conor (Mule skinner) Tonra , Teri (sweeties) Donaghy , Mary(Jafra) Hande , Domo (The chip shop magnate) Delicato , Edwina (The Gypsy) Benton , Keedue (The carpet seller) McGirl , and Mithereen (A very silly person) McLoughlin , for their friendship during the lab days . I would like also to thank Frank , Barry and The Bud for their advice and friendship especially during the transfer days .

I would like to thank Barbara Murphy and Rosaleen Kane for their contribution to this work and Dr. Paraic James for his help in the interpretation of NMR spectra .

I wish also to express my gratitude to the technical staff of the school of chemical sciences at Dublin City University especially Borris (Tubs) McGuirk for his expertise in the NMR field and his artistic skills . I would also like to thank the great Dynamo Benzene for diplaying their silken skills to all opposition and in particular Jasper (Fats) Gilly for the paper and the many scoops .

I would also like to thank the school of chemical sciences at Dublin City University and Westmeath VEC for financial support throughout this work .

Last , but not least , I would like to express my sincere gratitude to my family for their support over the many years I have spent in college and I hope now I will be able to repay them for their patience and kindness .

Declaration

This thesis is submitted in fulfilment of the requirements for Doctor in Philosophy by research and thesis . It has not been submitted as an exercise for a degree at this or any other university . Except where otherwise indicated this work has been carried out by the author alone , at Dublin City University .

Peter McLoughlin

Contents

Chapter 1.0

General Introduction

Chapter 2.0

OH radical and Cl atom reactions with a series of ethers and ketones

Chapter 3.0

A preliminary investigation into the gas phase photooxidation of the anaesthetics , isoflurane and enflurane

Abstract

The atmospheric lifetimes of a series of ethers and ketones was established , with respect to reaction with OH radicals and Cl atoms, using a relative rate smog chamber technique . Reactivity of these compounds was affected by , their C - H bond dissociation energies , the oxygen atom in their structure , steric effects , and polarity contributions . From the rate constant data calculated in this work it was concluded that the tropospheric lifetimes of these compounds is primarily determined by their reactivity with OH radicals . Only four of the compounds analysed (2-chloro,1,1,1-trifluoro ethyl ethyl ether, isoflurane, enflurane and acetone) had sufficiently long tropospheric lifetimes which will allow transportation of these species to the stratosphere . Three of these compounds were chlorinated ethers . These species may release their chlorine atoms in the stratosphere , ultimately resulting in ozone depletion .

Release figures for the two halogenated anaesthetic ethers , isoflurane and enflurane , were calculated in our laboratory and combined with atmospheric lifetime data to establish the possible contribution of the anaesthetics to ozone depletion . It was estimated that only a fraction of the released species will be effective in causing ozone depletion .

To establish the ulitimate atmospheric fate of the anaesthetics , stratospheric photooxidation reaction mechanisms were investigated for these species . Result data indicated that the anaesthetics will undergo reaction processes initiated by chlorine atoms produced from the photodecomposition of the parent species . These chlorine-sensitised photooxidation reaction mechanisms ultimately lead to the formation of CF_2O and CO_2 , both greenhouse gases .

Although the anaesthetics isoflurane and enflurane are released to the troposphere , their effect on stratospheric ozone and on world climate was estimated to be minimal compared with other CFCs . This work serves as a quick guide to the type of reaction processes which are important in environmental assessment of volatile anthropogenic species and also illustrates the significance of secondary factors such as emission figures , reaction products , etc., in atmospheric quality assessment .

CHAPTER 1

General Introduction

1.1 The Atmosphere and this thesis

Every year large quantities of chemicals are released into the atmosphere from natural as well as anthropogenic sources . These compounds are then transported both vertically and horizontally within the atmosphere by air circulation . Depending on the nature of the chemical , there are various mechanisms by which these species can be removed from the atmosphere. Compounds which are water soluble are readily removed by precipitation , i.e. in rain , while others such as chlorofluorocarbons (CFCs) are non-polar and stable in the lower atmosphere and thus can reside in the atmosphere for years before they are ultimately transformed / removed as a result of reaction in the upper reaches of the atmosphere . Much interest in the past 16 years has centred on the chemistry of those compounds which are volatile , non-polar and highly halogenated , i.e. CFCs . Due to the relative inertness of such compounds in the lower atmosphere , it was initially considered that these chemicals would have little effect on the quality of the atmosphere . However , such stability allows these compounds time to undergo transportation to the higher reaches of the atmosphere , where these species can then react disturbing the delicate balance existing there .

The atmospheric fate of a chemical released at the surface of the earth depends on a number of factors including the nature of the chemical , the presence and concentration of other species and the efficiency of transport and mixing processes within the atmosphere .

This thesis studies the atmospheric removal mechanisms of a series of volatile , non-polar , oxygenated (some halogenated) compounds . Chapter 2 deals with the rate of removal of these compounds by reactive species in the lower atmosphere , and Chapter 3 involves a study of removal mechanisms for two of these compounds in

the stratosphere . In this opening chapter we look briefly at characteristics of the atmosphere , at the pollutants themselves , their removal mechanisms , possible effects of these species especially in the stratosphere and the ultimate effects which these compounds may have on life at the earth's surface .

The earth's atmosphere consists of an envelope of gases extending to a height of approximately 2000 km, with the density of these gases decreasing rapidly with increasing altitude . Temperature variations also occur with altitude and it is this characteristic variation which is used to divide the atmosphere into layers . Figure 1.1 shows a plot of average atmospheric temperature for mid latitudes as a function of height above sea level . Ozone concentrations within the various regions of the atmosphere are also indicated .

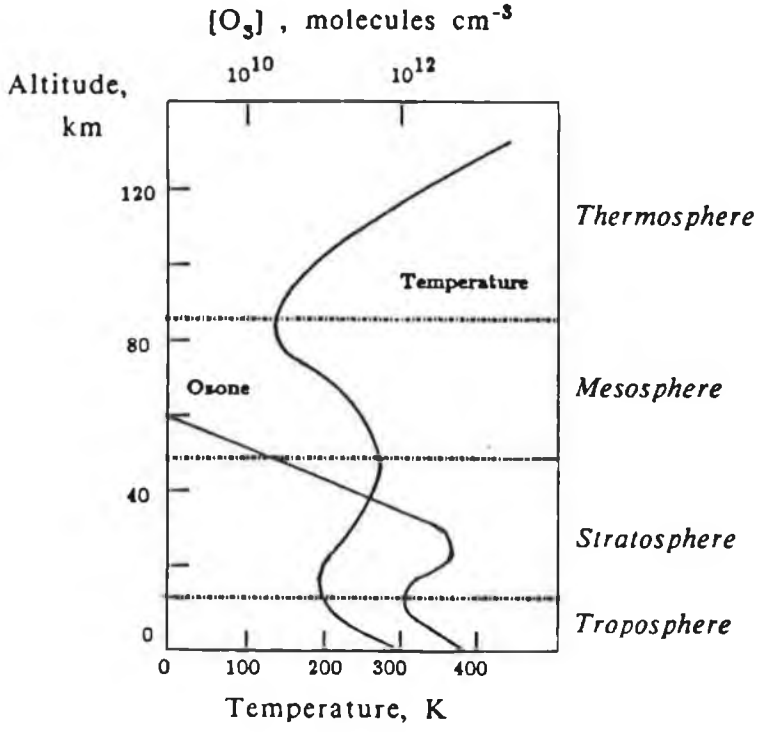

Figure 1.1
Temperature versus altitude profile for the first 120 km of the earth's atmosphere . Ozone concentrations are also indicated [1] .

The troposphere is characterised by a steady decrease in temperature with increasing altitude . It is maintained as a distinct layer of the atmosphere by the cooler air of the stratosphere which lies above . The decrease in temperature within the troposphere is due to the strong heating effect at the earth's sufrace from the absorption of visible and UV radiation . Accompanying this there is a strong circular and vertical mixing of constituents because warmer air near the ground rises and is replaced by cooler air from above . Thus pollutants released at the earth's surface can move to the top of the troposphere in a few days or less . Essentially all of the water vapour , clouds and precipitation in the earth's atmosphere are found in this region , so removal of water soluble pollutants by precipitation scavenging is an important atmospheric cleansing mechanism within this region .

The stratosphere shows a reversal of the temperature gradient found in the troposphere with temperature increasing with altitude . Relatively little vertical mixing occurs within this region since the cooler air is at the lower altitudes and does not readily rise . However , transport in the horizontal direction is quite rapid and a tracer may be dispersed around the world on a line of latitude from east to west in 1 to 4 weeks . There is a relatively slow rate of transport of materials across the tropopause . Upward moving air from the troposphere passes through the coldest region of the tropopause and this results in all but a few ppm of water vapour being precipitated out , hence the stratosphere is very dry and no precipitation scavenging occurs in this region .The stratosphere contains approximately one tenth of the earth's atmosphere by mass , and , apart from the presence of ozone and smaller amounts of trace species , it's chemical composition is close to that of the troposphere [2] .

The extent to which CFCs , HCFCs and all volatile compounds emitted to the atmosphere subequently deplete ozone is dependent on

the efficiency with which these compounds are removed from the troposphere . The tropospheric lifetime of a non - polar anthropogenic organic , (τ_a) is given by ;

$$\tau_a = {}^{1} / k_{ox}\,[Ox]$$

where : k_{OX} = Rate of Oxidation

[Ox] = Concentration of oxidant (NO_3 , Cl or OH)

The main tropospheric sinks for water insoluble volatile organic chemicals (VOCs) is oxidation by OH and NO_3 radicals and by Cl atoms . As photolysis is essential for the production of OH radicals , this process predominates during daylight hours . It fades in significance at dusk when oxidation via NO_3 radicals takes over . The latter process is only evident at night since sunlight readily photodissociates the NO_3 radical making it's daylight steady state concentration trivial . Recently the importance of Cl atom oxidation of VOCs in the troposphere has been recognised [3] . The sources and mechanisms of reaction of OH radicals and Cl atoms in the troposphere are discussed in detail in Chapter 2 of this thesis .

The temperature at the surface of the sun is approximately 6000^{o}C and hence solar radiation is largely in the UV and visible regions of the electromagnetic spectrum . Approximately 47% of the total radiation from the sun is received at the earth's surface while the remainder is lost either by reflection or absorption by atmospheric gases . The potentially lethal UV radiation between 200 and 300 nm is absorbed in the stratosphere , mainly by ozone and to a lesser extent by oxygen . Figure 1.2 compares the solar spectrum at the top of the atmosphere with the solar energy that reaches the earth's surface .

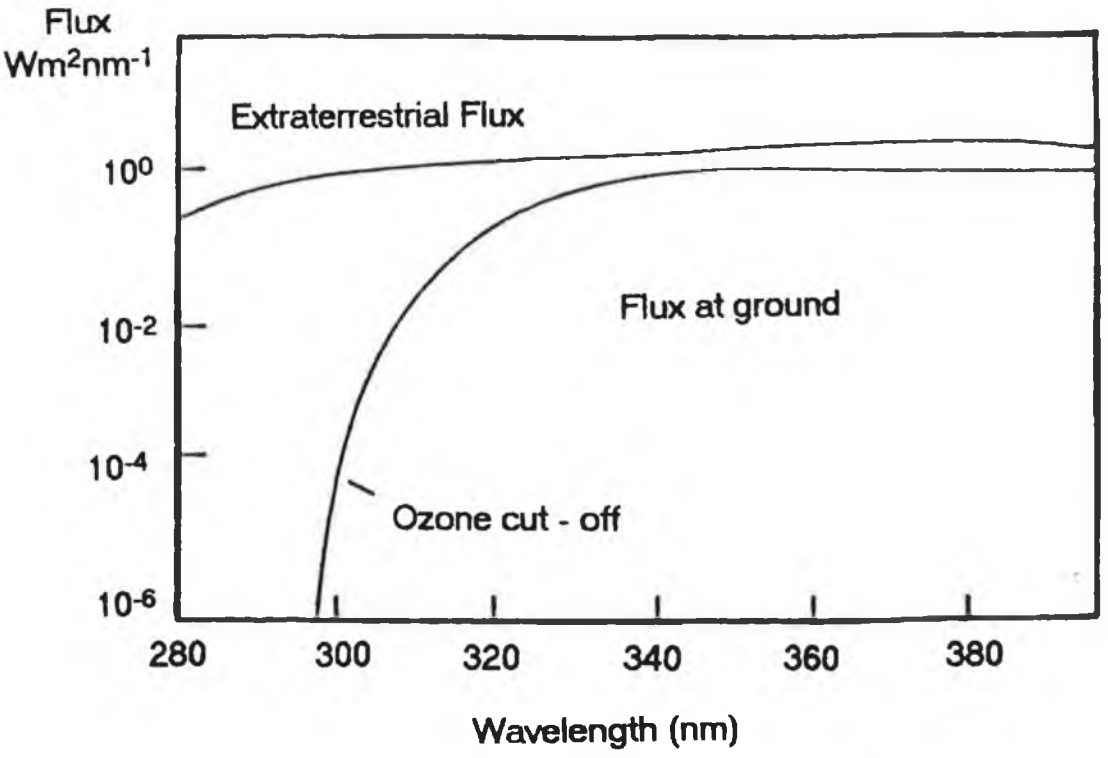

Figure 1.2
A comparison between light wavelengths incident on the earth's atmosphere to those which eventually reach the earth's surface [1] .

It is apparent that different regions exist in the atmosphere , with different conditions prevailing in each and therefore the types of chemical process which predominate at each level differs . Compounds which are not water soluble and react slowly with oxidising species in the troposphere will persist and eventually undergo transportation to the stratosphere . Here the lack of water and the higher energy (lower wavelength) light may lead to photodecomposition of these species . This light initiated decomposition is the main removal mechanism for certain compounds (halogen containing) in the stratosphere and it is this

breakdown which generates new problems , particularly with regard to ozone concentrations.

The importance of the earth's ozone "shield" has been known for many years . The absorption of solar UV radiation by the ozone layer provides the heat which maintains the stability of the stratosphere - the "cap" to the turbulent weather systems at lower levels - and this acts as one of the ultimate controls on the global climate . More importantly the absorption process shields the earth's surface from the most biologically damaging wavelengths of ultraviolet radiation (200 - 300 nm), UV(B) [4] .

Concern over O_3 depletion has arisen because of concern over corresponding increases in biologically harmful UV(B) radiation . It is therefore worth noting that a UV(B) monitoring network in the US (established in 1974) observed no increase in UV(B) radiaiton over the 11-year period 1974 - 1985 . On the contrary , downward trends in UV(B) intensity averaging from 0.5 - 1% per year were observed [5] . It is possible , however , that apparent trends in UV(B) intensities at the eight urban locations were influenced by either local air pollution (tropospheric O_3, particles etc) or by lack of selective sensitivity of the monitoring instruments to the biologically active wavelengths in the UV(B) spectrum [6] . It is most likely that no observed increase in the levels of UV(B) radiation have yet been observed in the U.S. because as yet the main areas of ozone depletion are confined to the southern hemisphere .

Any human disease that is induced or exacerbated by solar radiation will probably increase in frequency and severity with increased solar UV(B). This is due to the enhanced total dose of UV(B) , but also to the progressively greater contribution of the shorter wavelength , the more biologically effective dose . In human health issues this wavelength dependency reflects the greater absorption of the shorter wavelengths of UV(B) by DNA molecules . The two primary scientific issues underlying

the effects of enhanced UV(B) on human health are skin cancer and photoimmunology .

Scientific evidence that nonmelanoma skin cancer is caused by solar UV(B) is substantiative, strongly suggesting that projected increases in UV(B) due to stratospheric O_3 depletion would accelerate the incidence and severity of these tumors . Given an atmospheric amplification of 2 (i.e. a 1% depletion of stratospheric O_3 produces a projected 2% increase in UV(B) at ground level) , a 2% increase in UV(B) would result in a 2 - 5% increase in basal - cell carcinoma and a 4 - 10% increase in squamous - cell carcinoma . Among highly UV(B) - sensitive human populations from mid to upper latitudes (e.g. peoples of Celtic descent) who now inhabit regions of the world in which projected UV(B) increases are greatest (e.g. Australia) , the rate of occurrence of these skin cancers is expected to increase significantly . Melanoma is a much more serious concern . Melanoma kills three times as many people per year as other skin cancers . There is clearly a sunlight component to melanoma in that there is an inverse correlation of latitude and deaths from melanoma . With regard to increased UV(B) , most authorities in photocarcinogenesis believe there will be a concommitant increase in deaths by melanoma .

Beyond the direct effects of UV(B) exposure in contributing to skin cancer in humans , there is emerging data linking UV(B) with a change in the body's autoimmune system . Based on these studies , it is hypothesised that UV(B) - induced DNA lesions (thymine photoproducts such as cyclobutane pyrimidine dimers) in the skin are highly antigenic , elevating the bodies titre of antinuclear antibodies , which in turn elicit autoimmune - like reactions . These reactions are characteristic of certain sunlight - sensitive diseases such as systemic lupus erythematosus . The incidence and severity of this class of UV(B) - induced disease are expected to increase with enhanced exposure to UV(B) [6] . Moreover , it

is hypothesised that this same process is linked to the more complicated issue of photocarcinogenesis whereby UV(B) suppresses the body's intrinsic capacity to immunologically reject tumor growth and development . Consequently , even small changes in the ozone layer will have drastic biological implications at the earth's surface . Hence , stratospheric ozone concentrations have become matters of serious concern .

The ozone layer is thin ; in fact the total ozone overhead is equivalent to a column of about 0.3 cm at standard temperature and pressure [4] . Ozone is continually formed and destroyed in a series of photochemically - initiated reactions . The basic scheme for ozone equilibrium was established in 1930 by Chapman . He suggested the importance of reactions 1 - 4 below (now known as the Chapman cycle) in the formation and destruction of ozone in the atmosphere :

$O_2 + h\nu$ ($\lambda < 220$ nm)	------> $2O\cdot$ (O_2 abs. 135 -175 nm)	(1.2)
$O\cdot + O_2 + M$	------> $O_3 + M$	(1.3)
$O\cdot + O_3$	------> $2O_2$	(1.4)
$O_3 + h\nu$ ($\lambda < 320$ nm)	------> $O(^1D) + O_2$	(1.5)

In summary ozone is formed when oxygen atoms produced from the photodissociation of molecular oxygen combine with oxygen , with excess energy removed by another molecule , M . UV radiation in the wavelength range 240 to 320 nm can dissociate ozone and it is this absorption that shields the earth's surface from harmful UV radiation and also contributes to the characteristic temperature profile in the stratosphere (Figure 1.1) .

Catalytic cycles involving hydrogen containing and nitrogen containing species play an important role in natural ozone destruction mechanisms . It is estimated that 10% of ozone destruction is caused by

an OH radical reaction mechanism and 70% by reactions involving NO [1]. The Chapman cycle (reactions 1.2 to 1.5) predicts considerably more ozone than is actually present in the atmosphere and in fact it is generally believed that this cycle accounts for only some 20% of "natural" ozone destruction . If these cycles were the only processes contributing to atmospheric ozone loss , significantly larger concentrations of ozone would be found in the atmosphere .

The importance of atmospheric chlorine and it's oxide in the destruction of ozone was established by the pioneering work of Rowland and Molina [7] . Reactions (1.6) and (1.7) demonstrate the importance of the reaction of chlorine with ozone , the net result being ozone destruction:

$Cl\cdot + O_3$ ------> $ClO\cdot + O_2$ (1.6)

$ClO\cdot + O\cdot$ ------> $Cl\cdot + O_2$ (1.7)

$O_3 + O\cdot$ ------> $2O_2$ Net Reaction

There are a number of sources of chlorine containing compounds , both natural and anthropogenic which can serve as sources of chlorine for the propagation of the catalytic cycles shown above . The relative contribution of indlvidual source gases to total atmospheric chlorine for the year 1985 is shown below [8] .

Industrial Source	% of Total
CFC - 11	22
CFC - 12	25
CFC - 113	3
CFC - 114	< 1
CFC - 115	< 1
HCFC - 22	3
CCl_4	13
CH_3Cl_3	13

Natural Source

Methyl Chloride 20

The known natural sources of chlorine make up only 20% of the total and the eight CFCs listed under the Montreal Protocol (International accord which limits the release of CFCs) account for about 50% . Not all chlorine released in the stratosphere catalyses ozone destruction . The formation of hydrochloric acid (HCl) , chlorine nitrate ($ClONO_2$) and hypochlorous acid (HOCl) sequesters 90% [9] or more of stratospheric Cl· and ClO· ,

$$Cl\cdot + CH_4 \text{ ------> } HCl + \cdot CH_3 \qquad (1.8)$$

$$ClO\cdot + NO_2 \text{ ------> } ClONO_2 \qquad (1.9)$$

$$ClO\cdot + \cdot HO_2 \text{------> } HOCl + O_2 \qquad (1.10)$$

Although chemically bound these compounds remain as a reservoir for chlorine atoms in the stratosphere and are implicated as a major source of Cl atoms which have caused significant reductions in observed ozone concentrations over the Southern hemisphere and in particular over Antarctica in the past 15 years (the ozone hole) .

One of the most important sources of chlorine atoms in the stratosphere has been due to the increased release of CFC compounds from industrial and household activities . CFCs (chlorofluorocarbons) are compounds containing chlorine , fluorine , carbon and possibly hydrogen . The principal CFCs are CCl_3F , CCl_2F_2 and $CHClF_2$, abbreviated CFC - 11 , - 12 and - 22 respectively . The first number denotes the number of hydrogens plus one , and the second gives the number of fluorine atoms [10] . For CFCs containing two or more carbon atoms , a three digit numbering system is used . The first digit gives the number of carbon atoms minus one , the second the number of hydrogens plus one and the

third the number of fluorine atoms . Thus CCl_2FCClF_2 is abbreviated as CFC - 113 .

By 1988 the world consumption of CFCs had grown to over 10^9 kg / year . In the United States some 5,000 businesses at nearly 375,000 locations produce CFC - related goods and services worth more than $28 billion a year . CFC - related jobs total more than 700,000 [11] . Within the United States , the three major uses of CFCs are as refrigerants (30%) , as foam - blowing agents for polystyrene and polyurethane (28%) and as industrial solvents and cleansing agents (19%) . Outside North America , significant amounts (> 1.5 x 10^8kg) of CFCs have continued to be used as aerosol propellants even though that appplication was essentially banned in the US in 1978 .

The first real evidence that caused concern in relation to CFCs and the atmosphere , was Lovelock's measurement of atmospheric CFC - 11 concentrations in the early 1970's [12]. A comparison of estimated releases of the compound with it's concentration indicated that very little , if any , had decomposed and thus that the stable CFCs were accumulating in the atmosphere . The first reaction to this information was a Du Pont - organised , "Seminar on the Ecology of Fluorocarbons" for the world's CFC producers in 1972 . As a result of this symposium , a research program sponsored by 19 companies was established to investigate the fate and impact of CFCs in the atmosphere . Lovelock's measurements also initiated Molina and Rowland's research [7] into the atmospheric fate of CFCs .

CFCs have been found to have very long lifetimes in the troposphere . This is a consequence of the fact that they do not absorb light of wavelengths above 290 nm and do not react at significant rates with O_3 , OH , Cl , or NO_3 [10] . In addition to the lack of chemical sinks , there do not appear to be substantial physical sinks ; they are not very

soluble in water and hence are not removed rapidly by rainout . As a result CFCs reside in the troposphere for years (CFC - 11 and CFC - 12 have estimated tropospheric lifetimes of 74 and 111 years respectively [13]) slowly diffusing across the tropopause into the stratosphere . Once in the middle stratosphere , they are decomposed by short wavelength solar UV radiation [14] as follows :

$$CCl_2F_2 + h\nu\ (\lambda < 220\ nm) \text{ ------> } Cl\cdot + \cdot CClF_2 \qquad (1.11)$$

The chlorine atom released can then react rapidly with O_3 , reaction mechanism (1.6) , followed by reaction of the ClO radical with atomic oxygen , reaction (1.7) , once again releasing Cl atoms . The reaction sequence outlined in (1.6) and (1.7) constitutes the ClO_x free radical catalytic chain reaction which repeats itself over and over again in the stratosphere before finally being terminated as follows :

$$O\cdot + O_3 \text{ ------> } O_2 + O_2 \qquad (1.12)$$

The net effect of reactions (1.6) and (1.7) as shown in reaction (1.12) converts back to molecular oxygen , one ozone molecule and one atom of oxygen which would otherwise have formed ozone , thus making this ClO_x chain an exceptionally efficient method for ozone destruction .

In 1985 a large decrease in springtime ozone concentrations over Hailey Bay , Antarctica , throughout the previous decade was reported by British researchers [15] (Figure 1.3) . This phenomenon is now referred to as the Antarctic ozone "hole" .

Ground based and satellite data have shown a rapid decrease in total ozone over all of Antarctica during the Spring since the late 1970's . Total column ozone at all latitudes south of 60°S was lower in the 1987

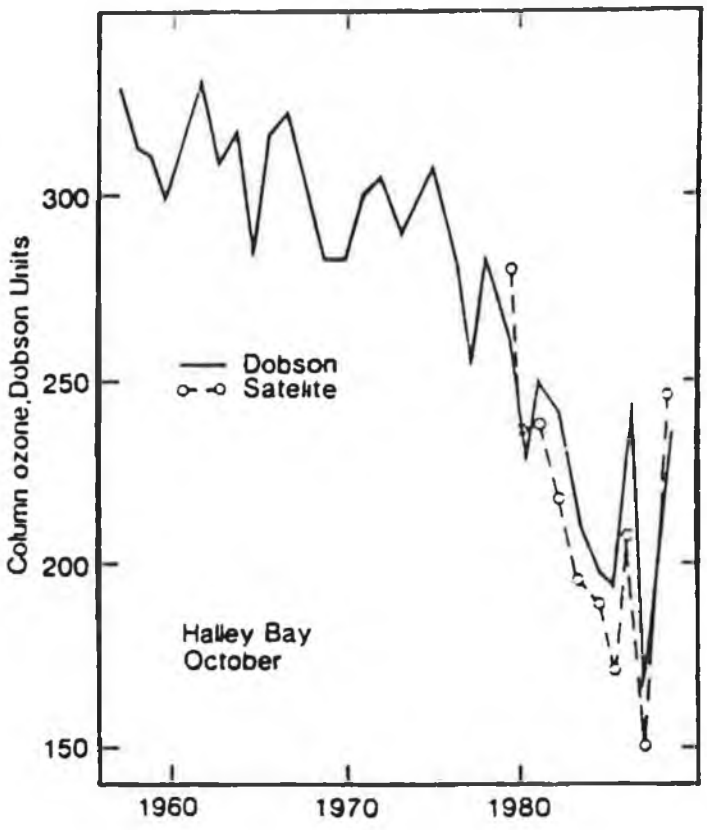

Figure 1.3

October average total ozone over Halley Bay (76°S) Antarctica [15] .

Spring than in any previous Spring since satellite measurements began in 1978 .

In 1987 ozone at 20 km over Antarctica decreased by more than 95% from values observed in August and the ozone "hole" lasted until early December , the latest this ozone "hole" has persisted . At all latitudes south of 60°S annual total ozone has decreased by 5% or more since 1979 [9] . Ozone changes of this magnitude were not predicted . During 1987 comprehensive measurements within the "hole" were made from the ground , from aircraft , satellites and balloons (the 1987 Antartic Airborne Ozone Expedition - AAOE [16]) . The AAOE established that the springtime depletion of Antartic ozone is due to photochemical destruction following a preconditioning phase involving heterogenous reactions on stratospheric clouds .

The unique meteorology during Winter and Spring over Antarctica forms an isolated air mass (polar vortex) with temperatures sufficiently

cold to form polar stratospheric clouds (PSCs) and perturb the chemical composition . These PSCs are thought to play a key role in the formation of the Antarctic ozone "hole" . There is substantial evidence that stratospheric temperatures during October - November 1987 were 8°C colder than in 1979 consistent with the ozone loss observed .

Based on 1986 - 87 observations , anthropogenic chlorine has been implicated as the primary cause of the Antarctic ozone "hole" . The chlorine abundance in all forms within the polar vortex is similar to the rest of the global stratosphere , however the balance is shifted from inactive to reactive chlorine species that destroy ozone . Within the "hole" ClO· is enhanced by a factor of 100 - 500 compared to levels observed at mid - latitudes [9] , yet total chlorine levels are similar . To obtain high concentrations of ClO· , active chlorine must be released from reservoir species such as $ClONO_2$ and HCl :

$$HCl + ClONO_2 \text{ -------> } Cl_2 + HNO_3 \qquad (1.13)$$

- a reaction which proceeds rapidly on ice surfaces . Molecular chlorine (Cl_2) is released and nitric acid remains on the ice . This process occurs during the Antarctic Winter -Spring when ice particles (PSCs) are present.

The penultimate step , resulting in substantial ozone losses in September , is the reappearance of sunlight after the polar night . Cl_2 photodissociates to release Cl· :

$$Cl_2 + h\nu \ (\lambda > 320 \text{ nm}) \text{ ------> } 2Cl\cdot \qquad (1.14)$$

which is converted to ClO· by reaction with O_3 :

$$Cl\cdot + O_3 \text{ ------> } ClO\cdot + O_2 \qquad (1.15)$$

NO_2 is removed by reaction with ClO· to form $ClONO_2$ further converting remaining HCl to Cl_2 . All HCl inside the polar vortex is converted to ClO· , and NO_2 to HNO_3 .

A catalytic cycle to remove ozone is achieved [9] by a mechanism involving the ClO· dimer :

$ClO\cdot + ClO\cdot$	------> Cl_2O_2	(1.16)
$Cl_2O_2 + uv$	------> $Cl\cdot + \cdot ClOO$	(1.17)
$\cdot ClOO$	------> $Cl\cdot + O_2$	(1.18)
$2(Cl\cdot + O_3$	------> $ClO\cdot + O_2)$	(1.19)
NET REACTION	**$2O_3$ ------> $2O_2$**	(1.20)

Substantial quantities of Cl_2O_2 were found in the ozone "hole" and a strong inverse - correlation was established between ClO· and ozone in mid - September (Figure 1.4) . No such inverse - correlation existed prior to the Antarctic sunrise .

This extraordinary ozone loss in the region of high ClO· concentrations strongly indicates that chlorine chemistry is most probably responsible for the Antarctic ozone "hole" . Coupling this information with the fact that increased release of CFCs to the atmosphere is implicated as a major source of Cl· in the stratosphere , we can better understand why the quantities of CFCs released has quickly risen to the forefront of the environmental stage .

The release of CFC - 12 to the atmosphere has averaged about 400 kilotons per year for the past 15 years , while CFC - 11 yearly emissions

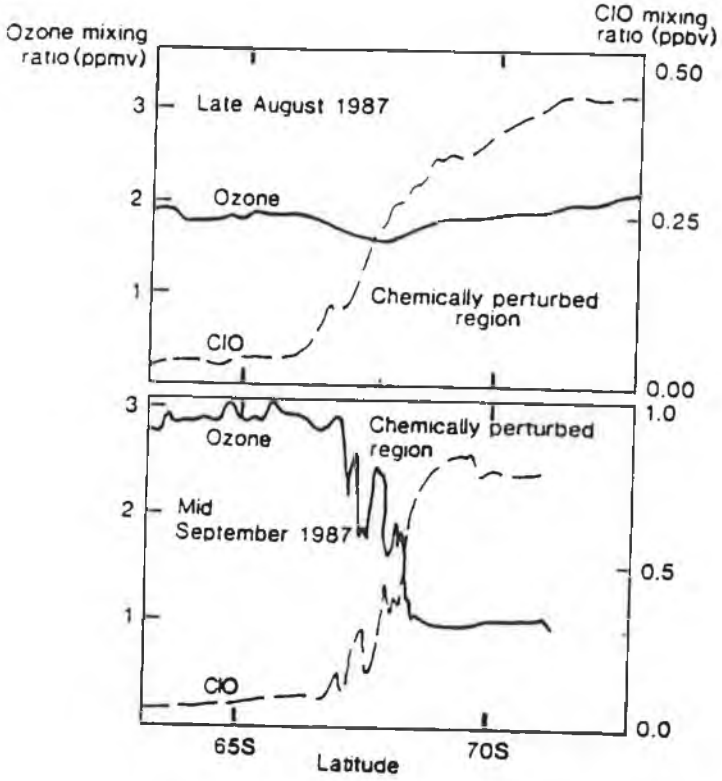

Figure 1.4

Antarctic ozone and ClO· at 18 km during (a) late August , and (b) mid - September 1987 [16] .

have been in the 250 - 300 kiloton range over the same period . Manufacture and atmospheric release of the third major CFC , CCl_2FCClF (CFC - 113) , have increased sharply over the past decade and are now also approximately 300 kilotons per year [14] . Forecasts project continued demand due largely to the recognition that developing countries will require the benefits provided by CFCs . These growth forecasts coupled with improved understanding of the potential for O_3 depletion by these CFCs has led to international efforts to limit long - term growth of CFC emissions [17] .

Attempts were made in the mid - 1970's to legislate a ban on the use of CFCs as an aerosol propellent . A joint administrative ban on nearly all aerosol uses was issued by the US environmental protection

agency (EPA) and the Food and Drug Administration (FDA) in 1978 . Although the US ban on aerosols was not implemented until 1978 , industry foresaw the ban and began to phase in non - CFC propellants and technologies .

In 1985 , an international conference on the status of the ozone layer was held in Vienna . The Vienna Convention for the Protection of the Ozone Layer was adopted by this conference . The Convention provided a framework for international cooperation with regard to the ozone layer . Among the provisions agreed were cooperative scientific evaluation of the status of the ozone layer , vetting rights of convention members , the adoption of protocols , and the exchange of information . Among the resolutions adopted by the conference and appended to the Vienna Convention were :

- a resolution on institutional and financial agreements ; and
- the resolution on a protocol concerning CFCs .

The second of these resolutions called for a protocol , or treaty , to protect the ozone layer . This resolution ultimately led to the Montreal Protocol .

In September 1987 a conference was convened in Montreal for the purpose of obtaining signatures to the Protocol to the Vienna Convention . The Montreal Protocol as it has become known , is an international treaty regulating the consumption and production of substances which deplete the ozone layer . Eight chemicals were controlled through the protocol ,

i.e.,

GROUP 1 (CFCs)	GROUP 2 (Halons)
CFC - 11	Halon - 1211
CFC - 12	Halon - 1301
CFC - 113	Halon - 2402
CFC - 114	
CFC - 115	

The regulated substances were divided into two groups . Beginning July 1 , 1989 , six months after the Protocol entered into force , annual production and consumption of group 1 compounds was curtailed to 1986 levels . By July 1 , 1993 , production and consumption of group 1 compounds was to decrease to 80% of 1986 levels . Finally , by July 1 , 1998 , production and consumption must be reduced to just 50% of 1986 levels . This agreement was strengthened by the London meeting in June 1990 , which called for an essentially complete phaseout of CFC production and release by the year 2000 .

Group 2 compounds were treated somewhat differently in Montreal . Calculated production or consumption of Group 2 compounds was to be frozen at 1986 levels 3 years after the agreement entered into force (January 1 1992) . No further constraints were imposed on Group 2 substances .

A number of exceptions were included in the Montreal Protocol notably with regard to developing countries , however this leniency may become balanced as major CFC - producing countries are independently committed to an even faster phaseout schedule for CFCs . Nevertheless , the amounts of CFCs emitted to the atmosphere during the past five years from 1985 to 1989 exceeded the emissions in any preceding five year period and measurements of the CFCs in the atmosphere do not yet show any slackening in the rate of increase in their atmospheric concentrations.

For example the total organochlorine concentration of the atmosphere at the end of 1990 is illustrated in Figure 1.5 . Levels are now approaching 4.0 parts per billion by volume (ppbv) compared with only 1.8 ppbv Cl in 1974 and 0.8 ppbv in 1950 , an increase by a factor of 5 in only 40 years .

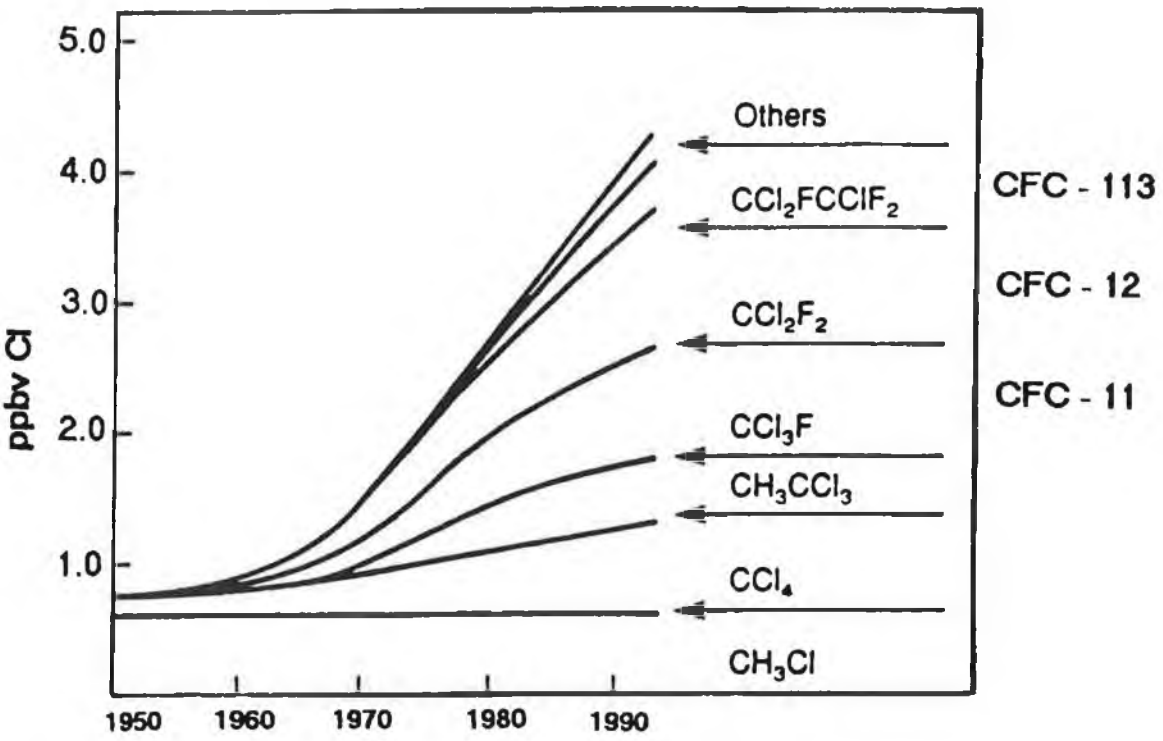

Figure 1.5

Organochlorine concentrations in the atmosphere , 1950 - 1990 [14] .

A recent market projection by Du Pont has attempted to determine how the current markets that use CFCs will be satisfied in the year 2000 . Increased environmental awareness coupled with a switch to less expensive , not - in - kind replacements are estimated to account for approximately 60% of the market . The remaining 40% of the projected market will still require fluorocarbon - based products . Hydrofluorocarbons (HFCs) and hydrochlorofluorocarbons (HCFCs) , have emerged as alternative fluorocarbon products for the remaining

It has been pointed out thus far that the chemistry of the atmosphere is very complex , with conditions varying with altitude . Also that stratospheric ozone in the atmosphere is responsible for regulating the levels of harmful UV(B) radiation which reaches the earth's surface . Increased levels of UV(B) reaching the earth may lead to increases in skin cancer and possible changes in biotic resources in terestrial systems (crops , forest trees , grasslands and thundra) and oceans (phytoplankton). Chlorine can catalyse the destruction of ozone and a ready source of these atoms in the stratosphere is from the increased release of stable CFC compounds into the troposphere . A direct relationship has been established between Cl atom concentrations in the stratosphere and the Antarctic ozone "hole" . As a result international legislation in the form of the Vienna Convention and the Montreal Protocol has set out to limit the emission of CFCs . A result of this has been the search for CFC alternatives such as HCFCs and HFCs . To establish the possible effects of these new compounds on the ozone layer and to increase the data base with respect to existing compounds , the rate of loss of these volatile organic chemicals with respect to OH radicals and Cl atoms (two major tropospheric sink reaction processes) must be determined ; hence the importance of the work carried out in our laboratory and summarised in Chapter 2 of this thesis .

Chapter 2 summarises the work carried out to determine the tropospheric lifetimes of a series of ethers and ketones . The lifetimes of these compounds were calculated from their OH radical and Cl atom rate constants . Two of the ethers (isoflurane and enflurane) studied are halogenated and routinely used as inhalational general anaesthetics . Their lifetimes are sufficiently long for a certain proportion of these compounds to reach the stratosphere . Once a chemical reaches the stratosphere it is important that the reactions which it may undergo are

studied . This is fundamentally important in determining possible adverse effects which a compound or it's reaction products may exhibit in the stratosphere . Chapter 3 of this thesis summarises the results obtained from a study of the photooxidation of the anaesthetic ethers , isoflurane and enflurane . This photooxidation mechanism is an important reaction pathway for these and analogous compounds in the stratosphere , hence the importance of this type of experimental study .

1.2 References

[1] I. Shanahan , *Irish Chemical News* , 12 , Winter , (1989) .

[2] B.A. Thrush , *Phil. Trans. R. Soc. London* , **A296** , 149 , (1980) .

[3] H.B. Singh , and J.F. Kasting , *J. Atmos. Chem.* , **7** , 261 , (1988) .

[4] I.S.A. Isaksen , and F. Stordal , *Ambio* , **10** , 1 , 9 , (1981) .

[5] J. Scotto , G. Cotton , F. Urbach , T. Berger , and T. Flars , *Science* , **239** , 762 , (1988) .

[6] R.I. Van Hook , P.A. Fairchild , W. Fulkerson , A.M. Perry , J.D. Regan , and G.E. Taylor , Report by U. S. Department of Energy , ORNL - 6552 (DE90004404) , 42pp , November , (1989) .

[7] M.J. Molina , and F.S. Rowland , *Nature* , **249** , 810 , 28 June , (1974) .

[8] M.J. Prather and R.T. Watson , *Nature* , **344** , 729 , 19 April , (1990).

[9] P.J. Fraser , *Chem. Aust.* , **56** , 8 , 272 , August , (1989) .

[10] B.J. Finlayson - Pitts , and J.N. Pitts Jr. , Atmospheric Chemistry , J. Wiley & Sons , (1986) .

[11] L.E. Manzer , *Science* , **249** , 31 , 6 July , (1990) .

[12] J.E. Lovelock , *Nature* , **230** , 379 , (1971) .

[13] M.J. Kurylo , *Int. J. Refrig.* , **13** , 62 , March , (1990) .

[14] F.S. Rowland , *Environ. Sci. Technol.* , **25** , 4 , 622 , (1991) .

[15] J.C. Farman , B.G. Gardiner , and J.D. Shanklin , *Nature* , **315** , 207 (1985) .

[16] United Kingdom Stratospheric Ozone Review Group (Eds) , "Stratospheric Ozone 1988" , HMSO , London , 71pp , (1988) .

[17] S.C. McDonald , Report by the US Department of Energy , PNL -- 7163 (DE90-001813) , 54pp , Oct. , (1989) .

CHAPTER 2.0

OH radical and Cl atom reactions with a series of ethers and ketones .

2.1 Introduction

Concern over the occurence and effects of airborne toxic and hazardous chemicals has emerged over the past twenty years as a dominant air pollution issue on a regional , national and international basis. Coupled with concern relating to toxic chemical pollution is the global problem of ozone depletion caused by the increased release and subsequent reactions of CFC compounds in the stratosphere .

Increased environmental awareness and hence monitoring has led to recognition of the wide range of sources of volatile chemicals entering the atmosphere . Among these sources are toxic waste disposal sites , landfills , releases from industrial or commercial processes , releases from household appliances , and emissions resulting from the application of pesticides and herbicides during agricultural operations .

Because of the complexity of atmospheric processes , the use of computer models is necessary to elucidate and predict the effects of anthropogenic and biogenic emissions to the atmosphere . Chemical mechanisms with varying degrees of detail are integral components of these atmospheric computer model studies . The ultimate accuracies of the chemical mechanisms used in these computer models are dependent on the accuracy of the individual rate constants and products of the many hundreds of elementary reactions which occur in the atmosphere . The troposphere , and , in particular , polluted urban atmospheres , contain hundreds of different organic species of much complexity and there is a need for evaluation of the chemical reactions occuring for these compounds .

Important elements of the data base which must be developed for each compound released to the atmosphere are [1]

- the atmospheric degradation pathway for the compound ;
- it's corresponding atmospheric lifetime ; and ,
- the products formed from the parent compound and their fates in the atmosphere .

From such information , exposure assessments can be developed and the radius of impact of a toxic or hazardous volatile compound can be characterised as being local , regional , or global in scale .

It is now well established that organic chemicals emitted into the troposphere (Figure 1.1) are removed by reaction with a number of reactive intermediates including OH , HO_2 and NO_3 radicals and O_3 , by photolysis and by wet and dry deposition [2] . In general the reactive species in the atmosphere that will attack emissions from ground or airborne sources with typical concentrations at 20 km are listed below .

SPECIES	**Concentration** (molecules cm^{-3})	**Concentration** (relative to OH)
H	5×10^5	0.35
O	1×10^6	0.7
OH	1.4×10^6	1.0
HONO	1.8×10^7	12
HO_2	3.5×10^7	25
H_2O_2	1.0×10^9	700
HNO_3	7.0×10^9	5000
NO_x	1.0×10^{10}	7000
Cl	1×10^3	0.001

Table 2.1.1
Concentrations of reactive atmospheric species at 20 km [1]

It is now accepted that the hydroxyl (OH) radical , nitrate radical (NO_3) and ozone (O_3) play a very important role in atmospheric reactions of anthropogenic organic chemicals in the troposphere [3 - 5] . In 1961 Leighton [6] suggested that OH radicals could be an important

intermediate species in photochemical air pollution . Subsequently the first kinetic data for the reaction of OH radicals with organic compounds were obtained (for a series of alkanes) by Greiner [7,8] . On the basis of these and subsequent data , Greiner [9] postulated that OH radical reactions might be important in photochemical air pollution .

Recognition of the importance of OH radical reactions as a removal mechanism in the troposphere has resulted in numerous kinetic and mechanistic studies of these reactions [5,10 - 15] .

The role of chlorine chemistry in the troposphere has received little attention because , "Cl atoms are sufficiently scarce that they could not compete with OH radicals as a dominant loss mechanism for hydrocarbons in the troposphere" , so stated Wofsy and McElroy in 1974 [16] . This scenario is supported by the fact that the reaction of Cl atoms with CH_4 is only 13 times faster than the corresponding OH radical reaction whereas OH radicals are nearly 1000 times more abundant in the lower troposphere . However by comparison , typical reaction rates of Non Methane HydroCarbons (NMHCs) with Cl atoms are nearly 100 - 1000 times faster than the corresponding OH radical rates . As the $^{Cl}/_{OH}$ ratio increases with altitude , and because of the lower activation energies of Cl atom reactions , it has been realised that Cl atoms should play an important role in NMHC oxidation in the lower stratosphere [17 - 19] . But what of the importance of Cl atom reactions in the troposphere ? Singh et al [20] have determined marine tropospheric levels of Cl atoms of 10^3 cm^{-3} or approximately 1000 times lower than OH radicals . Because of their greater reactivity towards NMHCs , Cl atoms may play an important role in NMHC oxidation at all latitudes . Singh et al [20] have calculated that between 20 to 40% of NMHC oxidation in the troposphere and 40 to 90% of NMHC oxidation in the stratosphere is caused by reaction with Cl atoms. Since Singh et al [20] highlighted the possible importance of Cl

atom oxidation of NMHCs in the troposphere , a number of articles have been published reporting Cl atom rate constants , pointing towards the importance of these values not only in stratospheric modelling but also in determining the fate of volatile organic chemicals (VOCs) in the troposphere [21 - 23] .

Advances in the kinetic and mechanistic aspects of OH radical and Cl atom chemistry has led to the elucidation of the atmospheric sources of these reactive species .

2.1.1 Sources of OH radicals and Cl atoms in the troposphere

2.1.1.1 *Sources of OH radicals in the troposphere*

In the troposphere the important direct sources of OH radicals are from the reaction of $O(^1D)$ atoms formed from the photodissociation of O_3 ($\lambda < 319nm$) with water vapour [2] :

$O_3 + h\nu$ ($\lambda < 320nm$)	---------->	$O(^1D) + O_2$	(2.1.1.1)
$O(^1D) + M$ ($M = O_2 + N_2$)	---------->	$O(^3P) + M$	(2.1.1.2)
$O(^1D) + H_2O$	---------->	$2\dot{O}H$	(2.1.1.3)

and from the photodissociation of HONO :

$HONO + h\nu$ ($\lambda < 400nm$)	--------->	$\dot{O}H + NO$	(2.1.1.4)

Another important source of OH radicals arises from the reaction of HO_2 radicals with NO :

$$\dot{HO}_2 + NO \text{ -------> } \dot{OH} + NO_2 \qquad (2.1.1.5)$$

with HO_2 radicals being generated from the photolysis of aldehydes and ketones , e.g. ,HCHO :

$$HCHO + h\nu \text{ --------> } \dot{H} + \dot{HCO} \qquad (2.1.1.6)$$

$$\dot{H} + O_2 + M \text{ ---------> } \dot{HO}_2 + M \qquad (2.1.1.7)$$

$$\dot{HCO} + O_2 \text{ --------> } \dot{HO}_2 + CO \qquad (2.1.1.8)$$

At higher altitudes applicable to the stratosphere and mesosphere , photodissociation of O_2 and N_2O are also sources of $O(^1D)$ atoms , while the photodissociation of H_2O yields OH radicals directly and H atoms .

The actual concentration of OH radicals in the troposphere and lower stratosphere is obviously of particular importance since reaction with these species is an important loss process for VOCs and their concentration will thus determine the lifetimes of these organics in the troposphere and thus the levels which are transported to the stratosphere.

Numerous directly measured and estimated atmospheric OH radical concentrations have been reported . In the lower troposphere , measurements using laser induced fluorescence and long pathlength UV absorption show that OH radical concentrations are generally $< 5 \times 10^6$ molecules cm^{-3} . Estimates for the average tropospheric OH radical concentrations have been derived from the ambient tropospheric levels of trichloromethane ($CHCl_3$) , 1,1,1 - trichloroethane (CH_3CCl_3) [24] and ^{14}CO. These ambient tropospheric measurements yield an average northern hemisphere tropospheric OH radical concentration of ca. 5×10^5 molecules cm^{-3} . More recently Crutzen [25] has carried out calculations which predict the annually averaged OH radical concentration in the troposphere during a 24 hour period at ca. 5×10^5 and 6×10^5 molecules

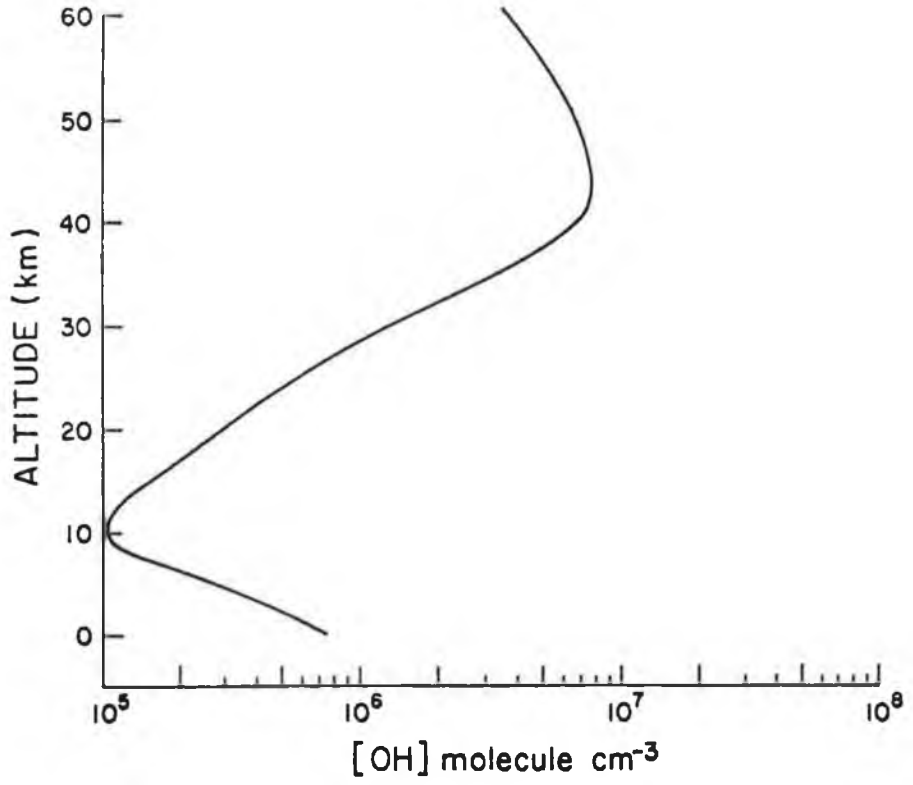

Figure 2.1.1
The profile was drawn on the basis of an annual daytime average (12 hr.) calculated in the Northern hemisphere at 30° latitude . This profile which appears in Atkinson et al [26] has the troposphere set at 15km .

cm^{-3} for the northern and southern hemispheres respectively . Figure 2.1.1 illustrates the atmospheric OH radical concentration profile as recently calculated by Crutzen et al [25] . The concentration of OH radicals locally may be much higher than the globally averaged value and the chemical lifetime of easily degradable substances is shorter in such circumstances . Directly measured [OH] values are typically of the order 1 x 10^6 radicals cm^{-3} , however during smog events , [OH] may be as high as 10^7 radicals cm^{-3} , so that the "local" chemical lifetime may only be $^1/_{10}$ - $^1/_{20}$ of the value calculated from the globally averaged value [27] . We can see therefore that in quoting atmospheric lifetimes for a volatile organic chemical (VOC) with respect to OH radicals , it is important to specify the concentration of OH radicals used to calculate these lifetimes .

The concentration of OH radicals chosen in this work to determine

the tropospheric lifetimes of the volatile organic compounds examined in this thesis was (7.7 ± 1.4) x 10^5 molecules cm^{-3} . This value was calculated by Prinn et al [24] and represents a globally averaged tropospheric concentration of OH radicals . From July 1978 to June 1985 , methyl chloroform concentrations were monitored by Prinn and coworkers [24] at a number of remote sites throughout the world . The principal recognised atmospheric sink for methyl chloroform is the reaction [28] :

$$CH_3CCl_3 + \dot{O}H \text{ -----> } \dot{C}H_2CCl_3 + H_2O \qquad (2.1.1.9.)$$

The global rate of loss of CH_3CCl_3 , which can be deduced from its known industrial emissions and observed global trends , was then used by Prinn et al [24] to deduce accurate globally averaged tropospheric concentrations of OH radicals .

2.1.1.2 *Sources of Cl atoms in the troposphere*

The chemical species and sources of gaseous chlorine in the troposphere have been the subject of controversy for many years . Gaseous inorganic chlorine (GIC) is known to be present in the marine boundary layer at concentrations of appoximately 1 to 2 ppbv [20] . There is general agreement that the major component of GIC is HCl which is released from sea salt aerosols that have been acidified to very low pH (2 to 3) by the addition of nitric or sulphuric acid produced within the atmosphere [29 - 32]:

$$HNO_3(g) + NaCl(p) \text{ -----> } HCl(g) + NaNO_3(p) \qquad (2.1.1.10)$$

$$H_2SO_4(p) + 2NaCl(p) \text{ -----> } 2HCl(g) + Na_2SO_4(p) \qquad (2.1.1.11)$$

The formation of the acids can be explained by looking at the reactions of sulphur and nitrogen oxides in the atmosphere . SO_2 in the atmosphere is steadily oxidised to SO_3 , which being extremely hygroscopic is adsorbed by any particulate matter as H_2SO_4 . This mechanism explains two things , namely , the often observed low pH of precipitation and the presence of chloride in the atmosphere . This marine source for GIC is supported by gaseous chloride concentration measurements . Highest levels of GIC are found in marine air and these decline as air moves over continental regions [33] .

Besides the proposed sea salt source of GIC in the troposphere other minor sources include man - made sources (combustion of coal and petrochemicals) and from volcanoes . The only specific (spectroscopic) measurement of HCl confirms it's 1 to 2 ppb abundance over the oceans but finds little HCl over land . More recently measurements in which HCl is converted to an organic derivative for quantification by GC have been reported [34]. These methods show somewhat lower HCl levels compared to previous determinations but these measurements represented a mix of both marine and continental air masses . For the determination of NMHC lifetimes with respect to Cl atoms in this report , a concentration of 10^3 atoms cm^{-3} was used [20] . This value is typical of a clean tropospheric marine environment .

2.1.2 Determination of rate constants for OH radical and Cl atom reactions

It has been demonstrated that OH radical and Cl atom reactions are important removal mechanisms for water insoluble volatile organic chemicals (VOCs) in the troposphere . It has been shown that there is a ready natural source of these reactive species in the troposphere and that numerous workers have determined accurate concentrations for these species in the atmosphere . To establish the tropospheric fate of a VOC and hence it's possible significance in stratospheric ozone depletion we must first determine the rate of reaction of this species with both OH radicals and Cl atoms and thus the efficiency with which it is removed from the troposphere .

Great effort has been devoted to devising experimental techniques which allow kinetic data to be obtained under simulated atmospheric conditions , i.e., in one atmosphere of air , with reactant and co - pollutant concentrations typical of those found in the troposphere . In many cases , precise duplication of atmospheric conditions is not possible so experiments are carried out over as wide a range of conditions as possible and the results extrapolated to atmospheric conditions .

The experimental techniques used to study the kinetics of OH radical and Cl atom reactions can be divided into two categories , absolute and relative rate techniques .

2.1.2.1 *Determination of OH radical rate constants*

Both absolute and relative rate techniques have been used for the determination of OH radical reaction rates with VOCs . Absolute rate constants are measured using techniques which allow the concentration

of the OH radical to be determined as a function of time . The OH radical is a very reactive , short lived species and hence absolute techniques rely on the use of extremely sensitive and rapid detection systems ,i.e., laser excitation and fluorescence detection . Because of this the use of absolute methods for determining reaction rates is very expensive. Another drawback of absolute techniques is the difficulty in simulating atmospheric conditions in the reaction area . These drawbacks have resulted in significant bodies of work being carried out using relative rate techniques to measure reaction rates . A reference reaction is chosen for which the absolute value of the rate constant is known with confidence and the rate constant of interest is then calculated from the experimentally determined rate constant ratio . As it is the concentration of the VOCs which is monitored in the relative rate technique , the time scale of reaction is much longer than in the absolute technique , hence the methods of detection are cheaper (GC is commonly used) . Due to the relatively easier experimental procedure employed in the relative rate technique , a greater precision (but not necessarily greater accuracy) is possible compared to the absolute techniques.

To achieve accurate and precise measurements of OH radical rate constants it is best to use a combination of the two techniques . For example in this work precise rate constant ratios were obtained using a relative rate technique and these were combined with accurate reference compound rate constants , obtained using an absolute rate technique . As the experimental procedure employed in our laboratory was a relative rate technique , only a quick review of absolute methods is given here .

(a) Absolute techniques

The main absolute techniques for monitoring OH radical rate constants include , fast flow discharge systems (FFDS) , flash photolysis

(FP) , and to a lesser extent , molecular modulation (MM) and pulse radiolysis (PR) .

A large proportion of reactions in the atmosphere are bimolecular :

$$A + B \text{ -----> Products} \qquad (2.1.2.1)$$

This simple mechanism can be used to help describe the principles of the above absolute techniques .

A can be taken as the OH radical and B the test compound under investigation . To study reaction kinetics , loss of small amounts of A in a large excess of B is usual . Hence the simple bimolecular rate equation :

$$-\frac{d[A]}{dt} = k_1 [A] [B] \qquad (2.1.2.2)$$

can be written as a pseudo-first order equation i.e. [B] remains essentially constant . The pseudo-first order expression can then be integrated to yield:

$$\ln \frac{[A]}{[A_o]} = -(k_1[B_o])_t \qquad (2.1.2.3)$$

Under these pseudo-first order conditions , a plot of $\ln\{[A]/[A_o]\}$ against time for a given value of $[B_o]$ is linear with a slope equal to $(-k_1[B_o])$. These plots are carried out for a series of concentrations of $[B_o]$ and the values of the corresponding decays determined . Finally , the absolute rate of interest , k_1 , is the slope of a plot of these decay rates against the corresponding values of $[B_o]$.

Pseudo - first order kinetic analysis is used to determine the rate constants for VOCs using each of the above mentioned absolute

techniques . This type of kinetic analysis requires only the monitoring of one species , A , as a function of time . Not only that , as a ratio of ($[A]/[A_0]$)appears in the pseudo-first order expression , the measurement of any parameter that is proportional to the concentration of A will suffice in determining k_1 .

Each of the absolute techniques now summarised utilizes the above pseudo-first order experimental technique to determine the rate of reaction of OH radicals with a test VOC .

Fast flow discharge systems (FFDS)

The term discharge system is used as a discharge is employed to generate OH radicals . Typically a microwave discharge of H_2 in a diluent gas (He or Ar) is followed by mixture with a known amount of NO_2 to generate OH radicals . Experimentally , two different approaches are used. In the first , OH radicals enter the flow tube at the upstream end and are mixed with the VOC . The decay of OH radicals is followed using a detector which moves along the length of the flow tube . In the second approach , one of the reactants enters at the upstream end of the flow tube and the second is added through a moveable inlet or through a series of fixed inlets . In this case the detection is fixed at the downstream end of the flow tube and the reaction time is varied by moving the mixing point for A and B relative to the detector .

The decay of OH radicals is typically monitored by resonance absorption (RA) [35] , resonance fluorescence (RF) [36] , electron paramagnetic resonance (EPR) [37] , mass spectroscopy (MS) [38] , laser magnetic resonance (LMR) [39] , or laser induced fluorescence (LIF) [40] .

The flow tube in the above experiments is typically 2 - 5 cm in diameter . As the reaction mixture travels down the flow tube at high linear flow speeds (typically 1000 cm s^{-1}) the OH radicals react with the test

organic . Using typical flow speeds , reactions occuring on a time scale of 100 ms can be studied in a 1 meter flow tube [2] .

Flash photolysis

A pulse of UV or vacuum UV radiation is produced by means of flash lamps [41] or by pulsed lasers . This pulse dissociates a parent molecule of H_2O [41] or HNO_3 [42] producing OH radicals . After an appropriate time following the photolytic flash , the concentration of the OH radicals is monitored using induced fluorescence (IF) or resonance fluorescence (RF) . Lasers are now commonly used to determine absolute rate measurements under tropospheric conditions [43] i.e. first a laser flash produces the OH radicals and a second can then determine it's concentration by induced fluorescence [44] or by long path absorption (LPA) [45].

Molecular modulation

$O(^3P)$ is produced by the mercury photosensitised decomposition of N_2O with 253.7 nm resonance radiation being used to excite the ground state Hg (6^1S_0) to the metastable ($^3P_1$) state ;

$$Hg\ (6^1S_0) + h\nu\ (253.7nm) \text{ -----> } Hg\ (6^3P_1) \qquad (2.1.2.4)$$

$$Hg(6^3P) + N_2O \text{ -----> } Hg + N_2 + O(^3P) \qquad (2.1.2.5)$$

$$O\ (^3P) + B \text{ -----> Products} \qquad (2.1.2.6)$$

The production of $O(^3P)$ is sinusoidally modulated by modulating the photolysing light which leads to the formation of $O(^3P)$.

If B is a hydrocarbon e.g propane , the $O(^3P)$ can abstract a hydrogen atom from it , thus producing OH radicals . The rate constant for the reaction of these OH radicals with a VOC can then be determined by

following the concentration of OH radicals (e.g. by absorption spectroscopy) [2] .

Pulse Radiolysis

OH radicals are produced by the pulse radiolysis of water vapour . The decay of OH radicals in a large excess of reactant is monitored by optical absorption and this [2] is used to study the kinetics of reactions . Although pulse radiolysis is a convenient technique for high temperature work and for application to atmospheric chemistry , since ,it can be used at total pressures of one atmosphere and more , the expense and complexity of the equipment has resulted in its use being limited [46-47] .

COMPARISON OF ABSOLUTE TECHNIQUES

The majority of absolute rate constants for atom and free radical reactions for atmospheric pollution assessment have been generated using FFDSs and FP . Flash photolysis is more useful for atmospheric determinations as pressures up to and greater than atmospheric pressure can be employed . As a consequence of these high pressures , rate constants as low as 10^{-18} $cm^3molecule^{-1}sec^{-1}$ can be measured . FP systems also employ large reaction cells and these large volumes coupled with the higher pressures possible in the system results in wall reactions being negligible . FFDSs were initially limited to </= 10 torr , however , flow tube studies have now been extended to 100 torr . Because of these low pressures , reaction rates below 10^{-16} $cm^3molecule^{-1}s^{-1}$ connot be determined . Another problem in FFDSs is wall reactions resulting from the relatively small dimensions of the reaction cell . The major advantage of FFDSs is the versatility with regard to detector options.

Typical errors of between ±10 and 30% are obtained when using

absolute techniques to determine OH radical rate constants . Errors obtained depend on the system used and the samples analysed .

(b) Relative rate techniques

Numerous methods have been employed to obtain relative rate constant data for the reaction of OH radicals with VOCs . The "smog chamber" has been the most widely used approach for relative rate studies. The design of a smog chamber can vary enormously depending upon the reaction to be simulated . In general , however , components of a smog chamber are similar and usually include :

-- a reaction chamber ;

-- a series of photolysis lamps ; and

-- a detection system .

Initially , glass type reactors were used , but these suffered many problems [2] and as a result , large smog chambers with inert surfaces are generally used today . Conditioned FEP Teflon films have found widespread use (an 86 dm^3 Teflon bag was used for our relative rate experiments) because of their low rates of surface destruction , the fact that their volume can easily be varied , they transmit solar radiation in the region 290 - 800 nm as opposed to >/= 350 nm for pyrex glass and they are cheap . During a normal smog chamber experiment using a Teflon bag , as samples are withdrawn , the bag collapses and hence a pressure of 1 atm is maintained throughout the analysis .

A problem with the collapsible bag type smog chamber is that temperature and pressure are not easily controlled . As a result , some evacuable smog chambers have been designed in order to control both temperature and pressure [48] . Ports are usually included in smog chambers for withdrawing samples for analysis . Included in some

chambers are ports for in situ spectroscopic measurements using techniques such as FTIR , GC and GCMS .

The irradiation sources used in most smog chamber systems to simulate solar radiation are :

-- black fluorescent lamps (output from 320 to 480 nm) ;

-- sunlamps (output from 270 to 440 nm) ; and

-- Xenon lamps (output from 280 - 700 nm) .

A combination of sunlamps and black lamps was employed in our experiments depending on the reaction under investigation .

For all of the work carried out in our laboratory the reactants were monitored by a gas chromatograph fitted with a flame ionization detector .

The relative rate technique employed in our laboratory has been described in detail by many workers [1,49] .This technique is based upon simultaneously monitoring the disappearance rates of a test compound (T) and a reference compound (R) whose OH radical rate constant (absolute) is known :

$T + \dot{O}H$	$\xrightarrow{k_1}$	PRODUCTS	(2.1.2.7)
$R + \dot{O}H$	$\xrightarrow{k_2}$	PRODUCTS	(2.1.2.8)
$T + h\nu$	------>	PRODUCTS	(2.1.2.9)
T + Walls	------->	Loss to walls.	(2.1.2.10)

The loss of T is defined by :

$$\frac{d(T)}{dt} = k_1(OH)(T) + k'(T) \qquad (2.1.2.11)$$

and the loss of R is defined by :

$$\frac{d(R)}{dt} = k_2(OH)(R) \qquad (2.1.2.12)$$

where k_1 and k_2 are the relative rate constants for the test compound , T ,

and reference compound R respectively .

The k' = (kp + kw) term , is the first order photodissociation constant and/or wall loss of the test compound . The integration and combination of equations 2.1.2.11 and 2.1.2.12 result in :

$$(1/ t - t_o)\ln(T_o / T_t) = (k_1/k_2)(1/ t - t_o)\ln(R_o / R_t) + k' \qquad (2.1.2.13)$$

Therefore , a plot of $(t - t_o)^{-1}\ln(T_o /T_t)$ vs $(t - t_o)^{-1}\ln(R_o /R_t)$ yields a straight line with a slope of (k_1/k_2) and intercept k' .

If k' = 0 , Atkinson et al [3] recommend evaluating k_1 by eliminating the time dependence from equation 2.1.2.13 , which then reduces to :

$$\ln(T_o /T_t) = (k_1/k_2)\ln(R_o /R_t) \qquad (2.1.2.14)$$

and again solving for k_1 by calculating the product of the slope $(k_1/k_2)$and k_2 .

Atkinson et al [3] , noted that the use of regression analysis with equation 2.1.2.13 to solve for (k_1/k_2) and intercept (k') , places the most weight on those data points collected in the earliest part of the irradiation where the least amount of the test compound has reacted . Equation 2.1.2.13 (or 2.1.2.14) requires that the loss of test or reference compounds be measured in the presence of OH , as a function of time .

It has been recommended by Bufalini et al [1] that the reference should be chosen with the following criteria :

(a) it should have an accurately known room temperature rate constant which approximates that anticipated for the test compound ;

(b) it should not photolyse (at λ >/= 290 nm) or oxidise in air ;

(c) it should be sufficiently volatile to remain in the gas phase and not be adsorbed on the walls of the reaction chamber ;

(d) it should be accurately measurable by an available analytical technique; and ,

(e) it should not react with the test compound , ozone or NO_3 , NO_2 , or HNO_2 .

Similarly the test compound must satisfy certain criteria in order to be a canditate for the above protocols [1 , 49] :

(a) an accurate analytical method must be available for making repeat measurements of the test compound over a two hour period , and

(b) the rate of loss by photolysis and wall losses must not be greater than the loss due to reaction with OH radicals :

$$(k_{OH\text{-}T} \times OH) >> k_{photolysis} \qquad (2.1.2.15)$$

The OH radicals for this relative rate technique were generated in our laboratory by the photolysis of methyl nitrite in the presence of excess nitric oxide :

$$CH_3ONO + h\nu \text{ -----> } CH_3\dot{O} + NO \qquad (2.1.2.16)$$

$$CH_3\dot{O} + O_2 \text{ -----> } HCHO + H\dot{O}_2 \qquad (2.1.2.17)$$

$$H\dot{O}_2 + NO \text{ -----> } NO_2 + \dot{O}H \qquad (2.1.2.18)$$

Nitric oxide was added in excess in order to drive reaction (2.1.2.18) to completion and to prevent ozone formation since NO_2 produced in reaction (2.1.2.18) will also photodissociate :

$$NO_2 + h\nu \text{ -----> } NO + O^{\bullet} \qquad (2.1.2.19)$$

$$O^{\bullet} + O_2 \text{ -----> } O_3 \qquad (2.1.2.20)$$

$$O_3 + NO \text{ -----> } NO_2 + O_2 \qquad (2.1.2.21)$$

The use of CH_3ONO as an OH radical source avoids many of the disadvantages associated with previous chemical sources used in relative rate techniques [1] and allows OH radical rate constants of >/= 3 x 10^{-13} $cm^3molecule^{-1}s^{-1}$ [1] to be determined , in a comparatively inexpensive , uncomplicated and accurate manner .

2.1.2.2 *Determination of Cl atom rate constants*

Chlorine atom rate constants are determined by both absolute and relative rate techniques . A summary of the main techniques used to determine the reactivity of VOCs with chlorine atoms is given below . Only a brief outline of the absolute techniques is given as these are similar to the methods summarised for the determination of OH radical rate constants in Section 2.1.2.1 .

(a) Absolute techniques

DF / MS

Cl atoms are produced in a microwave discharge of Cl_2 in helium and their concentration determined by monitoring the molecular chlorine peak at $^m/_e$ = 70 . A number of variations have been applied by various workers [51-53] , common to all is the use of a discharge to form Cl atoms. A flow tube reaction cell and a mass spectrometer is generally used to carry out and to monitor reaction . The reactor is typically a Pyrex flow tube 2.5 cm in diameter and 50 cm in length coated with halocarbon wax . Cl atom decay is monitored by MS . Bartels et al [54] used DF/MS to determine Cl atom rate constant values for a series of alkanes . They employed a reference technique , i.e., both a reference and test

compound were added in excess and the decay of both species was monitored during the reaction . A value for k_1/k_0 was obtained and the results placed on an absolute basis using a literature value for k_0 . High errors are usually encountered in this technique with ratio errors of ± 20% typical [53] .

DF/RF

Similar flow tubes as in DF/MS are used in this system . Similar experimental conditions as outlined previously for the determination of OH radical rate constants are used . Usually measurements of k_1 are made by observing the decay of Cl atoms in the presence of excess analyte [50]. A typical chlorine resonance lamp is operated by passing a mixture of 1% Cl_2 in He through the lamp at ca. 0.6 torr of the total pressure . A thin BaF_2 window is often used to filter the atomic hydrogen line at 121.6 nm and the atomic oxygen lines at 130 nm . A typical DF/RF system plus the procedure used to measure reaction rates of Cl atoms with a series of alkanes is summarised by Lewis et al [55] .

Pulsed laser / time-resolved resonance fluorescence spectroscopy

Detailed experimental procedures are outlined in the literature [56-57] and hence only a brief summary is given here . Cl (^2P_J) atoms are produced by 355 nm pulsed laser pholysis of Cl_2 and detected by time-resolved resonance fluorescence spectroscopy . A CW electrodeless discharge lamp (gas mixture : 0.1% Cl_2 in He) is typically used as the fluorescence excitation light source [56] . This technique is similar to the corresponding OH radical absolute technique described earlier . Usually all experiments are carried out with test compounds in a large excess of Cl (^2P_J) . Wine and Semnes [56] estimate the absolute accuracy of the rate constants reported by this method to be approximately ±15% .

Very low pressure reactor (VLPR)

In the three absolute techniques described above , the use of the pseudo-first order approximation is only valid when the substrate concentrations (RH) is essentially unchanged during the course of the reaction and no secondary reactions occur . This is generally not the case in the reactions of Cl atoms with C_2H_6 or higher hydrocarbons when very fast bimolecular Cl-radical processes as well as fast radical-radical reactions can occur . These can give rise to systematic errors and anomalies that have been reported . Such anomalies can be found in the slight pressure dependence of the reaction with ethane in a flash photolysis system , and to a lesser extent , as a flow rate dependence of the same rate constant when compared to the results obtained with flow cell and discharge flow tube kinetic techniques .

All of these problems can be avoided by use of VLPR . By working in the millitorr pressure range , complexities due to atom-radical and radical-radical recombination are avoided . The VLPR falls into the category of flow cell reactor systems , but having no flow velocity profile since it is a well-stirred reactor . A detailed review of the VLPR technique is given by Dobis and Benson [58] and Lazarou et al [59] . From their results the accuracy of the VLPR technique is seen to be very high with rate constants for the reaction of Cl atoms with C_2H_6 quoted to ± 3% .

(b) Relative rate techniques

A relative rate technique was used in this thesis to determine the Cl atom reaction rates of a series of ethers and ketones . The experimental procedure is similar to that outlined in Section 2.1.2.1 for the determination of OH radical rate constants . The only difference being that chlorine gas photolysis was used as a source of Cl atoms :

$Cl_2 + h\nu$ ($\lambda > 320$ nm) -----> 2Cl· (2.1.2.22)

This technique has been used extensively in other laboratories [60-62] to determine Cl atom rate constants . Typical errors of $\pm 2\sigma$ equivalent to a maximum of 5% are obtained using this technique [60] . This does not include errors in the reference rate constant used to place these results on an absolute basis . Wallington et al [60] estimated that systematic errors could introduce an additional 20% uncertainty to results , while other publications by Atkinson et al [61] and Wallington et al [62] recommend an additional 10 - 15% for the reference error .

2.1.2.3 *Estimation techniques*

With the development of experimental procedures for the determination of atmospheric reaction rates (both absolute and relative rates) has come the publication of large data reviews to summarise the present knowledge with regard to the various classes of compounds and their reactions [10 - 15] . This data base has allowed the development and use of estimation techniques for the calculation of OH radical reaction rate constants (specifically) for a wide range of organic compounds . These estimation techniques have permitted cost-effective estimation of tropospheric lifetimes for organic compounds whose volatility or chemical complexity make direct experimental investigation difficult .

The simplest of these estimation techniques are those utilizing structure - activity relationships (SARs) . The first development of an SAR technique was carried out by Greiner [9] in 1970 . As more experimental data became available the technique was updated ay Darnall et al [63] , Heicklen [64] , Cohen [65] , Baldwin and Walker [66] and by Atkinson

[67,68] . Recently Atkinson [68] has further updated his approach to take account of neighbouring groups , a greater range of compounds and a wider temperature range .

As discussed by Atkinson [68] , the rate constants for the reaction of OH radicals with alkanes can be fitted to within a factor of 2 over the temperature range 250 - 1000 K by consideration of the CH_3- , -CH_2- and CH- groups in the alkane and the substituent groups around these groups. Thus :

$$k\,(CH_3\text{-}X) = k^o_{prim}\,F(X)$$

$$k(X\text{-}CH_2\text{-}Y) = k^o_{sec}\,F(X)F(Y)$$

and

$$k(X\text{-}CH{<}^{X}_{Y}) = k^o_{tert}\,F(X)F(Y)F(Z)$$

where k^o_{prim} , k^o_{sec} and k^o_{tert} are the OH radical rate constants per -CH_3 , -CH_2- and >CH- group respectively , and F(X) , F(Y) and F(Z) are the substituent factors for X , Y and Z substituent groups . Values derived by Atkinson (1987) , $k^o_{prim} = 4.47 \times 10^{-18} T^2 e^{-303/T}$ $cm^3 molecule^{-1} s^{-1}$, $k^o_{sec} = 4.32 \times 10^{-18} T^2 e^{-233/T}$ $cm^3 molecule^{-1} s^{-1}$, $k^o_{tert} = 1.89 \times 10^{-18} T^2 e^{711/T}$ $cm^3 molecule^{-1} s^{-1}$, $F(-CH_3) = 1.00$ and $F(-CH_2-) = F(>CH-) = F(>C<) = e^{76/T}$. This estimation technique not only allows calculation of OH radical reaction rate constants for alkanes for which experimental data do not exist, but also allows the isomeric alkyl radical distribution to be calculated for a given alkane . Thus , for example , for 2-methylbutane the calculated OH radical reaction rate constants at 298 K (and the percentage of the overall OH radical reaction) at the various C atoms (in units of 10^{-12} $cm^3 molecule^{-1} s^{-1}$) is:

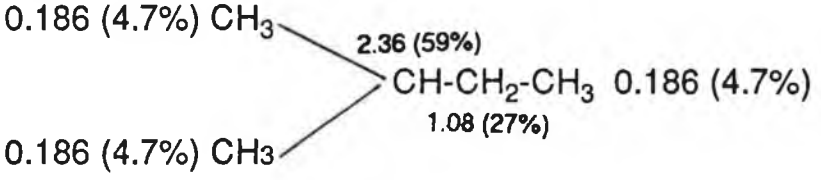

The following is a typical example of how the SAR technique can be used to predict the OH radical rate constant for ethyl methyl ether using the group reactivities suggested by Wallington et al [69] for the ethers :

CH_3 -- 1.2 x 10^{-12} $cm^3molecule^{-1}s^{-1}$ C_2H_5 -- 6.8 x 10^{-12} $cm^3molecule^{-1}s^{-1}$ (group reactivities for the ethers [69])

=> $k_{OH}(CH_3OC_2H_5)$ = 8.0 x 10^{-12} $cm^3molecule^{-1}s^{-1}$

This SAR technique predicts , to within a factor of two , the rate constants for approximately 300 compounds . The reliability of using this technique for estimating OH radical rate constants , depends on the applicability of the underlying assumptions , and on the accuracy and breadth of the kinetic data base from which the estimation technique was developed . So as more data becomes available , even more reliable predictions covering larger and more complex VOCs will be possible .

Other more complex estimation techniques include use of transition state theory (TST) developed by Kaufmann and co-workers ([70-71], [65]) and the development of gas/solution phase reactivity correlations [72] .

It has been pointed out that various experimental techniques , both absolute and relative rate , are available for the experimental examination of atmospheric processes . A relative rate - smog chamber technique was employed in our laboratory to determine the OH radical and Cl atom rate constants for a series of ethers and ketones . A Teflon bag - smog chamber system was used to carry out these studies due to it's low cost and it's suitable low contamination effects . A relative rate procedure was adopted again because of it's low cost and due to the availability of a suitable detection system (GC -FID) .

Based on the large number of experimentally determined rate

constants which have accumulated from both absolute and relative rate experimental techniques , reliable estimation procedures have now been established . All of this kinetic information must also be combined with product analysis to further broaden the data base and study the atmospheric impacts in relation to VOCs . As kinetic and product information grows , so too will the accuracy of computer modelling of the atmosphere , which relies on the accuracy of inputed data to predict future environmental quality .

Using the relative rate technique described the reaction of OH radicals and Cl atoms with a series of ethers and ketones was studied . To explain the observed rate data and to determine the ultimate atmospheric fate of these compounds , it is necessary to summarise present atmospherically important kinetic and mechanistic information regarding not just the ethers and ketones , but also the simpler alkanes .

2.1.3 OH radical and Cl atom reactions with the alkanes

2.1.3.1 *OH radical reactions with the alkanes*

Alkanes are released into the troposphere from natural and anthropogenic sources . The single , naturally produced organic , present in the largest concentrations in ambient air throughout the world is methane . Larger alkanes such as , ethane , propane , and butane are also released natually from sources such as seepage and bacterial fermentation . The major loss process for these alkanes in the troposphere is reaction with OH radicals . Because of this , numerous studies have been made of the reaction of OH radicals with these compounds .

The reaction of OH radicals with the alkanes has been extensively studied and Atkinson [15] has comprehensively reviewed the current kinetic data base for these compounds . For those reactions for which sufficient experimental data was available , the temperature dependence of these rate constants was also included in the Atkinson review [15] .

Kinetic studies of the alkanes with OH radicals has greatly increased the understanding of the mechanisms of these reactions . Evaluated sets of rate constants , often verified in several laboratories , are available [10 - 15] , and have been used to establish relationships between structure and reactivity [73] . For example , experiments have shown that a secondary C - H bond reacts approximately 40% faster if it is bonded to two other - CH_2 - groups rather than a - CH_2 - and one - CH_3 [2] .

The reaction of alkanes in the troposphere proceeds predominantly with OH radicals . This reaction involves a hydrogen abstraction mechanism with room temperature rate constants increasing with decreasing C - H bond dissociation energy [74] . These reactions are all

exothermic which is consistent with the low Arrhenius activation energies observed .Reaction exothermicities of 62.7 kJ mol^{-1} for methane , 87.9 kJ mol^{-1} for secondary C - H bonds and 113.0 kJ mol^{-1} for tertiary C - H bonds have been measured [75] .

OH radicals react with alkanes , abstracting a hydrogen atom and producing an alkyl radical and water vapour :

$$RH + \dot{O}H \quad \text{--------}> \quad R\cdot + H_2O \qquad (2.1.3.1)$$

This alkyl radical then reacts rapidly with O_2 to form alkyl - peroxy radicals,

$$R\cdot + O_2 \quad \text{--------}> \quad RO_2\cdot \qquad (2.1.3.2)$$

Atmospheric data indicates that the subsequent fate of these alkyl peroxy radicals in the troposphere is reaction with either HO_2 or NO :

$$RO_2\cdot + \dot{H}O_2 \text{ --------}> \quad ROOH + O_2 \qquad (2.1.3.3)$$

$$RO_2\cdot + NO \quad \text{--------}> \quad RO\cdot + NO_2 \qquad (2.1.3.4)$$

Nitric oxide reactions with alkyl peroxy radicals have been recognised for many years [76] as playing an important role in the photooxidation of organic molecules under atmospheric conditions. The alkoxy radical produced in the above mechanism (2.1.3.4) can then react with O_2 and for >/= C_3 , the alkoxy radical can unimolecularly decompose or unimolecularly isomerize via a hydrogen atom shift mechanism .

In general the degradation of an alkane in the troposphere (and other unsaturated organics) initiated by OH radicals abstracting a H - atom , is similar to the mechanism outlined in Figure 2.1.2 .

Rate constants for the gas phase reactions of OH radicals with a

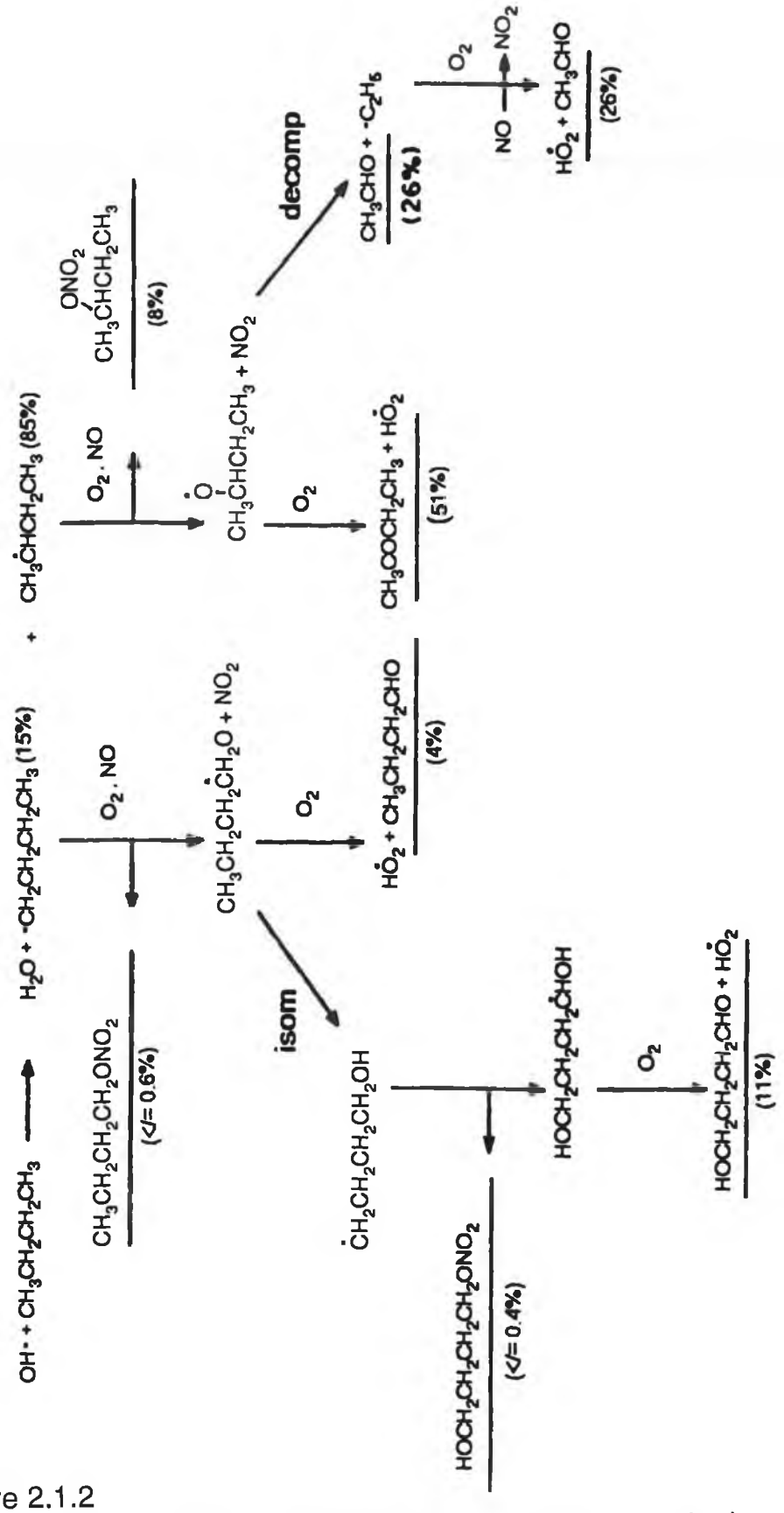

Figure 2.1.2
Major reaction pathways occuring during the tropospheric degradation of n-butane . Reaction is initiated by the abstraction of H-atoms by OH radicals .

number of cycloalkanes have also been reviewed by Atkinson [15] . These ractions are similar to the aliphatic alkanes , with reaction proceeding via a H - atom abstraction mechanism . Table 2.1.2 compares the room temperature rate constants for a series of alkanes to the corresponding cycloalkanes . Table 2.1.2 illustrates that there is a decrease in reactivity between propane and butane and the corresponding cyclic alkanes .

Number of carbons	k_{alkane} x 10^{-12} (cm^3 $molecule^{-1}s^{-1}$)	$k_{cycloalkane}$ x 10^{-12} ($cm^3molecule^{-1}s^{-1}$)
C_3	1.15	0.08
C_4	2.54	1.2
C_5	3.94	5.16
C_6	5.61	7.49
C_7	7.15	13.1

Table 2.1.2
Room temperature rate constants for the reaction of a series of alkanes and cycloalkanes with OH radicals [15] .

The presence of ring strain leads to a reduction in the room temperature rate constant over those expected on the basis of data for the strain free alkanes [3 , 77]. The effects of ring strain are unnoticeable for the >/= C_5 cycloalkanes , with a reversal of reactivity observed , i.e., the cycloalkanes react quicker . The absence of ring strain effects above C_4 results in the abstraction of H - atoms from the cycloalkanes in a similar manner to the alkanes . Because the cycloalkanes above C_4 contain more secondary hydrogens (the reactivity of hydrogens follow the order 2^o H's > 1^o H) than the corresponding alkanes , they react faster , hence the reversal in reactivity observed above C_4 .

The reaction of OH radicals with haloalkanes has been extensively studied as the ozone depleting chlorofluorocarbons (CFCs) are included

in this class . The available rate constant data for the gas phase reaction of OH radicals with haloalkanes are in general agreement apart from a few exceptions in earlier studies [78] . The majority of the rate constants reported for the haloalkanes have been determined using absolute techniques (FP - RA , DF - RF , etc.) due to the slow reaction of these species with the hydroxyl radical .

Atkinson's review [15] illustrates that Cl and Br substitution for H - atoms in methane leads to an increase in the room temperature rate constant , while F atom substitution initially enhances the room temperature rate constant (in CH_3F) , but in more highly substituted halomethanes (CHF_3 or CHF_2Cl) F atom substitution decreases the observed rate .

The addition of a halogen to the alkane structure has the effect of decreasing the bond dissociation energies of the C - H bonds , thus accounting for the observed increase in reaction rate of $CBrH_3$, CFH_3 and $CClH_3$ relative to CH_4 [15] . Additional substitution especially in higher alkanes leads to more complex reaction processes . It is possible that steric effects and induced polarity effects may significantly influence the reaction of OH radicals with these higher polyhalogenated compounds [28, 79] .

One important point must be highlighted with regard to the reaction of OH radicals with haloalkanes . As the level of substitution increases so too does the reaction time . Hence compounds containing large numbers of halogens , and thus few abstractable hydrogens , will persist in the troposphere for years . This observation is fundamental in explaining the long tropospheric lifetimes of CFCs . CFCs have few if any abstractable H - atoms and hence persist in the troposphere . This chemical inertness coupled with the insolubility of CFCs in water facilitates their transport to the stratosphere where they can subsequently result in ozone depletion

as outlined in Chapter 1 of this thesis .

Haloalkanes react with OH radicals in a similar manner to the alkanes [75] . The radicals produced in the initial H- atom abstraction reaction can then react rapidly with O_2 to form peroxy radicals :

$$CH_3Cl + \dot{O}H \text{ -------> } \cdot CH_2Cl + H_2O \quad (2.1.3.5)$$

$$\cdot CH_2Cl + O_2 \text{ -------> } \cdot O_2CH_2Cl \quad (2.1.3.6)$$

These haloalkylperoxy radicals can then react with NO or NO_2 :

$$\cdot O_2CH_2Cl + NO \text{ -------> } \cdot OCH_2Cl + NO_2 \quad (2.1.3.7)$$

$$\cdot O_2CH_2Cl + NO_2 \text{ -------> } CH_2ClOONO_2 \quad (2.1.3.8)$$

The haloalkoxy radical formed in mechanism (2.1.3.7) can then react with O_2 in an analogous reaction to the alkoxy radical yielding a stable carbonyl compound :

$$\cdot OCH_2Cl + O_2 \text{ -------> } HCOCl + \dot{H}O_2 \quad (2.1.3.9)$$

For haloalkoxy radicals which do not contain a H - atom,elimination of a halogen atom with formation of a carbonyl derivative appears to occur :

$$\cdot CF_3O \text{ -------> } CF_2O + \cdot F \quad (2.1.3.10)$$

Thus CF_2O is the expected oxidation product from the CF_3O radical . This reaction is not expected to be an elementary reaction .

It is clear that the reaction of alkanes , cycloalkanes and haloalkanes with OH radicals occurs via a hydrogen atom abstraction mechanism . Numerous factors affect the rate of this reaction including ,

the extent of halogen substitution , ring strain and the number and type of hydrogens present in the compound .

2.1.3.2 *Cl atom reactions with the alkanes*

Reaction of chlorine atoms with organic compounds proceeds via a hydrogen abstraction mechanism in a similar manner to OH radical reactions :

$$\cdot Cl + C_2H_6 \text{ -------> } \cdot C_2H_5 + HCl \quad (2.1.3.11)$$

$$\cdot C_2H_5 + O_2 + M \text{ -------> } C_2H_5O_2\cdot + M \quad (2.1.3.12)$$

$$C_2H_5O_2\cdot + C_2H_5O_2\cdot \text{ -------> } 2C_2H_5O_2 + O_2 \quad (2.1.3.13)$$

$$C_2H_5O_2\cdot + C_2H_5O_2\cdot \text{ -------> } CH_3CHO + C_2H_5OH + O_2 \quad (2.1.3.14)$$

$$C_2H_5O_2\cdot + C_2H_5O_2\cdot \text{ -------> } C_2H_5O_2C_2H_5 + O_2 \quad (2.1.3.15)$$

Both OH radicals and Cl atoms are electrophilic which explains their similar reaction processes . Wallington et al [60] has demonstrated a linear correlation between the reactivities of Cl atoms and OH radicals towards the alkanes . Such a correlation may be used to estimate the reactivities of alkanes towards Cl atoms from the corresponding reactivities towards OH radicals .

The reaction of Cl atoms with the alkanes although proceeding by a similar mechanism , occurs much faster reflecting the more electronegative character of Cl atoms compared to OH radicals . Payne et al [80] illustrated that the increased reactivity of Cl atoms compared to OH radicals with acetaldehyde , is largely due to the order of magnitude greater preexponential A factor for Cl atom reactions , the activation energy for both Cl and OH reactions being zero or near zero . This relatively high reactivity of the Cl atom has given rise to increased speculation about the importance of Cl atom reactions as a loss mechanism for VOCs in the troposphere [20] .

The reaction of Cl atoms with halogenated alkanes has been

extensively studied [56,80 - 86] . In the case of the chloroalkanes , all are less reactive than the corresponding parent alkane [83] . The deactivating effect of the chlorine substituent is probably attributable to steric considerations and is most pronounced for the smaller chloroalkanes and for chloroalkanes bearing the chlorine at a secondary site . The increase in reactivity along the series , 1 - chloropropane , 1 - chlorobutane , 1 - chloropentane essentially parallels the corresponding increase in reactivity from propane to n - pentane . This indicates that the deactivating effect of the chlorine substituent on the reactivity of the chloroalkanes is restricted to groups α to the carbon carrying the substituent . Attempts to explain the reactivity trends for chlorine attack on chlorinated and fluorinated hydrocarbons has been made in the literature [82,81,56] . The influences of inductive effects , electronegativity arguments , resonance interactions , steric effects , Van der Waals repulsion , attractive interactions due to dispersion forces , dynamic effects as well as electronic effects have been discussed . It is possible that different factors control reaction of Cl atoms with different compounds , i.e., factors affecting reaction may depend on the type of compound and the type , number and position of substituent halogens .

2.1.4 OH radical and Cl atom reactions with ethers

2.1.4.1 *OH radical reactions with ethers*

Saturated ethers react with OH radicals in a manner similar to the alkanes i.e. H-atom abstraction from C -H bonds [3] :

$$\dot{O}H + H_3COCH_3 \text{ -----> } H_2O + H_2\dot{C}OCH_3 \qquad (2.1.4.1)$$

Previous studies have shown that the C -H bonds for CH_x (x = 1-3) groups adjacent to the oxygen atom have significantly lower bond dissociation energies than do the corresponding C - H bonds in the alkanes [87,88] . The enhanced reactivity of the ethers is explained by the activating effect of the oxygen atom . Atkinson et al [3] thought that the C - H bond dissociation energies would increase as the CH_x groups moved from the oxygen atom . More recently however , Wallington et al [89] have shown increased reactivity along the series of ethers , CH_3OCH_3 , $C_2H_5OC_2H_5$, $C_3H_7OC_3H_7$, $C_4H_9OC_4H_9$ and $C_5H_{11}OC_5H_{11}$. Such linearity suggests that the - CH_2 - groups in these molecules display essentially similar reactivities which are approximately a factor of three greater than those observed in the alkanes [3] and are not dependent on the position of these - CH_2 -groups relative to the oxygen atom . Thus it appears that the oxygen atom has an activating effect which is operative over long distances in these aliphatic systems . In a more recent study Wallington et al [69] have illustrated the importance of longer range effects in both alcohols and ethers extending to positions 4 carbons from the oxygen atom .

Following H - atom abstraction , the subsequent reactions are expected to be totally analogous to those of the alkanes [3] :

$$\dot{O}H + CH_3OCH_3 \text{ -------> } H_2O + \cdot CH_2OCH_3 \qquad (2.1.4.2)$$

$$\cdot CH_2OCH_3 + O_2 \text{ -------> } \cdot O_2CH_2OCH_3 \qquad (2.1.4.3)$$

$$NO \text{ ----------> } NO_2$$

$$\cdot OCH_2OCH_3$$

Up to the publication of this thesis no information had been reported on the reaction of OH radicals with haloethers . However comparing the haloethers to the haloalkanes is useful in predicting the effect of halogen

substitution on the reaction rate of the ethers with the OH radicals . It is expected that initial halogenation will increase the rate of reaction due to the activating effect of the halogen . However highly halogenated ethers are expected to react only slowly with OH radicals and thus they may persist in the troposphere , eventually being transported to the stratosphere ultimately releasing Cl atoms which may then react with the destruction of stratospheric ozone . The current lack of information regarding the reaction of OH radicals with halogenated ethers illustrates the importance of the work reported here in increasing the kinetic data base with regard to such compounds .

2.1.4.2 *Reaction of Cl atoms with ethers*

The reactions of Cl atoms with aliphatic ethers have been studied by a number of workers [60,90] . A similar H-atom abstraction mechanism to that observed for the reaction of OH radicals with the ethers is expected :

$$Cl + CH_3OCH_3 \text{ -----> } HCl + \cdot CH_2OCH_3 \qquad (2.1.4.4)$$

Although correlation exists between the reactivities of OH radicals and Cl atoms with alkanes , no such correlation exists in the ethers [60] . One possible explanation is that reaction of either OH radicals or Cl atoms with these oxygenated species does not proceed via a simple direct concerted hydrogen abstraction mechanism [60] . As discussed in Section 2.1.4.1 , abstraction of H - atoms bound to an α carbon atom is enhanced relative to the corresponding alkane for both OH and Cl reactions . This activating effect (due to the oxygen) has been shown to operate up to five carbons away in the reaction of OH radicals with the ethers [69] .

However , for the reaction of Cl atoms with ethers , the increase in reactivity due to addition of further CH_2 groups to the alkyl chain are those expected on the basis of CH_2 group rate constants derived from reactions of Cl atoms with unsubstituted alkanes . Hence unlike OH radical reactions , Cl atom reactivity does not appear to be activated by the -O- group other than at the carbon atom directly bound to the ether functional group . It is possible that Cl atom reactions are sufficiently facile that any long range effects may be small and not easily identified [90] .

To date no information has been published regarding the reaction of Cl atoms with halogenated ethers , hence the importance of the kinetic data base established by the work carried out in our laboratory and summarised in this report .

2.1.5 Reaction of OH radicals and Cl atoms with ketones

2.1.5.1 *Reaction of OH radicals with ketones*

Aliphatic ketones are formed as intermediate stable chemical products during the atmospheric degradation reactions of a wide variety of organic compounds [91] :

$$C_3H_8 + \cdot OH \text{ -------> } CH_3\dot{C}HCH_3 \text{ -------> } CH_3CH(\dot{O}_2)CH_3$$
$$\text{-------> } CH_3CH(\dot{O})CH_3 \text{ -------> } CH_3COCH_3 \qquad (2.1.5.1)$$

In the atmosphere these carbonyls can photolyse and react with OH , NO_3, and HO_2 radicals . One of the dominant loss mechanisms for ketones in the troposphere is reaction with OH radicals , the kinetics and mechanisms of which have been reviewed by Atkinson [15] .

The accepted mechanism for the reaction of OH radicals with ketones is by H - atom abstraction [92] :

$CH_3C(O)R' + \cdot OH \text{ -------> } H_2O + \cdot CH_2C(O)R'$ (2.1.5.2)

For aliphatic ketones , it has been shown that the reactivity of the C - H bonds α to the carbonyl group is lower than in the alkanes [93,94] while it is higher in the β and γ positions . This enhancement in reactivity at the β and γ positions is explained by the formation of a six membered ring adduct prior to H - atom abstraction [93] :

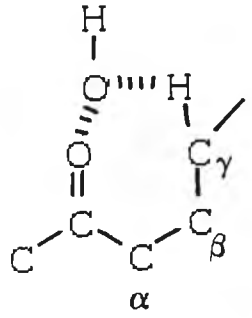

In addition it has been demonstrated that the reactivities of the aliphatic chains on either side of the carbonyl group are independent and additive [93] . This work has been extended to the kinetic study of the gas phase reactions of OH radicals with a number of cyclic ketones and diones [95] .

Literature kinetic data for the reaction of OH radicals with diones is consistent with that obtained for aliphatic ketones with the presence of an additional carbonyl group in the molecule affecting the kinetics of reaction with OH radicals in the same way as the first (the CH_n groups in β and γ positions to each of the carbonyl groups are activated) . The kinetic study of the reaction of OH radicals with cyclic ketones further supports the above ring adduct mechanism showing no enhancement of reactivity for the β - groups [95] .

As yet we can find no reference to the reaction of OH radicals with halogenated ketones . It is important that such work is carried out in order to determine the atmospheric fate of such compounds. It is possible that such halogenated ketones are produced in the troposphere by the action of OH radicals and Cl atoms on hydrofluorocarbons and hydrochlorofluorocarbons .

2.1.5.2 *The reaction of Cl atoms with ketones*

To date very little information regarding the reaction of Cl atoms with ketones has been published . Activation of the hydrogens to attack by the neighbouring carbonyl oxygen was indicated by Poulet et al [96,97] in the reaction of Cl atoms with H_2CO :

$$k_{Cl}\ CH_4 = 1.26 \times 10^{-13}\ cm^3\ molecule^{-1}s^{-1}$$
$$k_{Cl}\ H_2CO = 6.7 \times 10^{-11}\ cm^3\ molecule^{-1}s^{-1}$$

This activation towards reaction with Cl atoms is similar to that observed in many oxygenated organics . As the cyclic intermediate structure is not probable in the reaction of Cl atoms with the ketones our work is of interest from a mechanistic point of view and also serves to establish a data base with respect to the reaction of Cl atoms with such compounds .

2.1.6 References

[1] R.R. Arnts and J.J. Bufalini , EPA / 600 / 09 , Nov. , (1987) .

[2] B.J. Finlayson - Pitts and J.N. Pitts Jr , "Atmospheric Chemistry" , Wiley & Sons Publishers , (1986) .

[3] R. Atkinson , *Chem. Rev.* , **85** , 69 , (1985) .

[4] W.P.L. Carter , *Atmos. Environ.* , **24A** , 3 , 481 , (1990) .

[5] R. Atkinson , *Atmos. Environ.* , **24A** , 1 , 1 , (1990) .

[6] P.A. Leighton , "Photochemistry of Air pollution" , Academic Press , (1961) .

[7] N.R. Greiner , *J. Chem. Phys.* , **46** , 2795 , (1967) .

[8] N.R. Greiner , *J. Chem. Phys.* , **46** , 3389 , (1967) .

[9] N.R. Greiner , *J. Chem. Phys.* , **53** , 1070 , (1970) .

[10] W.B. DeMore , J.J. Margiton , M.J. Molina , and R.T. Watson , *Int. J. Chem. Kinet.* , **17** , 1135 , (1985) .

[11] D. L Baulch , R.A. Cox , R.F Hampson Jr. , J.A. Kerr , J. Troe , and R.T. Watson , *J. Phys. Chem. Ref. Data* , **9** , 2 , 295 , (1980) .

[12] D.L. Baulch , R.A. Cox , P,J, Crutzen , R.F. Hampson Jr. , J.A. Korr , J. Troe , and R.T. Watson , *J. Phys. Chem. Ref. Data* , **11** , 2 , 327 , (1982) .

[13] D.L. Baulch , R.A. Cox , R.F. Hammpson Jr. , J.A. Kerr , J. Troe , and R.T. Watson , *J. Phys. Chem. Ref. Data* , **13** , 4 , (1984) .

[14] R. Atkinson , D.L. Baulch , R.A. Cox , R.F. Hampson Jr. , J.A. Kerr , *Int. J. Chem. Kinet.* , **21** , 115 , (1989) .

[15] R. Atkinson , *J. Phys. Chem. Ref. Data* , Monograph 1 , (1988) .

[16] S.C. Wofsy and M.B. McElroy , *Can. J. Chem.* , **52** , 1582 (1974) .

[17] H.B. Singh , *Geophys. Res. Lett.* , **4** , 101 , (1977) .

[18] J. Ruldoph and D.H. Ehhalt , *J. Geophys. Res.* , **86**(C12) , 11959 , (1981).

[19] W.L. Chameides and R.J. Cicerone , *J. Geophys. Res.* , **83**(C2) , 947 , (1978) .

[20] H.B. Singh , and J.F. Kasting , *J. Atmos. Chem.* , **7** , 261 , (1988) .

[21] T.J. Wallington , J.M. Andino , I.M. Lorkovic , E.W. Kaiser , and G. Marston , *J. Phys. Chem.* , **94** , 3644 , (1990) .

[22] T.J. Wallington , M.M. Hinman , J.M. Andino , W.O. Siegl , and T.M. Japar , *Int. J. Chem. Kinet.* , **22** , 665 , (1990) .

[23] L.G. Yannis , M. Chrysostomos , and P. Panos , *J. Phys. Chem.* , **96** , 1705 , (1992) .

[24] R. Prinn , D. Cunnold , R. Rasmussen , P. Simmonds , F. Alyea , A. Crawford , P. Fraser , and R. Rosen , *Science* , **238** , 945 , (1987) .

[25] P.J. Crutzen , Atmos. Chem. , Ann Arbor Press , pp 313 - 328 , (1982) .

[26] R. Atkinson , K.R. Darnall , A.C. Lloyd , A.M. Winer , and J. Pitts Jr , *Adv. Photochem.* , **11** , 375 , (1979) .

[27] W. Klopffer , *EPA* Newsletter , **41** , 24 , March , (1991) .

[28] L. Nelson , I. Shanahan , H. Sidebottom , J. Treacy , and O.J. Nielsen , *Int. J. Chem. Kinet.* , **22** , 577 , (1990) .

[29] E. Eriksson ,*Tellus* XII , **11** , 63 , (1990) .

[30] R.A. Duce , *J. Geophy. Res.* , **74** , 18 , 4597 , (1969) .

[31] R.J. Cicerone , *Rev. Geophys. and Space Phys.* , **19** , 1 , 123 , (1981) .

[32] W.C. Keene , A. Pszenny , D.J. Jacob , R.A. Duce , J.N. Galloway , J.J. Shultz - Tokos , H. Sievering , and J.F. Boatmann , *Global Biochem. Cycles* , **4** , 4 , 407 , (1990) .

[33] T. Okita , T. Kanedo , T. Yanaka , and R. Sugai , *Atmos. Environ.* , **8** , 927 , (1974) .

[34] P. Matusca , B. Schwatrz , and K. Bachmann , *Atmos. Environ.* , **18** , 8 , 1667 , (1984).

[35] F. Kaufman , F.P. Del Greco , *9th Int. Sym. Comb.* , Academic Press , 659, (1963) .

[36] J.G. Anderson , F. Kaufman , *Chem. Phys. Lett.* , **16** , 365 , (1972)

[37] G. Dixon - Lewis , W.E. Wilson , A.A. Westenberg , *J. Chem. Phys.* , **44** , 2877 , (1966) .

[38] E.D. Morris Jr , D.H. Stedman , H.J. Niki , *Am. Chem. Soc.* , **93** , 3570 , (1971) .

[39] C.J. Howard , K.M. Evenson , *J. Chem. Phys.* , **61** , 1943 , (1974) .

[40] U. Meier , H.H. Grotheer , *Chem. Phys. Lett.* , **97** , 104 , (1984) .

[41] F. Stuhl , H. Niki , *J. Chem. Phys.* , **57** , 3671 , (1972) .

[42] A.R. Ravishankora , N.M. Kreuther , R.C. Shoh , P.H. Wire , *Geophys . Res. Lett.* , **7** , 861 , (1980) .

[43] V.H. Schmidt , K.H. Becker , *Phys. Chem. Behav , Atmos. Pollutants* , **177**, (1984) .

[44] V. Shimidt , 3rd Europ. Sym. , "Physico-chemical behaviour of Atmos. Pollutants" **177** , (1984) .

[45] A. Wahner , C. Zetzrch , *Ber. Bunsen. Chem.* , **89** , 323 , (1985) .
[46] W.A. Mulac , A. Liu , *J. Phys. Chem.* , **93** , 4092 (1984) .
[47] W.A. Mulac , A. Liu , C.D. Jonah , *Int. J. Chem. Kinet.* , **19** , 25 (1987) .
[48] H.M. Akimoto , *Environ. Sci. Technol.* , **13** , 471 , (1979) .
[49] R. Atkinson , W.P.L. Carter , A.M. Winer , and J.N. Pitts Jr. , *J. Air Pollut. Cont. Assoc.* , **31** , 10 , 1090 , (1981) .
[50] R. Simonaitis and M.T. Leu , *Int. J. Chem. Kinet.* , **17**, 293 , (1985) .
[51] W.A.Payne , J. Brunning , M.B. Mitchell and L.J. Stief , *Int. J. Chem. Kinet.* , **20** , 63 , (1988) .
[52] T. Khantoon , H. Edelbulttel-Einhaus , K. Hoyermann , and H.Gg. Wagner , *Ber. Bunsenges , Phys. Chem.* , **93** , 626 , (1989) .
[53] G. Poulet , G. Laverdet , and G. Le Bras , *J. Phys. Chem.* , **85** , 1892 , (1982) .
[54] M. Bartels , K. Hoyermann and U. Lange , *Ber Bunsen Phys. Chem.* , **93** , 423 , (1989) .
[55] R.S. Lewis , S.P. Sander , S. Wagner , and R.T. Watson , *J. Phys. Chem.* , **84** , 2009 , (1980) .
[56] P.H. Wine , and D.H. Semmes, *J. Phys. Chem.* , **87** , 3572, (1983) .
[57] P.H. Wine , D.H. Semmes , and A.R. Ravishankara , *Chem. Phys. Lett.* , **90** , 2, 128 , (1982) .
[58] O. Dobies and S.W. Benson , *J. Am. Chem. Soc.* , **112** , 1023 , (1990) .
[59] Y.G. Lazarou , C. Michael , P. Papagiannakopoulos , *J. Phys. Chem.* , **96** , 1705 , (1992) .
[60] T.J. Wallington , L.M. Skewes , W.O. Siegl , C.H. Wu , and S.M. Japar , *Int. J. Chem. Kinet.* , **20** , 867 , (1988) .
[61] R. Atkinson and S.M. Aschmann , *Int. J. Chem. Kinet.* , **19** , 1097 , (1987).
[62] T.J. Wallington , L.M. Skewes , and W.O. Siegl , *J. Photochem. Photobiol.* , A , **45** , 167 , (1988) .
[63] K.R. Darnall , R. Atkinson , *J. Phys. Chem.* , **82** , 1581 , (1978) .
[64] J. Heicklen , *Int. J. Chem. Kinet.* , **13** , 651 , (1981) .
[65] N. Cohen , *Int. J. Chem. Kinet.* , **14** , 1339 , (1982) .
[66] R.R. Baldwin , R.W. Walker , *J. Chem. Soc. Fara. Trans. 1* , **75** , 140 , (1979) .

[67] R. Atkinson and W.P.L. Carter , *Chem. Rev.* , **84** , 437 , (1984) .
[68] R. Atkinson , *Int. J. Chem. Kinet.* , **19** , 799 , (1987) .
[69] T.J. Wallington , P. Dagaut , R. Liu , and M.J. Kurylo , *Int. J. Chem. Kinet.* , **20** , 541 , (1988) .
[70] K.M. Jeong , F. Kaufmann , *J. Phys. Chem.* , **86** , 18116 , (1982) .
[71] K.M. Jeong , F. Kaufmann , *J. Phys. Chem.* , **88** , 1222, (1984) .
[72] P. Degaut , M.J. Kurylo , T.J. Wallington , *J. Phys. Chem.* , **92** , 5024 , (1988) .
[73] G.S. Jolly , G. Paraskavopoulos , D.L. Singleton , *Int. J. Chem. Kinet.* , **17** , 1 , (1985).
[74] R. Atkinson , *Int. J. Chem. Kinet.* , **12** , 761 , (1980) .
[75] S.W. Benson , "Thermochemical Kinetics" , 2nd ed. , Wiley , (1976).
[76] R. Atkinson , A.C. Lloyd , *J. Phys. Chem. Ref. Data.* , **13** , 315 , (1984) .
[77] R. Atkinson and S.M. Aschmann , *Int. J. Chem. Kinet.* , **20** , 339 , (1988) .
[78] R. Atkinson and R.A. Cosc , *Int. J. Chem. Kinet.* , **21** , 115 , (1989)
[79] P. McLoughlin , I. Shanahan , and R. Kane , *Int. J. Chem. Kinet.* , In press (1992) .
[80] W.A. Payne , D.F. Nava , F.L. Nesbitt , and L.J. Stief , *J. Phys. Chem.* , **94** , 7190 , (1990) .
[81] E. Tschuikow-Roux , J. Niedzielski , and F. Faraji , *Con. J. Chem.* , 63 , 1093 , (1985).
[82] E. Tschuikow-Roux , T. Yano , and J. Niedzielski , *J. Chem. Phys.* , **82**(1) , 65 , (1985) .
[83] T.J. Wallington , L.M. Skeves and W.O. Siegl , *J. Phys. Chem.* , **93** , 3649 , (1989) .
[84] E. Tschuikow-Roux , F. Faraji , S. Paddison , J. Niedzielski , K. Miyokawa , *J. Phys. Chem.* , **92** , 1488 , (1988) .
[85] E. Tschuikow-Roux , T. Yano , and J. Niedzielski , *J. Phys. Chem.* , **88** , 1408 , (1984) .
[86] T. Migita , M. Kougi , and Y. Nagai , Bulletin , *Chem. Soc. Japan .* **40** , 920 , (1967) .
[87] D.F. McMillan and D.M. Golden , *Ann. Rev. Phys. Chem.* , **33** , 493 , (1982) .

[88] O. Kendo and S.W. Benson , *Int. J. Chem. Kinet.* , **16** , 949 , (1984).
[89] T.J. Wallington , R. Liu , P. Degaut , and M.J. Kurylo , *Int. J. Chem. Kinet.* , **20** , 41 , (1988) .
[90] L. Nelson , D. Rattigan , R. Neavyn , H. Sidebottom , J. Treacy and O. Nielson , *Int. J. Chem. Kinet.* , **22** , 1111 , (1990) .
[91] H.B. Singh , P.L. Hanst , *Geophys. Res. Lett.* , **8** , 8 ,941 , (1981) .
[92] P. Dagaut , *J. de Chemie Phys.* , **86** , 3 , 595 , (1989) .
[93] T.J. Wallington and M.J. Kurylo , *J. Phys. Chem.* , **91** , 5050 , (1987) .
[94] R. Atkinson , S.M. Aschmann , W.P.L. Carter , and J.N. Pitts Jr. , *Int. J. Chem. Kinet.* , **14** , 839 , (1982) .
[95] P. Dagaut , T.J. Wallington , R. Liu , and M.J. Kurylo , *J. Phys. Chem.* , **92** , 4375 , (1988) .
[96] G. Poulet , G. Laverdel , and G. Le.Bras , *J. Phys. Chem.* , **85** , 1892 , (1981) .
[97] G. Poulet , G. LeBras , and J. Combourieu , Poster , WMO , Vol/Ed. **511** , 289 , (1978) .

2.2 General experimental to OH and Cl work

In this work , the first measurements of OH radical and chlorine atom rate constants for a series of ethers and ketones are reported . Furthermore, since this is the first report of rate data obtained using the present vacuum line - smog chamber system, a series of measurements were also performed on compounds for which generally reliable data already exists in order to validate the experimental procedures .

Hydroxyl radical and chlorine atom rate constants were measured using a relative rate technique which has been described in detail in the literature [1-3] and is summarised in Section 2.1 of this report . Briefly, OH radicals were generated by the photolysis of methyl nitrite in the presence of air and excess NO :

$CH_3ONO + h\nu$ (λ >/= 280 nm) -----> $CH_3O\cdot + NO$ (2.2.1)

$CH_3O\cdot + O_2$ -----> $HCHO + HO_2\cdot$ (2.2.2)

$HO_2\cdot + NO$ -----> $NO_2 + \cdot OH$ (2.2.3)

The system also contained the compound being tested as well as a reference compound for which the OH radical rate constant was accurately known . The only significant removal process for the test and reference compounds , assuming minimal loss to the smog chamber walls etc., (see Section 2.1) is reaction with OH radicals . These reactions may be represented by :

$OH\cdot + test \xrightarrow{k_1}$ products (2.2.4)

$OH\cdot + reference \xrightarrow{k_2}$ products (2.2.5)

As previously described in Section 2.1 , rate equations for the reaction mechanisms (2.2.4) and (2.4.5) can be combined and integrated to yield an expression of the form:

$$\ln([Test]_0 / [Test]_t) = (k_1/k_2)\ln([Ref.]_0 / [Ref.]_t) \qquad (2.2.6)$$

where $[Test]_0$ and $[Ref.]_0$ are the initial concentrations of the test and reference compounds respectively and $[Test]_t$ and $[Ref.]_t$ are the concentrations at some time t . According to expresssion 2.2.6, a plot of $\ln([Test]_0 / [Test]_t)$ versus $\ln([Ref.]_0 / [Ref.]_t)$ should be linear with a slope equal to (k_1/ k_2) and an intercept equal to zero . Given an accurate value for the rate constant of the reference compound (k_2) , the rate constant for the test compound (k_1) can be calculated immediately .

A similar procedure was used to determine chlorine atom reaction rates for the same compounds . Chlorine gas was photolysed to yield a supply of chlorine atoms for reaction :

$$Cl_2 + h\nu \ (\lambda >/= 320 \text{ nm}) \text{-----> } 2Cl\cdot \qquad (2.2.7)$$

The chlorine atoms produced then reacted with the test and reference compounds produced in a similar manner to the reaction of OH radicals outlined in mechanisms 2.2.4 and 2.2.5 . By use of expression 2.2.6 it was then possible to calculate the chlorine atom rate constant for the test compound (k_1) .

Having calculated the rate constants for the reaction of the test compounds with both OH radicals and chlorine atoms . it was then possible to calculate the tropospheric lifetimes (τ) of these compounds with respect to these species using the expression :

$$\tau_{OH(seconds)} = {}^{1}/_{k_{OH}[OH]} \quad \text{and} \quad \tau_{Cl} = {}^{1}/_{k_{Cl}[Cl]} \qquad (2.2.8)$$

k_{OH} and k_{Cl} are the rate constants for the reaction of OH radical and Cl atoms with the test species . [OH] and [Cl] are the tropospheric concentrations of OH radicals and chlorine atoms respectively .

2.2.1 Materials

Methyl Nitrite was prepared by the dropwise addition of 50% sulphuric acid (Analar grade) to a saturated solution of sodium nitrite (stated purity 96% , BDH Chemical Co.) in methanol (Analar grade) . The CH_3ONO that evolved was swept out of the reaction bulb by a stream of nitrogen (Air Products Ltd.), passed through NaOH to remove H_2SO_4 , dried by passing through calcium carbonate , and collected on the vacuum line in a trap using an acetone slush bath (temperature = 173 K) . The methyl nitrite was degassed by a freeze-pump-thaw procedure and purified by trap to trap distillation using an acetone slush bath . The purity of the prepared methyl nitrite was checked by IR spectroscopy and then stored in the dark on the vacuum line to prevent decomposition .

The dilution gas used in these experiments was zero grade air (B.O.C.) and the nitrogen used to clean the bag was supplied by Air Products Ltd. Prior to use all traces of moisture in the nitrogen were removed by passing the gas through a drying column (Phase - Sep) filled with molecular sieve and self-indicating silica gel . Before use in the smog chamber , the zero grade air was passed through a drying column (Phase - Sep) and a charcoal column (Phase - Sep) to remove traces of organics. Chlorine was obtained from Argo International Ltd., and had a stated purity of 99.5% . It was degassed several times and

stored in a blackened bulb on the vacuum line . The nitric oxide used in the system was supplied by BDH gas services and had a stated purity of 99% . This NO was degassed by the freeze-pump-thaw procedure and stored on the vacuum line . All test and reference compounds used , along with their suppliers and purities are listed in Sections 2.3 and 2.4 of this thesis . All of these compounds were used without futher purification and prior to use were degassed thoroughly by the freeze-pump-thaw procedure .

2.2.2 Apparatus

The vacuum apparatus employed in this work to accurately measure gas pressures is shown in Figure 2.2.1 . The apparatus consisted of a conventional mercury-free, high-vacuum line, made of "Pyrex" glass . Table 2.2.1 describes the various regions within the vacuum line . The volumes within these regions were important in accurately measuring concentrations of gases for analysis . The procedure used to determine these volumes and the volumes calculated are summarised in Section 2.2.3 .

A vacuum within the system was maintained by means of an Edward's high vacuum double stage rotary pump (Model E2M2) . Reactant pressures were measured on a pressure transducer (MKS Baratron, 122AA) . Pressure measurements within the vacuum line were made using an Edward's Pirani gauge (Model PEE 10K) for pressures down to 10^{-2} mBar and an Edward's Penning gauge (Model CP25-K) to measure pressures in the range 10^{-2} - 10^{-4} mBar . Greaseless taps using "Teflon" o-rings were used in all of the valve positions on the vacuum line and these were supplied by J. Young Ltd. .

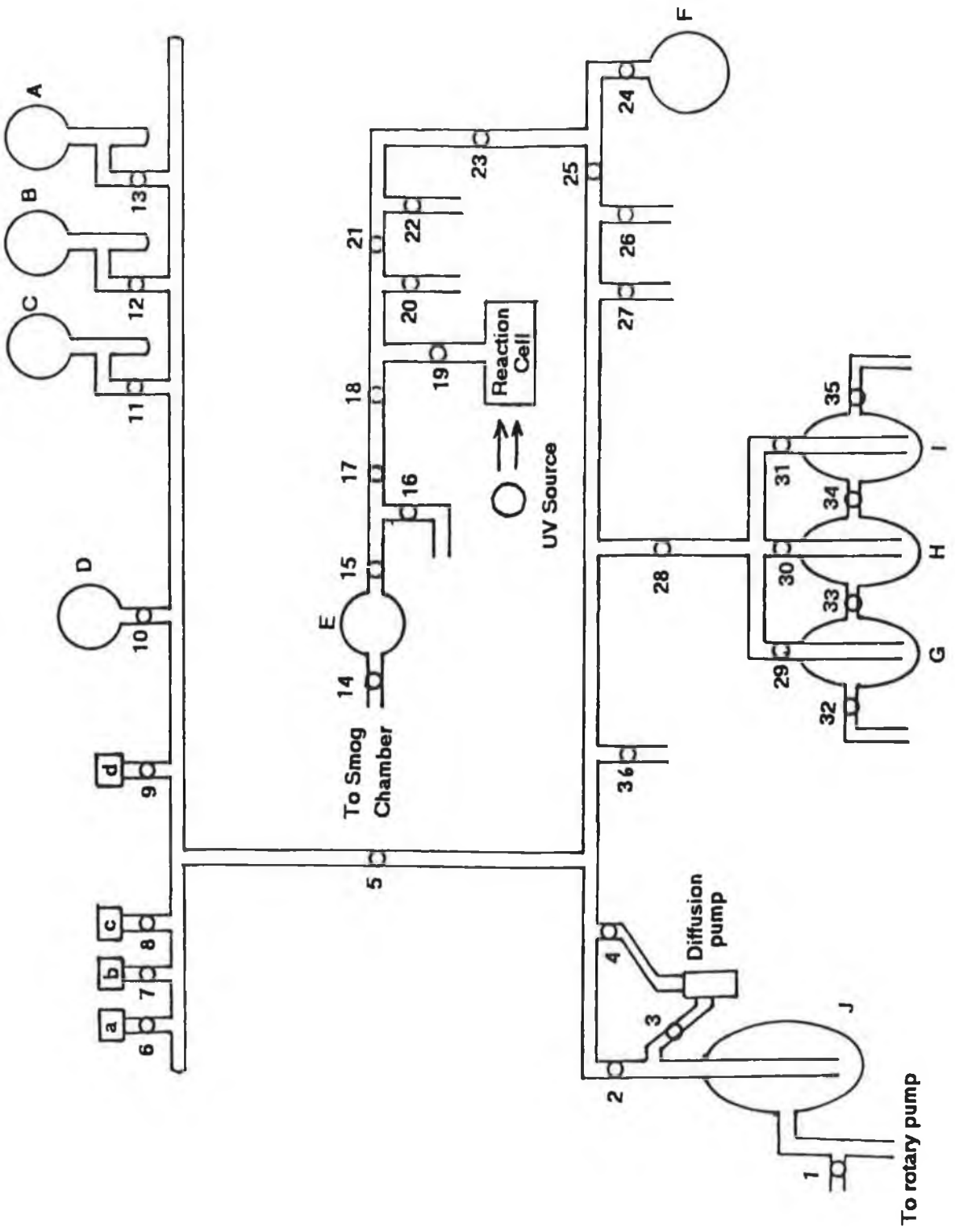

Figure 2.2.1

Mercury free high vacuum line used throughout this thesis .

VACUUM LINE SECTION	DESCRIPTION OF SECTION
Line 1	Tap 5 to taps 6,7,9,10,11,12 and 13 (includes volume to transducer c)
Line 2	Tap 5 to taps 2,4,36,28,26 and 25
Line 3	Tap 25 to taps 24 and 23
Line 4	Tap 23 to taps 22 and 21
Line 5	Tap 21 to taps 20,19 and 18
Line 6	Tap 18 to 17
Line 7	Tap 17 to taps 16 and 15
A,B,C and D	Storage bulbs
E and F	Mixing bulbs
a	Penning gauge
b	Pirani gauge
c	Pressure transducer (0 - 999.9Torr)
d	Pressure transducer (0 - 9.900Torr)

Table 2.2.1
The various regions and positions of transducers and gauges within the vacuum line.

Methyl nitrite was stored on the vacuum line in bulb C , Cl_2 in bulb B and NO in trap G . Samples of test and reference organics were stored in "Pyrex" glass fingers attached to the vacuum line at taps 36, 27 and 26.

Figure 2.2.2 is a schematic diagram illustrating how an 86 litre , conditioned "Teflon" bag was connected to the vacuum line and to the GC using "Teflon" tubing (1.5 mm i.d.) . The diagram demonstrates how samples were withdrawn from the bag for direct injection onto the column using a sampling pump (Perkin Elmer, Model 5-104) in conjunction with an automatic gas sampling valve (Valco) . The gas sampling valve was controlled by a series of electrical relays , which were in turn controlled by software on the GC . This enabled control of the "sampling time" (typically 2 minutes) from the GC keyboard .

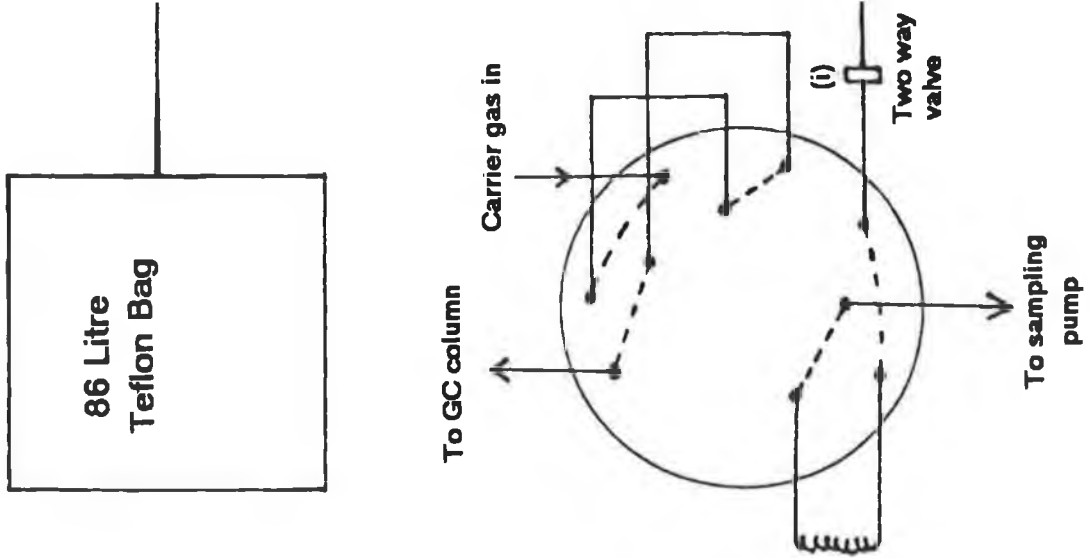

Figure 2.2 2
Schematic diagram illustrating the "Teflon" bag connected to the vacuum line and to the GC . The automatic gas sampling valve is in the fill position .

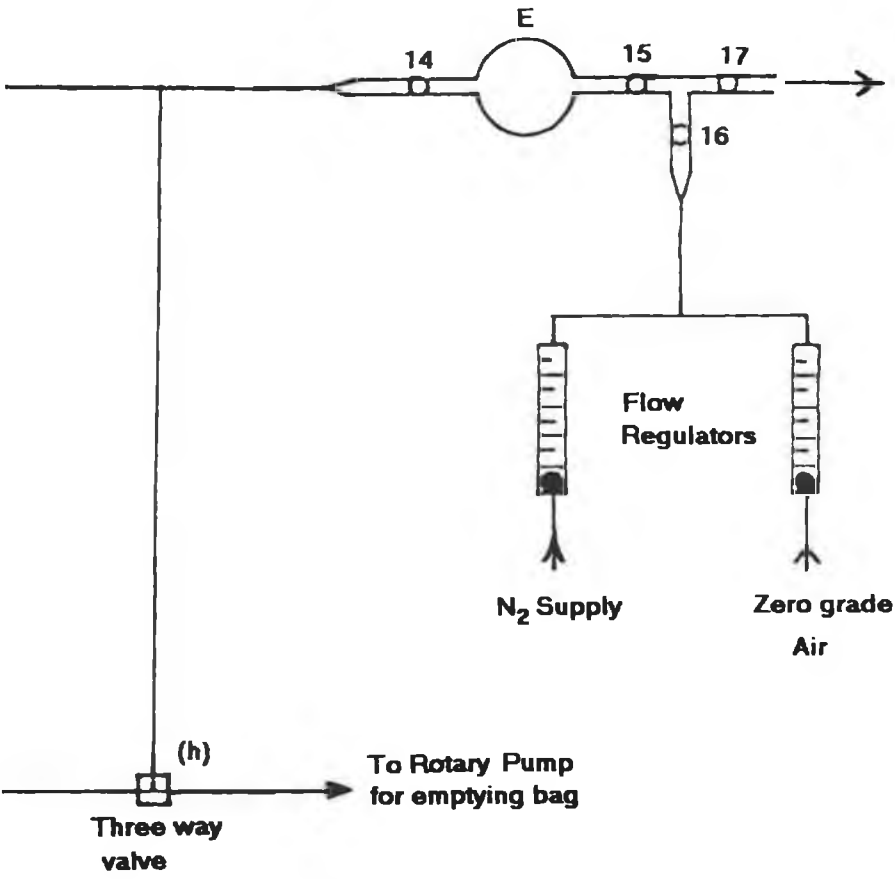
E
14
15
17
16
Flow
Regulators
N_2 Supply
Zero grade
Air
(h)
To Rotary Pump
for emptying bag
Three way
valve

To fill the smog chamber bag, valve (h) and tap (17) were closed and with taps (14), (15) and (16) open , flow regulators were used to flush the required volume of air or nitrogen into the bag . An Edward's Speedivac 2 single stage rotary pump was used to empty the bag . The irradiation chamber consisted of the "Teflon" bag (reaction chamber) and a bank of lights mounted on either side of a metal rectangular frame (124.5 cm x 96.5 cm x 87.5 cm) . Each bank of lights consisted of five black lamps (Philips TLD 18W / 08) and five sun lamps (Philips TL 20W / 09N). The entire irradiation chamber was surrounded by black cloth . A thermometer was mounted inside the chamber to measure the temperature during irradiation and atmospheric pressures were measured prior to reaction on a mercury barometer (Shaw Scientific Supplies Ltd) . As the reaction chamber lights warmed up , an opaque sheet (black plastic) was used to completely cover the "Teflon" reaction chamber . This sheet was also used to interrupt photolysis as required .

2.2.3 Procedure

To determine the correct pressure of reactants to release into the vacuum line and subsequently into the smog chamber , the volumes within the various regions of the vacuum line were first calculated . Bulb A in Figure 2.2.1 was the primary volume from which each volume within the vacuum line was calculated using the Boyle's law expressions :

$$\text{VOLUME} \quad \alpha \quad 1 / \text{Pressure} \qquad (2.2.9)$$

$$P_1 V_1 = P_2 V_2 \qquad (2.2.10)$$

The volume of bulb A was determined prior to it's attachment to the

vacuum line using a weight difference technique . Volumes within the vacuum line calculated using the above procedure are given in Table 2.2.2 below .

SECTION OF VACUUM LINE	VOLUMES (cm^3)
A	1168
B	1173
C	1167
D	556
E	297
F	284
Line 1	470
Line 2	318
Line 3	59.0
Line 4	60.3
Line 5	59.1
Line 6	21.0
Line 7	16.1
Reaction cell	177
IR Cell A	205
IR Cell B	272

Table 2.2.2

Volumes within the vacuum line and reaction cells used in this thesis .

A Perkin Elmer (model 8500) gas chromatograph fitted with a flame ionization detector (FID) was used to monitor reactant concentrations following irradiation . Thus an initial requirement before any rate data could be determined was the optimisation of chromatographic conditions to separate the test and reference and methyl nitrite (in the case of the OH radical reactions) .

Following irradiation of the gas mixtures , the formation of products which might interfere with the gas chromatographic analysis of either the test or reference organic or both had to be considered as a potential complication . As a test for interferences caused by secondary reactions in our system , experiments (decay profiles) were performed in which mixtures of methyl nitrite (or Cl_2 for the chlorine atom reactions) and either the test or reference organic were irradiated and analyses performed to check for the formation of potentially interfering products . In some instances GC conditions were optimised so as to separate test organics from reaction products . For all rate constants determined , reaction product interferences were not a problem over the irradiation times typical of the present work (30 minutes) .

Additionally , to test for any possible photodecomposition of the test and reference organics , mixtures of these reactants in zero grade air in the absence of methyl nitrite (or chlorine) were irradiated with the appropriate lamps . Irradiation times used for these photodecomposition experiments were similar to those for the experimental runs . No photodecomposition of any of the reactants was observed . Having optimised the analytical conditions , work could proceed on determining the relative rate constant ratios for the test compounds .

Initially the apparatus shown in Figure 2.2.1 was evacuated with liquid nitrogen around trap J to a vacuum of approximately 10^{-2} - 10^{-4} mBar . Boyles law ($P_1V_1 = P_2V_2$) was used to calculate the pressure of reactant required in bulb E such that when the contents of this bulb were swept into the bag using zero grade air , the required concentration of this reactant would result in the bag once a final bag volume of 50 litres was reached . The required pressure of reactants was measured into lines 1 - 7 + bulb E using pressure transducer d to monitor the concentration of reactants released . Tap (15) was then closed and the

entire vacuum line to tap 15 was again evacuated . Once a vacuum of less than 10^{-3} mBarr (as measured by an Edward's Penning gauge) was achieved , tap (17) was closed and taps (14), (15) and (16) opened . The reactant was then flushed into the bag at the appropriate flow rate (1.2 dm^3min^{-1} for this work) using zero grade air . Having added each of the reactants to the bag and a final volume of 50 litres within the bag (after 41.67 minutes) was achieved , the zero grade air was switched off and taps (14) , (15) , and (16) closed .

Similar initial concentrations of the test and reference organics were always used throughout this work , typically in the range 5-20 ppm depending on the limit of detection of the GC -FID for the particular reactants . For the hydroxyl radical reactions initial concentrations of CH_3ONO and NO were approximately 50 ppm and 25 ppm respectively . For chlorine atom reactions , the initial concentration of Cl_2 was 50 ppm . The final volume of the bag was 50 litres for all studies .

The reaction chamber was completely covered at all times except during photolysis . Before analysis , the reactants were allowed to mix for a minimum of 30 minutes . The temperature in the chamber fluctuated in the range 300 +/- 3K and atmospheric pressure was approximately 778 ± 20 mmHg throughout the analyses . For the OH radical reactions all 20 lamps were used for photolysis (λ >/= 260 nm) , while for the chlorine atom reactions , five black lamps were used for the photolysis (λ >/= 310 nm) . The lamps were switched on 30 minutes prior to use in order to achieve a stable output during subsequent photolyses . A minimum of two samples were taken before irradiation i.e. at t = 0 minutes . The black covering was then removed from around the "Teflon" bag and the reaction mixture irradiated for fixed periods (in the range 0 - 30 minutes, measured by means of a stop clock) . The covering was replaced at each photolysis time to stop reaction and a

sample taken (as described earlier) for GC analysis . This procedure was repeated several times so that the rate of loss of both the test and reference organics could be monitored . A maximum total irradiation time of approximately 30 minutes was used for both our Cl atom and OH radical work . When the last sample was taken, the bag was emptied by opening valve (h) to a single stage rotary pump and closing tap (14) and valve (i) .

To avoid carry over between experiments , the "Teflon" bag was filled and emptied at least twice with nitrogen . A sample was taken from the second fill and injected onto the GC to ensure the bag was clean. If this suggested that the bag was not completely free from reactants or products , the bag was emptied and the process repeated until a clear sample was obtained .

Peak heights were used to measure changes in concentration of the test and reference organics following irradiation , and the relative rate was determined as described in Section 2.1 of this report . To ensure experimental reproducibility and to Increase the accuracy of our rate data , the complete procedure as outlined above was repeated under identical conditions , a minimum of three times . The rate constant ratios determined from each experiment were then averaged to give the value reported .

2.2.4 Analysis

A Perkin Elmer Gas Chromatograph (Model 8500) fitted with a flame ionization detector (FID) was used to monitor the concentration of reactants before and after irradiation . The fuel gases for the FID used were air (Irish Industrial Gases) and hydrogen H-10 (Murex) and the carrier gas was nitrogen (I.I.G.) . Each of the gases were prefilled

through moisture traps (Phase - Sep) and charcoal filters (Phase - Sep) prior to entering the GC . Compressed air (I.I.G.) was also used to switch the injection ports from loop load to inject . All gas cylinders used needle valve controls . Two meter glass columns (3mm i.d.) were used with typical stationary phases of 10% SE-30 and PEG , on a Chromosorb WHP(80-100) support . The columns were operated isothermally at temperatures varying from 35°C to 150°C . Flow rates of the nitrogen carrier gas were maintained at approximately 35 cm^3min^{-1} . Injector and detector temperatures were set at 80 and 270°C respectively . Specific conditions employed for the analysis of the various test compounds are listed in Sections 2.3 and 2.4 . Chromatograms were recorded on a Perkin-Elmer GP-100 graphic printer . A Perkin-Elmer infrared spectrometer (Model 983G) was used to determine methyl nitrite purity . The methyl nitrite was scanned over the spectral region 4000 to 600 cm^{-1}.

2.2.5 References

[1] R.R. Arnts , and J.J. Bufalini , **EPA** / 600 / 09 , Nov. , (1987) .

[2] B.J. Finlayson - Pitts , and J.N. Pitts Jr. , "Atmospheric Chemistry" , Wiley & Sons Publishers , (1986) .

[3] R. Atkinson , W.P.L. Carter , A.M. Winer , and J.N. Pitts Jr. , *J. Air Pollut. Cont. Assoc.* , **31** , 10 , 1090 , (1981) .

2.3
The Reaction of OH radicals and Cl atoms with a series of Ethers

2.3.1 Introduction

Oxygenated hydrocarbons especially ethers are being released in increasing quantities into the atmosphere because of their use as solvents and fuel additives [1 - 2] . In order to increase the octane number of fuels and thereby prevent or minimize knock in spark - ignition engines , several gasoline additives have been used . These have included mainly organolead compounds such as $(CH_3)_4Pb$ and $(C_2H_5)Pb$ until their recent replacement by oxygenated organics . The switch to such oxygenated compounds has been in response to air quality regulations , which have necessitated the installation of catalytic converters whose longevity is affected by exposure to lead additives . In addition to their primary role in octane rating improvement , the organic oxygenates have the added benefit of reducing CO emissions . Presently two of the most widely used oxygenated organics for such applications are methyl tert - butyl ether (M.T.B.E.) and methyltetrahydrofuran (MTHF) . The use of these highly volatile compounds in amounts up to 20% in gasoline raises the fuel volatility making their evaporative emission to the atmosphere an important consideration [3] . The switch to the use of these oxygenated organics has been reflected in American chemical production figures . M.T.B.E. production in the United States has risen annually by approximately 27% from 1985 - 90 making it the 24th most abundantly produced chemical in the U.S. [4] . Besides fuel additives , ethers are also released into the troposphere as intermediates in hydrocarbon combustion [5] . Cyclic ethers such as furan and thiophene are also released into the troposphere from fuel conversion facilites [6] . Following such release , the main atmospheric fate of ethers is expected to be reaction with OH radicals and Cl atoms since photolysis , reaction with O_3 and reaction with NO_3 radicals are negligibly slow [7] . The reaction

mechanisms for OH radicals and Cl atoms with ethers is discussed in Section 2.1 of this thesis .

The reason for our interest in the ethers , specifically the ethyl methyl ethers , has been to assess the possible importance of the increased usage of halogenated anaesthetic agents such as isoflurane (1-Chloro-2,2,2,-trifluoro ethyl difluoro methyl ether) , $CF_3CHClOCF_2H$ and enflurane (2-Chloro-1,1,2-trifluoro ethyl difluoro methyl ether) , $CHClFCF_2OCF_2H$. These anaesthetics are the most widely used general anaesthetics in the western world and their use has led to some concern about their possible adverse effects on ozone concentrations [8 - 17] . Because of this concern work has been carried out in our laboratory to estimate the emission rates of these compounds into the atmosphere .

Initial concern centred on the fact that the anaesthetics halothane , isoflurane , and enflurane were volatile and substantially halogenated . Because of this , it seemed possible that these compounds might be emitted to the troposphere , and be sufficiently unreactive there to subsequently contribute to stratospheric ozone depletion in a similar manner to all CFC's [18] .

For the past 140 years that halogenated hydrocarbons have been administered for the purpose of anaesthesia , anaesthetists have been aware that during and following anaesthesia such molecules are exhaled by patients . In fact at least 99% of the volume of these anaesthetics used in the operating theatre is released into the atmosphere . Vapours of anaesthetic agents are discharged not only in the operating theatre . Significant levels of contamination have also been found in locations where anaesthetics are not usually administered , i.e. in corridors of operating room suites , anaesthetic workrooms and recovery rooms . The only regulation regarding pollution by anaesthetics in Britain is the Department of Health's recommendation for scavenging systems to

minimize concentrations of anaesthetic agents within the operating departments [17]. However most of these scavenging devices deliver their contents unchanged outside the theatre building .

Although both isoflurane and enflurane are released to the troposphere , their subsequent lifetime is limited by the hydrogen atoms in their structure . As the main sink for these anaesthetics in the troposphere is hydrogen abstraction reactions with hydroxyl radicals and chlorine atoms , it was reasonable to suggest that enflurane and isoflurane would react relatively fast in the troposphere with only a fraction of the emitted concentrations eventually reaching the stratosphere .

Since the first expressions of concern over these anaesthetics in relation to the ozone layer was published , reliable OH radical rate constants and tropospheric lifetimes have been calculated by A.C.Brown et al. [14 - 16] . From Brown's work the atmospheric lifetimes for isoflurane and enflurane (when compared to a uniform OH radical concentration of 7.7×10^5 radicals cm^{-3}) were found to be approximately 2 and 2.4 years respectively . These results indicate that a relatively small concentration of these compounds will indeed reach the stratosphere albeit in very small amounts compared with compounds such as CFC - 11 and CFC - 12 . Thus the overall contribution to ozone depletion by the anaesthetics was thought to be less than 5 parts in 10^4 of that produced by the CFC's . Brown et al [15] have estimated that the anaesthetics isoflurane , enflurane and halothane will contribute at most a fraction of approximately 5×10^{-4} to the overall atmospheric content of chlorine containing species .

To determine the overall effect of isoflurane and enflurane on the ozone layer , accurate production and emission figures must be examined in conjunction with experimental rate determinations . Table 2.3.1 compares the estimated global 1985 emissions of various CFC's [19] with

COMPOUND	*EMISSION/PRODUCTION FIGURES* / 10^{-6} kg/year	*DATA SOURCE*
CFC-11 ($CFCl_3$)	283 (emission)	[19]
CFC-12 (CF_2Cl_2)	412 (emission)	[19]
CH_3Cl_3	474 (emission)	[19]
HALON 1211 (CF_3ClBr)	3 (emission)	[19]
HALON 1301 (CF_3Br)	3 (emission)	[19]
ENFLURANE	5.0 (emission) 5.4 *(production) <0.220 (production)	This work [10] [13]
ISOFLURANE	5.7 (emission) 5.4 *(production) <0.800 (production)	This work [10] [13]
HALOTHANE	2.1 (emission) 1.0 (production) <1.0 (production)	This work [10] [13]

TABLE 2.3.1 :

Emission or production figures for some common CFCs plus some halogenated anaesthetics together with the source of the quoted data .

* = The production figure of 5.4 x 10^6 kg/year for isoflurane and enflurane is a combined figure i.e. isoflurane + enflurane .

production figures and estimated emission figures for the three anaesthetics , isoflurane , enflurane and halothane .

The emission figures for the three anaesthetics calculated in our laboratory is a conservative estimate . Figures are based on a survey of the quantities of anaesthetic agents used in a number of hospitals in the Dublin area from Nov. 1987 to Nov. 1988 . These values were used to conservatively estimate the amount of each anaesthetic used in hospitals throughout the country , and eventually a usage per million population . With a detailed knowledge of the countries in which these anaesthetics

are widely used together with population figures for these countries an estimate of yearly emission rates was calculated .

Rates of emission of these anaesthetic agents are very low relative to the rates of emission of other halogenated species , as can be seen from Table 2.3.1 . However , these species were only introduced into clinical practice in the early 1960's , and since then their production has increased dramatically . Furthermore , the level of emission of methyl chloroform , an industrial degreasing agent and solvent was of the same order of magnitude in the mid-1950's as the current levels for the three anaesthetics . However the increased usage of methyl chloroform eventually led to a situation where it has become a major source of chlorine in the atmosphere , so that it now poses a serious threat to ozone. While it is highly unlikely that the level of emissions of these anaesthetic agents will rise to that of methyl chloroform , it is possible that unchecked emissions of these and other compounds could lead to a situation where their combined emissions has greater significance than is currently anticipated . Consequently , it is important to determine the rates and mechanisms of atmospheric removal processes for these and analogous species and combine this knowledge with accurate emission figures for these compounds in order to assess their potential significance in the depletion of stratospheric ozone .

The work summarised in Chapter 2.0 of this thesis was carried out in order to establish the rate constants for the reaction of OH radicals and Cl atoms with a series of ethers including the two anaesthetics . Reaction of NO_3 with the anaesthetics and other HCFC's in general is thought to account for less than 10% of the removal of HCFC's from the troposphere [16] . The calculated rate constants were then considered in conjunction with the above calculated emission figures so that a more comprehensive environmental impact assessment could be constructed with regard to

these compounds . The rate constants for the reaction of OH radicals and Cl atoms with a number of other ethers (mostly halogenated) was also determined in order to investigate the effect of halogenation on the rate loss of these ethers in the troposphere . This work is of fundamental importance in gaining kinetic and mechanistic information regarding ethers in general and increasing the existing data base in relation to such compounds .

2.3.2 Experimental

The experimental procedures employed to determine the OH radical and Cl atom rate constants for the ethers are detailed in Section 2.2 of this thesis . Therefore only specific details pertaining to the ethers and their analyses is outlined here . Table 2.3.2 lists the various compounds studied , their corresponding purities and the suppliers from which they were obtained . All compounds were used without any further purification . Prior to use the samples were thoroughly degassed on the vacuum line using the freeze - pump - thaw procedure . Sample mixtures were subsequently prepared in the smog chamber as outlined in Section 2.2 . Separation of methyl nitite from the test and reference organics and from reaction products was then achieved on the gas chromatograph . The test and reference organics used plus the optimum analytical conditions established to determine the OH radical and Cl atom rate constants for the ethers are summarised in Table 2.3.3.

TEST	PURITY (%)	SUPPLIER
Hexane	> 95	Aldrich Chemical Company
Diethyl ether	99.9	"
2 - Chloro ethyl methyl ether	98	"
2,2 - Dichloro ethyl methyl ether	97	"
2 - Bromo ethyl methyl ether	95	"
2 - Chloro,1,1,1- trifluoro ethyl ethyl ether	97	Fluorochem Ltd
Di - *i* - propyl ether	> 99	Aldrich Chemical Company
Isoflurane	> 99.9	Abbott Laboratories Ltd.
Enflurane	> 99.9	Abbott Laboratories Ltd.

Table 2.3.2

Test compounds studied plus their associated purities and suppliers .

TEST	REFERENCE	COLUMN	G.C. CONDITIONS
Hexane	Pentane	10% SE 30 on Chromosorb WHP (80-100μm) ;2m	Column Temp. = 44°C Flow = 31cm³/min.
Diethyl ether	Ethane	10% SE30 on Chromosorb WHP (80-100μm) ;2m	Column Temp. = 55°C Flow = 45cm³/min.
2,2-Dichloro ethyl methyl ether	Diethyl ether	10% SE 30 on Chromosorb WHP (80-100μm) ;2m	Column Temp. = 65°C Flow = 35cm³/min.
Isopropyl ether	Diethyl ether	10% SE 30 on Chromosorb WHP (80-100μm) ;2m	Column Temp. = 50°C Flow = 35cm³/min.
2-Chloro ethyl methyl ether	Diethyl ether	10% P.E.G. (80-100μm) ;2m	Column Temp. = 65°C Flow = 35cm³/min.
2-Bromo ethyl methyl ether	Diethyl ether	10% SE 30 on Chromosorb WHP (80-100μm) ;2m	Column Temp. = 65°C Flow = 40cm³/min.
2-Chloro,1,1,1,-trifluoro ethyl ethyl ether	Ethane	10% SE 30 on Chromosorb WHP (80-100μm) ;2m	Column Temp. = 75°C Flow = 31.5cm³/min.
Isoflurane	Diethyl ether	10% SE 30 on Chromosorb WHP (80-100μm) ;2m	Column Temp. = 40°C Flow = 28cm³/min.
Enflurane	Diethyl ether	10% SE 30 on Chromosorb WHP (80-100μm) ;2m	Column Temp. = 40°C Flow = 28cm³/min.

TABLE 2.3.3

Summary of the analytical conditions established for the ethers .

2.3.3 Results

The kinetic data reported in this work represents the first measurements of this type using our present apparatus . To test our system , therefore , a series of experiments were carried out on compounds for which reliable rates of reaction have already been determined and published , i.e., OH + hexane and Cl + diethyl ether .

Table 2.3.4 lists the Cl atom and OH radical rate constants for a series of ethers measured in our laboratory . The corresponding tropospheric lifetimes calculated from the rate constants for these compounds are listed in Table 2.3.5 . A comparison is made between our result data and those quoted in the literature . Table 2.3.4 demonstrates that our calculated rate constants are within the quoted error limits established for these compounds . Each of the quoted slopes in Table 2.3.4 represent an average value calculated from repeat determinations .

Reaction mixtures for both OH radical and Cl atom rate studies were stable in the dark over time scales typical of the experimental runs . Typical dark reaction results are illustrated in Figures 2.3.1 and 2.3.2 . Similarly , no photodecomposition of either test or reference compounds was observed over the time scales used in our experiments . This stability of the ethers is illustrated from the result data plotted in Figures 2.3.3 and 2.3.4 .

Hence , we concluded that for our OH radical work , loss of test and reference was due to reaction with OH radicals alone , and in the case of our chlorine work , loss of test and reference was due to reaction with Cl atoms alone .

As stated in the experimental section , potential interferences from reaction products were investigated . Prior to studying the relative loss of

test and reference organics , reaction of each compound was studied on their own .

TEST	TEMP. (K)	k_1 / k_3	$k_{Cl} \times 10^{11}$ ($cm^3 molecule^{-1} s^{-1}$)	k_2 / k_4	$k_{OH} \times 10^{12}$ ($cm^3 molecule^{-1} s^{-1}$)	REF.
Hexane	301 ± 2	-----	-----	1.39 ± 0.05	5.53 ± 1.55	This Work
	298	-----	-----	-----	5.61 ± 1.40	[20]
Diethyl Ether	298 ± 1	4.4 ± 0.09	25.8 ± 4.4	-----	-----	This Work
	298 ± 2	-----	25.4 ± 1.7	-----	-----	[21]
	295 ± 2	-----	35.6 ± 2.8	-----	-----	[22]
2-Chloro ethyl methyl ether	300 ± 3	0.56 ± 0.02	14.4 ± 5.0	0.358 ± 0.021	4.92 ± 1.09	This Work
2,2-Dichloro ethyl methyl ether	300 ± 3	0.17 ± 0.01	4.4 ± 1.6	0.173 ± 0.008	2.37 ± 0.50	This Work
2-Bromo ethyl methyl ether	300 ± 3	0.64 ± 0.01	16.3 ± 5.4	0.507 ± 0.017	6.94 ± 1.38	This Work
2-Chloro,1,1,1-trifluoro ethyl ethyl ether	300 ± 3	0.05 ± 0.01	0.30 ± 0.10	N.D.	< 0.3 [(a)]	This Work
Di-l-propyl ether	300 ± 3	0.64 ± 0.01	16.3 ± 5.4	0.809 ± 0.032	11.08 ± 2.26	This Work
	298 ± 2	-----	15.1 ± 0.7	-----	10.7 ± 2.0	[21]
	298 ± 2	-----	-----	-----	11.3 ± 0.7	[21]
Isoflurane	300 ± 3	N.D.	< 0.1 [(b)]	N.D.	< 0.3 [(a)]	This Work
	300	-----	-----	-----	0.021 ± 0.005	[15] , [16]
Enflurane	300 ± 3	N.D.	< 0.1 [(b)]	N.D.	< 0.3 [(b)]	This Work
	300	-----	-----	-----	0.017 ± 0.005	[15] , [16]

Table 2.3.4
OH radical and Cl atom rate constants calculated in this work using a relative rate technique .

(a) , (b) Limits based on the sensitivity of the analytical procedures .

TEST	τ_{Cl} (days)	τ_{Cl} (days)	Reference
Hexane	-----	2.7	This Work
Diethyl Ether	45	-----	This Work
2-Chloro ethyl methyl ether	80	3.1	This Work
2,2-Dichloro ethyl methyl ether	263	6.3	This Work
2-Bromo ethyl methyl ether	71	2.1	This Work
2-Chloro,1,1,1-trifluoro ethyl ethyl ether	10.6 years	> 50	This Work
Di - *i* - propyl ether	71	1.4	This Work
Isoflurane	> 32 -----	> 50 2.0 years	This Work [15] , [16]
Enflurane	> 32 -----	> 50 2.4 years	This Work [15] , [16]

Table 2.3.5
Tropospheric lifetimes of the compounds studied in this work . Lifetimes were determined with respect to both OH radicals and Cl atoms .

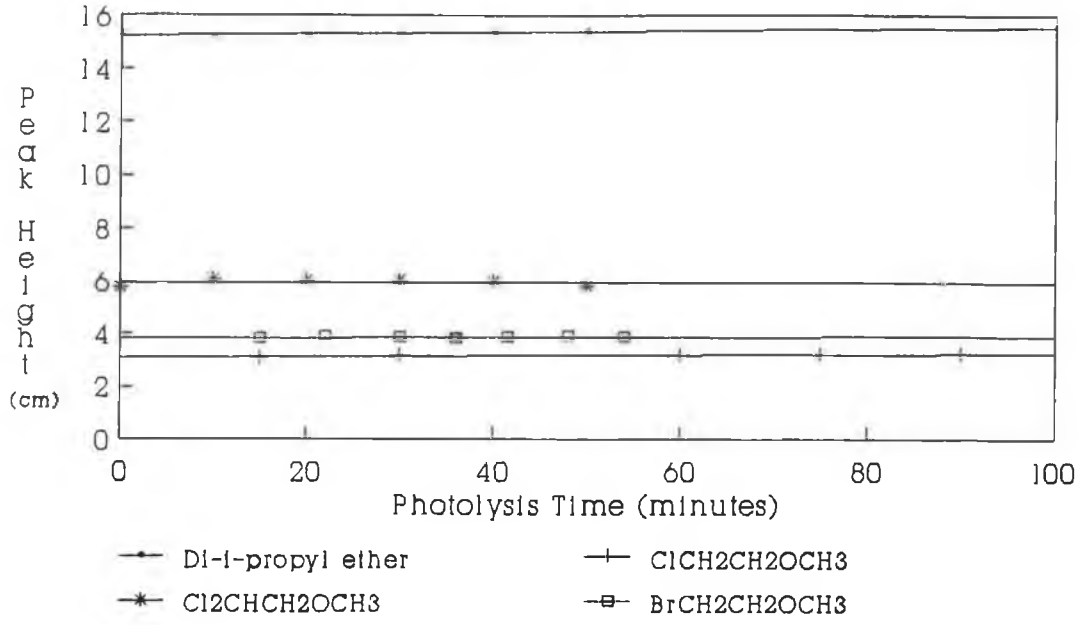

Figure 2.3.1
Dark reaction experimental observations for a number of ethers in methyl nitrite (OH radical experiments) .

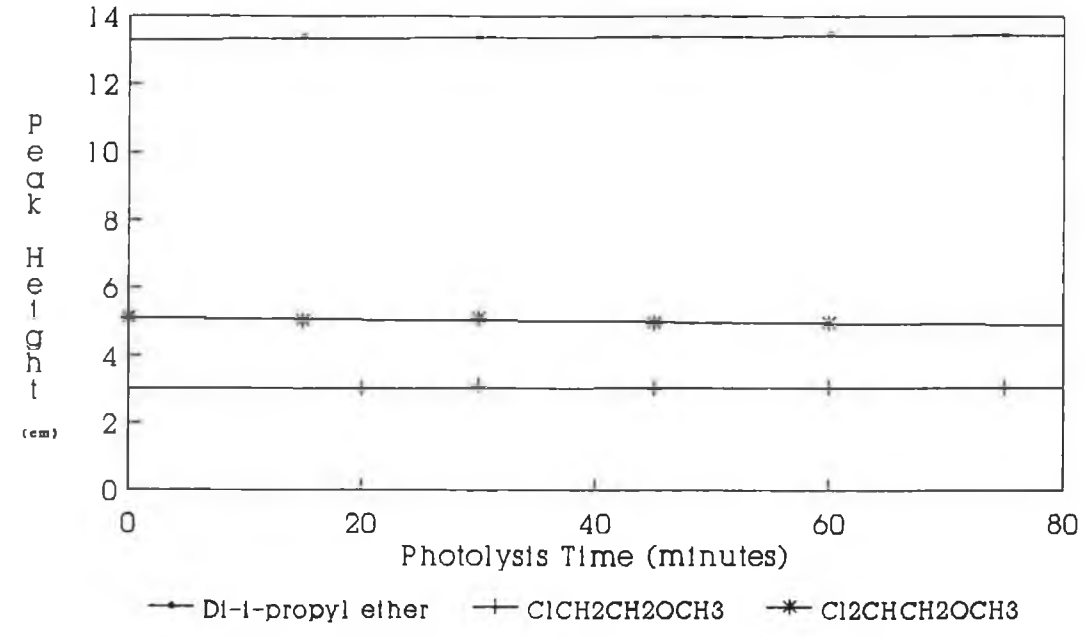

Figure 2.3.2
Dark reaction experimental observations for a number of ethers in molecular chlorine (Cl atom experiments) .

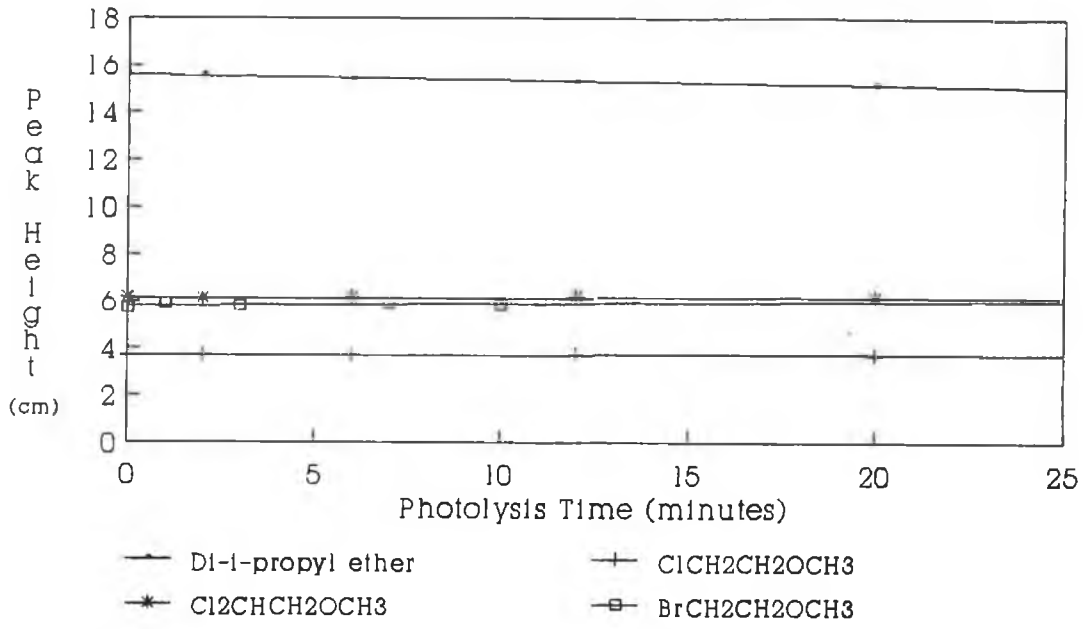

Figure 2.3.3
Photochemical stability of a series of ethers studied using experimental conditions typical of our OH radical work .

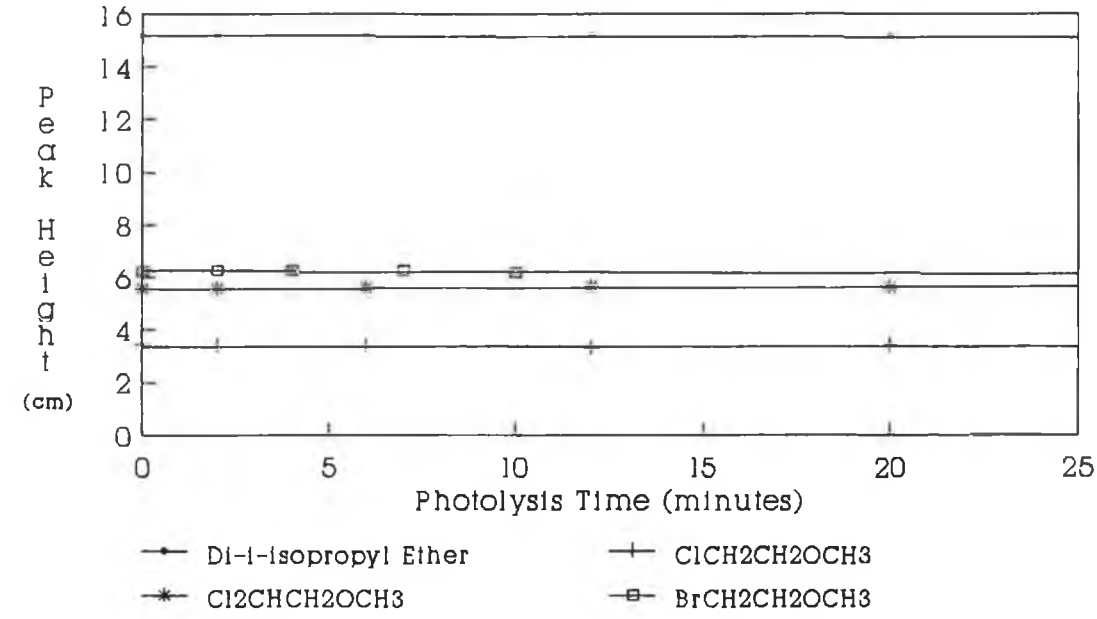

Figure 2.3.4
Photochemical stability of a series of ethers studied using experimental conditions typical of our Cl atom work .

It was thus possible to observe whether reaction products would interfere with other reaction mixture components and hence our result observations. Typical decay profiles for a selection of ethers is given in Figures 2.3.5 and 2.3.6 . Similar concentrations and the same reference organic were used in each of the studies illustrated , hence differences in the rates of decay illustrated are indicative of differences in the rate of reaction between the compounds . Any observed reaction product interferences were overcome by tailoring our analytical conditions to suit the system and therefore reaction products did not introduce errors into our results.

A high degree of precision in the result data was obtained using our system of analysis . For example, three repeat runs for the reaction of OH radicals with 2-chloro ethyl methyl ether yielded slopes of , 0.351 ± 0.004 . Similar reproducibility was obtained for the rate constant ratios for each of the compounds studied .

In both our OH radical and Cl atom work the slopes outlined in Table 2.3.4 were obtained from lines with correlation coefficients >0.995 and having minimal intercepts . Typical line plots are illustrated in Figures 2.3.7 and 2.3.8 .

Representative plots of our data for both OH radical and chlorine atom work are outlined in Figures 2.3.7 and 2.3.8 . The expression used to plot our data is given in equation (5). The concentration of test and reference at time, 0, and time , t, corresponded to the peak heights of each compound prior to irradiation and at some time, t, during photolysis. The slopes of the lines thus obtained correspond to $k_{reference} / k_{test}$. Knowing $k_{reference}$ allowed us to place our results on an absolute basis.

In the case of our OH radical work, two reference compounds were used. Pentane was used as the reference compound for the

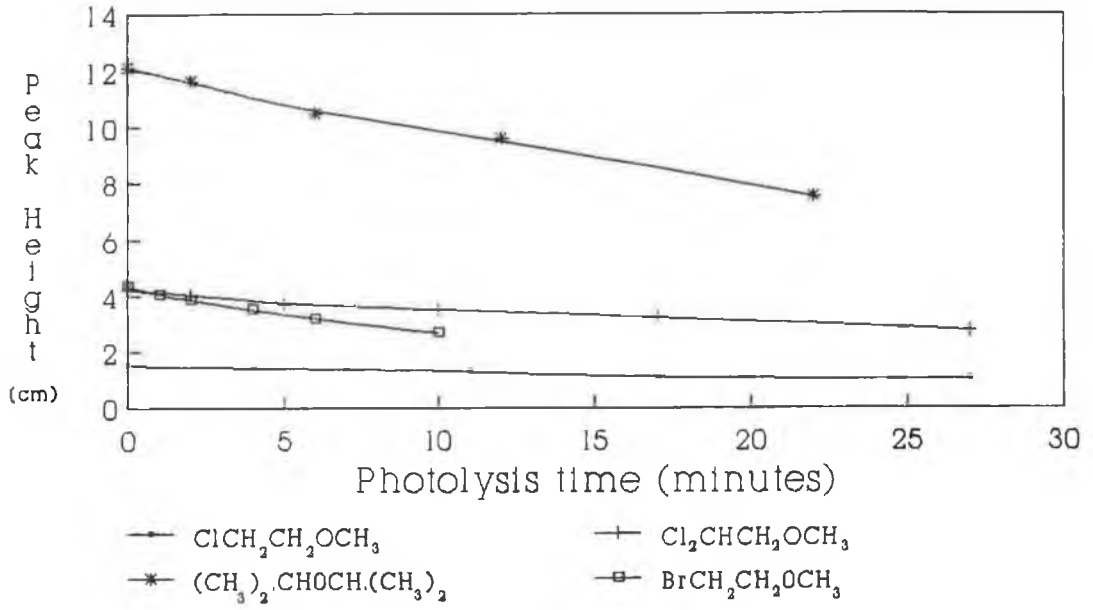

Figure 2.3.5
Decay curves obtained for the reaction of OH radicals with a selection of the ethers studied in this work .

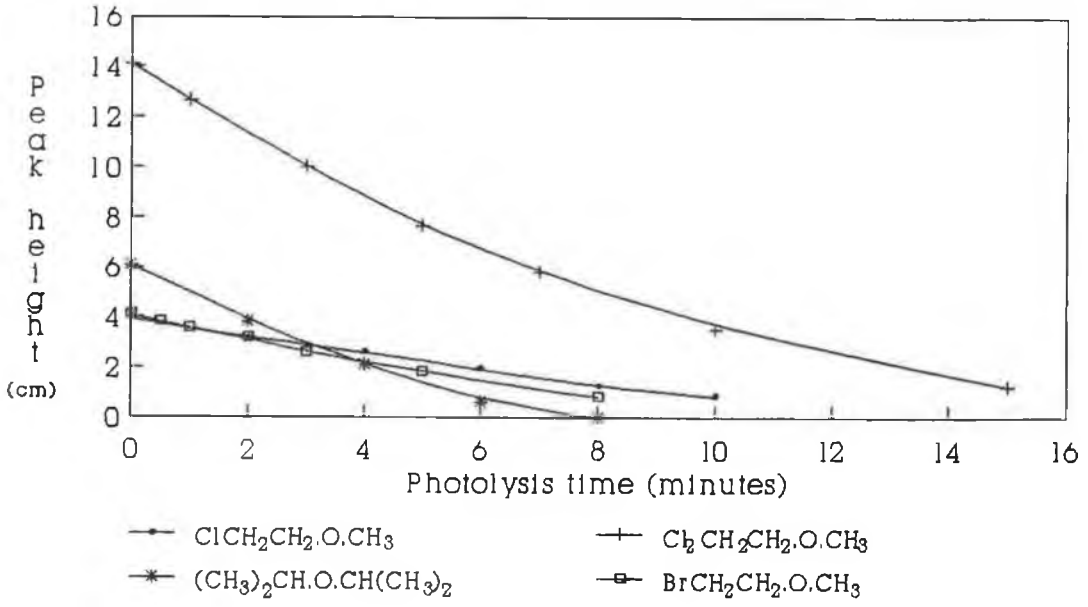

Figure 2.3.6
Decay curves obtained for the reaction of Cl atoms with a selection of the ethers studied in this work .

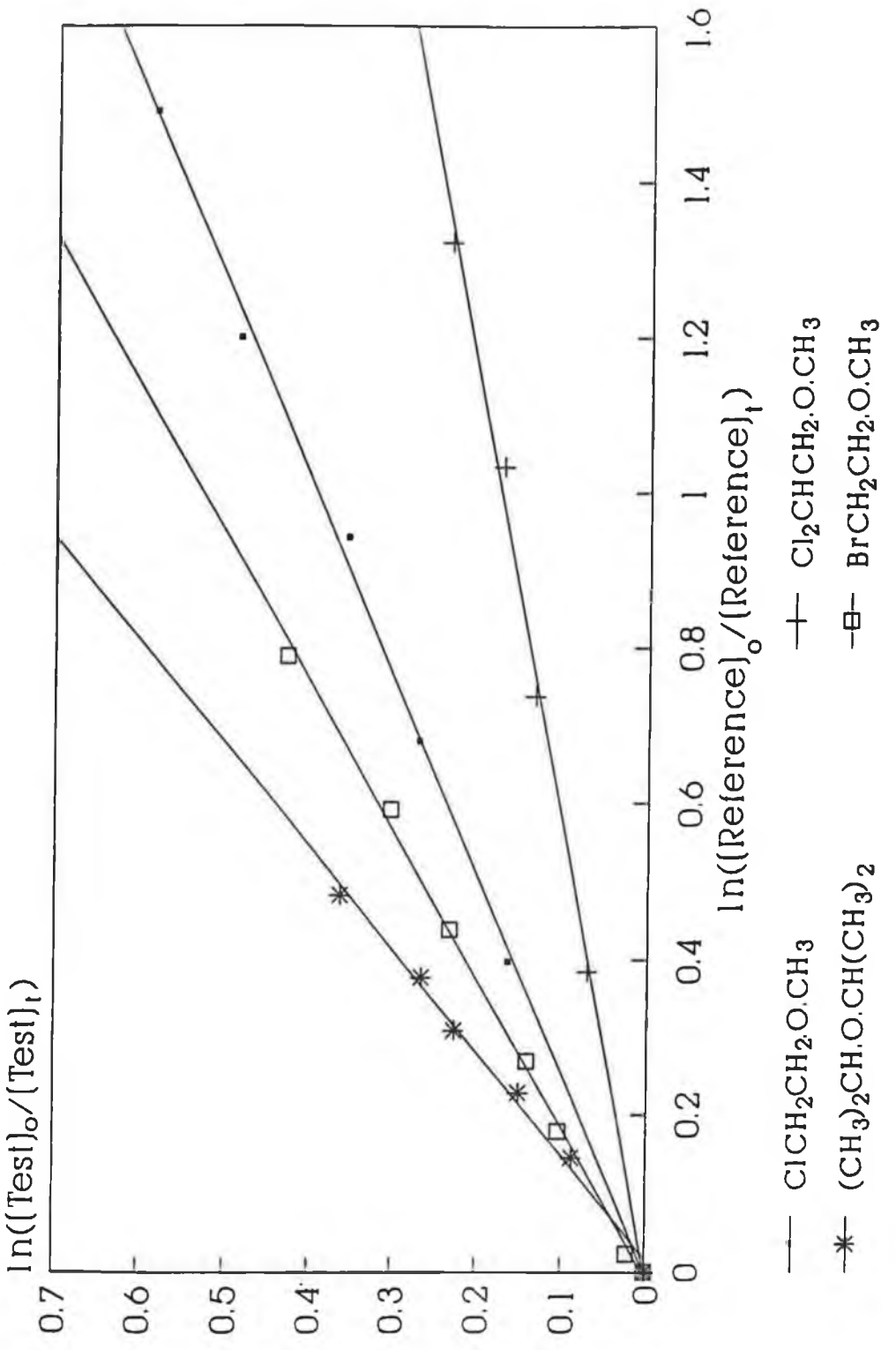

Figure 2.3.7
Typical plots for the determination of OH radical rate constants for a selection of ethers using a relative rate technique .

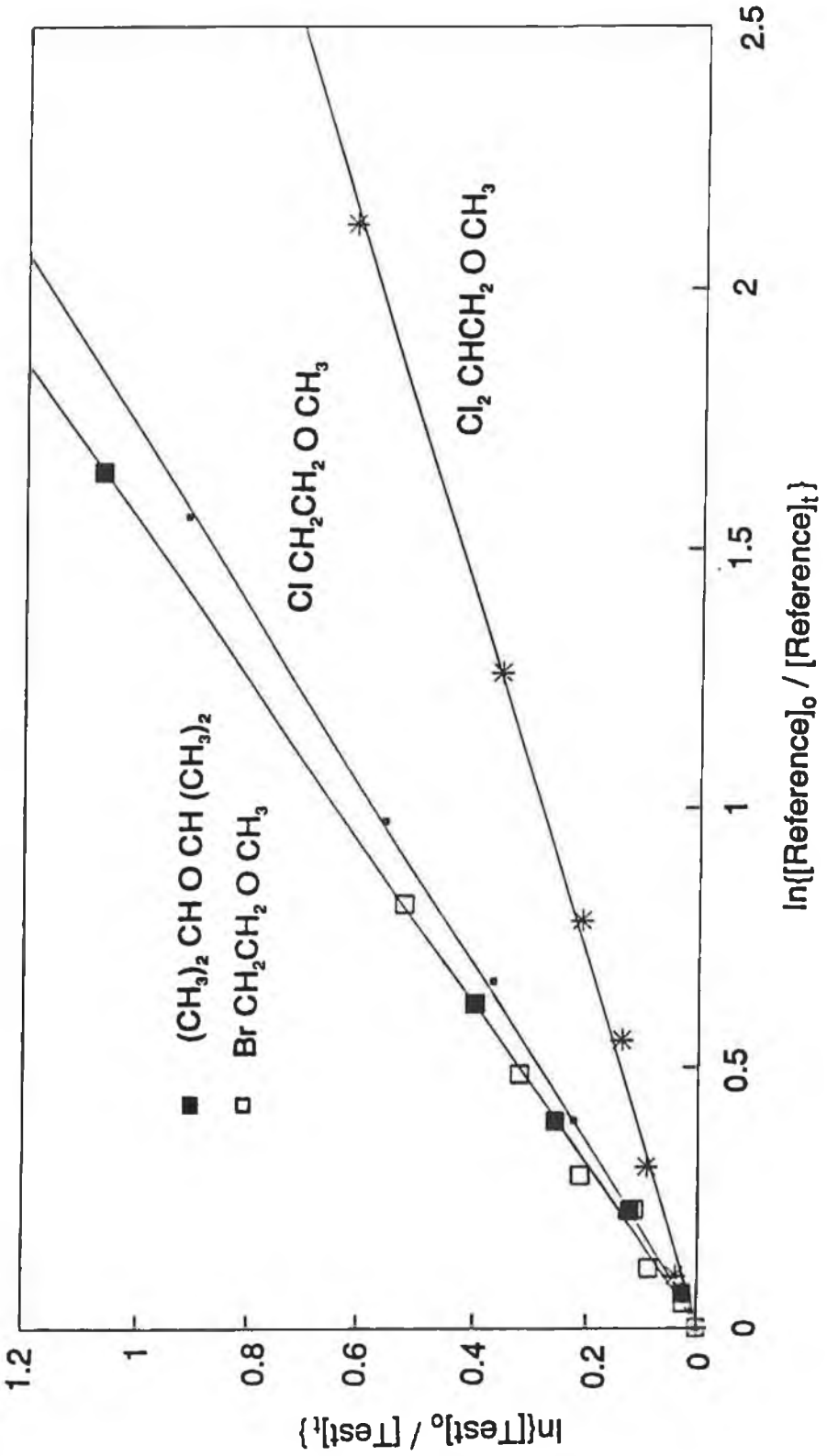

Figure 2.3.8
Typical plots obtained for the determination of Cl atom rate constants for a selection of using a relative rate technique .

determination of the rate constant for the hexane reaction , while diethyl ether was used for each of the other compounds studied . A value of k (OH + diethyl ether) = 13.6 ± 2.26 x 10^{-12} $cm^3molecule^{-1}s^{-1}$ was obtained from Wallington et al [23] . This figure was calculated using an absolute technique and includes all of those errors incurred in its calculation (i.e. ±2σ plus a maximum possible experimental error of 10%) . A value of k (OH + pentane) = 3.94 ± 0.98 x 10^{-12} $cm^3molecule^{-1}s^{-1}$ [20] was used , and included total errors associated with its determination . Although the OH radical rate constant for pentane was obtained using a relative rate technique , our reason for examining the reaction of OH radicals with hexane was purely as a system check . We wished to determine whether our new experimental set - up could be used to obtain rate constant values similar (within experimental error) to those recommended by Atkinson [32] . Reference rate constants were chosen which were calculated at similar temperatures to those of our experiments and which are representative of reported rate constants for these compounds .

In the case of our Cl atom work, two reference compounds were also chosen . Ethane was used as the reference for diethyl ether and 2-chloro,1,1,1-trifluoro ethyl ethyl ether and diethyl ether was used as the reference for the remaining compounds . The value of k (Cl + Ethane) = (5.84 ± 0.88) x 10^{-11} $cm^3molecule^{-1}s^{-1}$ [24] used represents an average of 4 absolute values and includes all errors associated with it's determination ,i.e.,± 15% . The value of k (Cl + diethyl ether) = (25.4 ± 8.05) x $10^{-11}cm^3molecule^{-1}s^{-1}$ [21] used is traceable to an absolute value and includes all experimental errors associated with it's determination (i.e., 2σ ± 25% error on $k_{Reference}$) . The error bars for the diethyl ether rate constant above differ from those quoted from the same reference in Table 2.3.4 as only errors corresponding to ±2σ are included in Table 2.3.4 and not total

experimental errors as above. Both reference rates were determined at similar temperatures to those in our experiments .

The stability of the anaesthetics towards OH radical and Cl atom attack is illustrated in Figures 2.3.9 and 2.3.10 . Although some decay is observed in chlorine , this reaction became very difficult to monitor once a reference organic was added to the reaction mixture . Because of the stability of these compounds , limits of reactivity for the anaesthetics and 2-chloro ,1,1,1-trifluoro ethyl ethyl ether were established and the calculated values quoted in Table 2.3.4 . The limits quoted for the OH radical rate constants are those recommended by Bufalini et al. [25] for the relative rate technique employed in our laboratory. The chlorine atom rate limits were established using a technique employed by Bufalini et al. [25] to set OH radical rate constant limits for the relative rate technique.

Table 2.3.5 lists the tropospheric lifetimes of each of our test compounds with respect to both OH radicals and Cl atoms. A value for the OH radical concentration of (7.7 ± 1.4) x 10^5 radicals cm^{-3} was used to determine the tropospheric lifetimes of our test compounds with respect to OH radicals . This value was calculated by Prinn et al. [26] and represents a globally averaged tropospheric value, calculated over a seven year period.

A value for the Cl atom concentration of 1 x 10^3 atoms cm^{-3} was used to determine the tropospheric lifetimes of our test compounds with respect to Cl atoms[27] .

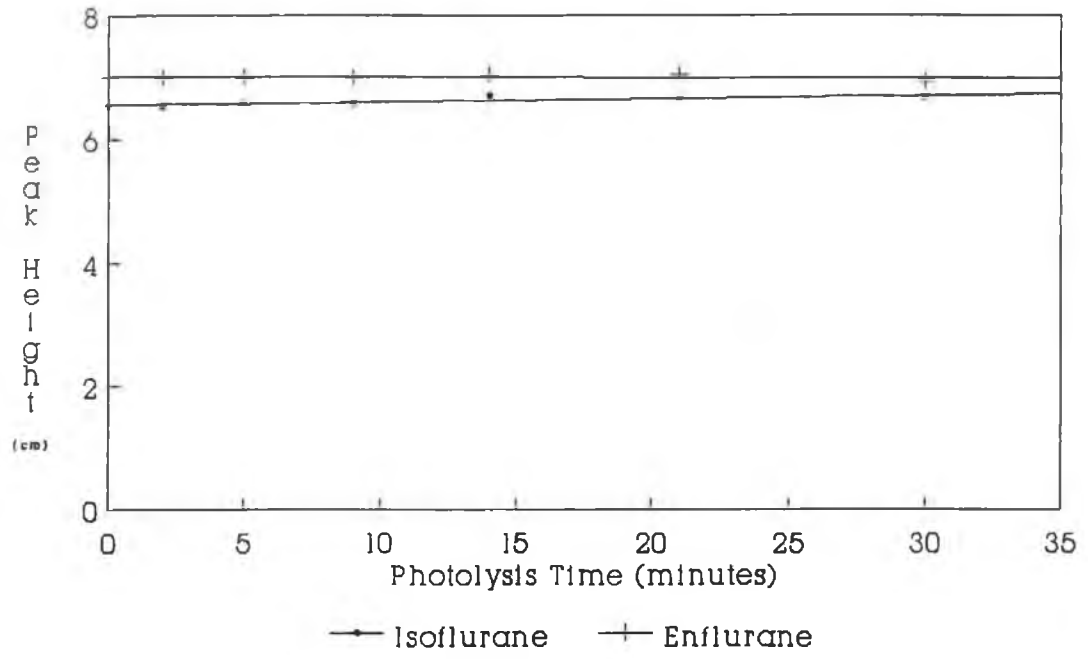

Figure 2.3.9
OH radical reaction observed with the anaesthetics , isoflurane and enflurane .

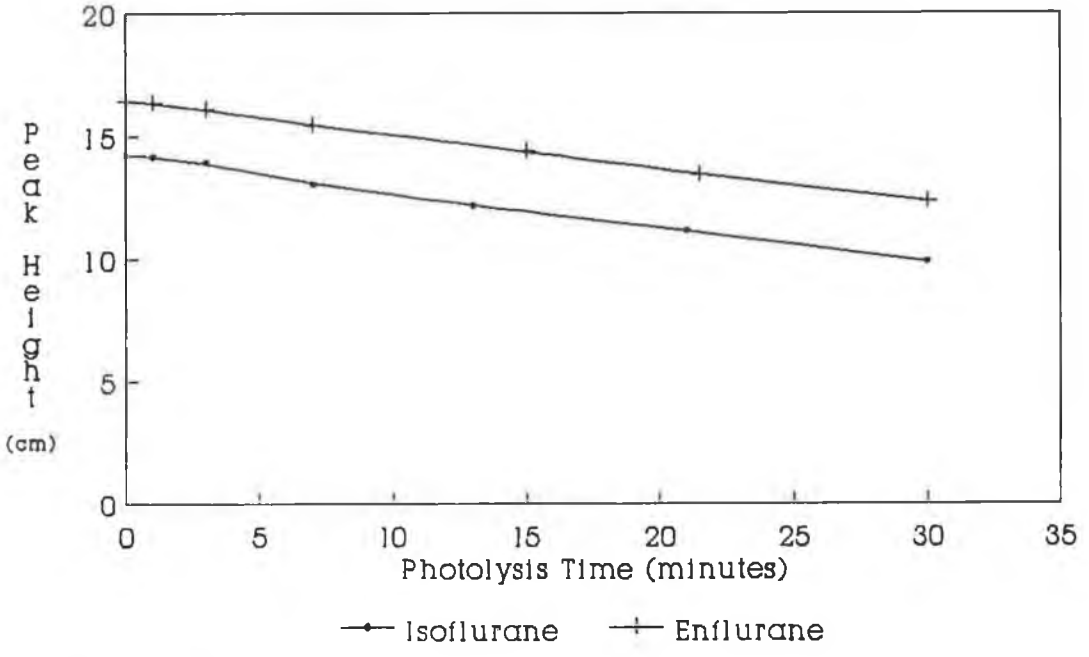

Figure 2.3.10
Cl atom reaction observed with the anaesthetics , isoflurane and enflurane.

2.3.4 Discussion

The kinetic data reported in this work is among the first dealing with the reaction of OH radicals and Cl atoms with halogenated ethers . Table 2.3.4 lists the OH radical and Cl atom rate constants and Table 2.3.5 the corresponding atmospheric lifetimes calculated from these rate constants for all of the compounds studied in this work . Prior to calculating the rate constants the stability of our test compounds in the dark and with respect to photodecomposition was established , Figures 2.3.1 - 2.3.4 . Possible interferences were also studied by establishing decay curves for each compound , Figures 2.3.5 and 2.3.6 . As similar conditions were used for each compound the decay curves visible in Figures 2.3.5 and 2.3.6 demonstrate the relative reactivity of each of the ethers towards both OH radicals and Cl atoms ,i.e., the sharper the decay , the greater the reactivity.

The slopes obtained indicate the precision of our results . The large error bars quoted for the rate constants are due to the inclusion of the total uncertainty associated with the reference rate constants used to place our results on an absolute basis .

Aliphatic ethers are expected to react with OH radicals and Cl atoms via a H-atom abstraction mechanism in a similar manner to the alkanes [20] :

$$\dot{O}H + CH_3OCH_3 \longrightarrow H_2O + \dot{C}H_2OCH_3 \qquad (2.3.1)$$

In the atmosphere the radicals produced in the abstraction reaction further react to give stable oxygenates :

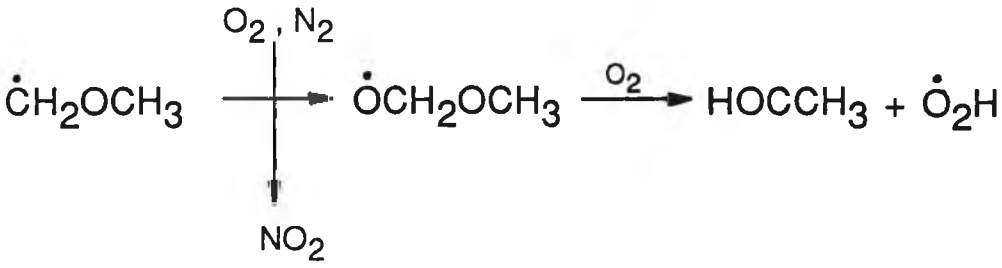

(2.3.2)

As expected from the bond energy of 93 +/- 1 kcal mol^{-1} for the primary C-H bonds in CH_3OCH_3 compared with the primary C - H bond energy of 98 +/-1 kcal mol^{-1} for the alkanes, the ethers are much more reactive than the corresponding alkanes (k_{OH} CH_3OCH_3 = 2.98 x 10^{-12} ,k_{OH} C_2H_6 = 0.268 x 10^{-12} $cm^3molecule^{-1}s^{-1}$ [20]) . This difference in bond dissociation energy is due to the activating effect of the oxygen , which has been shown to operate up to 5 carbons from the ether link [21] . The presence of chlorine in the ethers is expected to lower the C - H bond dissociation energy due to it's electron withdrawing effect, and thus give rise to an increase in the observed hydroxyl radical and chlorine atom rate constants for the abstraction process .

The majority of the ethers studied in this work were ethyl methyl ethers . Experimentally determined rate constants were not obtained for methyl ethyl ether , however a value for the OH radical rate constant was calculated using Wallington's group reactivity technique [28] . A value of 8.0 x 10^{-12} $cm^3molecule^{-1}s^{-1}$ was obtained thus indicating a drop in reactivity with respect to OH radicals on going from the unhalogenated to the dichlorinated ethyl methyl ether . This trend is not observed in the alkanes and may be accounted for by an increase in steric hindrance with increased halogenation .

Very little information is currently available on the effects of halogenation on the rate of reaction of ethers with OH radicals and Cl atoms . However, as a similar H-atom abstraction mechanism is expected for both ethers and ethanes (mechanism 2.3.1 and 2.3.2) , it is useful to

compare the effect of halogenation on the rates of reaction of ethanes and ethers . Table 2.3.6 demonstrates the effect of chlorine substitution on the OH radical rate constants for a series of chloroalkanes .

Compound	Temperature (K)	k x 10^{12} ($cm^3 molecule^{-1} s^{-1}$)	Estimated uncertainty	Reference
CH_3CH_3	298	0.268	± 20%	[20]
CH_3CH_2Cl	298	0.390	± 35%	[20]
CH_3CHCi_2	296	0.260	± 23%	[29]
$CHCl_3$	298	0.0119	± 30%	[20]

Table 2.3.6
The influence of Cl substitution on the rate constant for the reactlon of OH radicals with substituted ethanes .

Table 2.3.6 demonstrates that OH radicals react quicker with monosubstituted ethane than with ethane , suggesting that the Cl atom lowers the C - H bond dissociation energy causing a corresponding increase in the rate of H - atom abstraction , as expected. However, it is of interest to note that the OH radical rate constant for the disubstitued ethane is lower than that of the monosubstitued compound . A similar trend in reactivity was observed with regard to the mono- and di-chloro ethyl methyl ethers studied in our laboratory (Table 2.3.4). This apparent decrease in the rate of reactivity cannot be explained by bond dissociation energies alone. One possible reason for this deactivating effect of the chlorine substituent may be attributed to steric considerations . Another possible reason for the observed rate decrease may be due to polarity

changes associated with the incorporation of an extra Cl atom into the ether structure . It is possible that the inductive effect of an extra chlorine may result in a partial positive charge on the β - hydrogen :

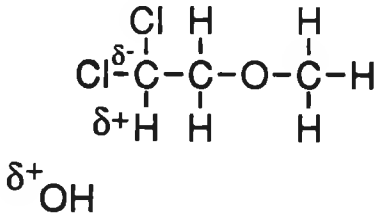

This would reduce the stability of the transition state for H abstraction by introducing repulsive forces between the H atom and the OH radical which may also be considered to carry a partial positive charge . This argument is not without precedent [30 , 31] for an electrophilic radical such as OH and the effect is expected to increase with increasing number and influence of electron withdrawing α substituents ; e.g.

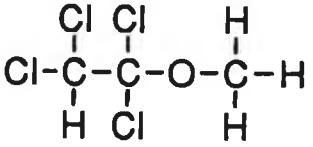

This hypothesis is reinforced by Taylor et al [30] who pointed to the similarity in bond dissociation energies of the α - hydrogens in CH_2ClCH_2Cl and CH_3CH_2Cl (96.5 ± 1 and 96.7 ± 3 kcal mol^{-1} respectively) , while the reaction rate of CH_2ClCH_2Cl with OH radicals is much smaller than with CH_3CH_2Cl . This also indicated that the reduction in reactivity of CH_2ClCH_2Cl was not due to small increases in bond strength .

The above decrease in reaction rate noted for the reaction of OH radicals with the chlorinated ethyl methyl ethers, was also found in the reaction of Cl atoms with these compounds, however the observed decrease was more significant. As both OH radicals and Cl atoms react via a similar H - atom abstraction mechanism (mechanism 2.3.1 and 2.3.2) , and due to the relatively larger size of the Cl atom to the OH radical, it would appear that steric effects may significantly influence the rate of such Cl atom reactions . To gain further knowledge with regard to possible steric influences, further work on the reaction of Cl atoms and OH radicals with other halogenated ethers is required .

The OH radical and Cl atom rate constants quoted in Table 2.3.4 for bromo ethyl methyl ether are both slightly larger than those for chloro ethyl methyl ether. This slight increase in reactivity of the bromo-substituted relative to the chlorine substituted compound has also been observed by a colleague in our laboratory studying halogenated alkanes. However, the difference in reactivities between the compounds may not be significant, as the reaction rates for both compounds lie within the error limits quoted for each rate constant. This similarity in reactivity between chlorinated and brominated compounds is consistent with data published by Atkinson [20] for CH_3Br and CH_3Cl.

The order of reactivity of the compounds studied is similar for both our OH radical and Cl atom data, reflecting the similarity of the reaction mechanisms involved. One surprising result was the unexpected similarity between the rates of reaction of bromo ethyl methyl ether and di-i-propyl ether. From the trends in the OH radical rate constant data, we would have expected a greater Cl atom reaction rate for di-*iso* -propyl ether. One possible reason for this could be due to the activating effect of the oxygen atom having less of an effect on distant C - H bonds in the case of Cl atom reactions [21] . Thus the H-atoms on the branched methyl groups of

di-*iso* - propyl ether are relatively more difficult to remove than in the corresponding OH radical reaction ; in fact , ease of removal of the hydrogens may be similar to that in the corresponding alkane . The value for k_{OH} di-*Iso* -propyl ether is greater than the corresponding alkane , 2,3-dimethyl butane, (k_{OH} = 6.2 x 10^{-12} $cm^3molecule^{-1}s^{-1}$ [20]) illustrating the activating effect of the oxygen atom in the ether .

One of the drawbacks of the relative rate technique employed in our laboratory is the difficulty in monitoring slow reactions . Compounds with OH radical rate constants < 0.3 x 10^{-12} $cm^3molecule^{-1}s^{-1}$ and Cl atom rate constants of < 0.1 x 10^{-11} $cm^3molecule^{-1}s^{-1}$ were not determined over the time scales employed in our laboratory (30 minutes) . These limits (also quoted in Table 2.3.4) were studied using a procedure outlined by Bufalini et al [25] . Both of these limits are defined by the sensitivty of the analytical technique used to measure the concentrations of the test and reference compounds . By modifying the concentration of Cl_2 and the nature of the reference compound it may be possible to determine Cl atom rate constants below 0.1 x $10^{-11}cm^3molecule^{-1}s^{-1}$ using our present experimental design .

Atmospheric lifetimes in Table 2.3.5 were calculated using the relationships ,

$$\tau_{Cl} = {}^{1}/_{k_{Cl}[Cl]} \quad \text{and} \quad \tau_{OH} = {}^{1}/_{k_{OH}[OH]} \qquad (2.3.3)\ ,\ (2.3.4)$$

where k_{Cl} and k_{OH} are the chlorine atom and hydroxyl rate constants respectively and [Cl] and [OH] the concentration of chlorine atoms and hydroxyl radicals respectively . The concentration of OH radicals of (7.7 ± 1.4) x 10^5 radicals cm^{-3} [26] used to calculate the atmospheric lifetimes of the ethers with respect to OH radicals, approximates that of a relatively

clean troposphere. The concentration of Cl atoms of 1 x 10^3 atoms cm^{-3} used to calculate the atmospheric lifetimes with respect to Cl atoms, is typical of a clean marine troposphere [27] .

The stability of isoflurane, enflurane and 2-chloro,1,1,1-trifluoro ethyl ethyl ether is demonstrated by their long tropospheric lifetimes in Table 2.3.5 and is illustrated in Figures 2.3.9 and 2.3.10 . These long lifetimes are consistent with the small number of abstractable hydrogens present in these compounds, and also the high degree of hindrance associated with these compounds. A limit of > 50 days was established for our OH radical tropospheric lifetime. Using an absolute technique, Brown et al [15 , 16] calculated the tropospheric lifetimes of isoflurane and enflurane (using a similar OH radical concentration to that employed in our studies) to be 2 and 2.4 years respectively , which is consistent with our data. From the results obtained by Brown et al [15] and from the release figures for isoflurane and enflurane calculated in our laboratory and presented in Table 2.3.1 , it is evident that only a small quantity of these anaesthetics will be emitted to the atmosphere . Since transport of material throught the tropopause into the stratosphere occurs on a time scale of roughly two years , an even smaller quantity will reach the stratosphere . As a means of quantifying the relative effect of the anaesthetics on stratospheric ozone , a number of factors were calculated from literature data coupled with the emission figures calculated in this work .

The factors commonly employed to quantify the relative effect of a compound on stratospheric ozone are , the ozone depletion potention (ODP) and the chlorine loading potential (CLP) [16] . For chlorinated halocarbons , the chlorine loading, CL , is proportional to the emission rate E , the lifetime and the number of chlorine atoms n_{Cl} :

$$CL\ (RH)\ \alpha\ E_{RX} \times \tau_{RH} \times n_{Cl} / M_{RH} \qquad (2.3.5)$$

The product τ x E/M is the steady - state concentration in moles , of any species in the atmosphere and for the same emission rate , the chlorine loading potential CLP, is given by :

$$CLP\ (RH) = \tau_{RH} / \tau_{CFC-11} \times M_{CFC-11} / M_{RH} \times n_{Cl} / 3 \qquad (2.3.6)$$

where M_{CFC-11} and M_{RH} are the relative molecular masses of CFC - 11 and RH . To obtain more accurate CLPs for the anaesthetics the emission figures for both our anaesthetics (Table 2.3.1) and CFC - 11 were incorporated into calculations :

$$CLP_{anaes} = (\tau_{anaes} / \tau_{CFC-11}) \times (E_{anaes} / E_{CFC-11}) \times (M_{CFC-11} / M_{anaes}) \times n_{Cl} / 3 \qquad (2.3.7)$$

The CLPs calculated for the anaesthetics are given in Table 2.3.7 . The ODP is defined as the ratio of the calculated ozone column change for each mass unit of gas emitted into the atmosphere relative to the calculated depletion for the reference gas CFC - 11 .

The relative importance of the active halogenated species in destroying ozone is altitude dependent because some of the halogenated compounds are photodissociated at shorter wavelengths than others . The vertical distribution of the compounds and the solar flux have to be considered in the model calculations . The consequence is that the ODP and the CLP are different , being related by a chlorine effectiveness factor (CEF) defined as :

$$ODP(RH) = CLP(RH) \times CEF(RH) \qquad (2.3.8)$$

The CEF for the reference compound , CFC - 11 is unity by definition .

The above relationships were used to calculate the ODP for both our anaesthetics and these are listed in Table 2.3.7 . The values for the CEF used to calculate the ODPs were obtained from the literature [32] . The difference in CLPs and ODPs between the reported data in Table 2.3.7 and that reported by Brown et al [16] is attributable to the fact that our calculations include emission figure contributions from the anaesthetics and CFC - 11 , while those by Brown et al [16] do not . If the ODPs of Brown are adjusted to take into account these emission differences , values for the ODPs of 7×10^{-5} and 8×10^{-5} are obtained for enflurane and isoflurane respectively .

Compound	**CLP**	**CEF**	**ODP**	τ_{OH} (years)
CFC - II	1.0	1.0 [32]	1.0	60 [32]
Isoflurane	0.0003	0.35 [32]	0.04 [16] 1.05×10^{-4}	2 [16] This work
Enflurane	0.0003	0.25 [32]	0.04 [16] 7.5×10^{-5}	2.4 [16] This work

Table 2.3.7
Ozone delpetion potentials (ODP) , chlorine loading potentials (CLP) and chlorine efficiency factors (CEF) for the anaesthetics and CFC - 11 . CLPs were calculated relative to tropospheric lifetimes with respect to OH radicals .

The values of the ODPs for the anaesthetics illustrate the minute contribution which these compounds exhibit on the ozone layer relative to CFC-11 . Although release of the anaesthetics to the atmosphere may be very small compared with other sources of potentially ozone - depleting or

greenhouse - effect - enhancing gases , the emission of such compounds could be almost negated by changes in operating room practices . It is calculated [17] that by appropriate use of absorption breathing systems with fresh gas flow rates of perhaps 1 dm^3min^{-1} , the total emissions might be reduced immediately by 50 - 75% . Although the extent to which isoflurane and enflurane will effect stratospheric ozone levels is minimal compared to compounds such as CFC - 11 and 12, the role of such trace compounds in atmospheric chemistry can not be overlooked , and must be considered in context with all such minor contributors .

To gain mechanistic information on OH radical and Cl atom reactions with haloethers , further work is required on compounds containing different halogens at different carbon sites. Product studies should also be carried out so that a complete environmental impact assessment can be made regarding the release of such haloether compounds.

2.3.5 Conclusion

Table 2.3.4 shows the similarity between the result data in the literature to that presented in this work . This result data also demonstrates the high level of precision obtained using our smog chamber - GC system . Typical errors on the rate constant ratios were approximately ± 5% . We can conclude therefore that accurate and precise rate constants were obtained using our system of analysis , and that the major source of error in these results is from the reference rate constant .

Cl atom reaction rates were on average approximately 25 to 30 times higher than the OH radical rate constants for the halogenated ethyl methyl ethers studied in this work . However , as OH radicals in the troposphere are approximately 1000 times more abundant than Cl atoms , we can conclude that the major loss process for the halogenated ethers in the atmosphere , including the anaesthetics , is reaction with OH radicals .

Rate of reaction of the halogenated ethers with Cl atoms and OH radicals appears to be influenced by the bond dissociation energies within the ethers . There may also be a steric hindrance contribution and/or an induced polarity effect influencing the rate of reaction of these species .

Result data shows that the etheral oxygen has less of an effect on the distant carbons in the reaction of the ethers (specifically di- *iso* -propyl ether) with Cl atoms . However , the activating effect of this oxygen atom extends over the entire di- *iso* - propyl ether molecule in the reaction of this compound with OH radicals .

Atmospheric lifetimes and emission figures for the anaesthetic ethers , isoflurane and enflurane were used to calculate the ozone depleting potential (ODP) of these anaesthetics . From these values , it can be concluded that these anaesthetic ethers will have negligible deleterious effects on stratospheric ozone levels .

2.3.6 References

[1] A.M. Winer , A.C. Lloyd , R. Atkinson , and J.N. Pitts Jr , *Chem. Phys. Letters* , **51** , 2 , 221 , (1977) .

[2] E.V. Anderson , *Chem. Eng. News* , **65** , 7 , (1987) .

[3] T.J. Wallington , P. Dagaut , R. Liu , and M.J. Kurylo , *Environ. Sci. Technol.* , **22** , 842 , (1988) .

[4] M.S. Reisch , *C&EN* , 13 - 19 , April 8 , (1991) .

[5] J.H. Lee , and I.N. Tang , *J. Chem. Phys.* , **77** , 9 , 4459 , (1982) .

[6] P.H. Wine , and R.J. Thompson , *Int. J. Chem. Kinet.* , **16** , 867 , (1984) .

[7] T.J. Wallington , J.M. Andino , L.M. Skewes , W.O. Siegl , and S.M. Japar , *Int. J. Chem. Kinet.* , **21** , 993 , (1989) .

[8] J. Norreslet , S. Friberg , T.M. Nielson , and U Romer , *The Lancet* , 719 , April 1 , (1989) .

[9] P. Hutton , and J.A. Kerr , *The Lancet* , 1011 , May 6 , (1989) .

[10] J.M.T. Pierce , and S.P.K. Linter , *The Lancet* , 1011 , May 6 , (1989) .

[11] K.J. Hopkins , and R.A. Albanese , *The Lancet* , 1209 , May 27 , (1989) .

[12] B.D. Joyner , *The Lancet* , 1209 , May 27 , (1989) .

[13] R.C. Rodgers , and J.A.S. Ross , *The Lancet* , 1209 , May 27 , (1989) .

[14] A.C. Brown , C.E. Canosa - Mas , A.D. Parr , R. Wayne and J.M.T. Pierce , *The Lancet* , 279 , July 29 , (1989) .

[15] A.C. Brown , C.E. Canosa - Mas , A.D. Parr , J.M.T. Pierce , and R.P. Wayne , *Nature* , **341** , 635 , (1989) .

[16] A.C. Brown , C.E. Canosa - Mas , A.D. Parr , and R.P. Wayne , *Atmos. Environ.* , **24A** , 9 , 2499 , (1990) .

[17] M. Logan , and J.G. Farmer , *Br. J. Anaes.* , **63** , 6 , 645 , (1989) .

[18] F.S. Rowland , and Molina .

[19] J.K. Hammitt , F. Camm , P.S. Connell , W.E. Mooz , K.A. Wolf , D.J. Wuebbles , and A. Bamezai , *Nature* , **330** , 711 , (1987) .

[20] R. Atkinson , *J. Phys. Chem. Ref. Data* , Monograph No. 1 , (1989).

[21] L. Nelson , O. Rattigan , R. Neavyn , H. Sidebottom , J. Treacy , and O.J. Nielson , *Int. J. Chem. Kinet.* , **22** , 1111 , (1990) .

[22] T.J. Wallington , L.M. Skewes , W.O. Siegl , C - H. Wu , S.M. Japar, *Int. J. Chem. Kinet.* , **20** , 867 , (1988) .

[23] T.J. Wallington , R. Lin , P. Dagnaut , *Int. J. Chem. Kinet.* , **20** , 41, (1988) .

[24] R. Atkinson , and S.M. Aschmann , *Int. J. Chem. Kinet.* , **17** , 33 , (1985) .

[25] J.J. Bufalini , and R.R. Arnts , **E.P.A.** / 600/3 - 87/046 , (1987) .

[26] R. Prinn , D. Cunnold , R. Rasmussen , P. Simmonds , F. Alyea , A. Crawford , P. Fraser , and R. Rosen , *Science* , **238** , 945 , (1987) .

[27] H.B. Singh , and J.F. Kasting , *J. Atmos. Chem.* , **7** , 261 , (1988) .

[28] T.J. Wallington , P. Dagaut , R. Liu , and M.J. Kurylo , *Int. J. Chem. Kinet.* , **20** , 541 , (1988) .

[29] C.J. Howard , and K.M. Evenson , *J. Chem. Phys.* , **64** , 4303 , (1976) .

[30] P.H. Taylor , S. McCarron , and B. Dellinger , *Chem. Phys. Lett.* , **177** , 1 , 27 , (1991) .

[31] L. Nelson , I. Shanahan , H.W. Sidebottom , J. Treacy , and O.J. Nielson , *Int. J. Chem. Kinet.* , **22** , 577 , (1990) .

[32] United Nations Environmental Programme and World Meteorological Organization Scientific Assessment : Volumes I and II , 21 August , (1989) .

2.4

The Reaction of OH radicals and Cl atoms with a series of ketones

2.4.1 Introduction

Apart from the many permanent components of the earth's atmosphere , N_2 , O_2 etc , a large number of minor components also exist i.e. HCl , hydrocarbons etc. The levels of these minor constituents vary greatly depending on time and place , since these species are the result of a very complex set of physical and chemical phenomena [1] :

(1) emission of primary compounds either by natural processes (volcanos, ocean spray , wind erosion , biogenic activity , etc.) or by anthropogenic processes (industrial , domestic or agricultural) ;
(2) chemical transformations leading to the formation of secondary compounds in the atmosphere ;
(3) transport and dispersion of atmospheric components because of shifts in air masses , turbulence , and convection ;
(4) phase transfers , i.e. the various phenomena involving exchange between the gaseous phase and solid or liquid phases in suspension (condensation , adsorption , evaporation , etc.) ;
(5) elimination by wet or dry deposition , absorption by vegetation or corrosion of various materials .

Among the most important chemical derivatives affected by these phenomena , carbonyl compounds , increasingly attracting the attention of atmospheric researchers because they play an important role in several of the processes mentioned above :

(1) they are fairly common primary compounds , (ketones are widely used in paints , as solvents and as degreasing agents [2]) . In fact acetone and methyl ethyl ketone (butan-2-one) are two of the most highly produced organic compounds (on a volume basis) in the United States [3] ;

(2) they are frequently produced intermediates in the photooxidation of organic compounds in the atmosphere ;

(a) methyl vinyl ketone ($CH_3COCH=CH_2$) is produced from the gas phase reactions of isoprene , (a vegetative emission) with the OH radical in the presence of NO_x [4] ;
(b) acetone is produced from the gas phase reaction of 2 - methylbutane with OH radicals [5] :

Mechanism 2.4.1.1

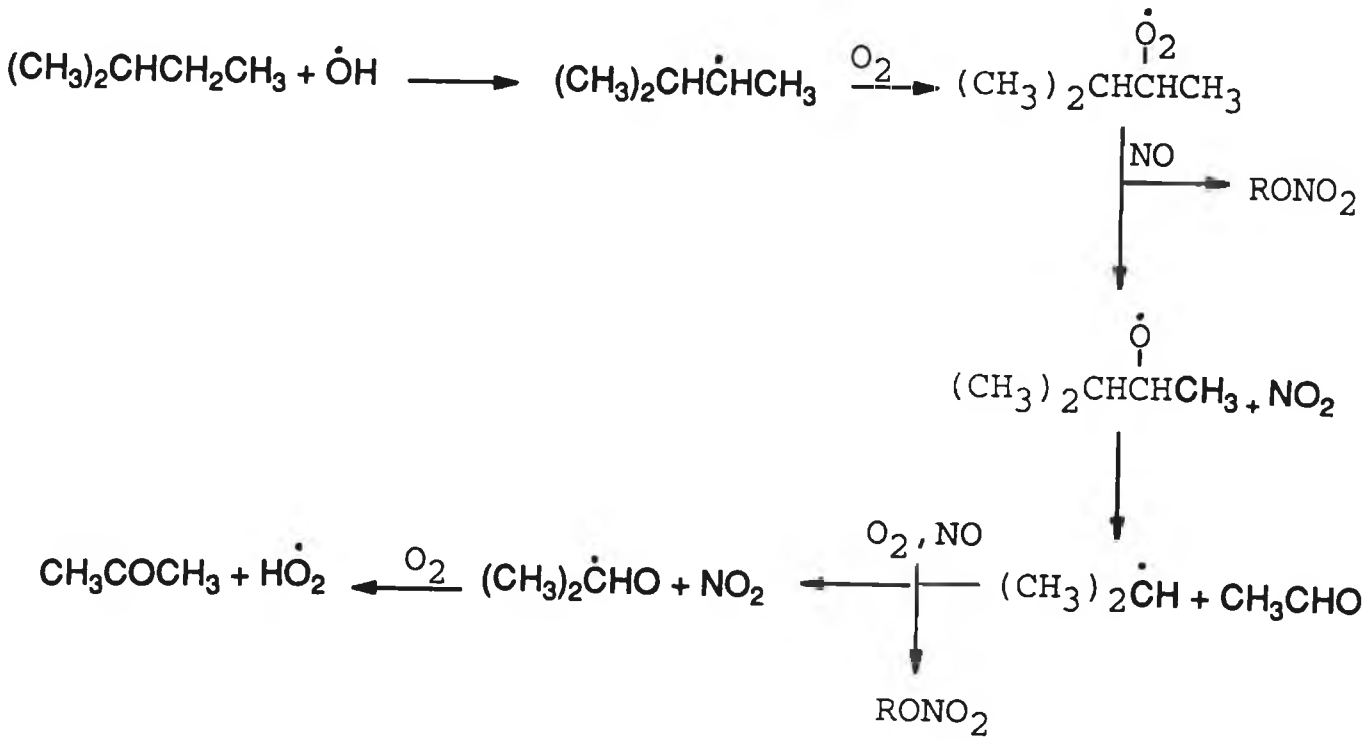

(3) carbonyl species are easily photolysed in the atmosphere and thus are an essential source of free radicals for tropospheric photochemistry and probably the most important source in moderately and strongly polluted atmospheres ;

(4) because carbonyl compounds are polar , they can easily interact with particles of condensed matter , adsorb onto soots and form solutions with rain and fog .

The atmospheric importance of carbonyl compounds has led to detailed reviews of the sources of these species and to both kinetic and mechanistic studies of the atmospheric reactions of these compounds [5,6]. As stated above , ketones are relesed to the atmosphere from their use in industry and in the household . To gain an insight into the atmospheric role of the ketones , we must first study their sources in detail and then combine this information with the available kinetic and mechanistic degradation pathways for these species in the troposphere . Three primary sources of ketones exist in the troposphere , natural sources, anthropogenic sources and as products from the atmospheric oxidation of organic compounds .

The emission of carbonyl compounds in general from natural sources is very small . However , certain insects produce ketones and traces have also been detected in volcanic gases . Much more important sources of ketones are due to emission from animal excrete and forest fires [1] . It should be noted that man has a marked effect on the impact of these sources (stockfarming , deforestation) .

Many industries are likely to emit a great variety of carbonyl compounds including ketones . As state earlier , butan-2-one and acetone are produced in large volumes by the American chemical industry . The use and production of such ketones is inherent in refining and petrochemistry , coal chemistry , plastics , paint and varnish industries , sewage treatment plants , and even coffee roasting . The main anthropogenic sources of ketones are rubbish incineration and the exploitation of fossil fuels for energy production , industrial and domestic heating and motor-vechicle traffic .

The most important reason for the study of atmospherically important ketones is due to their production as secondary reaction products in atmospheric gas phase processes e.g. the gas phase OH radical oxidation of 2 - methylbutane (mechanism 2.4.1.1) . Carlier et al [1] have estimated that secondary aldehydes and ketones account for an average of $^{7}/_{8}$ of the total carbonyl compounds in the polluted air above Los Angeles , despite the strength of the sources of primary compounds .

Any organic radical (R·) with an unpaired electron on a carbon atom reacts in the atmosphere as follows :

$R\cdot + O_2$	------->	$RO_2\cdot$	(2.4.1.2)
$RO_2\cdot + NO$	------->	$RO\cdot + NO_2$	(2.4.1.3)
$RO\cdot + NO$	------->	Carbonyl compound + $HO_2\cdot$	(2.4.1.4)

Reactions 2.4.1.2 to 4 are very fast during the daytime , and therefore the production of carbonyl compounds including ketones is virtually controlled by the formation of free radicals from organic compounds in the atmosphere . This depends both on the concentrations of the reactive species ($OH\cdot$, O_3 , $NO_3\cdot$, etc.) and on the rate constants between these species and the organic compounds of the troposphere . Table 2.4.1 illustrates the type of ketone identified as secondary reaction products in the gas phase reactions of certain primary alkanes under simulated atmospheric conditions [1] .

Primary compounds	Ketones identified as 2° reaction products
Propane	Acetone
Isobutane	Acetone
2,3-Dimethyl butane	Acetone
Pentane	2-Pentanone, 3-pentanone
Isopentane	Acetone
2-Methylpentane	Acetone

Table 2.4.1
Primary alkanes and their major identified photooxidation reaction products (ketones) .

It has been illustrated that ketones are produced from primary sources (both natural and anthropogenic) as well as being formed as intermediate "stable" chemical products during the atmospheric degradation reactions of a wide variety of organic compounds . The ketones therefore are a very important class of hydrocarbons in the troposphere . But what of the fate of these species in the atmosphere ? To assess the importance of the ketones in the atmosphere , we must first determine the removal mechanisms for these compounds , as well as the speed of these important removal reaction processes . In the atmosphere , ketones can photolyze or react with Cl atoms , OH , NO_3 , and HO_2 radicals .

In order to evaluate the photolysis rates of ketones or carbonyls in general , under atmospheric conditions , the radiation flux , J , the carbonyl absorption cross section , σ , and the photolytic quantum yield , Φ , all as a function of wavelength , need to be known . Thus [5] ,

$$k_{photolysis} = \int_{290nm}^{800nm} J_\lambda \sigma_\lambda \Phi_\lambda d_\lambda \qquad (2.4.1.5)$$

The radiation flux , J , is either experimentally measured or calculated for clear study conditions and is not dealt with further here . The absorption cross-sections and quantum yields are obtained from experimental studies.

The photodissociation of acetone has recently been studied by Meyrahn et al [7] . At 750 torr total pressure of air , the quantum yield for CH_3CO formation was determined to be 0.55 at 280 nm , 0.30 at 290 nm , 0.15 at 300 nm , 0.05 at 310 nm , 0.028 at 320 nm and 0.033 at 330 nm . This data is consistent with an average photodissociation quantum yield of 0.33 ± 0.06 for the wavelength region 280 - 330 nm measured by Cox et al [8] . No data is available concerning the photodissociation quantum yields for the higher ketones . As for acetone , these quantum yields are [5] , espically at wavelengths typical of the troposphere .

For ketones which do not contain C = C bonds , their reactions with O_3 are of negligible atmospheric importance , and indeed only upper limits to the rate constants of $< 10^{-20}$ $cm^3molecule^{-1}s^{-1}$ have been obtained for the analogous compounds , HCHO , CH_3CHO and CH_3COCHO [9] .

For the reactions of the NO_3 radical with the ketones , no data is currently available , however , rate constants for such reactions are expected to be in the range 10^{-17} to 10^{-16} $cm^3molecule^{-1}s^{-1}$ at room temperature [5] . With rate constants of this magnitude , these reactions with the NO_3 radical are of minimal atmospheric importance as a ketone loss process .

Because of the slow reaction rates for the ketones with O_3 and NO_3 and the low photodissociation of the ketones above 300nm , it is predicted that the major loss process for these species in the troposphere is reaction with OH radicals [1,5,10] . The importance of this OH radical degradation pathway for the ketones has resulted in a number of investigations of the kinetics of this process [11 - 16] . Current kinetic

information with regard to the reaction of OH radicals with the ketones has been summarised by Atkinson [6] .

As stated in Section 2.1.5.1 reaction of OH radicals with ketones proceeds via a H - atom abstraction mechanism . However enhancement in reactivity at the β and γ positions may be due to the formation of a six membered ring adduct prior to H - atom abstraction [11] . It is hoped that the present study may further support the kinetic data obtained by Wallington et al [10] and Atkinson et al [12] thus adding credence to such a ring adduct mechanism .

Since Singh et al [17] proposed Cl atom reactions with volatile organic chemicals (VOCs) in the troposphere as being an important loss mechanism for these species , a number of articles have been published reporting Cl atom rate constants . These reports point towards the importance of these values not only in stratospheric modelling but also in determining the fate of VOCs in the troposphere [18 - 20] . Although Cl atom reactions with the ketones is possibly an important loss mechanism for these species in the troposphere no published kinetic data was found in this area up to the publication of this thesis .

The work carried out in this section involved the use of a relative rate technique to determine OH radical and Cl atom rate constants for a series of ketones . This information is important in establishing a data base for the reaction of Cl atoms with ketones , and also serves to reaffirm published kinetic data relating to the reaction of OH radicals with the ketones . Both sets of rate constants are used to study factors effecting the mechanisms of these reactions and to establish relationships between the structures of the ketones and their corresponding reactivities.

2.4.2 Experimental

The apparatus and experimental procedures used in this thesis to determine OH radical and Cl atom rate constants for a series of ketones are detailed in Section 2.2 of this report . Only specific details pertaining to the ketones and their analysis is therefore given here .

Table 2.4.2.1 lists the ketones studied their corresponding purities and their suppliers . Both the test and reference compounds were used without further purification . Prior to use the samples were thoroughly degassed on the vacuum line using the freeze - pump - thaw procedure . Samples were prepared on the vacuum line and subsequently flushed into the smog as outlined in Section 2.2 . Separation of methyl nitrite from the test and reference organics and from the reaction products was then achieved on the gas chromatograph . The test compounds (ketones) plus the optimum analytical conditions established to determine their OH radical and Cl atom rate constants are summarised in Table 2.4.2.2 .

COMPOUND	PURITY (%)	SUPPLIER
Propan-2-one	>99.5%	BDH Chemicals Ltd.
Butan-2-one	>99%	BDH Chemicals Ltd.
Pentan-2-one	>98%	BDH Chemicals Ltd.
Hexan-2-one	>99%	Aldrich Chemical Co. Ltd.
Heptan-2-one	>98%	Aldrich Chemical Co. Ltd.
Pentan-3-one	>98%	Aldrich Chemical Co. Ltd.
Hexan-3-one	>98%	Aldrich Chemical Co. Ltd.
4-MethylPentan-2-one	>99.5%	Aldrich Chemical Co. Ltd.
Cyclopentanone	>99%	Aldrich Chemical Co. Ltd.
Cyclohexanone	>99.8%	Aldrich Chemical Co. Ltd.

Table 2.4.2.1
The ketones studied in this work plus their corresponding stated purities and suppliers .

COMPOUND	GC CONDITIONS			
	Oven Temp. (°C)	Inj. Temp. (°C)	Det. Temp. (°C)	Flow Rate ($cm^3\ min^{-1}$)
Propan-2-one	90	105	160	35
Butan-2-one	75	105	160	35
Pentan-2-one	100	105	160	33
Hexan-2-one	85	100	180	33
Heptan-2-one	90	100	180	33
Pentan-3-one	80	100	180	35
Hexan-3-one	90	100	180	35
4-Methyl Pentan-2-one	85	100	180	33
Cyclopentanone	95	150	180	35
Cyclohexanone	110	150	180	35

Table 2.4.2.2
The ketones studied in this work and the corresponding GC conditions used for their analysis . The column used was a 2 metre glass column (id = 3 mm) packed with 10% PEG on chromosorb WHP (80-100 μm) .

2.4.3 Results

The technique employed in this work to determine the OH radical and Cl atom rate constants for a series of ketones is outlined in Section 2.2 of this thesis . These determinations were carried out in the temperature range 297 ± 6K and at atmospheric pressures of 769.62 ± 13.58 mm Hg .

The technique employed resulted in the determination of rate constant ratios (k_{Test}/ $k_{Reference}$) , which are given in Table 2.4.3.1 . The error bars on these ratios represent ± 2σ from a least squares analysis of our data . Accurate reference rate constants (for OH + cyclohexane and Cl + cyclohexane) were then used to place the data on an absolute basis . The reference rate constant used for the OH radical rate determinations was k_{OH} cyclohexane = (8.28 ± 1.24) x 10^{-12} $cm^3molecule^{-1}s^{-1}$. This value represents an average of two absolute figures determined by Droege and Tully [21] and Bourmada et al [22] . The error bars on this reference rate represents the total estimated uncertainty in it's determination . The reference rate constant used for the Cl atom rate calculations was k_{Cl} Cyclohexane = (31.1 ± 4.67) x 10^{-11} $cm^3molecule^{-1}s^{-1}$. This value was obtained from Atkinson et al [23] and was calculated using a relative rate technique . Although it is not advisable to use a relative rate constant to establish another reaction rate , the only available absolute value for k_{Cl} Cyclohexane was determined by Davis et al [24] . The value obtained , (18 ± 2) x 10^{-11} $cm^3molecule^{-1}s^{-1}$ is not consistent with the values of 36.1 and 31.1 x 10^{-11} $cm^3molecule^{-1}s^{-1}$ calculated by Wallington et al [25] and Atkinson et al [23] and hence was not used . Table 2.4.3.1 lists the OH radical and Cl atom rate constants calculated in this work .

The large error bars resulted from the inclusion of all errors inherent in the determinations, including those associated with the reference

TEST	TEMP. (K)	k_1 / k_3	$k_{Cl} \times 10^{11}$ (cm^3 molecule^{-1} s^{-1})	k_2 / k_4	$k_{OH} \times 10^{12}$ (cm^3 molecule^{-1} s^{-1})	Ref.
Propan-2-one	299 ± 4	----	[a] < 0.1	----	[b] < 0.3	This work
	298	----	----	----	0.23 ± 0.07	[6]
Butan-2-one	299 ± 4	0.103 ± 0.003	3.21 ± 0.56	0.154 ± 0.008	1.28 ± 0.26	This work
	298	—	----	----	1.15 ± 0.29	[6]
Pentan-2-one	299 ± 4	0.327 ± 0.007	10.17 ± 1.75	0.604 ± 0.010	5.00 ± 0.84	This work
	298	----	----	----	4.9 ± 1.5	[6]
Hexan-2-one	298 ± 4	0.609 ± 0.012	18.94 ± 3.22	1.091 ± 0.014	9.03 ± 1.47	This work
	298	----	----	----	9.1 ± 2.7	[6]
Heptan-2-one	299 ± 4	0.757 ± 0.014	23.54 ± 3.97	1.493 ± 0.021	12.36 ± 2.03	This work
	----	----	----	----	8.67 ± 1.27	[11]
Pentan-3-one	299 ± 4	0.227 ± 0.009	7.06 ± 1.34	0.330 ± 0.011	2.73 ± 0.50	This work
	298	----	----	----	2.0 ± 0.6	[6]
Hexan-3-one	295 ± 4	0.476 ± 0.005	14.80 ± 2.38	0.851 ± 0.019	7.05 ± 1.21	This work
	----	----	----	----	6.96 ± 1.68	[12]
4-Methyl Pentan-2-one	299 ± 4	0.407 ± 0.009	12.66 ± 2.18	1.633 ± 0.016	13.52 ± 2.16	This work
	298	----	----	----	14.1 ± 4.23	[6]
Cyclopentanone	297 ± 4	0.282 ± 0.010	8.77 ± 1.63	0.338 ± 0.018	2.8 ± 0.57	This work
	----	----	----	----	2.94 ± 0.47	[27]
Cyclohexanone	301 ± 1	----	----	0.576 ± 0.017	4.77 ± 0.86	This work
	----	----	----	----	6.36 ± 1.15	[27]

Table 2.4.3.1

OH radical and Cl atom rate constant ratios and the corresponding rate constants for the ketones studied in this work .

[a],[b] Reaction rate limits were establilshed based on the sensitivity of the analytical procedures using a technique outlined by Bufalini et al [26] .

compounds . Rate constant data for the reaction of OH radicals with the ketones obtained from the literature is also included for comparison with the data calculated in this work .

Table 2.4.3.2 lists the tropospheric lifetimes of the ketones studied with respect to OH radicals and Cl atoms . These tropospheric lifetimes were calculated using the expression :

$$\tau = {}^{1}/_{[OH]([or\ Cl])\ x\ k_{OH}\ or\ (k_{Cl})} \qquad (2.4.3.1)$$

where [OH] and [Cl] are the tropospheric concentration of these species and k_{OH} and K_{Cl} are the rate constants for the reaction of OH radicals and Cl atoms with the ketones respectively .

The concentration of OH radicals used to calculate the tropospheric lifetimes of the ketones with respect to the reactive OH species was (7.7 ± 1.4) x 10^5 radicals cm^3 . This value calculated by Prinn et al [28] was determined from observed mean methylchloroform trends at various isolated locations throughout the world from July 1978 to June 1985 . These measured trends were combined with knowledge of industrial emissions and a globally averaged tropospheric hydroxyl radical concentration obtained (1σ uncertainty) .

The concentration of Cl atoms used to determine the tropospheric lifetime of the ketones with respect to Cl atoms was 1 x 10^3 atoms cm^{-3} . This value was calculated by Singh et al [17] and represents an average value typical of a clean marine troposphere .

As in all smog chamber - relative rate techniques ,the stability of the test compounds was evaluated prior to rate constant determination . The stability of a series of ketones studied in the absence of light is illustrated in Figures 2.4.3.1 and 2.4.3.2 . The stability of the ketones with respect to

Compound	τ_{OH} (days)	τ_{Cl} (days)
Propan-2-one	> 50	> 31.7 years
Butan-2-one	11.7	362
Pentan-2-one	3.0	114
Hexan-2-one	1.7	61
Heptan-2-one	1.2	49
Pentan-3-one	5.5	164
Hexan-3-one	2.1	78
4-Methyl Pentan-2-one	1.1	91
Cyclopentanone	5.4	132
Cyclohexanone	3.2	---

Table 2.4.3.2
Tropospheric lifetimes of the ketones studied in this work . Lifetimes were calculated relative to [OH] = 7.7 ± 1.4 x 10^5 radicals cm^{-3} [28] and [Cl] = 1 x 10^3 atoms cm^{-3} [17] .

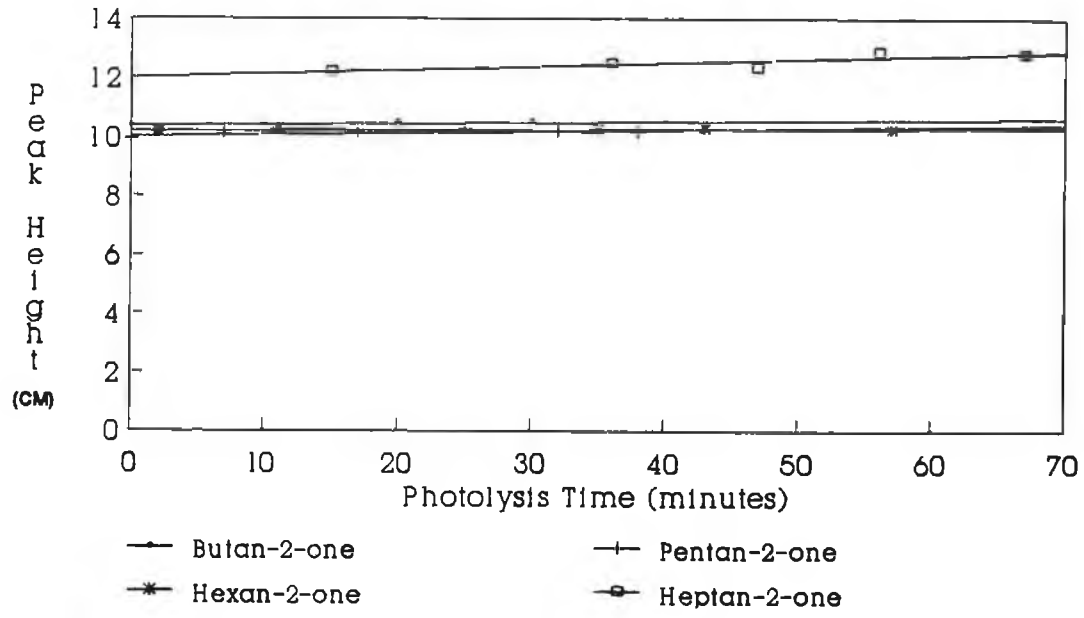

Figure 2.4.3.1
The stability of a series of ketones in synthetic air at room temperature and atmospheric pressure (769.62 ± 13.58 mmHg) in the presence of methyl nitrite and NO .

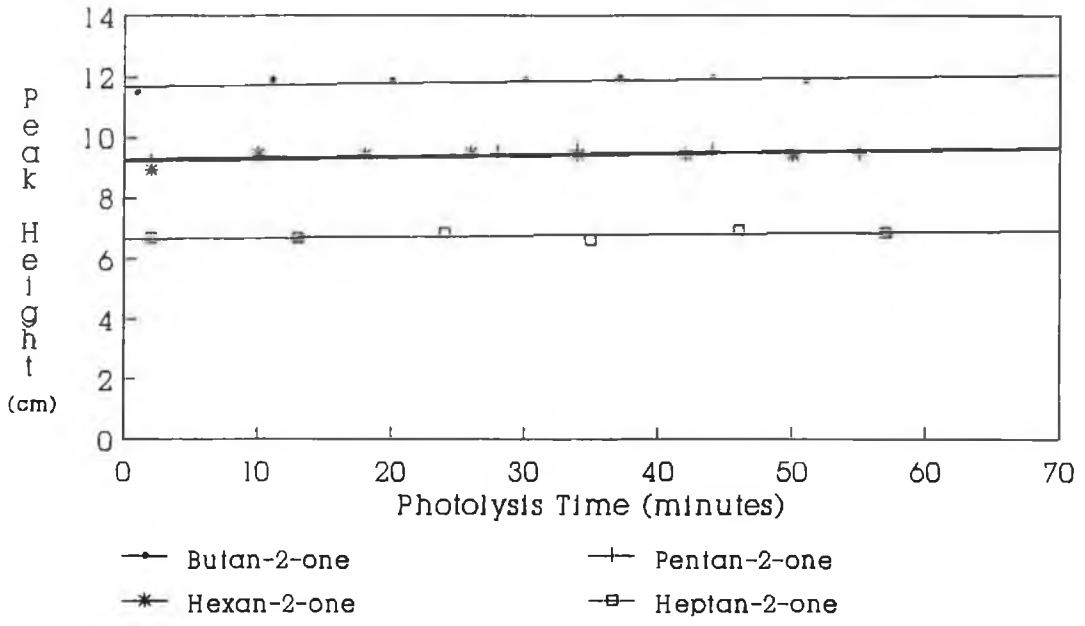

Figure 2.4.3.2
The stability of a series of ketones in synthetic air at room temperature and atmospheric pressure (769.62 ± 13.58 mmHg) in the presence of Cl_2.

photodecomposition is illustrated in Figures 2.4.3.3 and 2.4.3.4 .

To optimize the analytical conditions for analysis , it was necessary to ensure that no reaction products interferred with the determination , i.e. that products from the reaction of OH radicals or Cl atoms with the test compounds did not elute from the GC column at the same retention time as that of the reference organic and vice versa . Hence , prior to determining rate constants ,"decay curves" for both the test and reference organics was established . These "decay curves" involved monitoring the reaction of the test or reference on their own , with OH radicals or Cl atoms . Examples of typical "decay curves" are given in Figures 2.4.3.5 and 2.4.3.6 .

Having ensured that photodecomposition or dark reactions were not responsible for loss of test or reference organics , and having optimized analytical conditions , the determination of rate constant ratios was

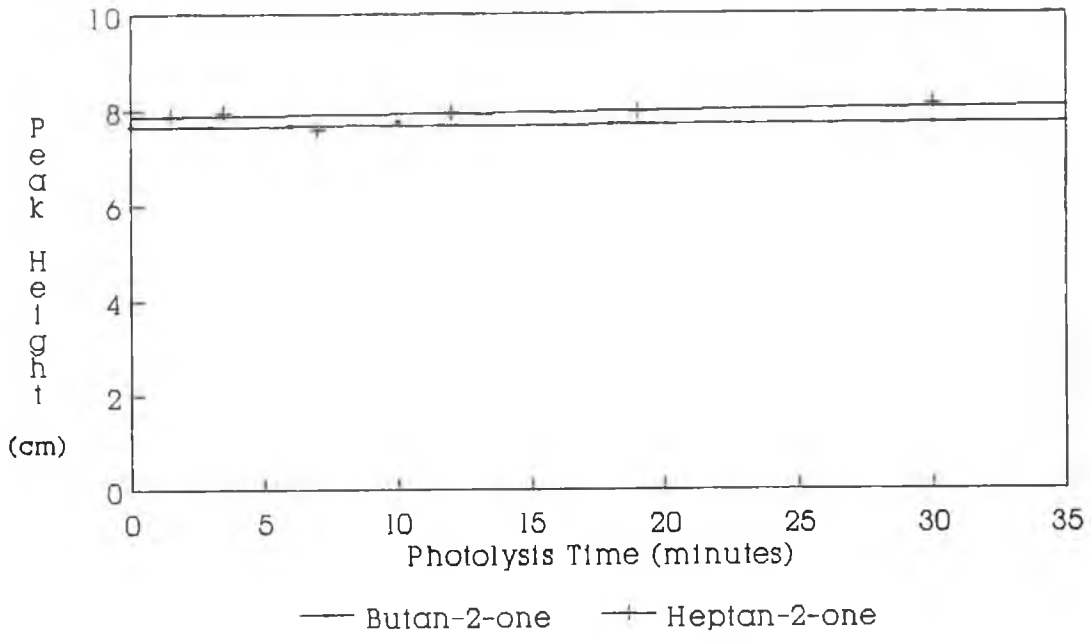

Figure 2.4.3.3
The stability of two test ketones with respect to photodecomposition . Stability was tested at 297 ± 6 K and atmospheric pressure (796.62 ± 13.58 mmHg) using all 20 sun and dark lamps (λ = 270 - 470 nm) in the smog chamber for irradiation .

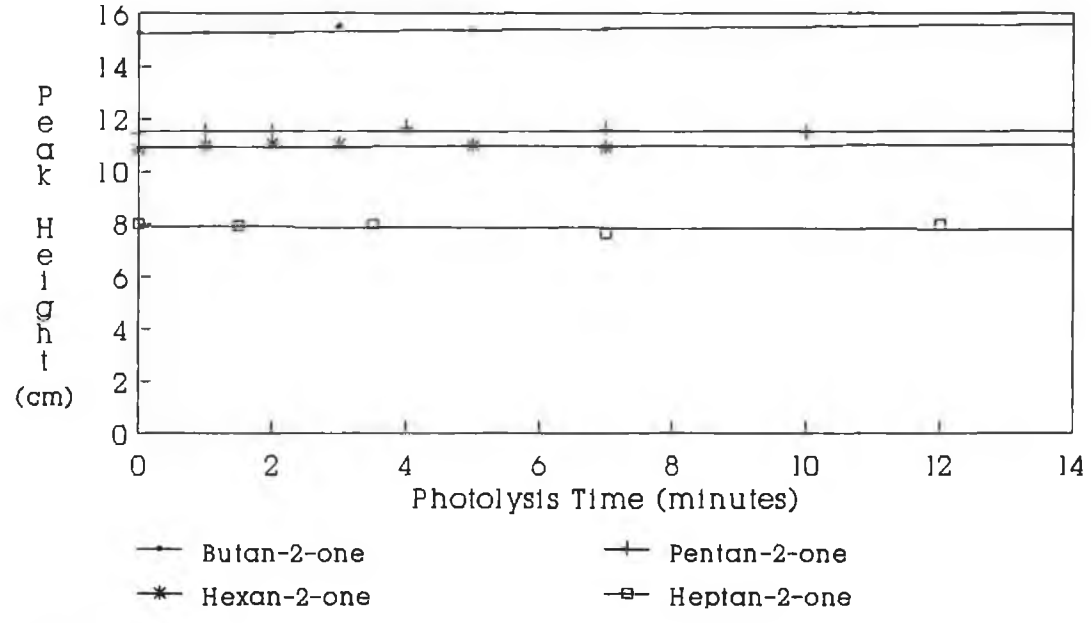

Figure 2.4.3.4
The stability of four test ketones with respect to photodecomposition . Stability was examined at 297 ± 6 K and atmospheric pressure (769.62 ± 13.58 mmHg) using 5 black lamps (λ = 315 - 470 nm) in the smog chamber for irradiation .

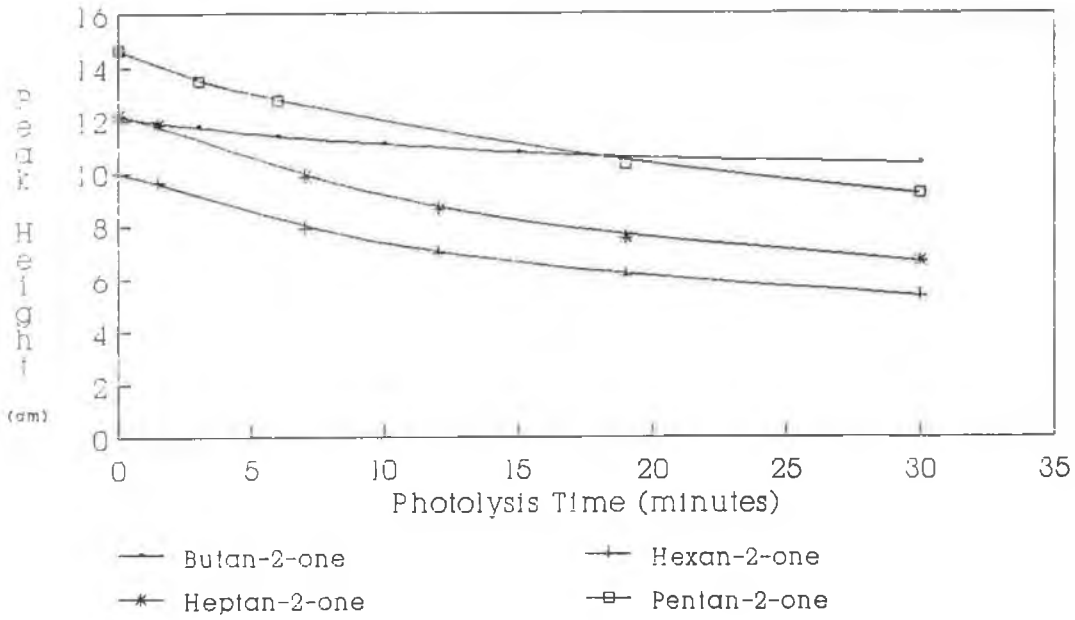

Figure 2.4.3.5
"Decay curves" for the reaction of OH radicals with a series of ketones . Experiments were carried out at 297 ± 6 K and at atmospheric pressure of 769.62 ± 13.58 mmHg .

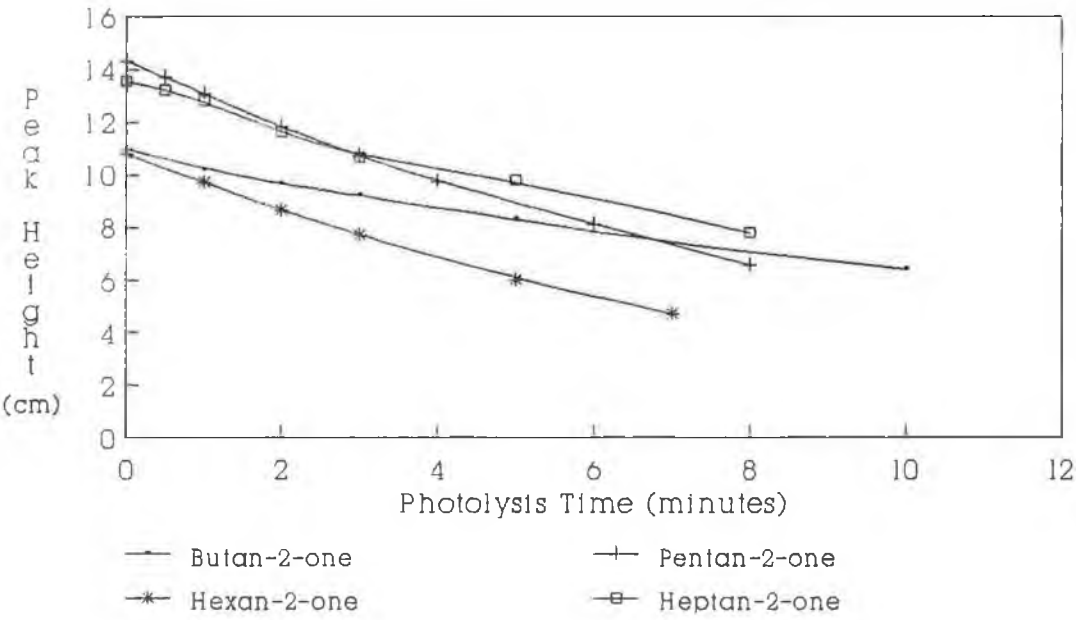

Figure 2.4.3.6
"Decay curves" for the reaction of Cl atoms with a series of ketones . Experiments were carried out at 279 ± 6 K and at atmospheric pressure of 769.62 ± 13.58 mmHg .

possible . Figures 2.4.3.7 and 2.4.3.8 illustrate typical plots obtained for the reaction of a series of ketones with OH radicals and Cl atoms . Plots were constructed by monitoring the concentration of test and reference at various photolysis times and then plotting this data as outlined in Figures 2.4.3.7 and 2.4.3.8 . The slopes of the lines indicated in these diagrams correspond to the values of (k_1/k_2) and (k_2/k_4) , given in Table 2.4.3.1 .

From the OH radical rate constants in Table 2.4.3.1 , and using literature values for k_{OH} (CH_3) it was possible to determine the reactivity of aliphatic chains in the ketones . The values obtained together with those previously quoted in the literature for the ketones is given in Table 2.4.3.3. Values for the corresponding alkane reactivities , calculated from the rate constant values for these compounds recommended by Atkinson [6] are also included for comparison .

Using the Cl atom rate constants calculated in our laboratory and listed in Table 2.4.3.1 , it was also possible to determine the reactivity of aliphatic chains in the ketones with respect to Cl atoms . The reactivity data calculated together with the corresponding alkane reactivities obtained from Atkinson et al [23] are given in Table 2.4.3.4 .

From the rate constant data in this work and from literature values for CH_3 reactivity , it was possible to calculate $-CH_2-$ reactivities for the ketones with respect to OH radicals and Cl atoms (Tables 2.4.3.5 and 2.4.3.6) . Literature values for OH and CH_3 reactivities were obtained from Wallington et al [11] . The reactivities of CH_3 groups further than 2 carbons from the carbonyl group were assumed to be equal i.e. approximately 0.37. Values for k (Cl + CH_3) were established from the rate limit established in our laboratory for the reaction of Cl atoms with acetone i.e. $(0.1 \times 10^{-11} / 2)$ $cm^3molecule^{-1}s^{-1}$. As in the OH radical reactions , the reactivity of the CH_3 group was assumed to remain constant , regardless of the distance from the carbonyl group .

R	$CH_3(CO)R \times 10^{12}$ ($cm^3molecule^{-1}s^{-1}$)			CH_3R ($cm^3molecule^{-1}s^{-1}$)
	THIS WORK	[6]	[11]	[6]
CH_3	< (0.3/2)	0.115	0.11	0.13
C_2H_5	[a]1.17 [b]1.37	[a]1.04 [b]1.0	[a]1.04 [b]1.37	1.02
C_3H_7	[c]4.89 [d]5.68	[c]4.79	[c]3.89	2.41
C_4H_9	[c]8.92	[c]8.99	[c]6.53	3.81
C_5H_{11}	[c]12.25	----	[c]8.56	5.48

Table 2.4.3.3

The reactivity of linear aliphatic chains in the ketones calculated from the OH radical rate constants determined in our laboratory and listed in Table 2.4.3.1 . Literature values for the ketones and the alkanes are also included for comparison .

[a] Value obtained from k_{OH}(butan-2-one) - $k_{OH}(\alpha\text{-}CH_3)$

[b] Value calculated from $\{k_{OH}$(pentan-3-one)/2$\}$

[c] Value calculated from k_{OH}(ket-2-ones) - $k_{OH}(\alpha\text{-}CH_3)$

[d] Value calculated from k_{OH} {Hexan-3-one - (Pentan-3-one /2)}

R	$CH_3(CO)R \times 10^{11}$ ($cm^3molecule^{-1}s^{-1}$) [This work]	$CH_3R \times 10^{11}$ ($cm^3molecule^{-1}s^{-1}$) [23]
CH_3	[a]0.05	3.19
C_2H_5	[b]3.16	10.21
C_3H_7	[b]10.12	16.51
C_4H_9	[b]18.89	22.01
C_5H_{11}	[b]23.49	27.11

Table 2.4.3.4

The reactivity of linear aliphatic chains in the ketones calculated from the Cl atom rate constants determined in our laboratory and listed in Table 2.4.3.1 . Literature values calculated for the alkanes are included for comparison .

[a] Calculated from half the rate limit established for acetone in this work .

[b] Calculated from k_{Cl}(Ket-2-ones) - $k_{Cl}(\alpha\text{-}CH_3)$.

Position relativeto C=O	Reaction rates 10^{12} $cm^3molecule^{-1}s^{-1}$		Ref.
	[a]CH_3	CH_2	
α	0.11	0.8 0.7 0.9	This work [12] [11]
β	0.37	3.72 3.6 >/= 2.6	This work [12] [11]
γ	0.37	4.03	This work
δ	0.37	3.33	This work
[b]Cyclic CH_2	----	0.7 0.74	This work [27]

Table 2.4.3.5
Calculated CH_2 reactivities (with OH) in aliphatic ketones . Previous determinations are also included for comparison .
[a] Values for CH_3 reactivities used to calculate the CH_2 data was obtained from Wallington et al [11] .
[b] Cyclic CH_2 reactivity was calculated from , k_{OH}(cyclopentanone)/4 .

Position relative to C=O	Reaction Rates 10^{11} $cm^3molecule^{-1}s^{-1}$	
	[a]CH_3	CH_2
α	0.05	3.06
β	0.05	7.01
γ	0.05	8.77
δ	0.05	4.66
[b]Cyclic CH_2	----	2.19

Table 2.4.3.6
CH_2 reactivities (with Cl) in aliphatic ketones .
[a] CH_3 reactivities were set at half the reaction rate limit for Cl atoms with acetone which was established in this work .
[b] Cyclic CH_2 reactivity was calculated from k_{Cl}(cyclopentanone)/4 .

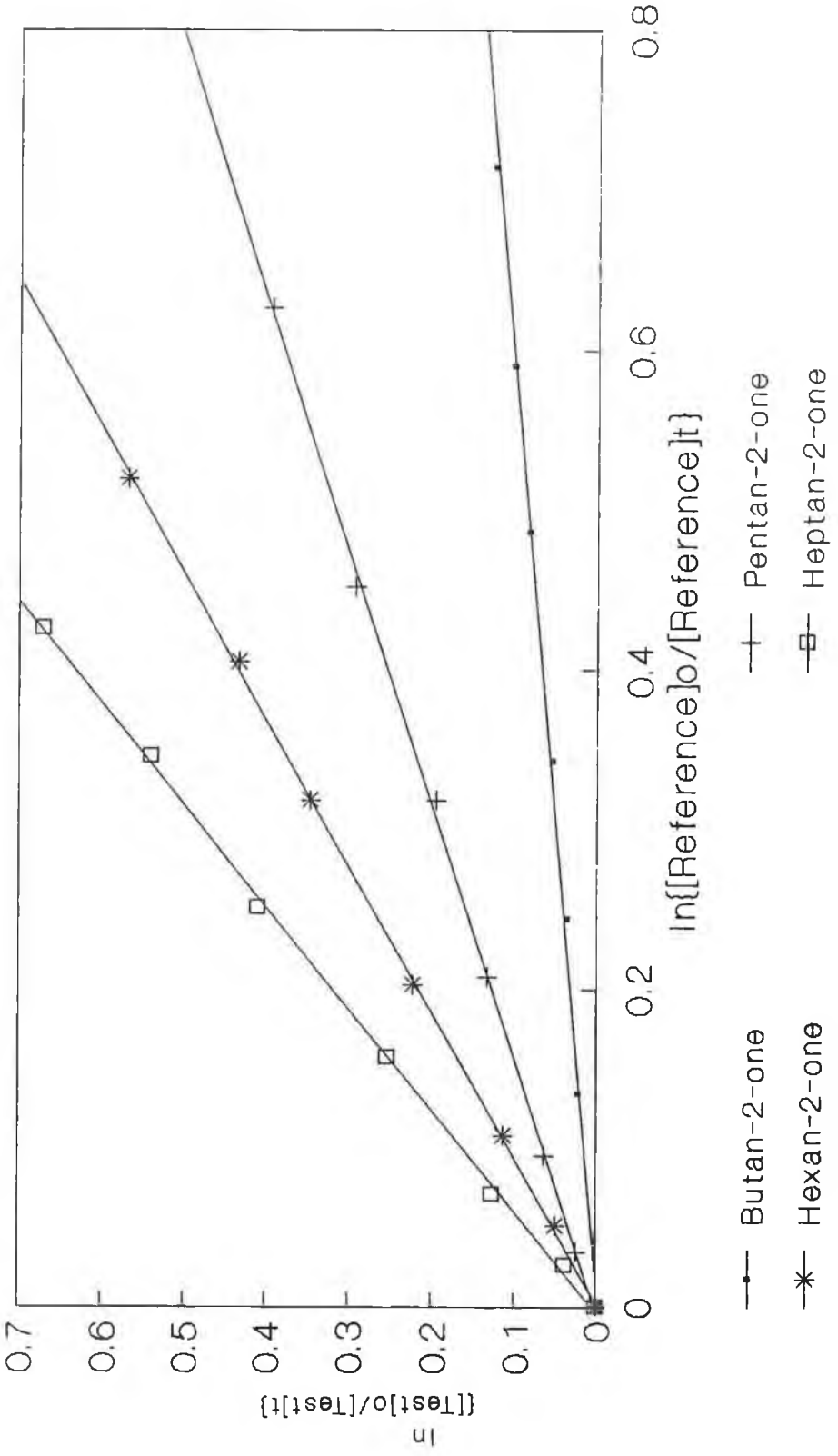

Figure 2.4.3.7
Typical relative rate plots for the reaction of a series of ketones with OH radicals using cyclohexane as a reference . Experiments were carried out at 297 ± 6 K and at atmospheric pressures of 796.62 ± 13.58 mmHg .

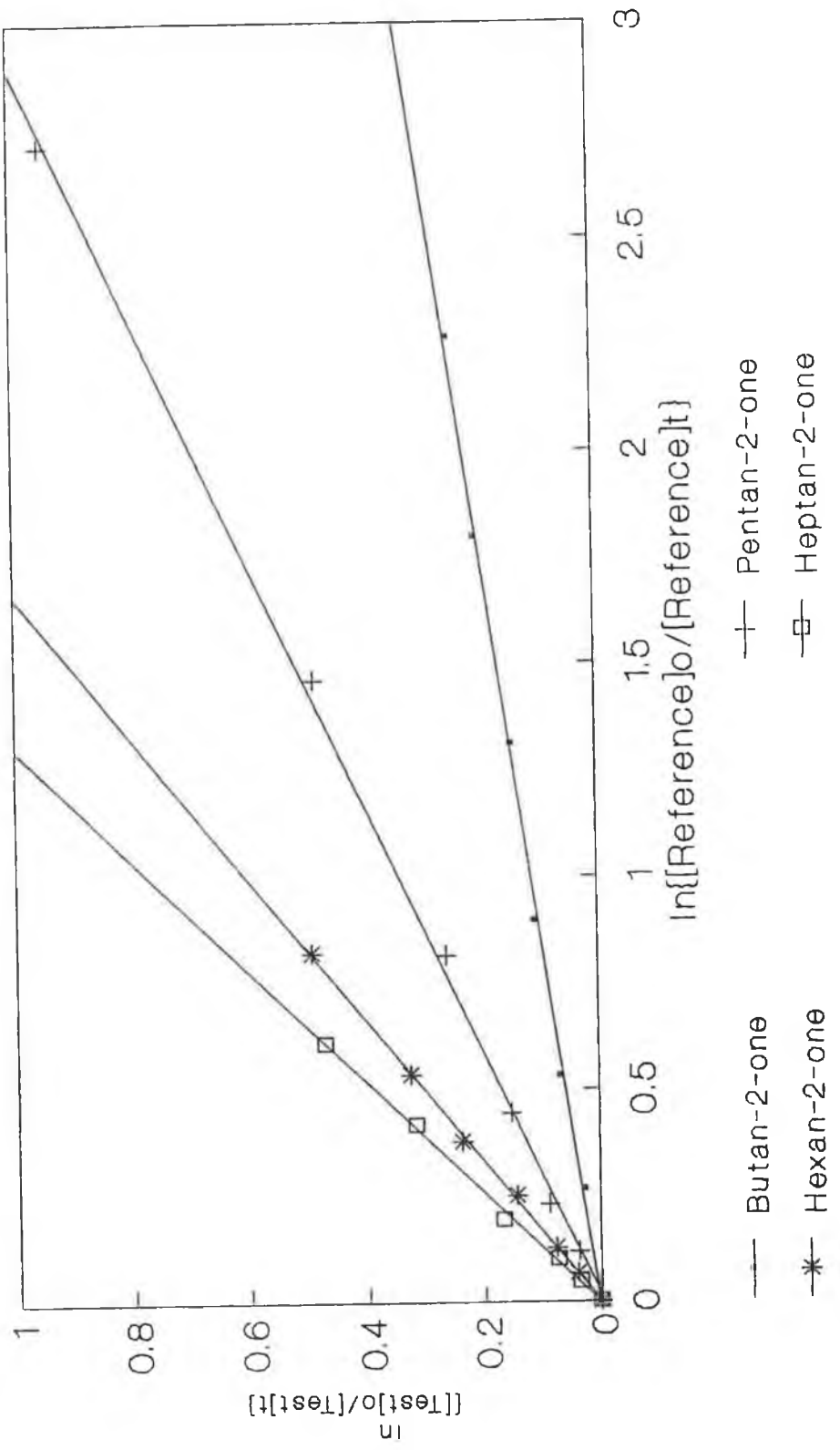

Figure 2.4.3.8

Typical relative rate plots for the reaction of Cl atoms with a series of ketones using cyclohexane as a reference . Experiments were carried out at 297 ± 6 K and at atmospheric pressures of 769.62 ± 13.58 mmHg .

The reactivity of cyclic -CH_2- groups , calculated from the reactivity of cyclopentanone , is also given in Tables 2.4.3.5 and 2.4.3.6 .

To help determine the extent to which the carbonyl group in the ketones influenced reaction , plots of ketone versus alkane reactivity were constructed , Figures 2.4.3.9 and 2.4.3.10 . The alkane rate constants used for comparison were obtained from the literature [23,6] .

To illustrate the differences in reactivity between the various pentanones (pentan-2-one , pentan-3-one etc.) with OH radicals and Cl atoms , typical relative rate plots for these species were combined as indicated in Figures 2.4.3.11 and 2.4.3.12 .

To illustrate differences in the reactivity of the various hexanones (hexan-2-one , hexan-3-one etc.) towards OH radicals and Cl atoms , typical relative rate plots for these test compounds were combined and are indicated in Figures 2.4.3.13 and 2.4.3.14 .

To determine whether a relationship existed between OH radical and Cl atom reactivities , the rate constants obtained for the reaction of each of these species with the ket-2-ones were plotted against each other as in Figure 2.4.3.15 . The limits established for the reactivity of OH radicals and Cl atoms with propan-2-one are included .

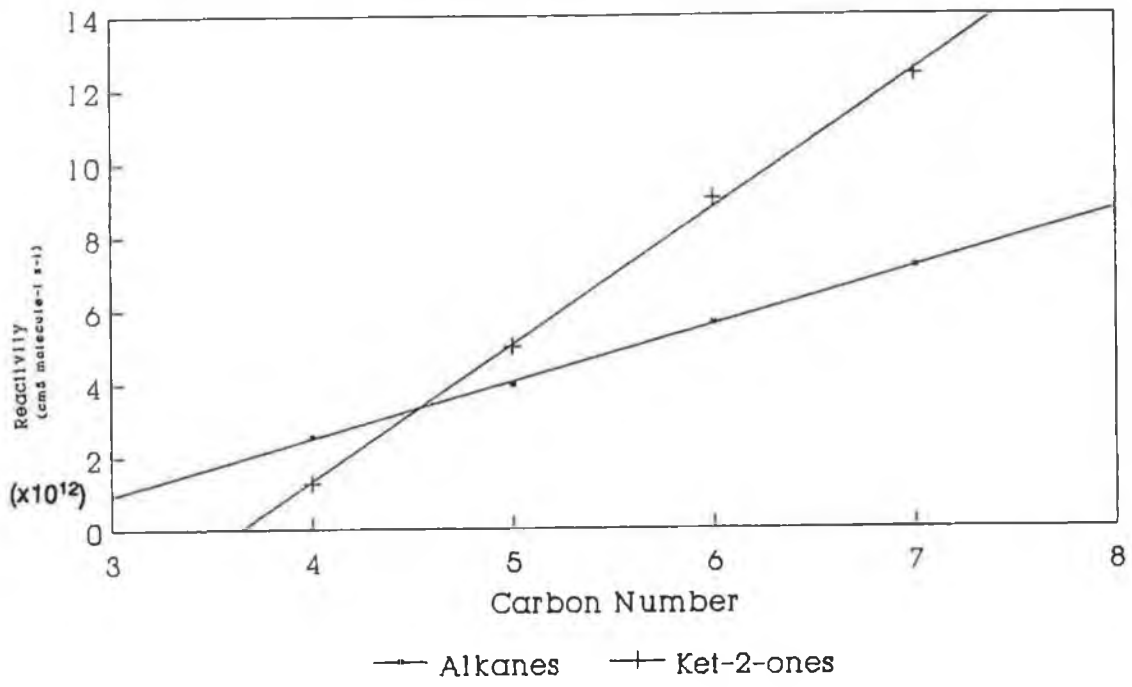

Figure 2.4.3.9
The reactivity of C_4 - C_7 ketones with OH radicals versus the corresponding alkane reactivities .

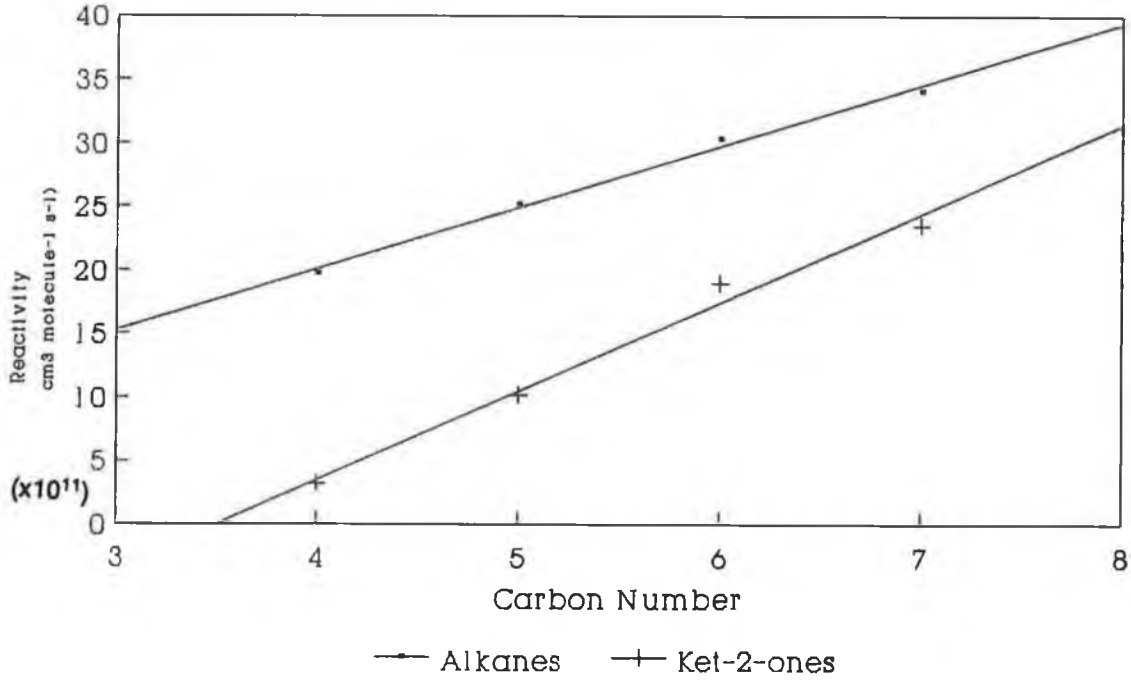

Figure 2.4.3.10
The reactivity of C_4 - C_7 ketones with Cl atoms versus the corresponding alkane reactivities .

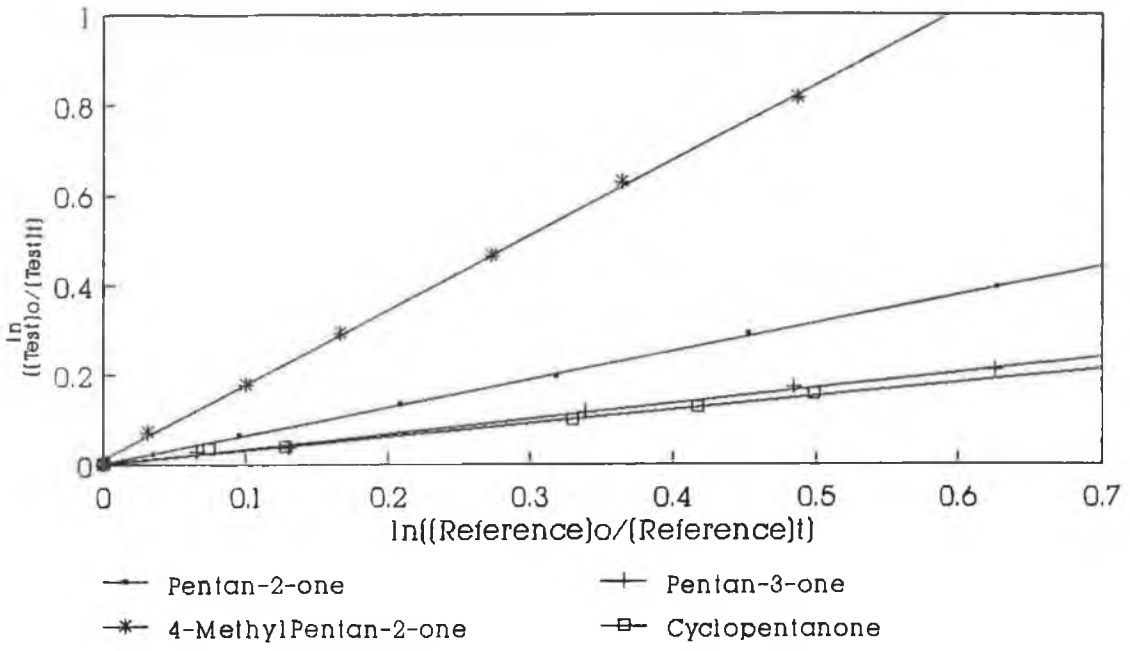

Figure 2.4.3.11
Relative rate plots typical of the reaction of OH radicals with a series of pentanones . The reference organic used was cyclohexane . Experiments were carried out at temperatures of 297 ± 6 K and atmospheric pressures 769.62 ± 13.58 mmHg .

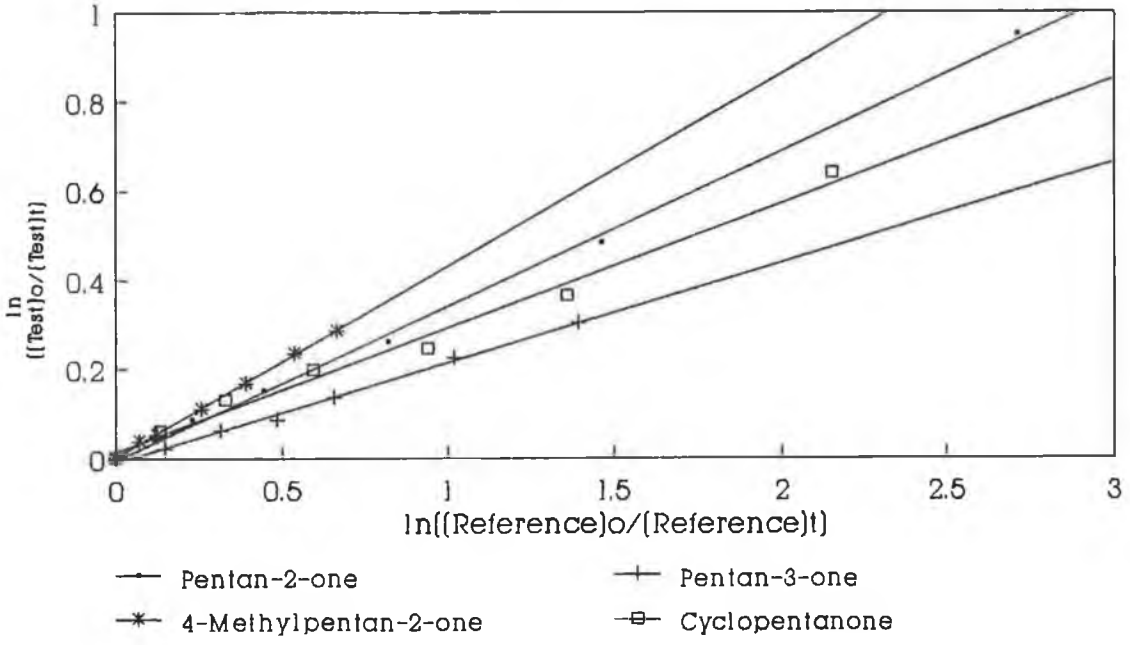

Figure 2.4.3.12
Relative rate plots typical of the reaction of Cl atoms with a series of pentanones . The reference organic used was cyclohexane . Experiments were carried out at 297 ± 6 K and atmospheric pressure of 796.62 ± 13.58 mmHg .

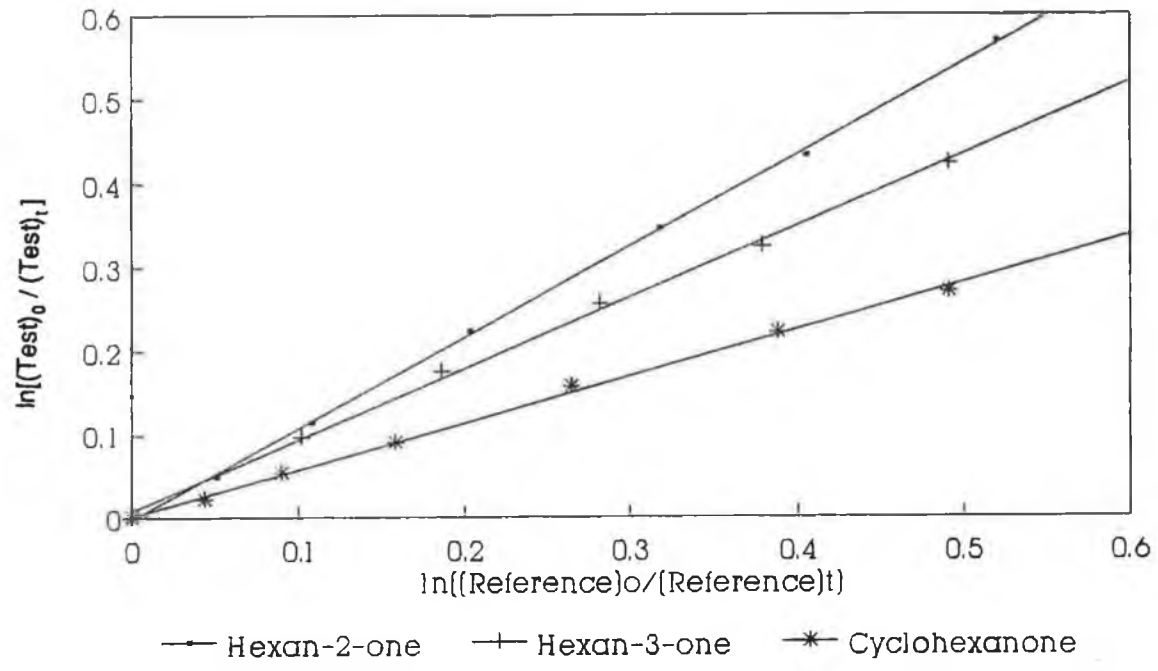

Figure 2.4.3.13
Relative rate plots typical of the reaction of OH radicals with a series of hexanones . Cyclohexane was used as the reference organic . Experiments were carried out at 297 ± 6K and at atmospheric pressure of 769.62 ± 13.58 mmHg .

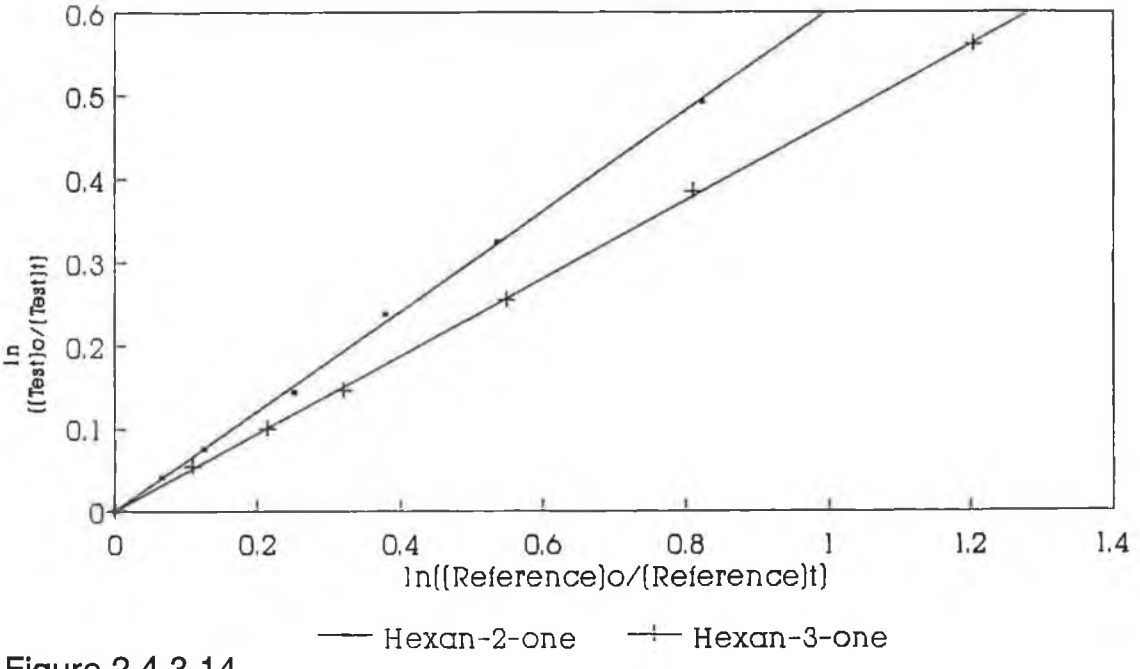

Figure 2.4.3.14
Relative rate plots typical of the reaction of Cl atoms with a series of hexanones . Cyclohexane was the reference used and experiments were carried out at 297 ± 6 K and atmospheric pressure of 769.62 ± 13.58 mmHg .

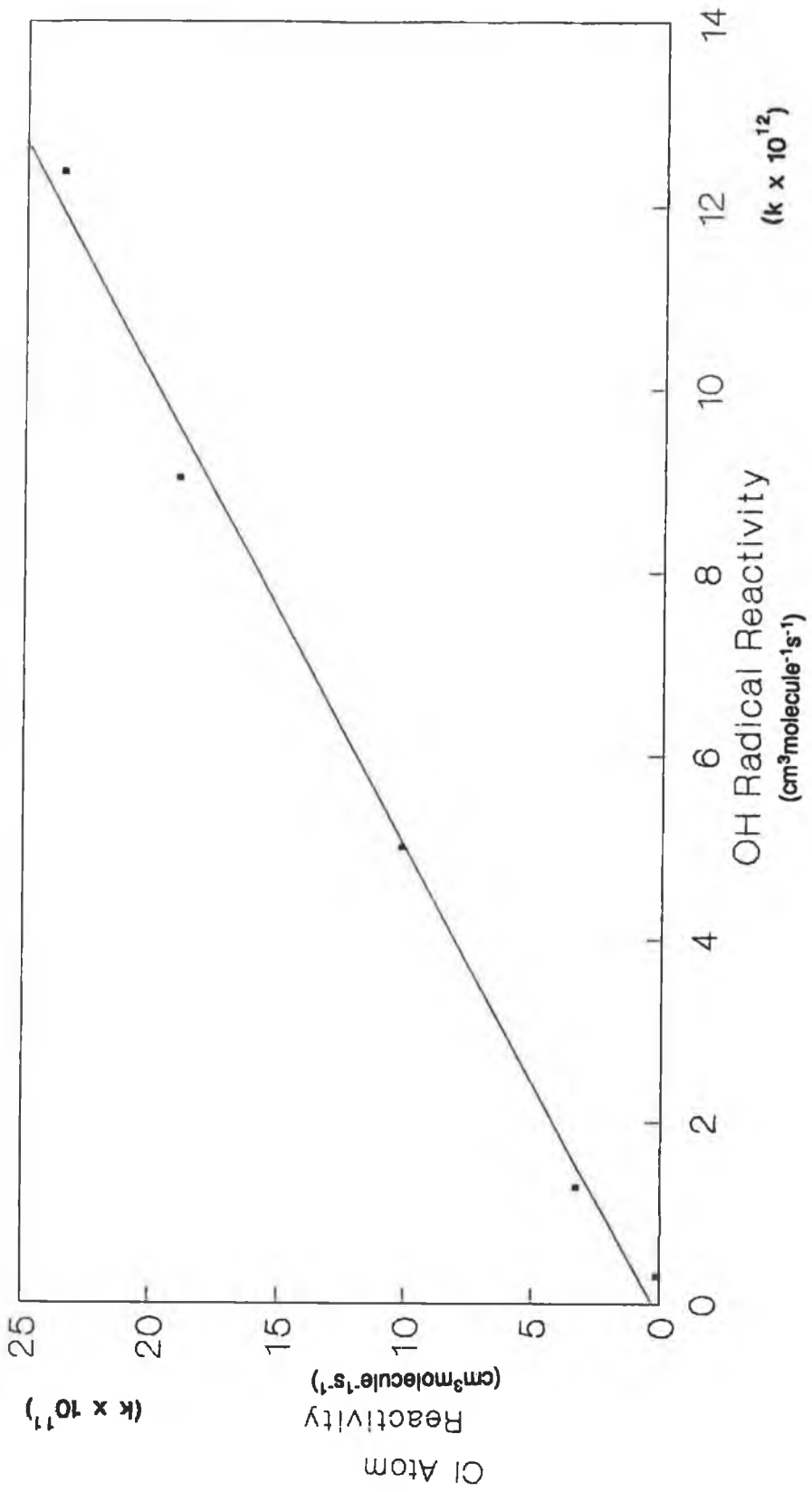

Figure 2.4.3.15
OH radical versus Cl atom rate constants for a series of ket-2-ones . Rate constants were determined at 297 ± 6 K and atmospheric pressure .

2.4.4 Discussion

The relative rate technique was used to determine accurate room temperature rate constants for a series or ketones , Table 2.4.3.1 . The majority of the values obtained are in good agreement , within experimental error , to those cited in the literature [6,11,12,27] . The large error bars quoted in Table 2.4.3.1 , for both the reference data and that obtained in our laboratory reflects the total errors (experimental + 2σ) inherent in their determination . The rate constant ratios calculated in this work and summarised in Table 2.4.3.1 indicate the high precision of the data obtainable using this system of analysis . The error bars on the slope values represents ± 2σ from a least squares analysis of our data , and did not exceed ±5% in all determinations . The large error bars quoted on the actual rate constants is due predominately to the uncertainty in the reference rate constant used to place this data on an absolute basis .

From Table 2.4.3.1 the relative importance of Cl atoms to OH radicals as a loss mechanism for the ketones in the troposphere is reflected in the difference in magnitude of the two sets of rate constants , An interesting observation is the fact that in most cases the OH radical rate constants in Table 2.4.3.1 are approximately 20 times slower than the corresponding Cl atom rate values . Therefore from a knowledge of the OH radical rate constants , estimates of the Cl atom reaction rates can be made and vice versa . However , 4-methyl pentan-2-one reacts only ca. 9 times faster with Cl atoms than with OH radicals . It is possible that the two extra methyl groups may hinder attack on the ketone by the larger Cl atoms , relative to the OH radicals giving a decrease in the Cl atom rate constant . Cl atoms were found to react almost 30 times faster with cyclopentanone than OH radicals . The greater reactivity of Cl atoms may negate the effects of ring strain which is more noticeable in the slower

reacting OH radical species , thus giving rise to this greater gap in reactivity .

By comparing the reaction rates for the ketones with OH radicals and Cl atoms listed in Table 2.4.3.1 , it is possible to determine which of these loss processes will dominate in the troposphere . Although the Cl atom rate constants are between 10 and 30 times that of the OH radical rate constants , it is estimated that OH radicals are approximately 1000 times more abundant in the troposphere [17] . Therefore , the dominant loss mechanism for the ketones studied in this work will be reaction with OH radicals . This high reactivity of the ketones with OH radicals is also indicated in Table 2.4.3.2 , i.e. the tropospheric lifetimes of the ketones with respect to OH radicals are much shorter than the corresponding lifetimes relative to reaction with Cl atoms . From the lifetimes indicated in Table 2.4.3.2 , it can be concluded that only propan-2-one (acetone) will persist for any significant time in the troposphere . It is likely therefore that acetone may reside long enough in the troposphere to facilitate transportation of a small concentration to the stratosphere where the major loss process for this species would be photodecomposition .

Before any rate constant data could be determined , the stability of the ketones in the dark and relative to photodecomposition was established . Figues 2.4.3.1 to 2.4.3.4 illustrates the stability of a number of the ketones under various experimental conditions .

Having established that loss of both test and reference organics would proceed solely by reaction with OH radicals and Cl atoms , we then optimized the analytical conditions to ensure no interference from reaction products . As mentioned in Section 2.4.3 "decay curves" were established for the test and reference organics to ensure reaction products from each of these species did not interfere in the subsequent relative rate determinations . Typical decay curves are given in Figures 2.4.3.5 and

2.4.3.6 . As a similar reference organic was used in these determinations , the rate of decay in these diagrams illustrates the differences in reactivity between the species i.e. the greater the decline the faster the reaction .

Once the preliminary requirements of the relative rate technique had been satisfied , rate constant ratios were then calculated as outlined in Section 2.1 . Ratios were obtained from the slopes of relative rate plots similar to those examples indicated in Figures 2.4.3.7 and 2.4.3.8 . An interesting observation from the relative rate plots in Figures 2.4.3.7 and 2.4.3.8 is the increased slopes from butan-2-one to heptan-2-one i.e. as the number of abstractable hydrogens increases so too does the OH radical and Cl atom rate constants . This similarity in reaction order for the ketones with respect to both OH radicals and Cl atoms reflects the similarity in reaction mechanisms involved . The example plots illustrated in Figures 2.4.3.7 and 2.4.3.8 demonstrate the high level of linearity (all regression values were above 0.995) and low intercepts obtainable using our system of analysis .

From the calculated rate constant ratios , precise and accurate rate constants for the reaction of a number of ketones with OH radicals and Cl atoms was established . Cyclohexane was used as the reference organic for the determination of OH radical and Cl atom rate constants . Total errors were included in all calculations so that a clearer picture of the typical uncertainties associated with these experiments is obtained . In general a misleading picture of rate constant errors is given by atmospheric researchers where it has become common practice to site result data with error bars equivalent to $\pm 2\sigma$ from least squares analysis of their result data . In reality , however , experimental errors or errors inherent in the reference rate compound may result in an overall error as high as ±30% .

The accuracy of the rate constant data listed in Table 2.4.3.1 is illustrated by the similarity of these results to those of previously published rate data . (Rate data was only available with regard to the reaction of OH radicals with the ketones) . The precision of these rate constant ratios is reflected in the small error bars on these values .

Having calculated rate constants for the reaction of OH radicals and Cl atoms with a number of ketones , it was then possible to use this data to investigate effects of ketone structure on reactivity . From the OH radical rate constants for the C_3 to C_7 aliphatic ketones , it was possible to calculate the reactivity of these linear chains :

e.g.

k_{OH} Pentan-3-one ($CH_3CH_2COCH_2CH_3$) = 2.73 x 10^{-12} $cm^3molecule^{-1}s^{-1}$

- hence the reactivity of the C_2H_5 group in this ketone is approximately (2.73 / 2) x 10^{-12} $cm^3molecule^{-1}s^{-1}$ or 1.37 . A similar method was used to calculate reactivities for C_3H_7 , C_4H_9 and C_5H_{11} groups with the ketones and the results are presented in Table 2.4.3.3 . As only a rate limit was established for the reactivity of OH radicals with acetone in this work , values for the reactivity of ketone CH_3 - groups calculated by Wallington et al [11] were used to calculate the reported linear chain reactivities . Values calculated from rate constant data obtained by Wallington et al [11] and Atkinson [6] are included in Table 2.4.3.3 for comparison . Alkane linear chain reactivities calculated from rate constant data recommended by Atkinson [6] for the C_2 - C_6 alkanes is also illustrated . Very close correlation exists between the ketone reactivity data reported in this work and that of Atkinson [6] , while significant differences are observed with data calculated by Wallington et al [11] . As the data recommended by Atkinson [6] reflects an average best estimate of all published ketone -OH radical rate data up to 1989 including that of Wallington et al [11] , it would

be expected that these values may be the best estimate of the true reactivity for these species .

The alkane chain reactivity closely matches that of the ketones when R is a CH_3 group . However , activating of the ketones towards OH radical attack is illustrated by the greater chain reactivity of the ketones over the corresponding alkanes in Figure 2.4.3.3 . This activation effect is due to the presence of the oxygen in the carbonyl group of the ketones . Such an activating effect is evident in many oxygenated organic systems .

No enhancement of the CH_3 group reactivity is evident in the ketones relative to the corresponding alkane CH_3 moiety . This supports Wallington et al's [11] ring adduct formation theory i.e., there are no groups further than the α-position in acetone to form a ring structure with OH radicals . Hence reaction of acetone with OH radicals proceeds via a straightforward H-atom abstraction process .

Similar linear chain length reactivities were calculated for the reaction of Cl atoms with the ketones and these are listed in Table 2.4.3.4 . A rate limit was established for the reaction of Cl atoms with acetone and this figure was used to calculate a maximum value for the reactivity of ketone CH_3 groups with Cl atoms :

i.e.

$$k_{Cl}\ CH_3OCH_3 = < 0.1 \times 10^{-11}\ cm^3\ molecule^{-1}\ s^{-1}$$

$$=> k_{cl}\ CH_3 \text{ in acetone} = < 0.05 \times 10^{-11}\ cm^3 molecule^{-1} s^{-1}$$

From this value it was then possible to calculate the reactivity of C_2-C_5 aliphatic ketone chains with Cl atoms . The values for these reactivities are compared with the corresponding alkane chain reactivities calculated from rate constant data obtained by Atkinson et al [23] . Unlike OH radical reactivites the reaction of the alkane chains with Cl atoms is greater than the corresponding ketones . As in the case of the ethers [29] the

activating effect of the oxygen may have a less dramatic effect on the reactivity of the hydrogen atoms especially those on distant carbons . The very low reactivity of the ketone CH_3 groups (calculated from the reactivity of acetone) relative to the CH_3 groups in ethane illustrates that a ring adduct mechanism may be an intermediate step in the H-atom abstraction process for these ketones . As shown by Wallington et al [11] this adduct formation gives rise to activation in reactivity of groups β and γ to the carbonyl group in OH radical reactions with the ketones . Other possible reasons for the smaller ketone chain reactivities relative to the alkanes could be due to steric hindrance or polarity effects caused by the presence of the oxygen atom in the ketones .

To further investigate the factors affecting ketone reactivity with OH radicals and Cl atoms , the rate constant data was coupled with published rate data to obtain group reactivities (-CH_2- groups primarily) for these species .

Table 2.4.3.5 lists the OH radical -CH_2- group reactivities for the ketones calculated using our OH radical rate data and Wallington's [11] CH_3 group reactivities . The value of 0.11×10^{-12} $cm^3molcule^{-1}s^{-1}$ calculated by Wallington et al [11] for the CH_3 reactivity in the ketones was calculated from the OH radical reactivity of acetone i.e. k_{OH} CH_3OCH_3 = 0.22×10^{-12} $cm^3molecule^{-1}s^{-1}$. Similar reactivity calculations allowed determination of β-CH_3 group reactivities [11] . In our calculation of -CH_2- group reactivities , it was assumed that the reactivity of CH_3 groups relative to OH radicals remained essentially constant once beyond the α-position . Therefore a fixed value of 0.37×10^{-12} $cm^3molecule^{-1}s^{-1}$ was used for CH_3 group reactivities in the β , γ and δ positions in the ketones (with OH) . Using these values of CH_3- group reactivities , it was then possible to calculate the -CH_2- reactivities listed in Table 2.4.3.5 . From these values for CH_2 group reactivities the activating effect at the β and γ

positions is clear . From this present study activation of the ketones to attack by OH radicals is indicated as far as the δ position . Similar α and β-CH_2-group reactivities were obtained to those calculated by Atkinson et al [12] and Wallington et al [11] . This activation of the β and γ -CH_2- groups is also indicated by comparing the reactivity at these groups to those of -CH_2- groups in the alkanes. A value of k_{OH}-CH_2- for the alkanes of 1.2 x 10^{-12} $cm^3molecule^{-1}s^{-1}$ was recommended by Atkinson et al [30] . Thus , α-CH_2- group reactivities with OH radicals approximates that of -CH_2- groups in the alkanes whereas -CH_2-groups at the β, γ and δ positions in the ketones are approximately 3 times more reactive . Similar observations were made by Atkinson et al [12] thus it would appear that the ring adduct mechanism proposed by Wallington et al [11] is indeed probable .

Further supportive evidence for this ring intermediate is found in the OH - CH_2-group reactivities calculated for the cyclic ketones . Cyclic -CH_2- group reactivites for the ketones studied are below those calculated for the analogous alkanes and well below that of -CH_2- groups in the aliphatic ketones ;

i.e.

Carbons in ring structure	[a]Alkane-CH_2- reactivity	Ketone-CH_2-reactivity
C_5	1.03	0.7
C_6	1.25	0.95

Table 2.4.4.1
Comparison of cyclic-CH_2-group reactivites in the ketones to those in the corresponding alkanes .
[a]Cyclic alkane reactivities were calculated from rate constant data recommended by Atkinson [6] .

Since the ring structure of these cyclic ketones would inhibit the formation of the adduct intermediate , similar -CH_2- group reactivities to those of the alkanes would be expected . Lower group reactivities for the ketones relative to the alkanes may result from hindrance caused by the oxygen in the carbonyl group . As in the alkanes , the average -CH_2- group reactivity in the cyclic species increases on going from the C_5 to the C_6 ring structure. This is as expected due to a concommitant decrease in ring strain effects.

Similar Cl atom -CH_2- group reactivities were calculated for the ketones and these are presented in Table 2.4.3.6 . CH_3-reactivity in the ketones was established from the rate limit established for the reaction of Cl atoms with acetone . This reactivity (0.05×10^{-11} $cm^3 molecule^{-1} s^{-1}$) was assumed to remain constant irrespective of the position of this CH_3 group in the ketone chain .

As in the case of OH radical reactions with the aliphatic ketones attack at the α - position is not favoured . However the distance of activation seems to extent only to the β and γ positions . The magnitude of the β and γ -CH_2- group reactivities in the ketones is only slightly higher than that for the alkanes (ca. 6.5×10^{-11} cm^3 $molecule^{-1}$ s^{-1} -- estimated from the Cl - alkane chain reactivities in Table 2.4.3.4) . It is possible that attack on the ketones by Cl atoms proceeds via a ring adduct mechanism. The high -CH_2- group reactivities at the β and γ position may be due to the formation of this ring adduct prior to H-atom abstraction (similar to the formation of the ring adduct mechanism proposed by Wallington et al [11] for the attack of OH radicals on aliphatic ketones) . Attack at the α-CH_2 group in the ketones may be effected not only by this intermediate ring formation , but also by steric hindrance caused by the carbonyl oxygen .

The -CH_2-group reactivities in cyclopentanone are low , not just in relation to the other ketone -CH_2- reactivities , but also compared to that

calculated for $-CH_2-$ groups in the alkanes (i.e. k_{Cl} $-CH_2-$ cyclohexane = 6.08×10^{-11} $cm^3molecule^{-1}s^{-1}$ [6]) . This reduction in reactivity is probably due to the inability of the cyclic ketone to form a stable adduct intermediate in a similar manner to the straight chain ketones . Coupled with this , attack by large Cl atoms may be significantly hindered by the carbonyl oxygen and by the ring structure of the cyclic ketone .

From the group reactivities in Tables 2.4.3.5 and 2.4.3.6 it would appear that attack at the γ position is the most favoured by both OH radicals and Cl atoms . It may be that this position in the ketones forms the most stable ring adduct with the reactive species ,

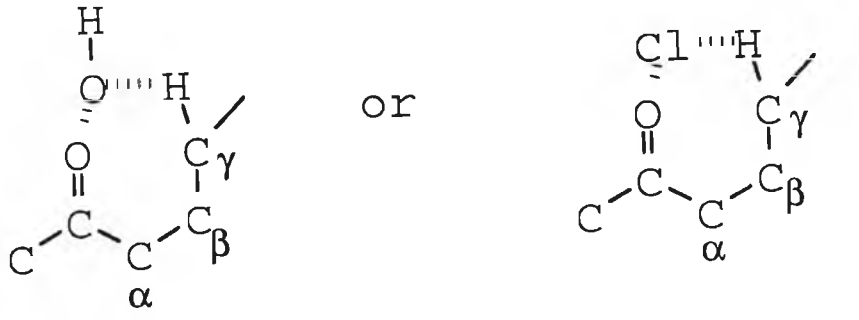

To examine possible differences in reaction mechanisms between the ketones and the alkanes with OH radicals and Cl atoms the reactivity of a series of aliphatic ketones was plotted versus those of the corresponding series of alkanes . These comparison plots are given in Figures 2.4.3.9 and 2.4.3.10 .

In Figure 2.4.3.9 the similarity in reaction rate between the C_4 ket-2-one and C_4 alkane with OH radicals is illustrated . However above C_5 the ket-2-ones react much faster than the corresponding alkanes . This difference in reactivity supports the formation of the ring adduct intermediate proposed .

In Figure 2.4.3.10 , activation of the ketones towards reaction with Cl atoms is not illustrated . From Table 2.4.3.6 it is evident that hydrogens close to the carbonyl group in the ketones are not at all reactive with Cl

atoms . The deactivating effect of this carbonyl moiety however is diluted to a certain extent with increasing aliphatic chain length , hence the convergence of the lines in Figure 2.4.3.10 . I would conclude that the formation of a ring adduct intermediate is very important in increasing the reaction of OH radicals with the ketones , however this activating effect is offset in the Cl atom reactions by steric hindrance effects at carbons close to the carbonyl moiety .

A number of pentanones were studied in this work with different factors effecting the magnitude of the OH radical and Cl atom rate constants obtained for these species . Figures 2.4.3.11 and 2.4.3.12 illustrate typical relative rate plots for the reaction of a number of pentanones with OH radicals and Cl atoms . The higher the observed slopes in these diagrams the faster the particular ketone reacts . In both the OH radical and Cl atom plots , 4-methyl pentan-2-one had the fastest reaction rate reflecting the high number of H - atoms available for abstraction in this compound . The second most reactive ketone in Figures 2.4.3.11 and 2.4.3.12 was pentan-2-one possibly owing to it's ability to form a stable cyclic intermediate at the β-CH_2 group thus facilitating abstraction of H - atoms with ease . Pentan-3-one on the other hand reacted only slowly with both OH radicals and Cl atoms . The main reason for this decreased reactivity is due to the absence of an activating -CH_2- moiety in it's structure . The relatively slow reaction of cyclopentanone is due to the effects of both ring strain and due to the inability of this ketone to form a stable cyclic intermediate prior to H - atom abstraction .

The reactivity of a number of hexanones were studied with both OH radicals and Cl atoms . As with the pentanones the ketone containing the carbonyl moiety on the second carbon reacted quickest . Since hexan-2-one contains two activating -CH_2- groups at the β and γ positions , it

reacts rapidly with both OH radicals and Cl atoms . Hexan-3-one reacted slower as it contains only one activating site at the β -CH_2- position .

Finally , the OH radical and Cl atom rate constants obtained for reaction with the ket-2-ones were plotted against each other (Figure 2.4.3.15) . This diagram supports the earlier arguement that with a knowledge of the OH radical rate constants for these species , it is possible to calculate the Cl atom rate constants and vice versa . As the limits of reactivity established for propan-2-one included in Figure 2.4.3.15 are linear with respect to the calculated rate data , I would conclude that the actual rate constant values for the reaction of propan-2-one with OH radicals and Cl atoms are very close to the esimated values presented in Table 2.4.3.1 .

Rate constants obtained for the reaction of OH radicals and Cl atoms with the ketones studied in this work points towards a more complex mechanism of reaction than just straightforward H - atom abstraction . The proposed ring adduct formation could be of great importance in assessing the atmospheric fate and thus significance of these ketones . Further work needs to be carried out to determine accurate values for CH_3 group reactivities . From these values the reactivity of hydrogens at the various carbon sites in the ketones could be accurately estimated and the formation of a ring adduct intermediate confirmed or disproved .

2.4.5 Conclusion

Using a smog chamber - relative rate technique accurate and precise rate constant data was calculated for the reaction of OH radicals and Cl atoms with a series of ketones . From this data it was observed that Cl atoms react approximately 20 times quicker with linear aliphatic ketones than OH radicals . This observation may be useful in predicting the reactivity of such ketones with one reactive species from a knowledge of the reaction rate of the ketone with the other reactive species . The magnitude of the difference between the rate constant values obtained for the reaction of Cl atoms with the ketones relative to the corresponding OH radical rate values , confirms reaction of the ketones with the later reactive species as the dominant loss process for these oxygenated hydrocarbons in the troposphere . Each of the ketones studied have low tropospheric lifetimes with respect to both OH radicals and Cl atoms , indicating that these compounds will be rapidly removed from the troposphere .

Formation of a cyclic adduct intermediate prior to H-atom abstraction is implicated in the reaction of OH radical and Cl atoms with aliphatic ketones . The mechanism is supported by :

(a) the low reactivity of α-CH_2 groups ;

(b) activation of β,γ and δ -CH_2-groups towards attack ;

(c) low reactivity of cyclic -CH_2 groups ;

(d) high linear chain reactivities above C_4 ; and

(e) greater reactivity of ketones above C_4 than the corresponding alkanes.

The reaction of Cl atoms with the ketones may be effected by steric hindrance from the carbonyl oxygen . This may account for the lower reactivity observed for these species with the ketones relative to the alkanes.

Rate constant result data also indicated that the effects of ring strain on the rate of OH radical attack on the cyclic ketones , decreases as the ring size increases .

2.4.6 References

[1] P. Carlier , H. Hannachi , and G. Mouvier , *Atmos. Environ.* , **20** , 11 , 2079 , (1986) .

[2] J.A. Kerr , and D.W. Stocker , *J. Atmos. Chem.* , **4** , 253 , (1986).

[3] C&EN , 28 , June 24 , (1991) .

[4] E.C. Tuazon , and R. Atkinson , *Int. J. Chem. Kinet.* , **21** , 1141 , (1989) .

[5] R. Atkinson , *Atm. Environ.* , **24A** , 1 , 1 , (1990) .

[6] R. Atkinson , *J. Phys. Chem. Ref. Data* , Monograph 1 , (1989) .

[7] H. Heyrahn , J. Pauly , W. Schneider , and P. Warreck , *J. Atmos. Chem.* , **4** , 277 , (1986) .

[8] R.A. Cox , M.C. Addison , J.P. Burrows , and R. Patrick , 14th Int. Conf. Photochem. , 30 March-3 April , (1980) .

[9] R. Atkinson and W.P.L. Carter , *Chem. Rev.* , **84** , 437 , (1984) .

[10] B.J. Finlayson-Pitts and J.N. Pitts Jr. , "Atmospheric Chemistry" , Wiley & Sons , Publishers , (1986) .

[11] T.J. Wallington and M.J. Kurylo , *J. Phys. Chem.* , **91** , 5050 , (1987) .

[12] R. Atkinson , S.M. Aschmann , W.P.L. Carter , and J.N. Pitts Jr. , *Int. J. Chem. Kinet.* , **14** , 839 , (1982) .

[13] R.A. Cox , K.F. Patrick , and S.A. Chant , *Environ. Sci. Technol.* , **15** , 5 , 587 , (1981) .

[14] C. Chiorboli , C.A. Bignozzi , A. Maldotti , P.F. Giardini , A. Rossi , and V. Carassiti , *Int. J. Chem. Kinet.* ,**15** , 579 , (1983) .

[15] R. Atkinson , S.M. Aschmann , and J.N. Pitts Jr. , *Int. J. Chem. Kinet.* , **15** , 75 , (1983) .

[16] A.M. Winer , A.C. Lloyd , K.R. Darnall , and J.N. Pitts Jr. , *J. Phys. Chem.* , **80** , 14 , 1635 , (1976) .

[17] H.B. Singh and J.F. Kasting , *J. Atmos. Chem.* , **7** , 261 , (1988) .

[18] T.J. Wallington , J.M. Andino , I.M. Lorkovic , E.W. Kaiser , and G. Marston , *J. Phys. Chem.* , **94** , 3644 , (1990) .

[19] T.J. Wallington , M.M. Hinman , J.M. Andino , W.O.Siegl , and S.M. Japar , *Int. J. Chem. Kinet.* , **22** , 665 , (1990) .

[20] L.G. Yannis , M. Chrysostomos , and P. Panos , *J. Phys. Chem.* , **96** , 1705 , (1992) .

[21] A.T. Droege , and F.P. Tully , *J. Phys. Chem.* , **91** , 1222 , (1987).

[22] N. Bourmada , C. Lafage , and P. Devolder , *Chem. Phys. Lett.* , **136** , 2 , 209 , (1987) .

[23] R. Atkinson , and S.M. Aschmann , *Int. J. Chem. Kinet.* , **17** , 33 , (1985) .

[24] D.D. Davis , W. Braun , and A.M. Bass , *Int. J. Chem. Kinet.* , **2** , 101 , (1970) .

[25] T.J. Wallington , L.M. Skewes , W.O. Siegl , C.H. Wu , and , S.M. Japar , *Int. J. Chem. Kinet.* , **20** , 867 , (1988) .

[26] J.J. Bufalini , and R.R. Arnts , **EPA** / 600 / 3-87 / 046 ,Nov., (1987) .

[27] P. Dagaut , T.J. Wallington , R. Liu , and M.J. Kurylo , *J. Phys. Chem.* , **92** , 4375 , (1988) .

[28] R. Prinn , D. Cunnold , R. Rasmussen , P. Simmonds , F. Alyea , A. Crawford , P. Fraser , and R. Rosen , *Science* , **238** , 945 , (1987) .

[29] L. Nelson , O. Rattigan , R. Neavyn , H. Sidebottom , J. Treacy , and O.J. Nielson , *Int. J. Chem. Kinet.* , **22** , 1111 , (1990) .

[30] R. Atkinson , K.R. Darnall , A.C. Lloyd , and A.M. Winer , *Adv. Photochem.* , **11** , 375 , (1979) .

CHAPTER 3.0

A preliminary investigation into the gas phase photooxidation of the anaesthetics , isoflurane and enflurane

3.1 Introduction

In chapter two , the tropospheric lifetime , and release figures for the two anaesthetic ethers , isoflurane and enflurane were established . From this result data and from rate constant data calculated by Brown et al [1] it is predicted that a small proportion of these ethers will persist in the troposphere for up to 2.5 years . As a consequence , a fraction of the volume of these anaesthetics released at the earth's surface may reach the stratosphere where the dominant loss process will involve photodecomposition and photooxidation . Therefore to complete the assessment of the potential atmospheric impact of these two compounds , the photooxidation of these species at wavelengths as low as 200 nm was studied .

Compounds of the type $R^1 - O - R^2$ are called ethers , the simplest of these are colourless and have a characteristic smell . The first member of the ether homologous series , dimethyl ether , is a gas and the lower ethers are liquids at room temperature . The boiling point of an ether is usually similar to that of the alkane from which it can be formally derived by substitution of an oxygen atom for a methylene group , and significantly lower than that of the isomeric primary alcohol . The relatively high boiling point of the alcohol is believed to be due to association of alcohol molecules in the liquid phase by intermolecular hydrogen bonding which cannot occur with ethers or alkanes , although ethers can participate with protic compounds in intermolecular hydrogen bonding . Ethers can also form ether-soluble complexes with a number of Lewis acids , they dissolve a variety of organic compounds and they are unreactive under various reaction conditions [2] . These properties make ethers useful solvents for organic reactions . Some ethers with low molecular weight , e.g. dimethyl ether , or with several ether groups , e.g.

1,2-dimethoxyethane , are immiscible with water and are extensively used for solvent extraction in organic chemistry .

Probably the most commonly known property of diethyl ether is it's ability to cause anaesthesia . It has been used as a general anaesthetic since it was first used for this purpose by a Boston dentist in 1848 . In concentrations in air or oxygen between 3.6 - 6.5% by volume , inhalation of diethyl ether causes anaesthesia but concentrations greater than 10% are usually fatal . The ether anaesthetics act on the central nervous system and are believed to interfere with transmission of nerve impulses . A serious disadvantage associated with mixtures of diethyl ether and oxygen used in anaesthesia , is that the mixtures are dangerously explosive and this hazard has prompted a search for safer alternatives . The search led to the discovery of new fluoroether anaesthetics such as isoflurane and enflurane . These highly halogenated ethers are now the most commonly used inhalation anaesthetics in the Western world .

The feature of ethers which is most important in determining the chemical and physical properties of this class of compound is the presence of the oxygen atom with it's lone pair of electrons . The central feature of much of the chemistry of ethers is their ability to act as bases and form coordination complexes with a wide variety of acids . This interaction involves one or more of the lone pairs of electrons on oxygen and ethers are therefore classified as n-donors .

Because of the greater electronegativity of the oxygen atom compared with carbon , the C - O bond will be polarised and alkoxy groups will attract electrons inductively [2] . The effect of this inductive withdrawal of electron density is most marked at the α-carbon atom and rapidly diminishes with distance through space or along a saturated chain of atoms . The strength of this withdrawal of electron density is such that it decreases H-atom bond dissociation energies on methylene groups in the

ethers , thus increasing the speed at which these H-atoms are removed by OH radical and Cl atoms [3] . Reactions with these reactive species are important as tropospheric removal mechanisms for ethers released to the atmosphere . The increased reactivity of the ethers towards reaction with OH radicals relative to the corresponding alkane reaction has been demonstrated by a number of workers ; this work has also shown that the activating effect of the oxygen in the ether is operative up to 5 carbons from the oxygen atom [4] .

In contrast to the above effect , because of the presence of the lone electron pairs on the oxygen atom , alkoxy groups can release electron density on demand to stabilize adjacent cations e.g. (3.1.1) , or radicals e.g. (3.1.2) , by resonance .

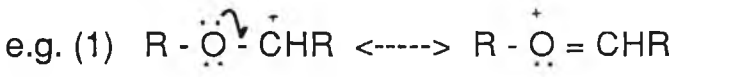

e.g. (1) (3.1.1)

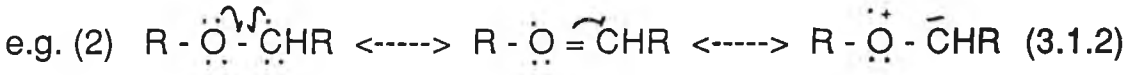

e.g. (2) (3.1.2)

The polarization of the C - O bond in the ethers caused by the different electronegativity of carbon and oxygen is not sufficiently marked to make the bond generally susceptible to cleavage by nucleophilic attack at the α-carbon .

The ability of the ether oxygen to facilitate the generation of a radical or carbonium ion at the α-position is believed to be a crucial factor in directing the reaction of oxidizing agents to this position . Two general types of mechanism for oxidation of ethers can be envisaged involving abstraction of hydrogen by radicals , as in the mechanism proposed for autooxidation (3.1.3) , or abstraction of hydride ion in oxidation by bromine (3.1.4) ,

$$R\cdot + H - CR_2OR \text{ ------> } RH + R_2\cdot COR \text{ ------> Products} \qquad (3.1.3)$$

$$Br \text{ -- } Br \text{ -- } H \text{ -- } CR_2OR \text{ ------> } R_2{}^+COR \text{ ------> Products} \qquad (3.1.4)$$

Generally , ethers are more resistant to oxidation than aldehydes or acetals , which are the first products of oxidation of primary ethers and therefore further oxidation to acids or esters is common . Reagents which have been used to oxidise ethers include bromine , chromic oxide - acetic acid , and mercuric acetate [2] .

Ethers tend to autoxidize readily in the presence of air or oxygen at normal temperatures to give peroxides . This autooxidation represents a potential hazard to users of ether solvents as these peroxide products which concentrate in the residue on evaporation can detonate . Autooxidation commences by production of radicals and so any radical source is an effective catalyst for this reaction . As well as a range of organic initiators , salts of manganese , iron , cobalt , copper , and lead greatly accelerate autooxidation by catalysing decomposition of peroxides into radicals .

The ability of alkoxyl groups to stabilise an adjacent cation promotes facile heterolysis of the carbon - halogen bond in α - haloethers and consequently these compounds are extremely reactive under conditions that favour both S_N 1 and S_N 2 mechanisms . Thus for example , it has been estimated that hydrolysis of chloromethyl methyl ether is 10^{13} times faster than hydrolysis of 1-chloropropane .

Saturated ethers only absorb light of wavelength less than 200 nm and because of technical difficulties of working at these short wavelengths , photoreactions of pure ethers were little studied prior to 1960 . Photosensitized reactions had been studied more extensively [5,6] .

Before studying the photochemistry of the ethers we must first look at the absorption characteristics of these compounds .

Saturated ethers absorb noticeably around 200 nm . The maximum of the first absorption band has been attributed to an $n \dashrightarrow \sigma^{*5}$ or Rydberg - type transition and lies near 185 nm . The absorption coefficient at shorter wavelengths is increasingly determined by the alkyl part of the molecule and tends to be larger the longer and more highly branched the alkyl chain [7] . With only a few exceptions , the liquid - phase absorption coefficients of ethers match those of the gas phase , at least over the range where both can be measured [7,8] .

The direct photolysis of the ethers by light wavelengths below 200 nm has been extensively studied by a number of workers [2,7,9 - 12] . Similar trends in reactivity have been noted by each of these research groups .

The major products formed in the direct photolysis of diethyl ether in the gas phase are , ethane , propane , butane , ethylene , ethanol and other minor products [2] . The yield of ethanol relative to hydrocarbon increases markedly with increasing pressure . Alcohols are the major products from direct photolysis of ethers in the liquid phase , carbonyl compounds and enol ethers are also obtained [10] .

The most important primary process in the direct photolysis of open chain ethers is homolytic C - O bond scission [2,9 -12] :

$$R\text{ -- }O\text{ -- }R' \xrightarrow{h\nu} R\cdot + \cdot O\text{ -- }R' \qquad (3.1.5)$$

$$R\text{ -- }O\text{ -- }R' \xrightarrow{h\nu} R\text{ -- }O\cdot + \cdot R' \qquad (3.1.6)$$

The alkoxyl radicals (RO· and R'O·) abstract a hydrogen atom from another ether molecule giving the alcohol (ROH and R'OH) , and alkoxyalkyl radicals ,

$$CH_3CH_2O\cdot + CH_3CH_2OCH_2CH_3 \text{ ---------> } CH_3CH_2OH + CH_3\cdot CHOCH_2CH_3 \quad (3.1.7)$$

The alcohol can also be formed by a molecular elimination process , an olefin being the other product :

$$CH_3CH_3OCH_2CH_3 \xrightarrow{h\nu} CH_3CH_2OH + CH_2 = CH_2 \quad (3.1.8)$$

The other molecular process involving the C - O bond is the formation of a carbonyl compound and an alkane in primary and secondary ethers :

$$CH_3CH_2OCH_2CH_3 \xrightarrow{h\nu} CH_3CHO + CH_3 - CH_3 \quad (3.1.9)$$

Alcohols and carbonyl compounds are key products for the determination of the photolysis mechanism of ethers because the alkoxyl radicals from reactions (3.1.5) and (3.1.6) readily abstract hydrogen atoms from neighbouring molecules to give alcohols (reaction (3.1.7)) but do not interact with other radicals under the conditions of these experiments [7] . The carbonyl compound is not formed by any process other than that exemplified in reaction (3.1.9) if the alkoxyalkyl radicals formed by H - abstraction are sufficiently stable with respect to fragmentation at the experimental conditions . Fragmentation of a saturated alkoxyalkyl radical is only observed if it is heavily loaded with methyl substituents :

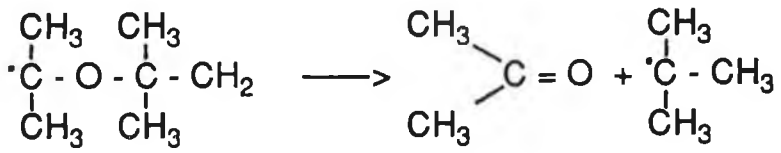

(3.1.10)

For this reason the quantum yield for the formation of alcohols and carbonyl compounds is a measure of the quantum yield of C - O bond scission in primary and secondary ethers . The scission of a C - H bond is indicated by the formation of H_2 , because the high abstractive power of the H - atom precludes it's interaction with other radicals in liquid systems . Radical addition to olefins would become important only at high conversion of the starting material . The various modes of reaction (homolytic scission and molecular processes , e.g., reactions (3.1.5) to (3.1.8) as well as minor processes such as C - C bond fragmentation can be assessed only if a complete product study has been made . Then with the knowledge of the disproportionation / dimerization ratios of the radicals in question a detailed picture of the primary processes can be given .

To explain the products formed in the liquid phase photolysis of diethyl ether at 185 nm , the following primary processes were proposed by Sonntag et al [7] :

	$MeCH_2O\cdot + \cdot CH_2Me$	(70%)	(3.1.11)
	$MeCH_2OH + CH_2 = CH_2$	(8.5%)	(3.1.12)
$MeCH_2OCH_2Me$ ===>	$MeCHO + MeMe$	(10%)	(3.1.13)
	$MeCH_2OCH = CH_2 + H_2$	(11%)	(3.1.14)
	$Me\cdot + \cdot CH_2OCH_2Me$	(0.5%)	(3.1.15)

$MeCH_2O\cdot$ --------> $Me\cdot + CH_2O$ (3.1.16)

$MeCH_2O\cdot + MeCH_2OCH_2Me \text{ -----> } MeCH_2OH + Me\cdot CHOCH_2Me$ (3.1.17)

$Bu^tOBu^t \text{ --------> } Bu^tOH + (Me)_2C = CH_2$ (3.1.18)

In the gas phase at low pressure , the vibrationally excited alkoxy radical formed in reaction (3.1.11) fragments as in (3.1.16) and the methyl radicals from this reaction and the ethyl radicals from (3.1.15) combine to give hydrocarbons . At higher pressures and in the liquid phase the vibrational energy of the ethoxy radical is lost by collision with other molecules , thus preventing the reaction in equation (3.1.16) , and the ethoxyl radical abstracts hydrogen from ether (3.1.17) , to give ethanol . Similar reactions occur with other primary and secondary ethers . Direct photolysis of liquid di - t - butyl ether also gives mainly the alcohol but in this case it arises primarily from the molecular process shown in equation (3.1.18) .

The photolysis of dimethyl ether and diethyl ether in the gas phase was first studied by Harrison and Lake [7] using a hydrogen discharge lamp ($\lambda < 192$ nm) . They reported the formation of formaldehyde from dimethyl ether , and ethylene , acetaldehyde , and formaldehyde from diethyl ether . Studies were subsequently carried out on dimethyl ether using wavelengths of approximately 147 nm , by Meagher and Timmons [14] . In the interpretation of their results , Meagher and Timmons [14] proposed the following mechanism :

$CH_3OCH_3 \text{ -------> } H\cdot + \cdot CH_2OCH_3^*$ (3.1.19)

$\cdot CH_2OCH_3^* \text{ ------> } CH_2O + \cdot CH_3$ (3.1.20)

$H_2 + CO + \cdot CH_3$ (3.1.21)

The primary process was thought to be scission of a C - H bond followed by the thermal decomposition of the vibrationally excited methoxymethyl radical . Meagher and Timmons [14] also considered the alternative mechanism :

$$CH_3OCH_3 \text{ ----------> } \cdot CH_3 + \cdot OCH_3^* \qquad (3.1.22)$$

$$CH_3O\cdot^* \text{ ----------> } CH_2O + H\cdot \qquad (3.1.23)$$

but gave it lower preference because they predicted that this would result in a pressure independence of methyl radical yield which they did not observe . These results were reinterpreted by Sonntag et al [7] according to reactions (3.1.22) and (3.1.23) . Such a mechanism falls in line with the photolytic behavior of all other ethers studied so far .

The photolysis of diethyl ether in the gas phase was also studied by Johnson and Lawson [15] . They showed that the distribution of the products measured is virtually the same at 147 nm and 124 nm , although at 124 nm the energy absorbed is sufficient for photoionization to occur . In general the photolysis of diethyl ether in the gas phase at 147 nm and 124 nm appears to follow the same lines that have been established for the liquid phase at 185 nm [10] . This C - O bond scission mechanism is also supported by results observed by Mikuni et al for the gas phase photolysis of dimethyl ether [16] and diethyl ether [9] at 184.9 nm .

The major product from the direct photolysis at 254 nm of oxygenated ether is ethyl acetate [17,18] . Work by Chien et al [19] , Kulevsky et al [20] , Stenberg et al [21] , and Wang [22] , has shown that the initial step in the photooxidation of liquid diethyl ether is absorption of light by a charge - transfer complex of molecular oxygen with ether .

Molecules capable of donating an electron pair are defined as electron donors (D) and molecules which can accept an electron pair are

called acceptors (A) . Donors and acceptors interact , usually weakly to form complexes :

$$D + A \rightleftharpoons D , A \; (<=> D^+, A^-) \qquad (3.1.24)$$

These complexes absorb light of different wavelengths than either D or A . During this process an electron is transferred from D to A :

$$D , A \; (<--> D^+ , A^-) \xrightarrow{h\nu} D^+ , A^- \; (<--> D , A) \qquad (3.1.25)$$

The associated species of electron donor and acceptor molecules with new spectral features are referred to as charge - transfer complexes .

Various workers [20 - 22] have shown that a number of ethers exhibit enhancement of absorption when saturated with oxygen , thus demonstrating the possible formation of charge - transfer complexes . Oxygen saturated diethyl ether exhibits a charge - transfer absorption band [2,20 - 22] , and absorption of energy is believed to be associated with transfer of charge from the ether to an oxygen molecule to give the ether radical cation and oxygen radical anion :

$$Et_2O: + O_2 \xrightarrow{h\nu} Et_2O^{\cdot +} \cdot O_2^- \qquad (3.1.26)$$

Loss of a proton from this radical cation gives the 1 - ethoxyethyl radical which reacts with oxygen to give products :

$$EtO\dot{C}H_2Me \xrightarrow{-H^+} EtO\dot{C}HMe \xrightarrow{(O_2)} Products \qquad (3.1.27)$$

Some preliminary work has been carried out by Wang [22] into the gas phase photooxidation of tetrahydrofuran . Although an attempt to measure the association constant between oxygen and the ether in the

gaseous phase was unsuccessful due to slow reaction and weak complexation , oxidation was noted by Wang [22] when tetrahydrofuran vapour was mixed with oxygen and irradiated .

Significant differences exist between photochemical processes in the gas and liquid phase . First , since molecules in the liquid phase are continually undergoing collisions , the excited molecules are easily deactivated . Secondly , since dissociation in the liquid phase leads to the production of two radicals within the same solvent cage , there is a high probability of primary recombination .

Consequently , unlike the liquid phase , tail end absorption by the ethers is thought to be important in gas phase photooxidation reactions of these species . Wang [22] observed that excited tetrahydrofuran (n --> σ^*) in the gas phase decomposes to give ethylene and acetaldehyde among it's many reaction products thus illustrating a complex photooxidation mechanism . Wang [22] found that in the gas phase reaction of an oxygen - tetrahydofuran mixture , a greater number of reaction products were obtained without the use of a Vycor filter (a filter which excluded light for excitation of tetrahydofuran alone but did not eliminate all wavelengths for charge - transfer excitation) . Only when using this filter did the nature of the products formed parallel those obtained in the liquid phase reaction . Hence , this work by Wang [22] demonstrated the possible formation of a charge - transfer complex between molecular oxygen and an ether as a possible reaction mechanism in the gas phase for the photooxidation of the ether . However , this charge - transfer mechanism may only be of secondary importance compared to reaction initiated by direct photolysis due to tail end absorption .

The photochemical reactions of liquid ethers with a variety of other compounds generally give α-substituted products which are believed to arise by reaction with the 1-alkoxylalkyl radical ,

e.g.,[23]

$$MeCH_2OCH_2Me + Cl_2 \xrightarrow{h\nu} MeCH_2OCHClMe + HCl \qquad (3.1.28)$$

The marked regioselectivity of these photoinduced radical substitutions can be rationalized because of the ability of oxygen to stabilize the adjacent unpaired electron in 1-alkoxyalkyl radicals .

The work carried out in this thesis involved a preliminary investigation into the gas phase photooxidation of two halogenated ethyl methyl ethers , isoflurane ($CF_2HOCHClCF_3$) and enflurane (CF_2HOCF_2CHFCl) at wavelengths above 200 nm . The introduction of halogens , particularly chlorine , into the ether structure shifts the absorption to higher wavelengths facilitating photooxidation at lower energy . The UV spectra of isoflurane and enflurane are similar (as these compounds are structural isomers of each other) and are located largely in the vacuum UV region . The band of lowest energy (highest wavelength) corresponds to a transition from an orbital of halogen lone pair character (X) to an orbital antibonding in the carbon -halogen bonds [24] . The first band in the enflurane vapour phase vacuum UV spectrum has its maximum near 156 nm , with a shoulder on it's low frequency side . Tail end absorption was noted by Dumas et al [24] at wavelengths up to 182 nm . The bands that occur at higher frequencies have been interpreted as X -----> Rydberg transitions . Cl -----> Rydberg bands are formed at 142 , 134 and 128 nm .

According to previous spectroscopic studies [25] only the hydrogen geminal to the chlorine atom in enflurane , is acidic . The role of the other hydrogen is not clear however it has been proposed [25] that enflurane might enter into repulsive interactions through it's -CHF_2 group and

attractive ones with stronger bases through its ClFHC - group . To this one might add the possible electron acceptor role of the oxygen .

Chapter three of this thesis involves a study of the gas phase photooxidation of isoflurane and enflurane using available techniques to monitor reaction in order to elucidate the mechanisms involved . Preliminary experiments involved a study of the UV absorption characteristics of the anaesthetics in the liquid phase and determination of the major gas phase photooxidation reaction products using IR spectroscopy . These fundamental investigations were used to establish the initiation process and were used as a guideline for further experiments. Techniques used in this photooxidation study included GC (with FID and MS detector options) , IR , and NMR .

3.2 Experimental

3.2.1 Materials

Isoflurane , (1-Chloro-2,2,2-trifluoroethyl difluoromethyl ether) trade name "Forane" , used throughout this project was supplied by Abbot Laboratories Ltd. , Ireland .

Enflurane , (2-Chloro-1,1,2-triflouroethyl difluoromethyl ether) trade name "Ethrane" was also supplied by Abbot Laboratories Ltd. . Both anaesthetics had stated purities of > 99.9% and no further purification (other than degassing) was carried out .

Oxygen (> 99.7%) , air , nitrogen(oxygen free) and hydrogen were supplied by Irish Industrial Gases , Dublin . Carbon dioxide (CO_2 >99.995) was supplied by Air Products of Dublin and carbonyl fluoride (CF_2O) by SCM Speciality Chemicals in America . CF_3COCl and Cl_2 (99.5%) were supplied by Fluorochem Ltd. , England and Argo International Ltd. respectively .

$CHCl_3$ (>99.8%) was supplied by F.S.A. supplies .

d-Chloroform (>99.8%) and d-acetone (99.5%) were supplied by the Aldrich Chemical Company of America .

3.2.2 Apparatus

(a) *Vacuum apparatus*

The vacuum line used throughout this work consisted of a conventional mercury free high vacuum line made of Pyrex glass . Figure 2.2.1 describes the vacuum system employed throughout this work , while Table 2.2.1 defines the various regions within the vacuum line . Chapter 2 of this thesis contains a detailed review of the operation of the vacuum line .

(b) *UV lamp and power supply*

The lamp used for most photolyses was a 400 Watt medium pressure mercury lamp (Photochemical Reactors Ltd.) . Output typical of this lamp design is shown in Figure 3.2.2.1 . The lamp was water cooled and powered by it's own intensity stabilised 220-240 Volts a.c. power supply . To minimise background radiation and to limit UV light leaking to the surrounding laboratory , the irradiation area was enclosed in black cloth .

(c) *UV / visible absorption data* :

UV / visible absorption properties of both anaesthetics and transmission characteristics of the various filters used were determined using two instruments . The first was a Hewlett Packard (model 8452A) diode array UV / visible spectrophotometer and the second a Shimadzu (model OV-240) with an option program / interface (model OP1/1) .

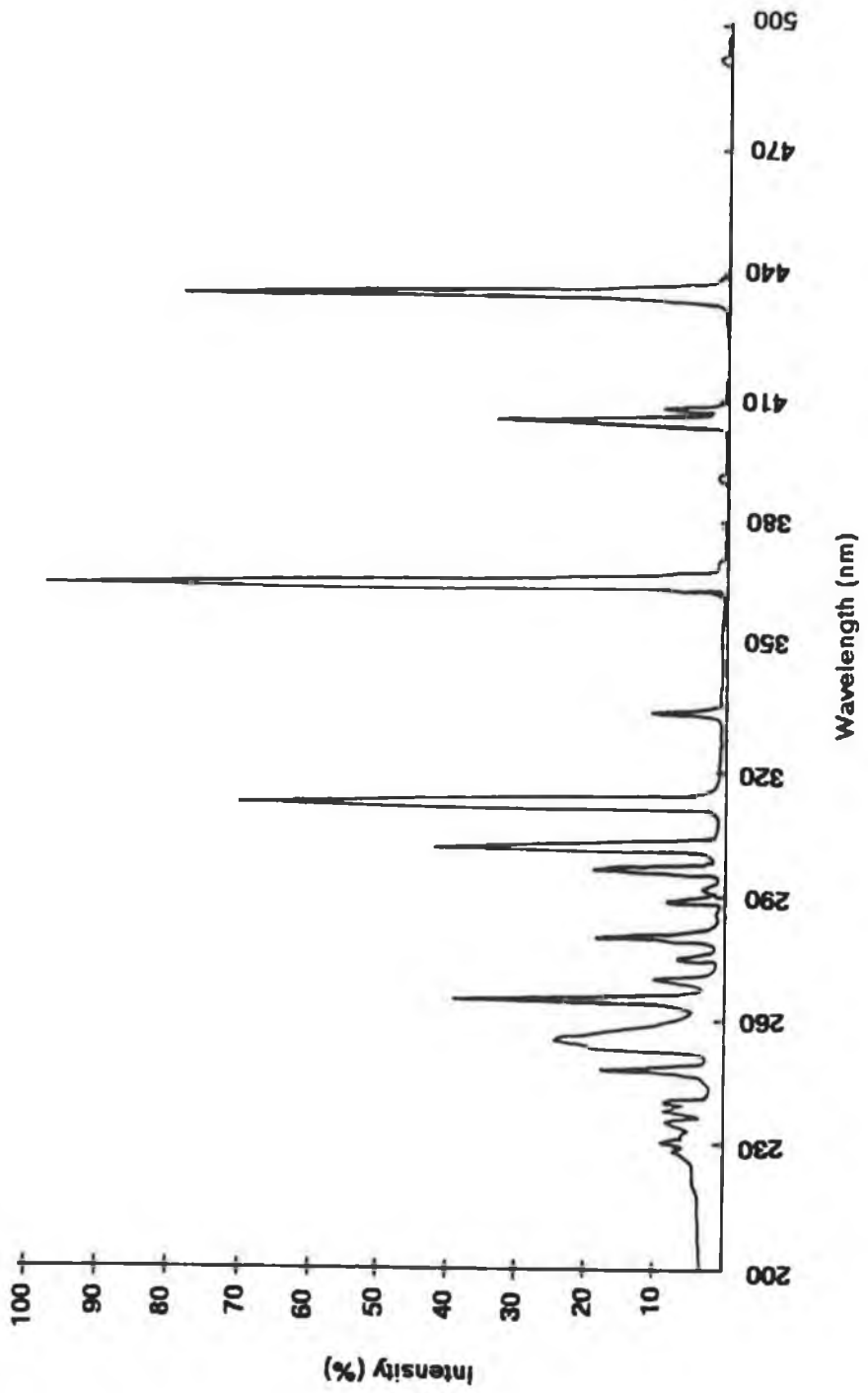

Figure 3.2.2.1
Output from the 400 Watt medium pressure mercury lamp (Photochemical Reactors LTD) employed throughout this work for photolysis .

(d) *Gas chromatography*

Most of the chromatographic analyses were performed on a Perkin Elmer (model 8500) gas chromatograph , fitted with a flame ionisation detector . Injection was achieved by use of a 10 - port , Valco (VICI Instruments) automatic gas sampling valve . Figure 3.2.2.2 illustrates this sampling valve in the fill position connected to the vacuum line . Oxygen free nitrogen was used as the carrier gas and was passed through a moisture trap (Phase - Sep) prior to entering the instrument . The columns used and the associated chromatographic conditions employed are listed in Tables 3.2.2.1 and 3.2.2.2 . Chromatograms complete with their integrated peak areas were recorded on a Perkin-Elmer, G.P. 100 graphic printer .

The GC - mass spectrometry in this research was carried out courtesy of Loctite Ireland Ltd . The system employed was a Hewlett Packard GC fitted with an ion trap detector . An injection temperature of 50^{o}C was used and an oven temperature of 40^{o}C. Helium , the carrier gas used, had a flow rate equivalent to a pressure of 2 psi . 50pl was injected onto the GC and total ion current traces were recorded over the mass range 35 - 300 .

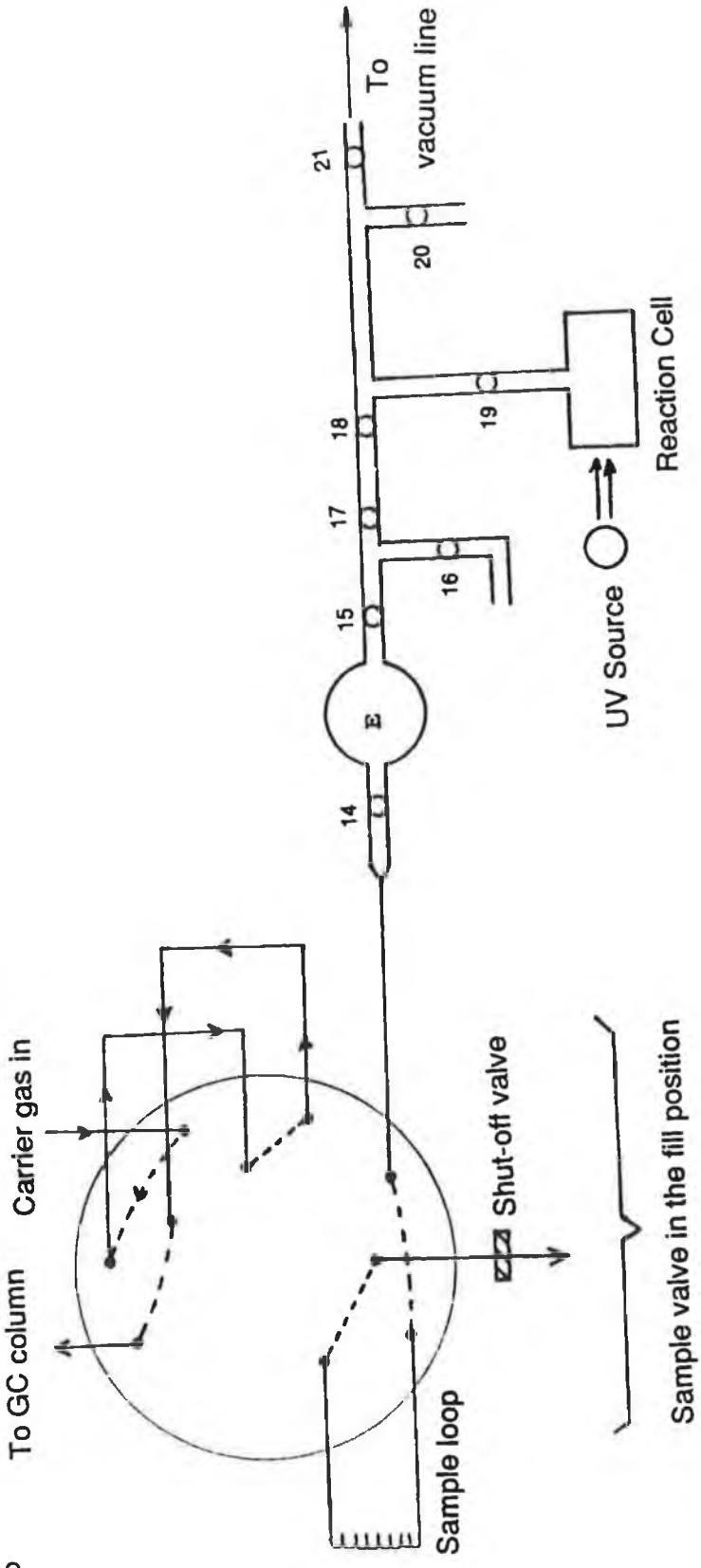

Figure 3.2.2.2
This diagram illustrates the Valco automatic gas sampling valve , in the fill position , connected to the vacuum line to facilitate injection from the reaction cell .

COLUMN	PORAPAK Q (Medium polarity)
Length	4 m (Stainless steel)
Internal Diameter	2.0 mm
Mesh Size	100 - 120 µm
Injector Temperature	25 °C
Oven Temperature	220 °C
Detector Temperature	270 °C
Carrier Gas	Nitrogen (oxygen free)
Flow Rate	40 cm^3 / min.

Table 3.2.2.1
Initial chromatographic conditions employed to study the photooxidation of the anaesthetics .

COLUMN	10% SE 30 on Chromosorb WHP (A non - polar column)
Length	2.0 m (glass)
Internal Diameter	3.0 mm
Mesh Size	100 - 120 µm
Injector Temperature	80 °C
Oven Temperature	40 °C
Detector Temperature	270 °C
Carrier Gas	Nitrogen (Oxygen free)
Flow Rate	30 cm^3 / min.

Table 3.2.2.2
Chromatographic conditions used to study the photooxidation products of the anaesthetics .

(e) *Infrared spectroscopy*

Most of the IR work was carried out in a T - shaped reaction vessel housed in the sample compartment of the IR spectrometer (Figure 3.2.2.3) , with sodium chloride plates in the IR beam and a pathlength of 10 cm . Along the perpendicular axis , with a pathlength of 10 cm was the mercury source and it's associated filter system . Some experiments in this work were carried out by clamping the reaction cell 10 cm from the medium pressure mercury lamp source and removing the cell to the IR spectrometer at selected photolysis times .

IR studies were carried out using two different instruments . The first , a Perkin Elmer model 983G was used for spectral subtraction work and some initial product studies . The second , a Perkin Elmer model 297 , was used for all other work . Both instruments were calibrated prior to use with a polystyrene test film and all spectra were recorded over the spectral range 4000 - 600 cm^{-1} .

(f) *Nuclear magnetic resonance work*

All of the NMR work carried in this thesis was performed on a 400 MHz Bruker AC 400 instrument . Samples were analysed at room temperature for proton NMR in high precision glass tubes .

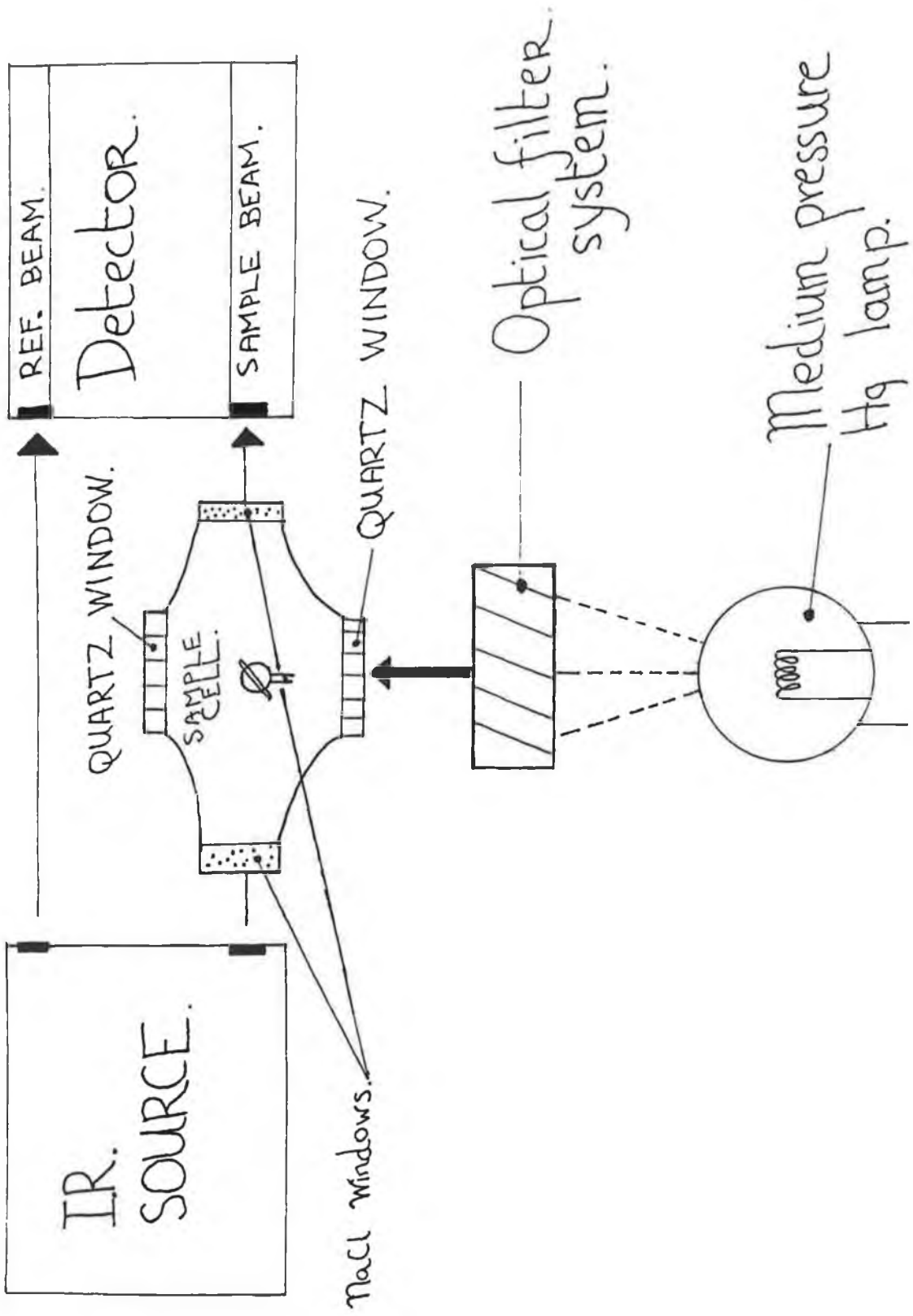

Figure 3.2.2.3
Vertical view of the experimental design used to study the photooxidation of the anaesthetics . IR spectroscopy was employed to determine the extent of reaction .

3.2.3 Procedures

3.2.3.1 *Vacuum line volumes*

To accurately measure reactant concentrations , the volumes within the various regions of the vacuum line needed to be established . Bulb A in Figure 2.2.1 was the primary volume from which each volume within the vacuum line was determined using Boyle's Law ,

$$\text{VOLUME} \quad \alpha \quad {}^{1}/_{\text{Pressure}} \qquad (3.2.3.1)$$

$$P_1V_1 \quad = \quad P_2V_2 \qquad (3.2.3.2)$$

The volume of bulb A was determined prior to it's attachment to the vacuum line . Volumes in the vacuum line calculated using the above procedure are summarised in Section 2.2 of this thesis .

3.2.3.2 *The preparation of gas mixtures*

Typically mixtures of anaesthetic and reactant gases (O_2,N_2, etc.) were prepared on the vacuum line in bulb F (Figure 2.2.1) . The correct pressures of reactant (calculated using line volumes and expression (3.2.3.2)) were frozen into bulb F , left to mix in the dark for 30 minutes and then allowed through to the reaction or IR cell . Prior to photolysis the medium pressure mercury lamp was warmed up for ten minutes with water flowing through the cooling jacket. Photolysis times were recorded using a stop clock , with reaction temperatures monitored by a mercury thermometer .

3.2.3.3 *UV / visible absorption spectra plus preliminary experiments*

Samples of the liquid anaesthetics were degassed using the freeze-pump-thaw method and their UV spectra measured on a diode array spectrophotometer in a 1 cm pathlength quartz cell . To establish whether oxygen saturation of the anaesthetics altered their absorption spectra , each of the degassed anaesthetics were then saturated with O_2 and UV spectra recorded as before .

To determine whether light was necessary for reaction to proceed , reaction mixtures of 20 torr anaesthetic plus 300 torr O_2 were monitored by GC in the presence and absence of light .

To illustrate the first law of photochemistry and to narrow down the wavelengths responsible for reaction , photolysis of 5 torr anaesthetic in 200 torr O_2 was carried out with and without a Corning 0-53 optical filter (which excluded light below 270 nm) .

In all of our photolyses output from the medium pressure mercury lamp was unfiltered resulting in the generation of significant levels of heat . Reaction cell temperatures typically reached 47 ± 4°C during photolysis . To determine whether this temperature was sufficient to initiate reaction , mixtures of anaesthetic and oxygen were prepared and transferred to the reaction cell . These mixtures were monitored by GC at temperatures of 47 ± 4°C over time periods up to 90 minutes . Similar mixtures of anaesthetics in oxygen were prepared , transfered to the reaction cell and then injected onto the GC . These mixtures were used for comparison with the heated samples .

In an attempt to determine whether loss of the anaesthetics took place in the absence of oxygen , reactions were performed in the presence and absence of oxygen and the extent of photooxidation

monitored by IR spectroscopy . Reaction mixtures were photolysed using output from the unfiltered medium pressure mercury lamp .

3.2.3.4 *Photooxidation Profiles*

(a) *Infrared*

Preliminary experiments in our laboratory with isoflurane and enflurane involved the photooxidation of the anaesthetics in oxygen, to establish if any change would be noted using infrared spectroscopy .

Mixtures of anaesthetics in oxygen were prepared on the vacuum line and transferred to the IR reaction cell . The cell was then clamped 10 cm from the medium pressure mercury lamp and reaction was monitored using IR spectroscopy .

The above preliminary investigations indicated that photooxidation of the anaesthetics yielded a number of different products including carbonyl containing compounds which were readily monitored using infrared spectroscopy . As a result detailed photooxidation profiles for the anaesthetics were established with reactions followed by IR spectroscopy . The experimental design used to establish these profiles is outlined in Figure 3.2.2.3 . To ensure differences in reaction were not due to pressure effects , each of the reaction mixtures were made up to a total pressure of 200 torr with oxygen free nitrogen . To ensure a steady light output during the above photolyses the medium pressure mercury lamp was allowed to warm up for 30 minutes prior to photolysis .

To determine whether oxygen concentration radically affected both the rate of loss of the anaesthetics and the photooxidation products formed , profiles were established in which firstly each anaesthetic was

added in excess over oxygen and secondly , in which each anaesthetic and oxygen were added in equal concentrations .

As in the previous profiles , the experimental setup described in Figure 3.2.2.3 was used and IR spectra were recorded to monitor reaction progress . The profiles in which the anaesthetic was added in excess were useful in determining minor reaction products formed that were not visible during the photolysis of small quantities of the anaesthetics .

(b) *GC*

When using gas chromatorgraphy to monitor the photooxidation profiles for the anaesthetics , it proved useful to construct standard curves. Having established these curves , it was then possible to determine the concentration of the anaesthetics at each photolysis time . Consequently it was also possible to demonstrate the complex nature of these gas phase photooxidation mechanisms by fitting this result data to a first order rate expression .

Standard curves for both anaesthetics were established in the concentration range from 0 to 20 torr in 300 torr O_2 . These reaction mixtures were prepared on the vacuum line and transferred to the reaction cell . After five minutes the cell contents were allowed to the GC , and injected using the Valco automatic gas sampling valve .

Photooxidation profiles for the anaesthetics were established by preparing reaction mixtures of 20 torr anaesthetic plus 300 torr O_2 on the vacuum line , transferring them to the reaction cell for photolysis , followed by injection onto the GC in a similar manner to the standards . Photolysis times ranging from 0 to 120 minutes were used . The concentration of anaesthetics at each photolysis time was determined by interpolation onto the standard curves .

3.2.3.5 *Effects of reaction parameters on anaesthetic photooxidation*

In this section the effect of reaction parameters such as oxygen and anaesthetic concentration , total pressure and light intensity were studied to determine their effect on the photooxidation of the anaesthetics and on their oxidation products .

(a) *The effect of oxygen concentration*

5 Torr of the anaesthetics was mixed with concentrations of oxygen varying from 0 to 195 torr . The initial reaction mixture pressure was maintained at 200 torr using oxygen free nitrogen . These reaction mixtures were prepared on the vacuum line and transfered to the IR reaction cell . The cell was then clamped 10 cm from the medium pressure mercury lamp and photolysis times of 30 minutes for isoflurane and 75 minutes for enflurane used . The rate of loss of anaesthetic was then calculated as follows ;

$$\left(\frac{\text{Loss Anaesthetic (torr)}}{760 \times 0.08205 \times 300}\right) \Big/ \text{Photolysis Time (seconds)} = \text{Rate of Loss (mol dm}^{-3}\text{ s}^{-1}\text{)} \qquad (3.2.3.3)$$

(b) *The effect of anaesthetic concentration*

In a similar manner to the study of effects of variation in oxygen concentration , the concentration of anaesthetic was varied. Concentrations of anaesthetic from 0 to 7 torr were prepared in 50 torr O_2. The total initial reaction mixture pressure was set at 200 torr using oxygen free nitrogen as the diluent gas. The reaction mixtures were prepared on the vacuum line and transferred to the infra-red reaction cell for photolysis. A photolysis time of 30 minutes was used for the isoflurane

study and 75 minutes for enflurane. The rate of loss of the anaesthetics was calculated using expression (3.2.3.3) .

(c) *The effect of total pressure*

To determine the effect of reaction mixture initial pressure on reaction rate, the following procedure was used .

5 Torr of anaesthetic plus 50 torr O_2 was photolysed with varying pressures of oxygen free nitrogen added . Pressures of nitrogen ranged from 0 - 150 torr resulting in total reaction mixture pressures of 55 - 205 torr . The reaction mixtures were prepared on the vacuum line , transferred to the IR reaction cell and clamped 10 cm from the light source for photolysis . Reaction times of 30 minutes and 75 minutes were used for isoflurane and enflurane respectively .

(d) *Effect of light intensity*

The effect of light intensity on the photooxidation of the anaesthetics was investigated as described below .

5 Torr anaesthetic in 195 torr O_2 was prepared on the vacuum line and transferred to the I.R. reaction cell . This cell was then placed in the IR spectrometer as outlined in Figure 3.2.2.3 . Reactions were monitored at 0, 25, 50 and 100% transmittance using reaction times of 75 minutes for isoflurane and 105 minutes for enflurane . The 25 and 50% transmission filters were fashioned from wire mesh and their transmittance determined by monitoring their UV / visible spectrum from 190 - 800 nm . Rate of loss of the anaesthetics was determined as previously described .

3.2.3.6 *Chlorine - sensitised photooxidation of the anaesthetics*

(a) *Preliminary investigations*

5 Torr anaesthetic , 1 torr chlorine and 194 torr O_2 mixtures were prepared on the vacuum line and transferred to the IR reaction cell. This cell was clamped in front of the unfiltered medium pressure mercury lamp for photolysis, and IR spectra taken to monitor the extent of reaction . The IR spectrometer used in these experiments was the Perkin Elmer 983G . To better visualise the loss of the anaesthetics and the appearance of IR bands due to reaction products , the IR spectrometer was operated in the spectral substraction mode .

Comparison of the photooxidation reactions of the anaesthetics with and without the addition of chlorine was then carried out . 5 Torr anaesthetic , 1 torr N_2 plus 194 torr O_2 mixtures were prepared on the vacuum line and transferred to the IR reaction cell . The cell , once clamped 10 cm from the unfiltered light source, was irradiated for varying lengths of time . IR spectra were taken at each photolysis time , to establish reaction profiles . Gas mixtures of 5 torr anaesthetic , 1 torr Cl_2 and 194 torr O_2 mixtures were then prepared and photolysis profiles established in a similar manner .

To establish the importance of the lower wavelengths in the medium pressure mercury lamp output , on the chlorine initiated photooxidation of the anaesthetics , the following experiments were carried out . 5 Torr anaesthetic , 1 torr of Cl_2 and 194 torr O_2 were prepared on the vacuum line and transferred to the IR reaction cell . This cell was then clamped inside the smog chamber and photolysis carried out by the black lamps ($\lambda > 320$ nm) .

The use of black lamps for photolysis ensured that the only reaction which would take place was initiated by chlorine atoms produced from the

photolysis of molecular chlorine . Reaction profiles were established for the anaesthetics by monitoring reaction progress using IR spectroscopy .

(b) *Quantum yield work*

The chemical actinometer employed for measurement of the quantum yield of the photooxidation reactions studied here was the reaction of atomic chlorine with chloroform at wavelengths above 300 nm . The reaction of chloroform with atomic chlorine proceeds as follows :

$$Cl_2 + h\nu\ (\lambda > 300nm) \text{ ----------} > 2Cl\cdot \qquad (3.2.3.4)$$

$$2CHCl_3 + Cl\cdot \text{ ----------} > 2HCl + C_2Cl_6 \qquad (3.2.3.5)$$

Since the quantum yield of formation of hexachloroethane , $\Phi_{C_2Cl_6}$, is unity over a wide range of experimental conditions , it was decided to monitor the disappearance of $CHCl_3$ rather than the appearance of C_2Cl_6 .

Mixtures containing 5 torr $CHCl_3$, plus 1 torr Cl_2 were prepared on the vacuum line and transferred to the IR reaction cell . The cell was placed in the IR as outlined in Figure 3.2.2.3 and photolysis carried out at wavelengths > 300 nm . A photolysis time of 45 minutes was used for all reactions and the rate of loss of $CHCl_3$ determined at 100 , 50 , 25 and 0 % transmittance .

5 Torr anaesthetic , 1torr Cl_2 and 194 torr O_2 mixtures were then prepared on the vacuum line and transfered to the IR reaction cell . Photolysis of these anaesthetic mixtures was carried out for the same length of time , at the same wavelengths and using the same incident light intensities used in the chloroform reaction . From the above experiments it was possible to determine :

(1) the effect of light intensity on the rate of loss of the anaesthetics initiated by reaction with chlorine ;

(2) the effect of light intensity on the concentration of the chlorine initiated photooxidation products of the anaesthetics ;
(3) the quantum yield for the loss of the anaesthetics ($\Phi_{anaes.}$) at each of the different light intensities :

$$\Phi_{anaes.} = \frac{R_{anaes.}}{I_A} = \frac{\text{Rate of loss of Anaesthetic (mol.dm}^{-3}\text{.s}^{-1})}{\text{Rate of loss of CHCl}_3\text{ (mol.dm}^{-3}\text{.s}^{-1})} \quad (3.2.3.6)$$

The rate of loss of $CHCl_3$ in Cl_2 is essentially equivalent to the rate of formation of C_2Cl_6 as $\Phi_{C_2Cl_6}$ is unity . The light intensity for our quantum yield work was therefore taken as the rate of loss of $CHCl_3$.

3.2.3.7 *Product studies*

This section of work involved an investigation of the reaction products arising from the photooxidation of the anaesthetics using both infrared spectroscopy and gas chromatography .

(a) *Infrared spectroscopy*

A large number of reaction products were visible in the IR spectra of the photooxidized anaesthetics . These product spectra were then compared with known or standard spectra to facilitate identification of reaction products . Spectra of CF_2O , CO_2 and CF_3COCl were obtained as follows . The gases were transferred to the vacuum line from their supplied cylinders and degassed thoroughly . These gases were then transferred to an IR cell and spectra obtained in the region 4000 - 600 cm^{-1} .

During the photooxidation of the anaesthetics , HCl was identified as a reaction product from it's characteristic vibration - rotation spectrum in the region 3100 - 2500 cm^{-1}. This region of the spectrum identifying HCl was expanded on the infrared spectrometer , to facilitate interpretation .

(b) *Gas Chromatography*

Mixtures of 20 torr anaesthetic plus 300 torr O_2 were prepared on the vacuum line and transferred to the reaction cell . These mixtures were subsequently photolysed for between 60 and 75 minutes, and then injected onto the GC , operated using the chromatographic conditions outlined in Table 3.2.2.1 . A pressure surge resulted when operating with these GC parameters , therefore , chromatographic conditions were changed to those in Table 3.2.2.2 . Reaction mixtures were again

prepared as before and after photolysis these mixtures were injected onto the GC using the injection system described in Figure 3.2.2.2 .

Although products were visible in the above GC / FID work , no information could be obtained as to their nature . As it was possible to separate these reaction products from the anaesthetics using gas chromatography , it was decided to carry out GC / mass spectrometry work on the reacted gas mixtures, in an attempt to facilitate identification of these product components . The samples were analysed at Loctite Ireland Limited , to whom I am indebted .

Gas mixtures containing 20 torr anaesthetic plus 300 torr O_2 were prepared on the vacuum line and transferred to the reaction cell for photolysis . Reaction times of 60 minutes for isoflurane and 90 minutes for enflurane, were used . The reaction mixtures were then transferred to gas tight sample holders with self-sealing rubber septa attached for sample withdrawal . To maximise the concentration of products in the sample holder , liquid nitrogen was used for a short period of time to freeze the reaction mixture components from the sample cell to the holders . The sample holders were covered with dark cloth to minimise further reactions during sample transit .

The instrument type and the analysis conditions used are summarised in Section 3.2.2 (d) of this report . On injection of 50pl of sample , total ion current traces (TIC) for each reaction mixture over the mass range 55 - 300 amu were obtained . These traces indicated the number of product components present in our reacted samples . From the TIC traces it was then possible to fractionate each of the reaction mixture components visible in the traces using an electron impact source, and obtain a mass spectrum for each .

(c) *NMR*

The final technique used in this project involved the analysis of reaction products using proton nuclear magnetic resonance (NMR) spectroscopy . NMR spectra were obtained for both anaesthetics in the deuterated solvents, d-chloroform and d-acetone . Product analyses were then attempted as follows .

Mixtures of 25 torr anaesthetic and 5 torr O_2 were prepared on the vacuum line and transferred to the IR reaction cell for photolysis . The experimental design outlined in Figure 3.2.2.3 was used in conjunction with IR spectroscopy to monitor the progress of the reaction . At photolysis times of 105 minutes for isoflurane and 90 minutes for enflurane , IR spectra indicated considerable quantities of reaction products present . The reacted samples were transferred from the IR reaction cell to a small glass "finger" surrounded by liquid nitrogen attached to the vacuum line . These products were then mixed with deuterated solvent and the mixture transfered to a high precision NMR tube . Useful results were obtained using d-acetone only, as the oxidation products were too polar to dissolve in d-chloroform . The NMR instrument used is described in Section 3.2.2 (f) of this report . By subtracting the pure anaesthetic NMR spectra from the reaction mixture spectra , it was possible to identify which portion of the reaction mixture NMR was due to reaction products .

3.3 Results

3.3.1 UV absorption data and reaction initiation

The reaction cells were checked for their transmission characteristics . The optical windows on all cells transmitted above 190 nm .

UV / visible spectra of the anaesthetics, both degassed and saturated with oxygen are given in Figures 3.3.1.1 - 3.3.1.4. To establish whether light was needed for reaction to take place, a mixture of 20 torr anaesthetic and 300 torr O_2 was prepared . This mixture was photolysed for two hours in the reaction cell and injected onto the GC . A similar mixture of 20 torr anaesthetic plus 300 torr O_2 was left in the reaction cell for two hours and then injected . It was found that no measuable loss of anaesthetic took place in the absence of light .

On photolysing 5 torr anaesthetic in 200 torr O_2 with a Corning 0 - 53 optical filter in place (which excluded wavelengths below 270 nm) , no photolysis took place .

Since the light source used in this work generated a significant amount of heat during use , the effect of temperature on the initiation of reaction was investigated . The temperature of the reaction cell typically reached 17.5 ± 2°C prior to photolysis, and rose to 40 ± 2°C after five minutes photolysis . A maximum temperature of 47 ± 4°C was reached at the longest photolysis times used in this work . In the absence of UV radiation , no significant loss of reactants was detected over a 90 minute time span at 47 ± 4°C .

Initial experiments carried out and followed by GC and IR over short photolysis times (30 - 60 minutes) on the anaesthetics seemed to indicate no loss of anaesthetic without O_2 present . However , Figures 3.3.1.5 -

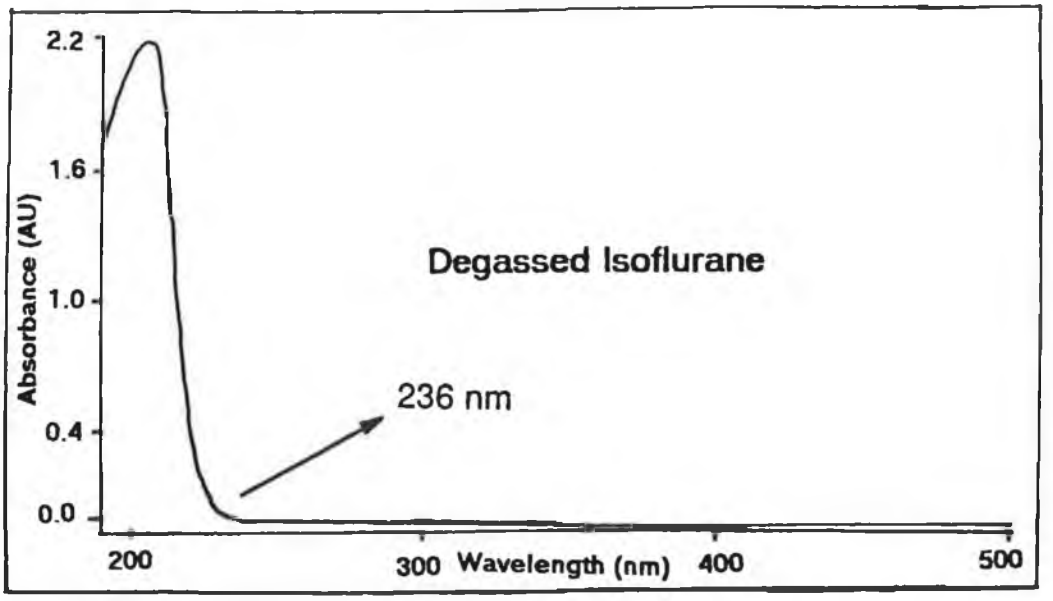

Figure 3.3.1.1

UV / visible spectrum of degassed isoflurane .

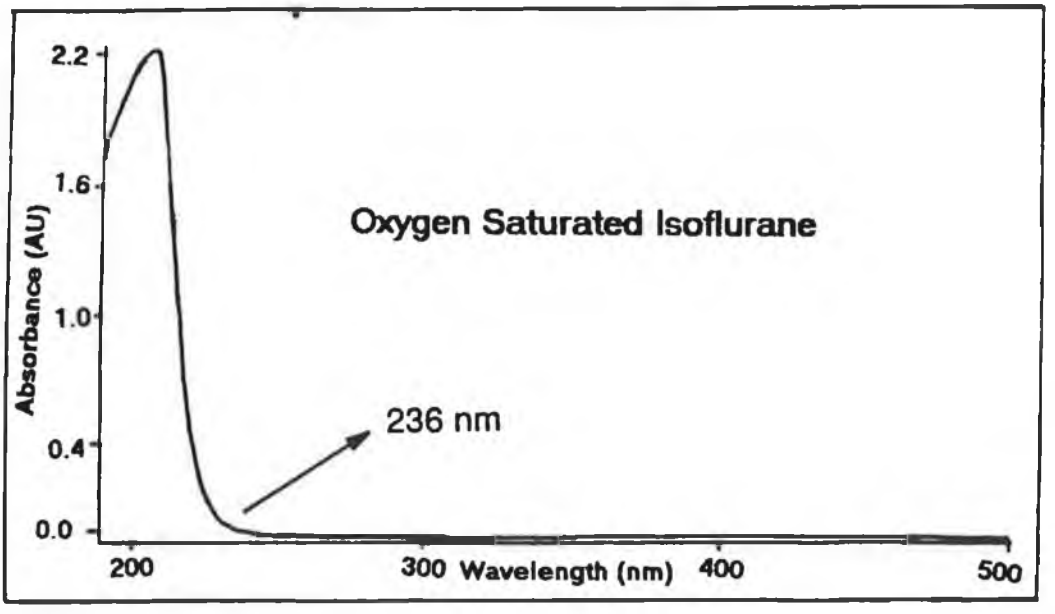

Figure 3.3.1.2

UV / visible spectrum of oxygen saturated isoflurane .

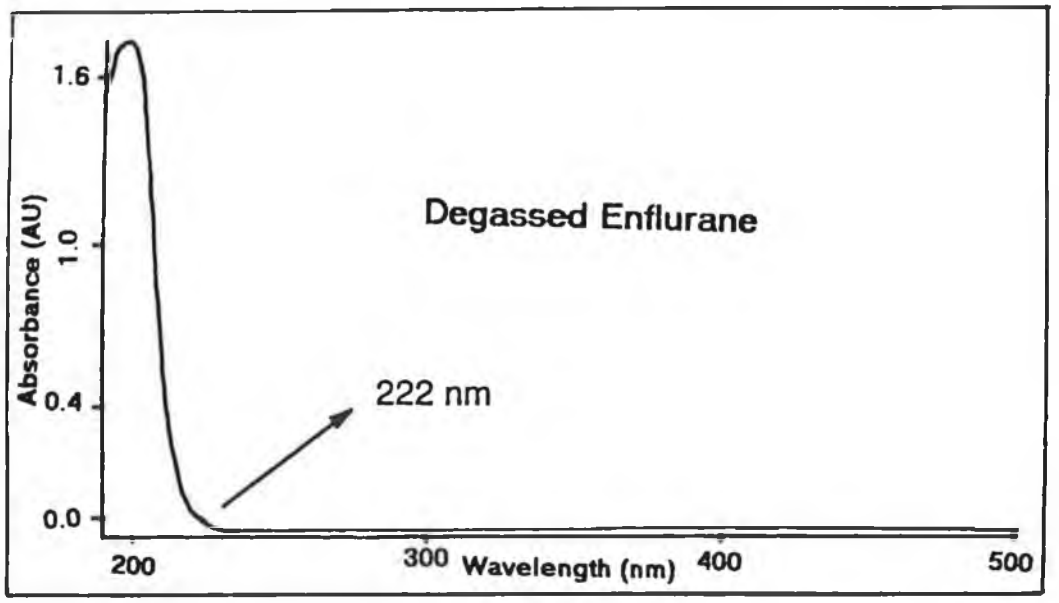

3.3.1.3

UV / visible spectrum of degassed enflurane .

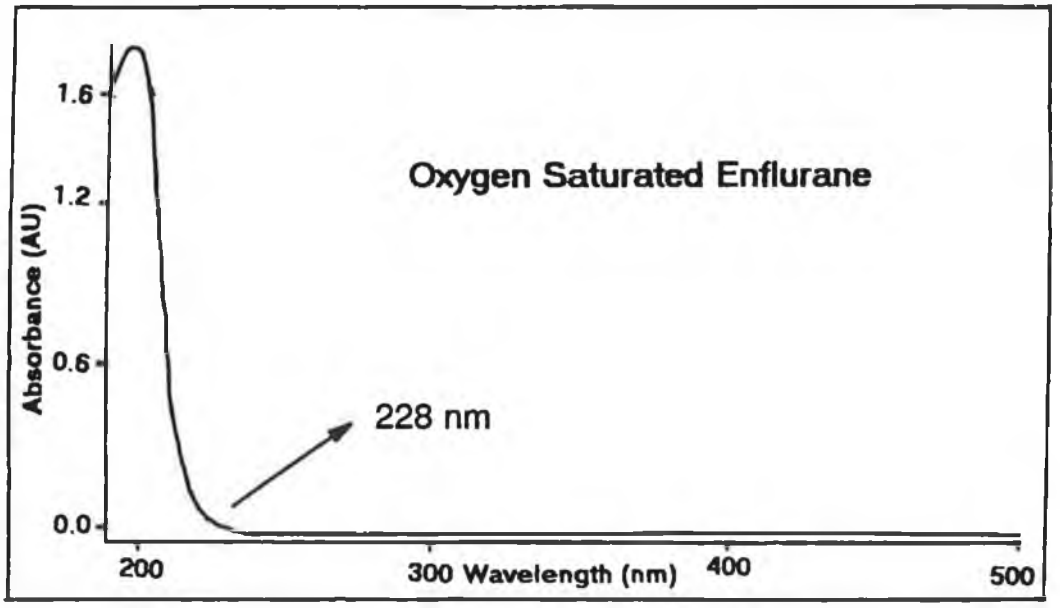

Figure 3.3.1.4

UV / visible spectrum of oxygen saturated enflurane .

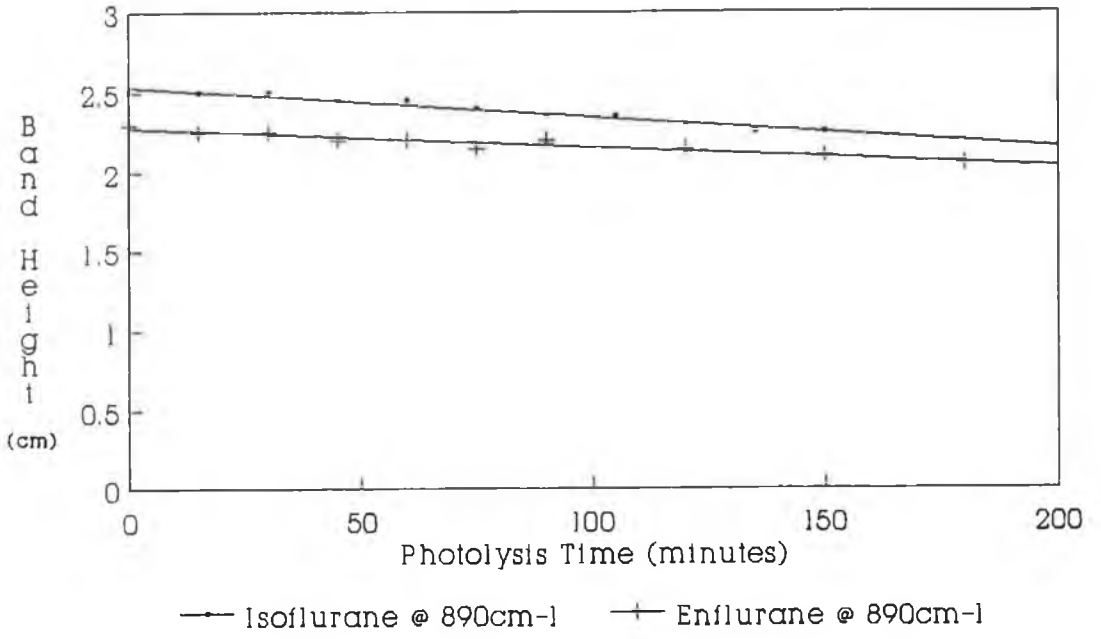

Figure 3.3.1.5
Reaction profiles obtained for the photolysis of 5 torr anaesthetic in the absence of O_2 or N_2 . Photolysis was carried our at 47 ± 4 °C at wavelengths above 200 nm .

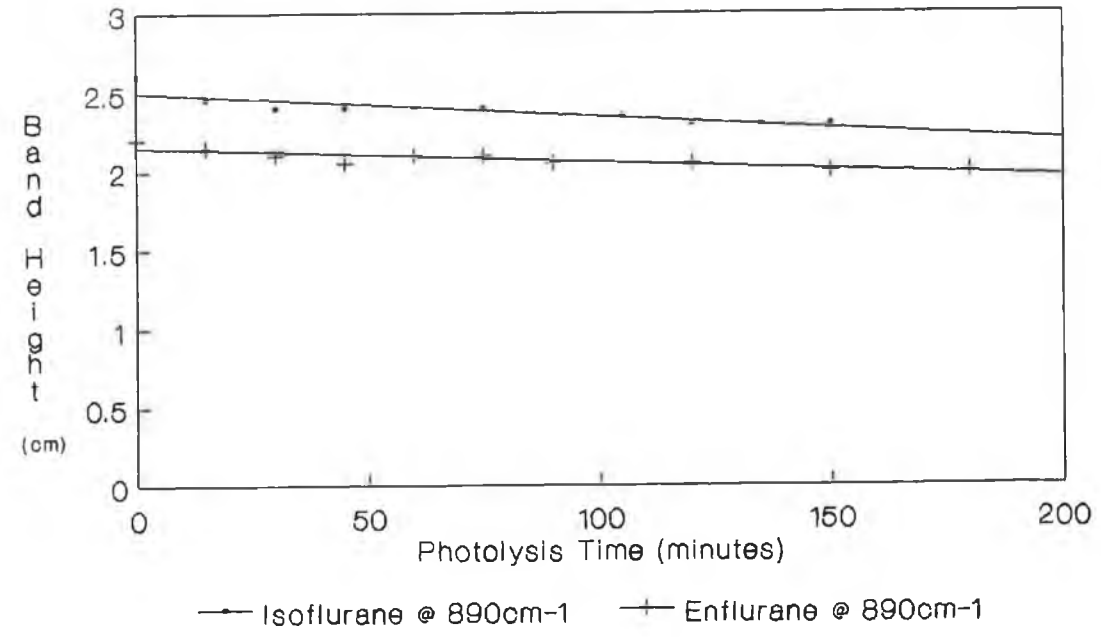

Figure 3.3.1.6
Reaction profiles obtained for the photolysis of 5 torr of the anaesthetics in 195 torr N_2 . Photolysis was carried out at 47 ± 4 °C using wavelengths above 200 nm .

3.3.1.6 demonstrate the results obtained during the photolysis of 5 torr anaesthetic , first on their own in the reaction cell and secondly in nitrogen at a total pressure of 200 torr. It is interesting to note that both anaesthetics exhibit slow losses over the long timescales used .

3.3.2 Photooxidation profiles

(a) *Infrared spectroscopic monitoring of reaction profiles*

Initial work involved monitoring the decay of the anaesthetics , plus the appearance of their reaction product IR bands over extended photolysis times . The output from the medium pressure mercury lamp was unfiltered in these experiments . Figures 3.3.2.1 show the absorption bands produced during the photolysis of isoflurane in oxygen .

As can be seen from Figure 3.3.2.1 two major carbonyl bands were initially evident at 1840 and 1940 cm^{-1} together with a series of sharp bands between 3100 and 2600 cm^{-1} . Prolonged photolysis resulted in the formation of a third carbonyl type band centred at 2350 cm^{-1} . The significance of these bands is discussed later in this report , particularly with regard to the elucidation of possible reaction mechanisms .

Figures 3.3.2.2 shows the IR absorption bands produced during the photolysis of enflurane in oxygen . These spectra demonstrate the production of a number of carbonyl vibrational bands during photolysis (at 1840 , 1910 , and 1940 cm^{-1}) . As in the reaction of isoflurane a further band at 2350 cm^{-1} was formed on prolonged irradiation . Sharp bands between 3100 and 2600 cm^{-1} were also formed during the photooxidation of enflurane .The significance of these bands is discussed later in this report .

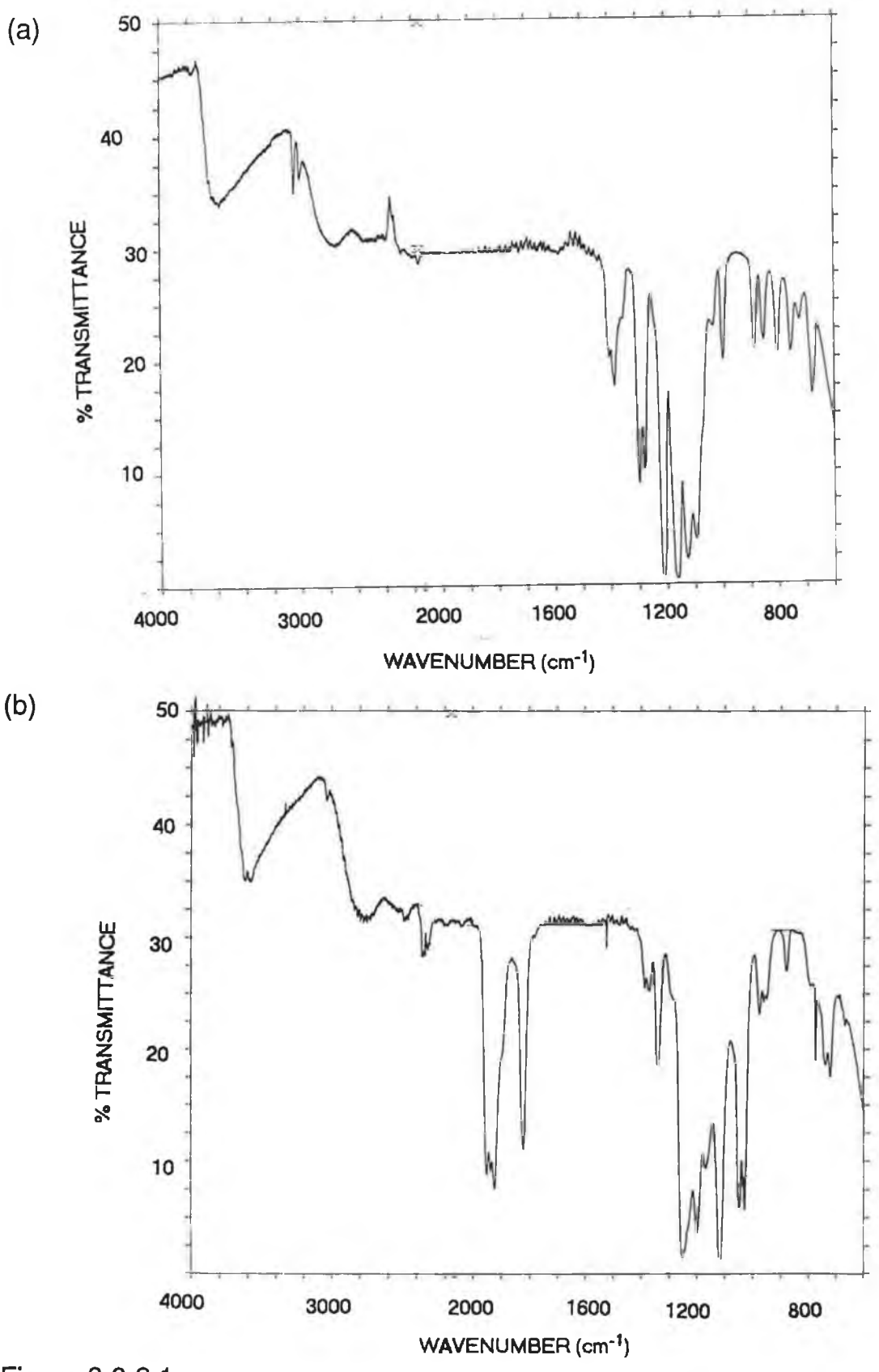

Figure 3.3.2.1
Photolysis of 5 torr isoflurane plus 200 torr O_2 at wavelengths above 200 nm and at a temperature of 47 ± 4 °C . IR spectra were recorded at (a) t = 0 , and (b) t = 270 minutes .

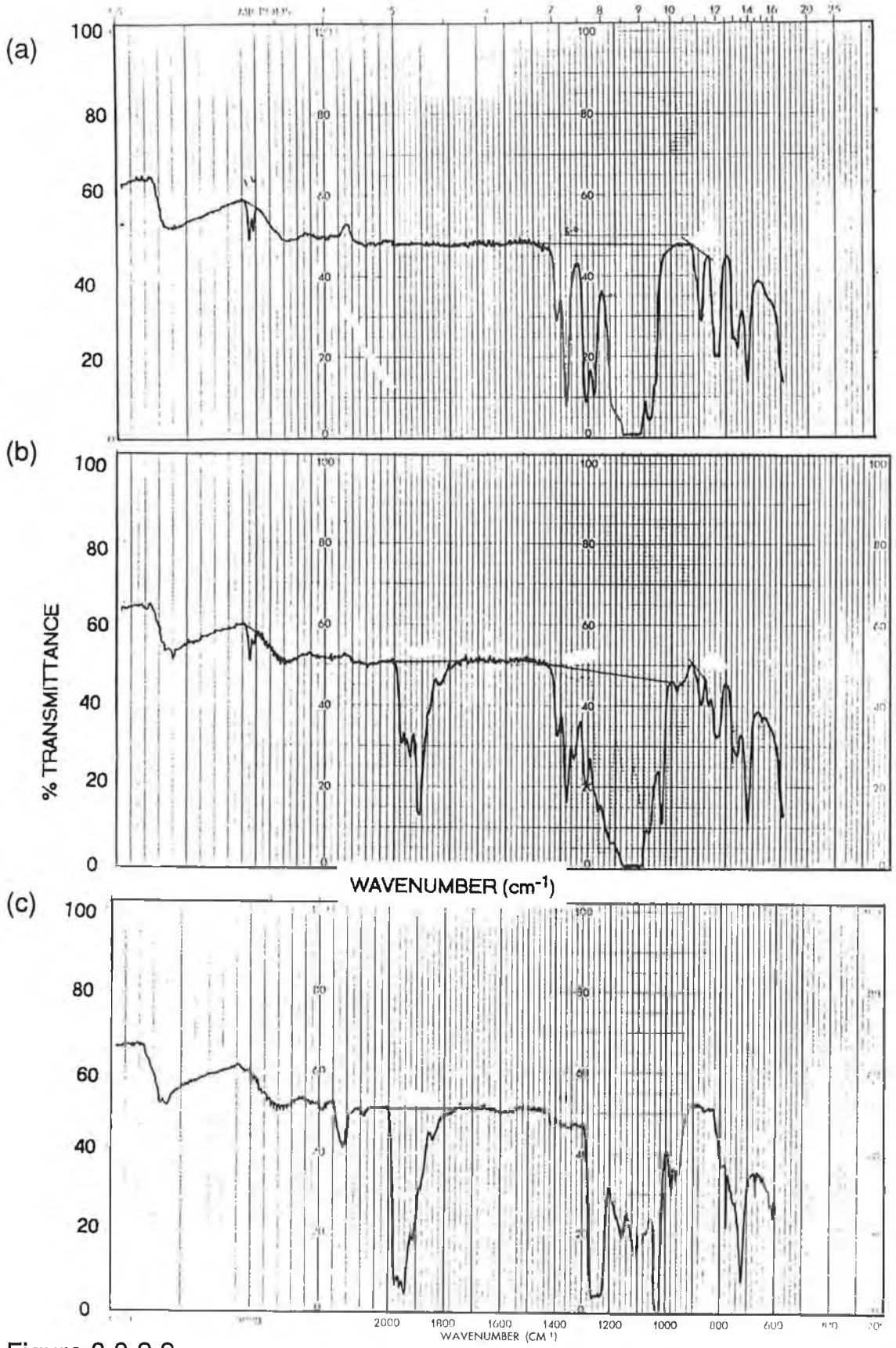

Figure 3.3.2.2

Photolysis of 10 torr enflurane plus 100 torr O_2 at wavelengths above 200 nm and at a temperature of 47 ± 4 °C . IR spectra were recorded at (a) 0 , (b) 105 and (c) 240 minutes .

Having completed preliminary IR investigations into the photooxidation of the anaesthetics, detailed reaction profiles were estabished, with both the disappearance of reactant and the formation of products monitored (Figures 3.3.2.3 to 3.3.2.8) .

Initally 5 torr isoflurane or enflurane was photolysed in 195 torr O_2 with the resulting profiles illustrated in Figures 3.3.2.3 and 3.3.2.4 . The profile for isoflurane (Figure 3.3.9) indicates an initial lag time at the beginning of reaction followed by the production of an unknown carbonyl compound (at 1840 cm^{-1}) plus CF_2O (band at 1940 cm^{-1}). Prolonged photolysis resulted in the production of CO_2 , indicated by the IR band at 2350 cm^{-1} . The photooxidation profile for enflurane (Figure 3.3.2.4) is similar to isoflurane in that an induction period is evident prior to reaction . Also , two unknown carbonyl compounds plus CF_2O and CO_2 are produced . Common to both reactions is the noticeable maximum exhibited with respect to the main carbonyl product , while CF_2O production continues to increase with photolysis time . The height of the sharp bands produced during the photooxidation of the anaesthetics and appearing in the IR spectra at wavelengths between 3100 and 2600 cm^{-1} were not monitored due to their small size .

Figures 3.3.2.5 and 3.3.2.6 illustrate the reaction profiles for 5 torr isoflurane or 5 torr enflurane in 5 torr O_2 and 190 torr N_2 . These profiles are very similar to those in 3.3.2.3 and 3.3.2.4 , indicating the minimal effect of O_2 concentrations above 5 torr .

Finally , Figures 3.3.2.7 and 3.3.2.8 demonstrate the photooxidation profiles obtained for the reaction of 25 torr isoflurane and enflurane , in 5 torr O_2 and 170 torr N_2 . Noticeable in these profiles is the incomplete reaction of the anaesthetics and the tailing off in CF_2O and CO_2 production . The fact that the main carbonyl product in both photolyses started to decrease , while the CF_2O and CO_2 concentrations levelled off

but did not fall , indicates that these latter compounds are probably secondary reaction products, possibly resulting from the breakdown of the main carbonyl products .

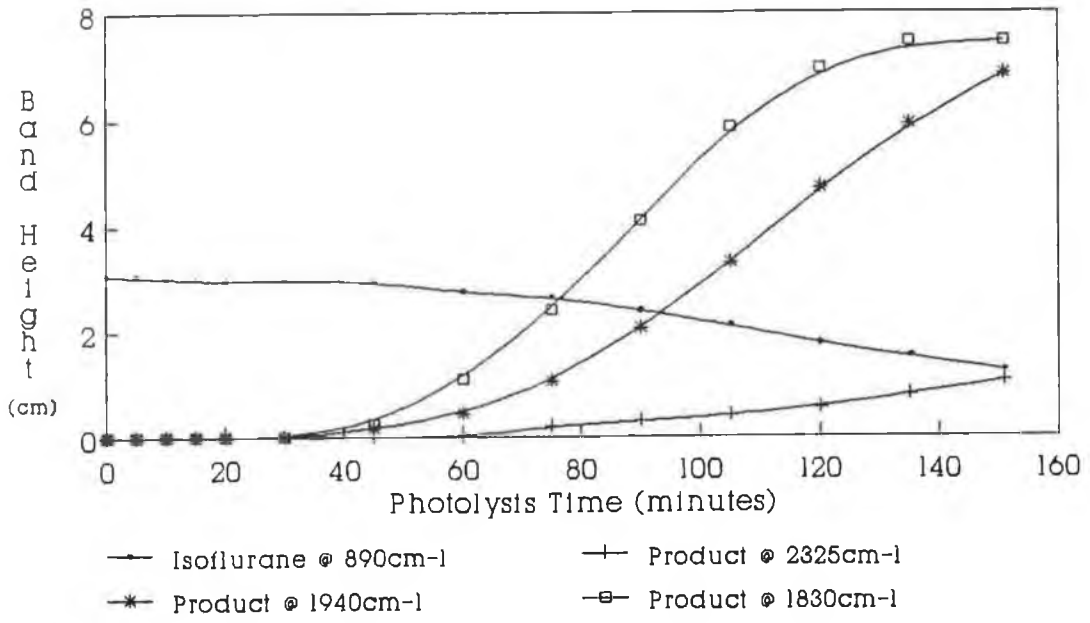

Figure 3.3.2.3
Photolysis profile obtained for the photooxidation of 5 torr isoflurane in 195 torr O_2 at wavelengths above 200 nm and at a temperature of 47 ± 4 ^oC . The appearance of reaction products is also illustrated .

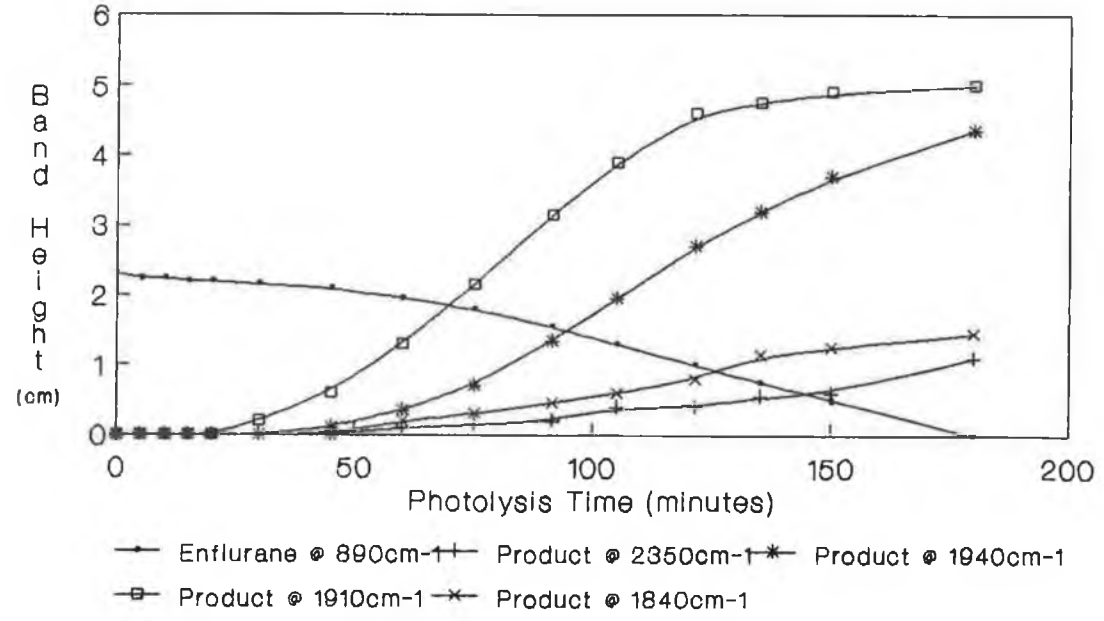

Figure 3.3.2.4
Photolysis profile obtained for the photooxidation of 5 torr enflurane in 195 torr O_2 at wavelengths above 200 nm and at a temperature of 47 ± 4 ^oC . The appearance of reaction products is also illustrated .

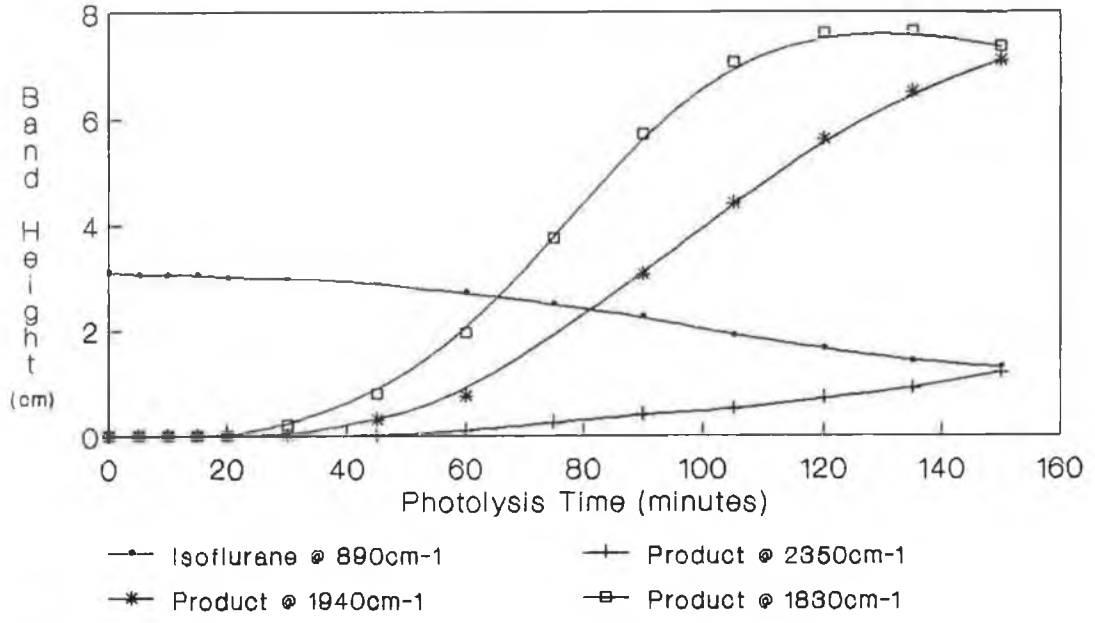

Figure 3.3.2.5
Photolysis profile for the photooxidation of 5 torr isoflurane in 5 torr O_2 and 190 torr N_2 at wvelengths above 200 nm and at a temperature of 47 ± 4 °C. Reaction product formation is also indicated .

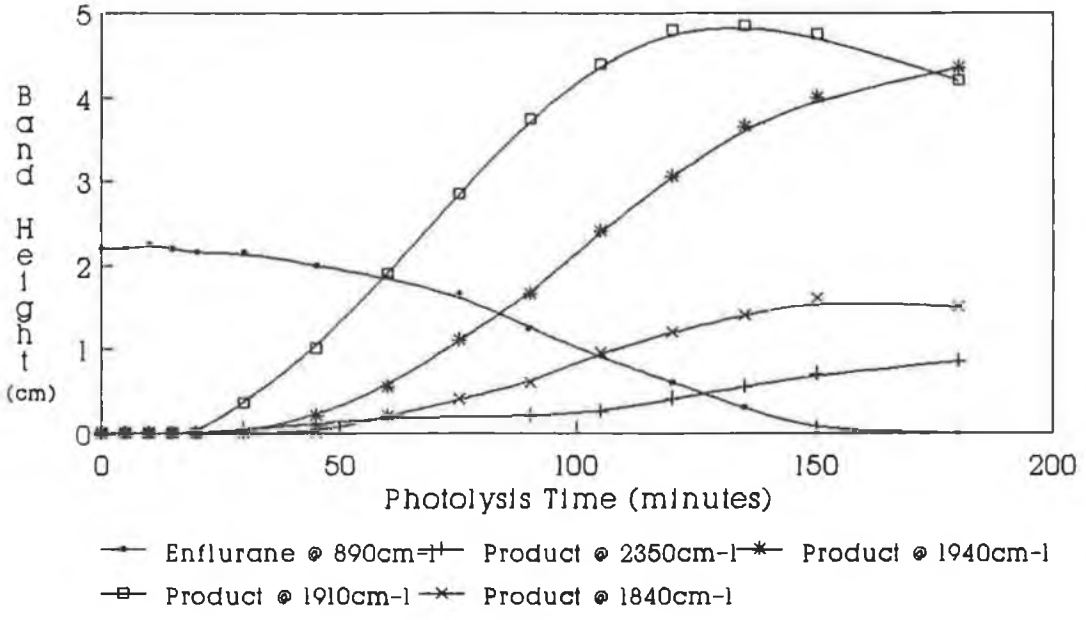

Figure 3.3.2.6
Photolysis profile for the photooxidation of 5 torr enflurane in 5 torr O_2 and 190 torr N_2 at wavelengths above 200 nm and at a temperature of 47 ± 4 °C . Reaction product formation is also indicated .

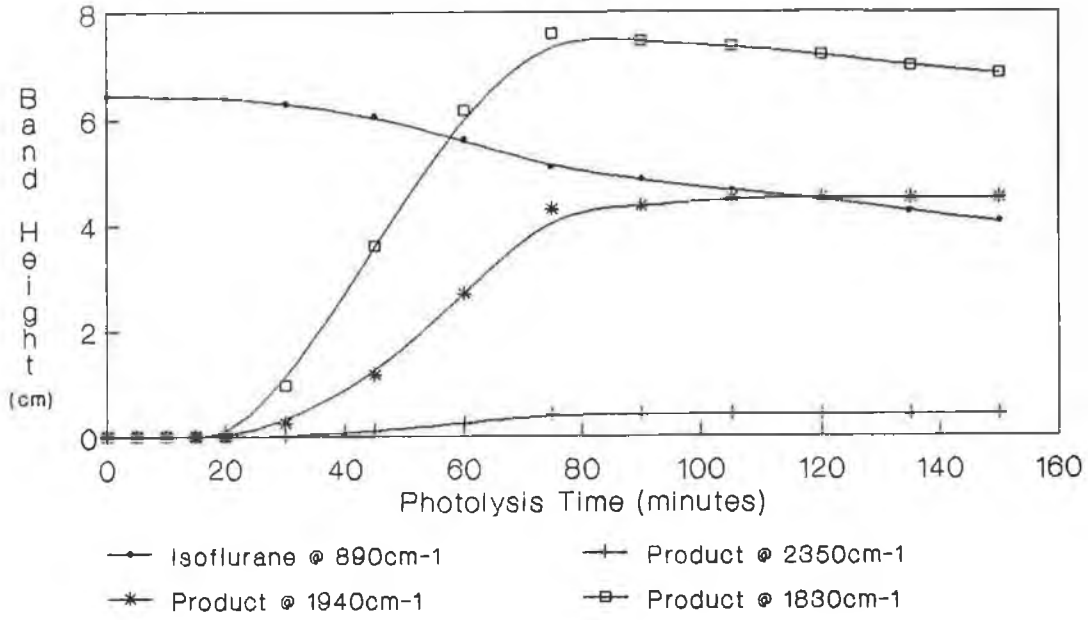

Figure 3.3.2.7
The photooxidation profile for 25 torr isoflurane in 5 torr O_2 and 170 torr N_2 at wavelengths above 200 nm and at a temperature of 47 ± 4 °C . Reaction product formation is also indicated .

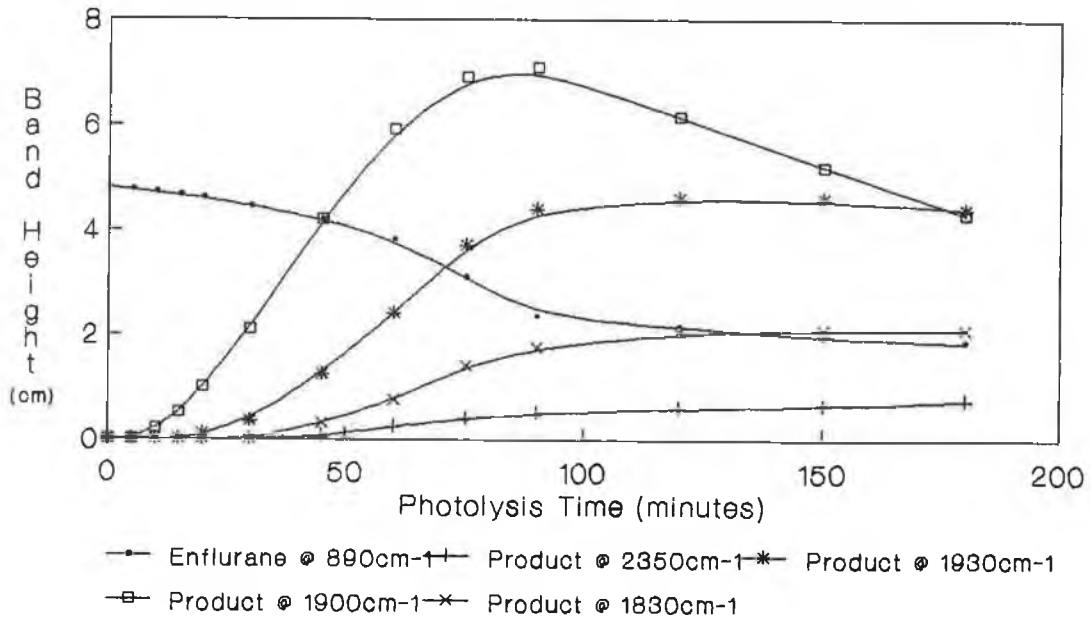

Figure 3.3.2.8
The photooxidation profile for 25 torr enflurane in 5 torr O_2 and 170 torr N_2 at wavelengths above 200 nm and at a temperature of 47 ± 4 °C . Reaction product formation is also indicated .

(b) *Gas Chromatographic monitoring of reaction profiles*

To calculate anaesthetic concentrations at each photolysis time , and to demonstrate the complex nature of the photooxidation processes involved, standard curves were initially established for each of the anaesthetics using GC . From these plots , illustrated in Figures 3.3.2.9 and 3.3.2.10 , the photooxidation profiles for isoflurane and enflurane were constructed , Figures 3.3.2.11 and 3.3.2.12 . The profiles obtained were similar to those determined by IR spectroscopy (Figures 3.3.2.3 and 3.3.2.4) , with a similar induction period indicated . Furthermore , the formation of reaction products was indicated by the appearance of a peak in the GC traces for both anaesthetic reaction mixtures at long photolysis times . Although no information could be obtained as to the nature of these products using GC / FID , it did highlight the possible usefulness of GC / mass spectrometry in this work.

To demonstrate the complexity of the reaction processes involved, first order plots were constructed using the standard curves and the profile data. These plots , given in Figures 3.3.2.13 and 3.3.2.14 are non-linear as expected.

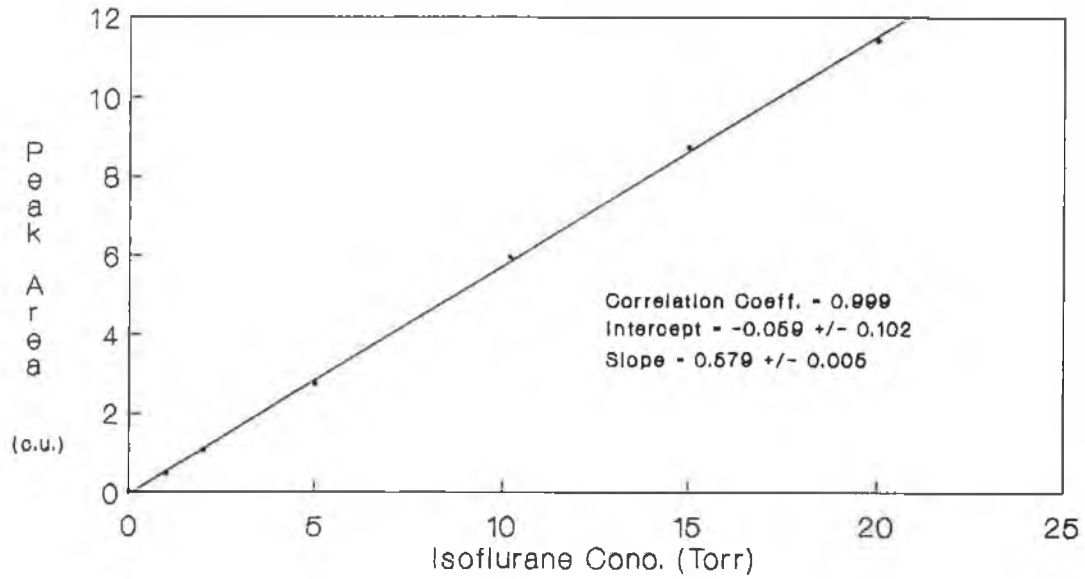

Figure 3.3.2.9

Isoflurane standard curve in 300 torr O_2 , determined by GC .

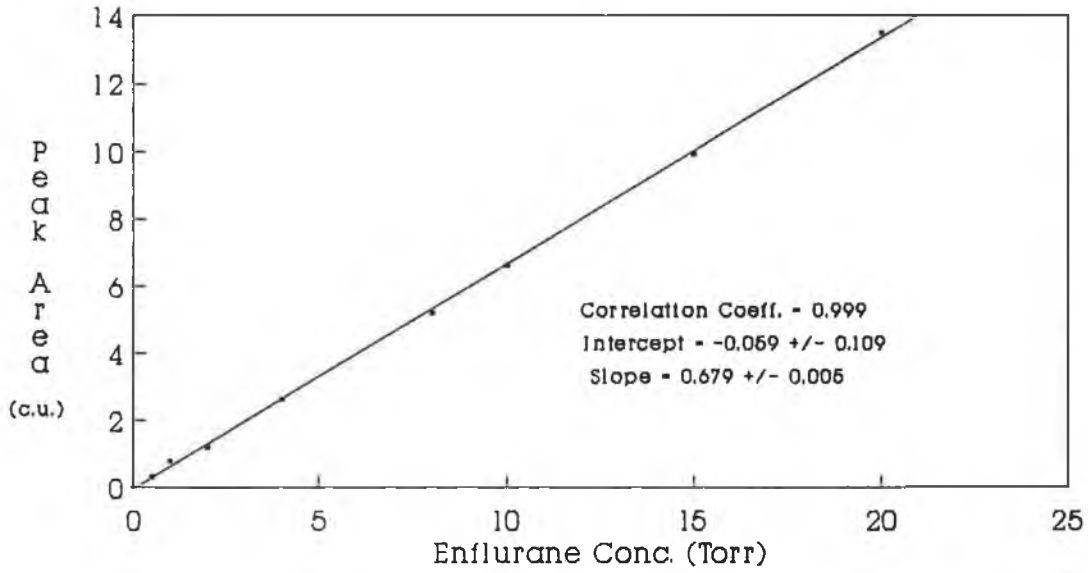

Figure 3.3.2.10

Enflurane standard curve in 300 torr O_2 , determined by GC .

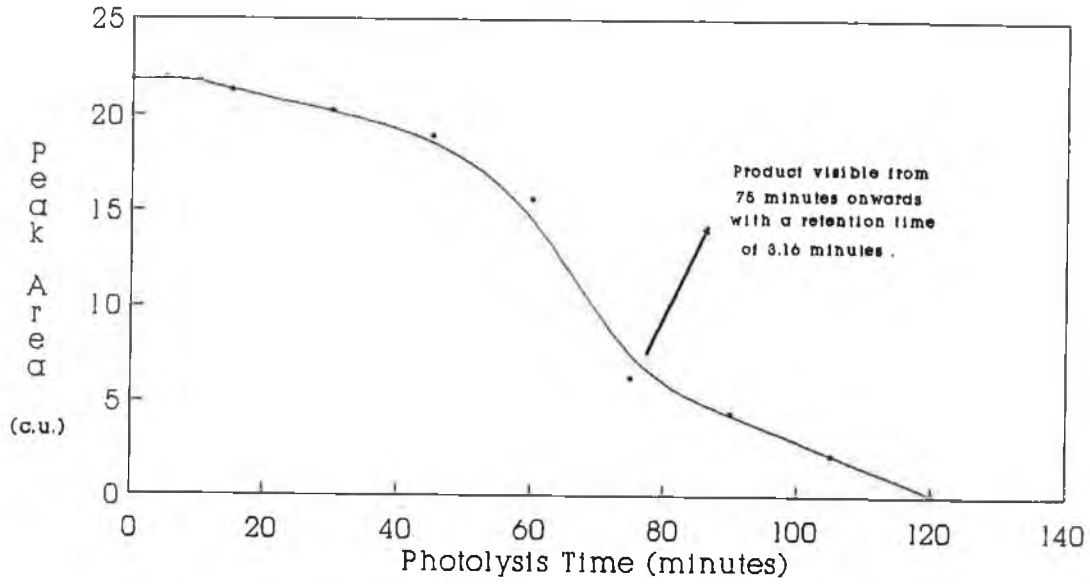

Figure 3.3.2.11
Photooxidation profile for 20 torr isoflurane in 300 torr O_2 using wavelengths above 200 nm and a temperature of 47 ± 4 °C . Reaction was followed by GC .

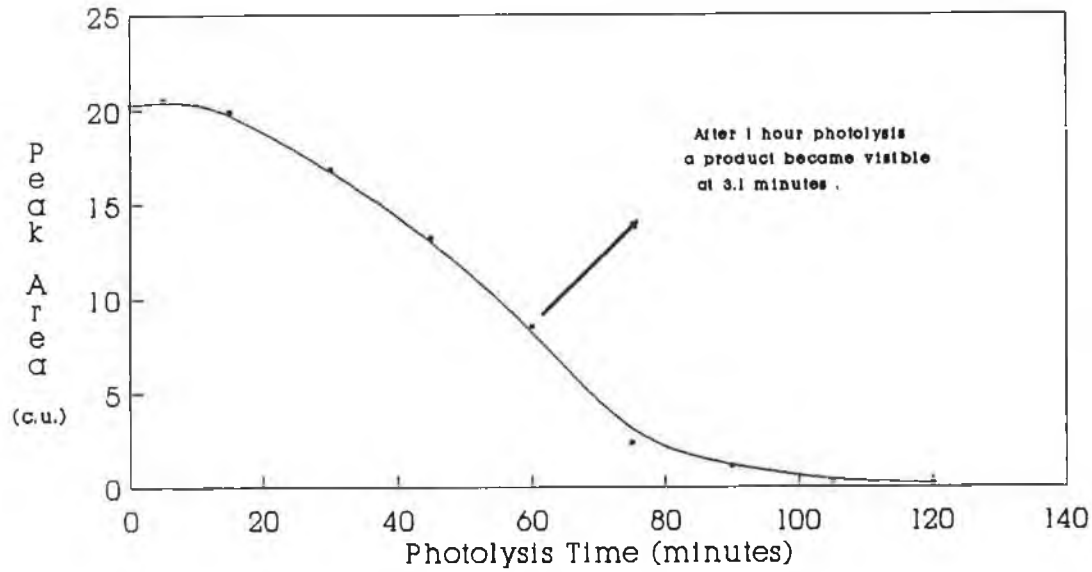

Figure 3.3.2.12
Photooxidation profile for 20 torr enflurane in 300 torr O_2 at wavelengths above 200 nm and at a temperature of 47 ± 4 °C . Reaction was followed by GC .

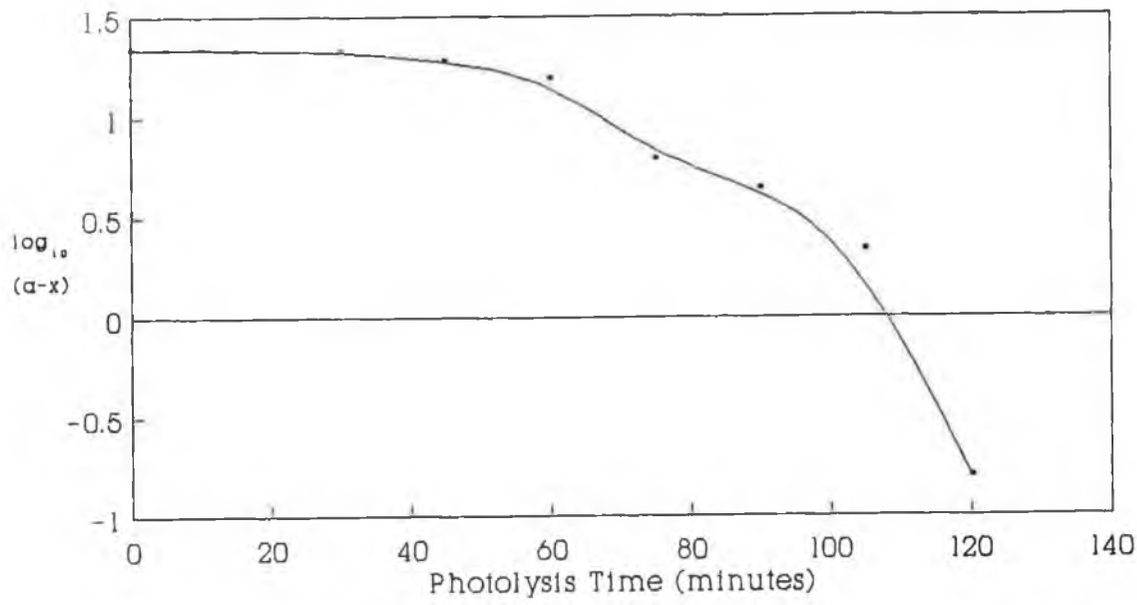

Figure 3.3.2.13
1st order plot for the photooxidation of 20 torr isoflurane in 300 torr O_2 at 47 ± 4 °C using wavelengths above 200 nm .

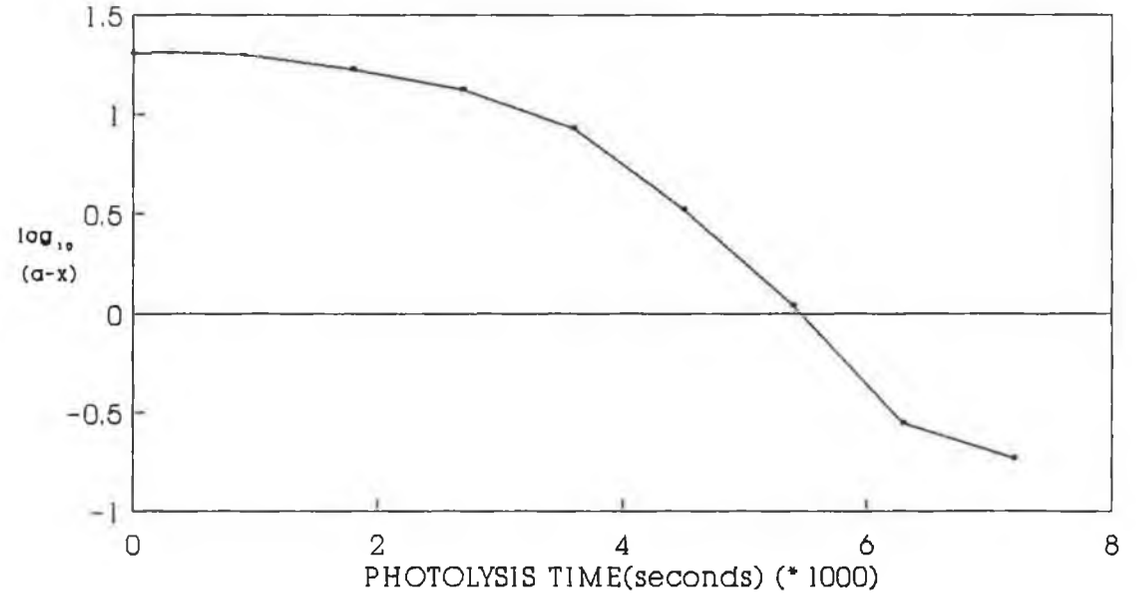

Figure 3.3.2.14
Ist order plot for the photooxidation of 20 torr enflurane in 300 torr O_2 at 47 ± 4 °C using wavelengths above 200 nm .

3.3.3 Effect of reaction parameters on the photooxidation of the anaesthetics

(a) *Effect of oxygen concentration*

Figures 3.3.3.1 and 3.3.3.2 , illustrate the effect which oxygen concentration exerted on the reaction rate of the anaesthetics . For both anaesthetics the rate of loss observed plus the concentration of the photooxidation products remained essentially constant once the oxygen pressure was above 5 torr . Only the effect of oxygen concentration on the main photooxidation products was examined and portrayed in Figures 3.3.3.1 and 3.3.3.2 . The reason for this was that the other reaction products were present only in small concentrations at the reaction times used in this experiment .

(b) *Effect of anaesthetic concentration*

Figures 3.3.3.3 and 3.3.3.4 show the linear relationship between the rate of loss of the anaesthetics , the levels of their photooxidation products formed and the concentration of the anaesthetic added to the initial reaction mixture.

(c) *Effect of total pressure*

Figures 3.3.3.5 and 3.3.3.6 , show the effect of total pressure on the rate of loss of both anaesthetics and on the levels of their photooxidation products formed . The total pressure of the reaction mixture exerted little effect on the rate of loss of isoflurane or on the concentration of it's photoxidation products (Figure 3.3.3.5). However, in the photooxidation of enflurane, greater loss of anaesthetic and more reaction products were observed at lower total pressures(Figure 3.3.3.6) . Possible explanations for these observations are contained in the discussion of this report.

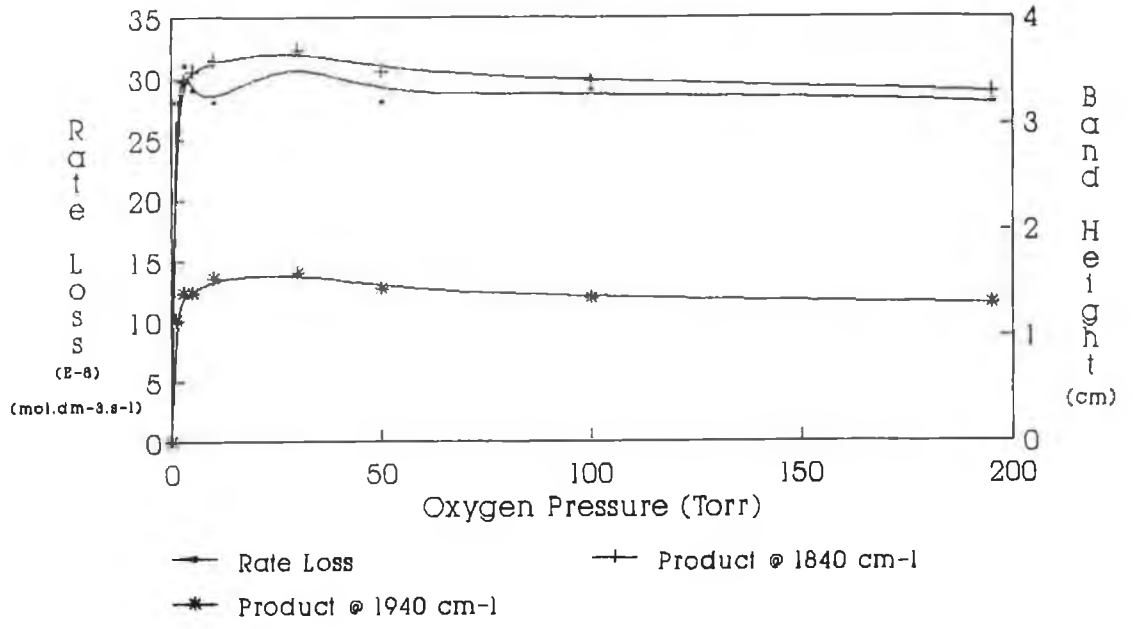

Figure 3.3.3.1
Effect of oxygen concentration on the rate of loss of isoflurane and on the formation of it's photooxidation products . Reaction was carried out at 47 ± 4°C , at a total pressure of 200 torr and using wavelengths above 200 nm .

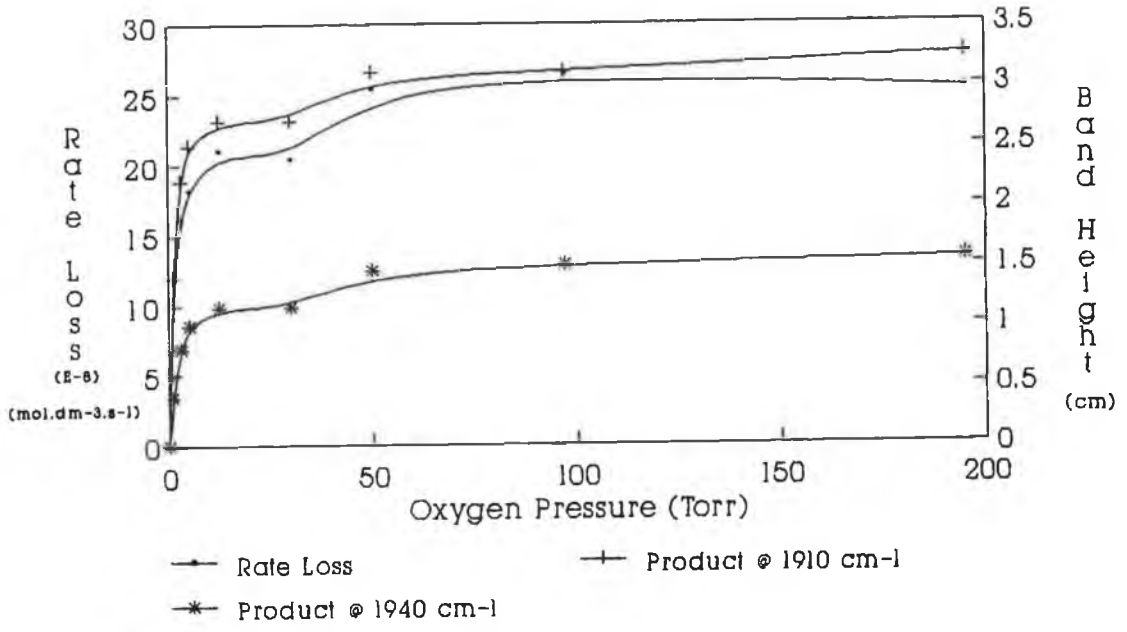

Figure 3.3.3.2
Effect of oxygen concentration on the rate of loss of enflurane and on the formation of it's photooxidation products . Reaction was carried out at 47 ± 4 °C and at a total pressure of 200 torr using wavelengths above 200 nm .

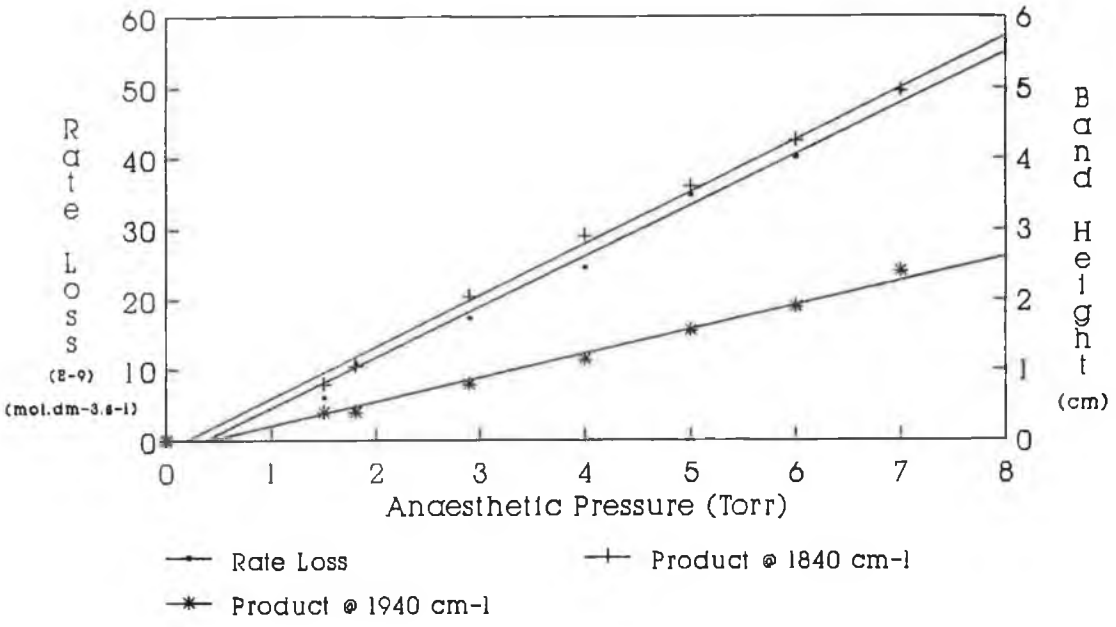

Figure 3.3.3.3
Effect of anaesthetic concentration on the rate of loss of isoflurane and on the rate of formation of it's photooxidation products . Reactions were carried out at 47 ± 4 °C using wavelengths above 200 nm and at a total pressure of 200 torr .

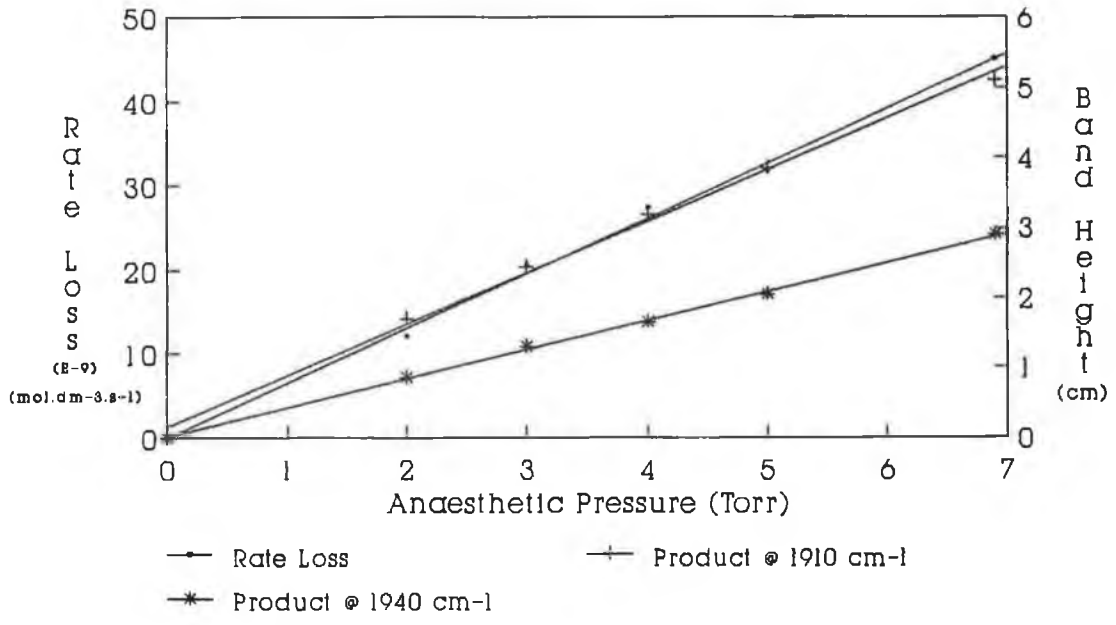

Figure 3.3.3.4
Effects of anaesthetic concentration on the rate of loss of enflurane and on the rate of formation of it's photooxidation products . Reactions were carried out at 47 ± 4 °C at a total pressure of 200 torr and using wavelengths above 200 nm .

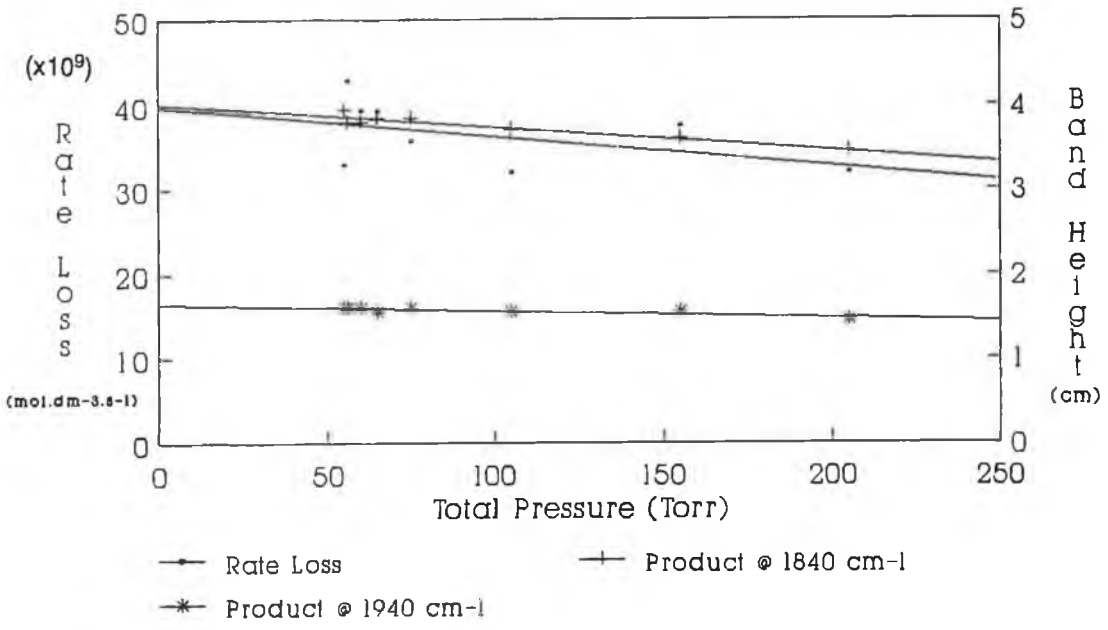

Figure 3.3.3.5
The effect of total initial reaction pressure on the rate of loss of isoflurane and on the concentrations of it's photooxidation products . Reactions were carried out at 47 ± 4 °C using wavelengths above 200 nm .

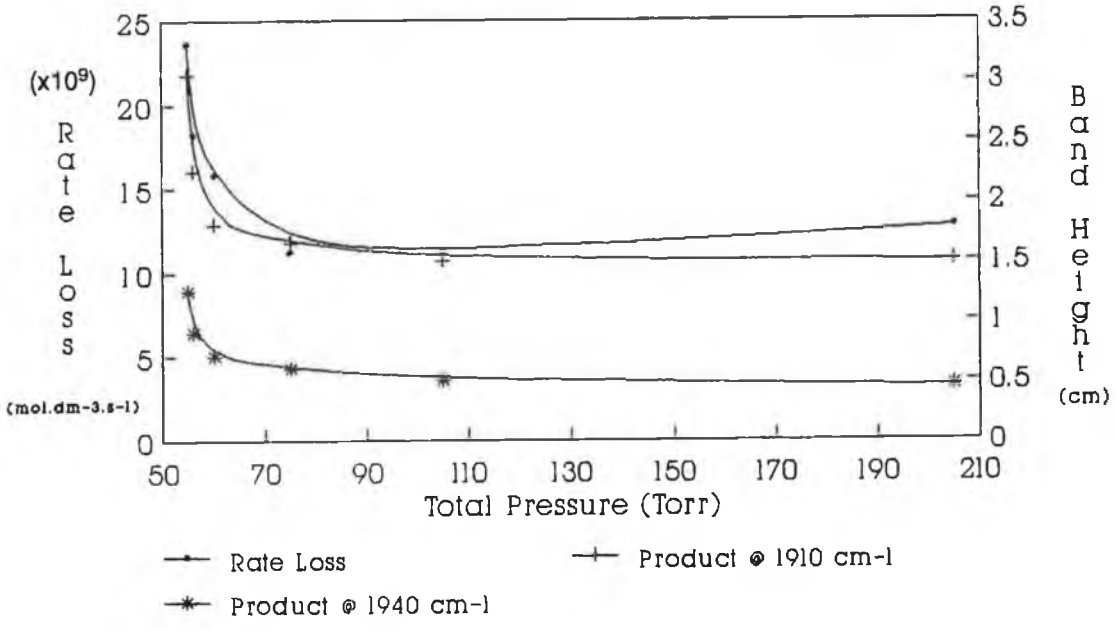

Figure 3.3.3.6
The effect of total initial reaction pressure on the rate of loss of enflurane and on the concentrations of it's photooxidation products . Reactions were carried out at 47 ± 4 °C using wavelengths above 200 nm .

(d) *Effect of light intensity*

The intensity of the medium pressure mercury lamp output, incident on the reaction mixtures affected the loss of anaesthetics and the concentration of their main photooxidation products in a linear fashion , as illustrated in Figures 3.3.3.7 and 3.3.3.8 .

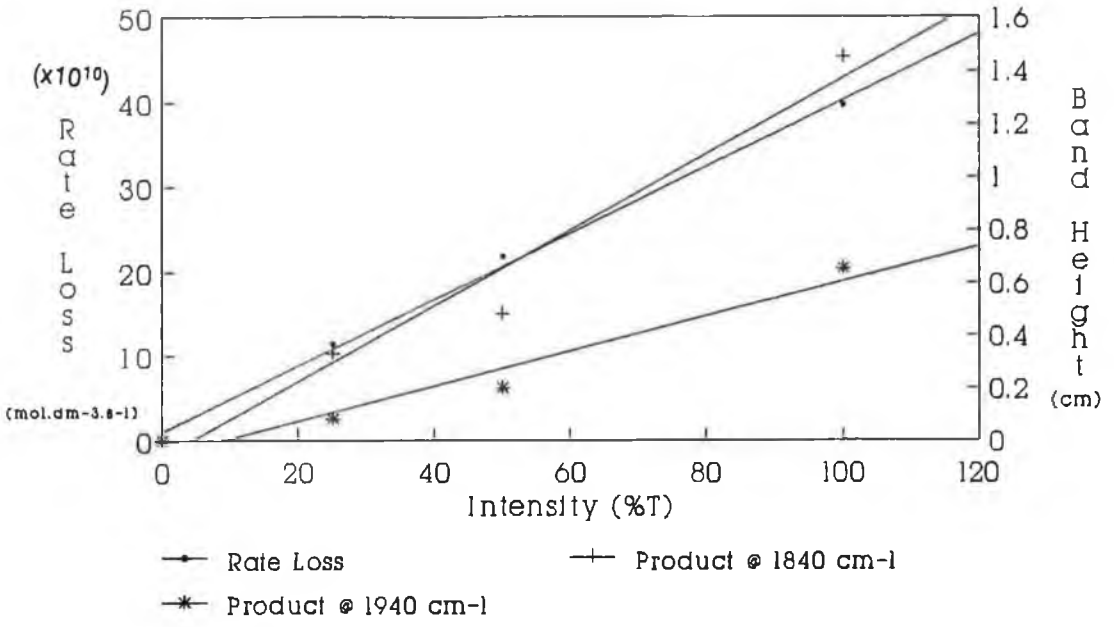

Figure 3.3.3.7
Effect of light intensity on the rate of loss of isoflurane and on the levels of it's photooxidation products . Reactions were carried out at a temperature of 47 ± 4 °C , at a total pressure of 200 torr and using wavelengths above 200 nm .

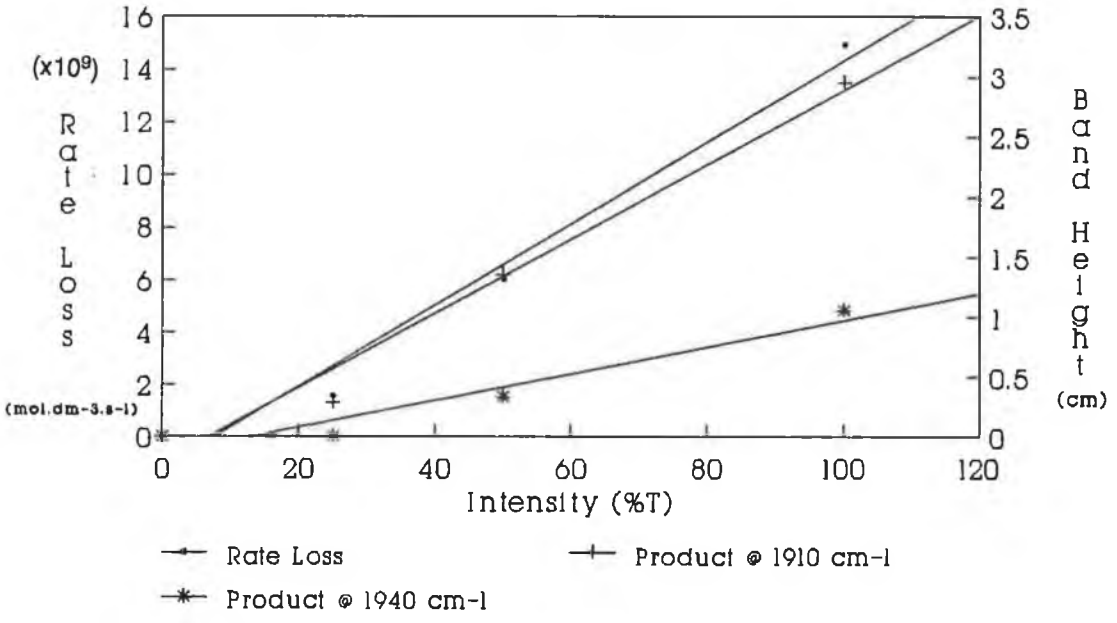

Figure 3.3.3.8
Effect of light intensity on the rate of loss of enflurane and on the levels of it's photooxidation products . Reactions were carried out at a temperature of 47 ± 4 °C , at a total pressure of 200 torr and using wavelengths above 200 nm .

3.3.4 Photooxidation of the anaesthetics in the presence of chlorine

As the reaction of chlorine atoms with the anaesthetics was thought to be important in the mechanism of photooxidation of these compounds, molecular chlorine was added to the reaction mixture prior to photolysis. Similar reaction products were obtained at shorter photolysis times , Figure 3.3.4.1 .

To investigate the effect of chlorine atoms on the photooxidation of the anaesthetics, photolysis was carried out with and without chlorine present. The resulting reaction profiles are given in Figures 3.3.4.2 to 3.3.4.5 . The main observation is that the presence of chlorine gives rise to further reactions with no observable induction time at the beginning of photolysis. Also as indicated in Figures 3.3.2.3 to 3.3.2.8 , and in Figures 3.3.4.3 and 3.3.4.5 , the main carbonyl product in both isoflurane and enflurane photolysis reaches a maximum and then starts to decline with prolonged photolysis. However, CF_2O production tends to steadily increase even at long reaction times. This could indicate that CF_2O may be a secondary reaction product.

To determine the overall importance of atomic chlorine reactions in the observed photooxidation of the anaesthetics mixtures containing 5 torr of anaesthetics , 1 torr Cl_2 and 194 torr O_2 were photolysed in a smog chamber using only the black lamps for photolysis ($\lambda > 320$ nm) . Figures 3.3.4.6 and 3.3.4.7 show the reaction profiles observed .

Having established that atomic chlorine reactions with the anaesthetics was very important in the photooxidation mechanism , the quantum yield for the chlorine - sensitized reaction of the anaesthetics with oxygen was determined . The actinometer used was $CHCl_3$ (reaction with Cl_2 at wavelengths > 300 nm) .

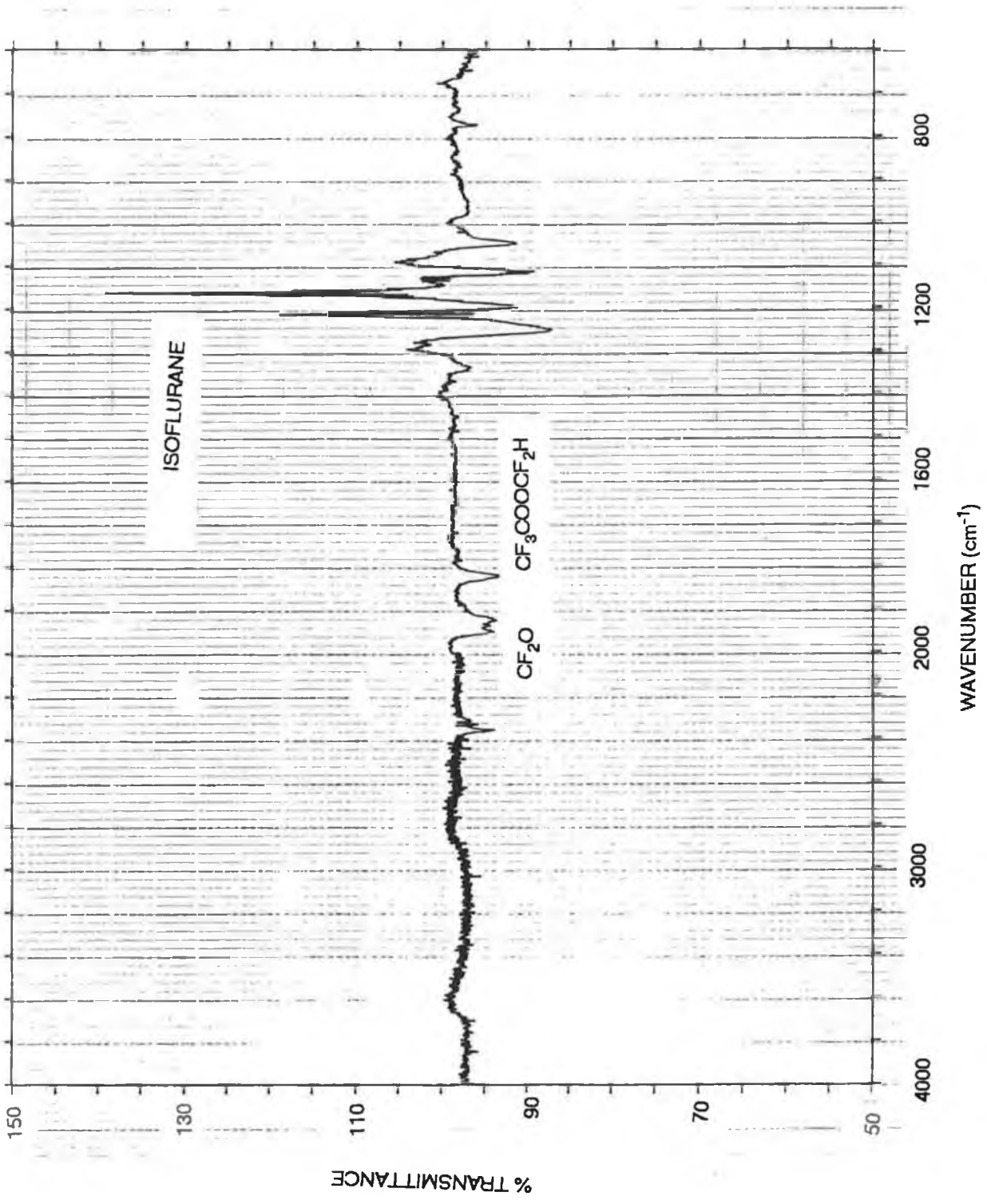

Figure 3.3.4.1
Infrared difference spectrum obtained during the photolysis of 5 torr isoflurane in 1 torr chlorine and 194 torr O_2 . Reaction was carried out at 47 ± 4 °C using wavelengths above 200 nm . The spectrum represents the difference between a reaction mixture at 30 and 60 minutes photolysis.

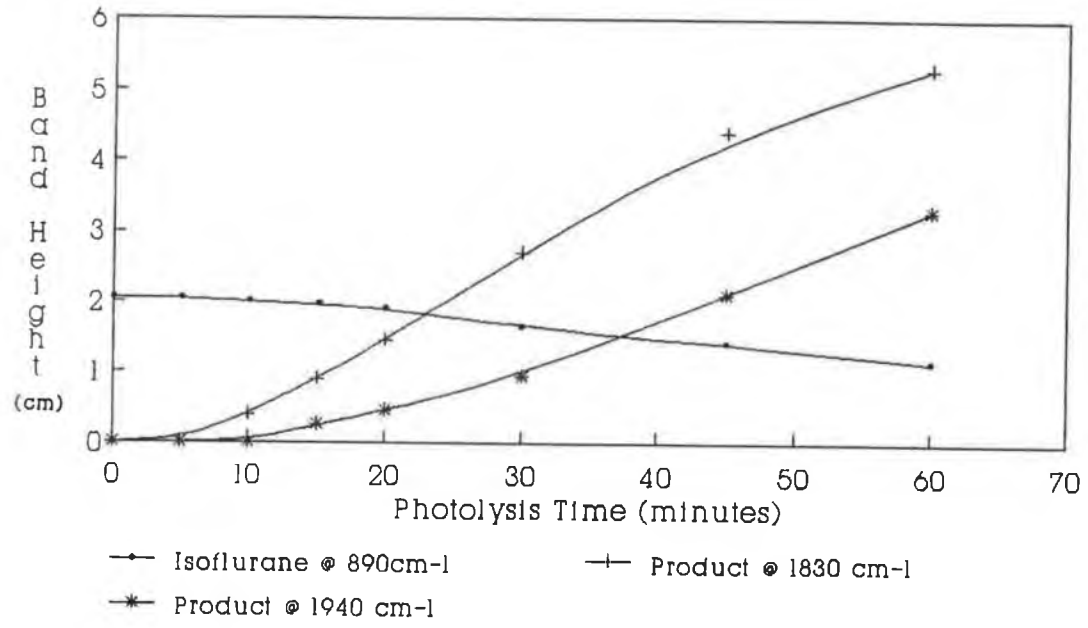

Figure 3.3.4.2
The photooxidation profile for 5 torr isoflurane in the absence of Cl_2 . Reactions were carried out in 194 torr O_2 at a temperature of 47 ± 4 °C using wavelengths above 200 nm .

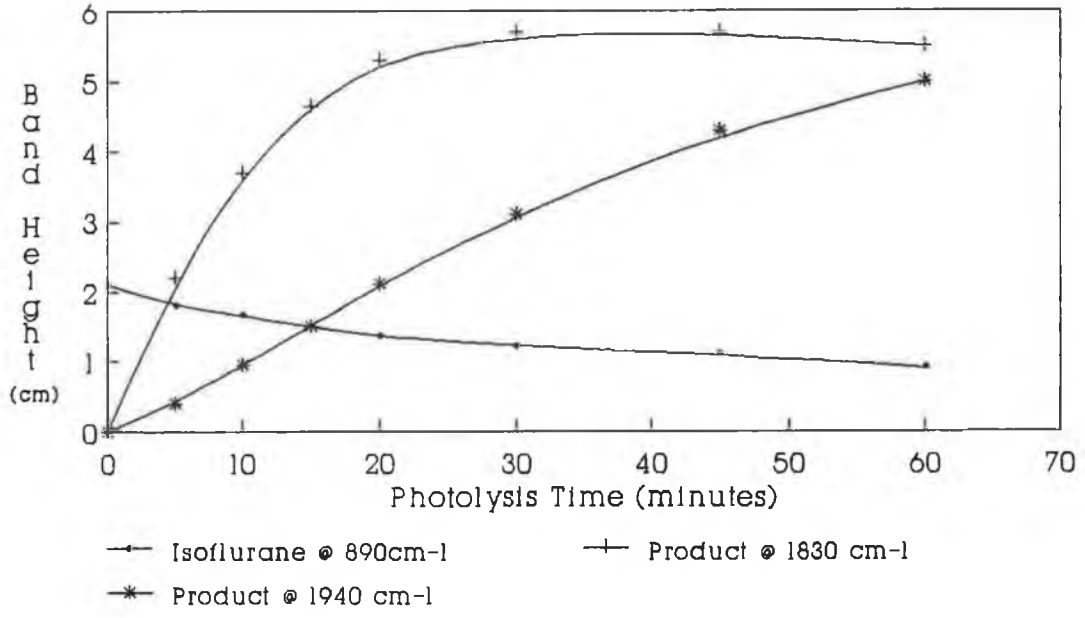

Figure 3.3.4.3
The photooxidation profile for 5 torr isoflurane in 1 torr Cl_2 and 194 torr O_2. Reaction was carried out at 47 ± 4 °C using wavelengths above 200 nm .

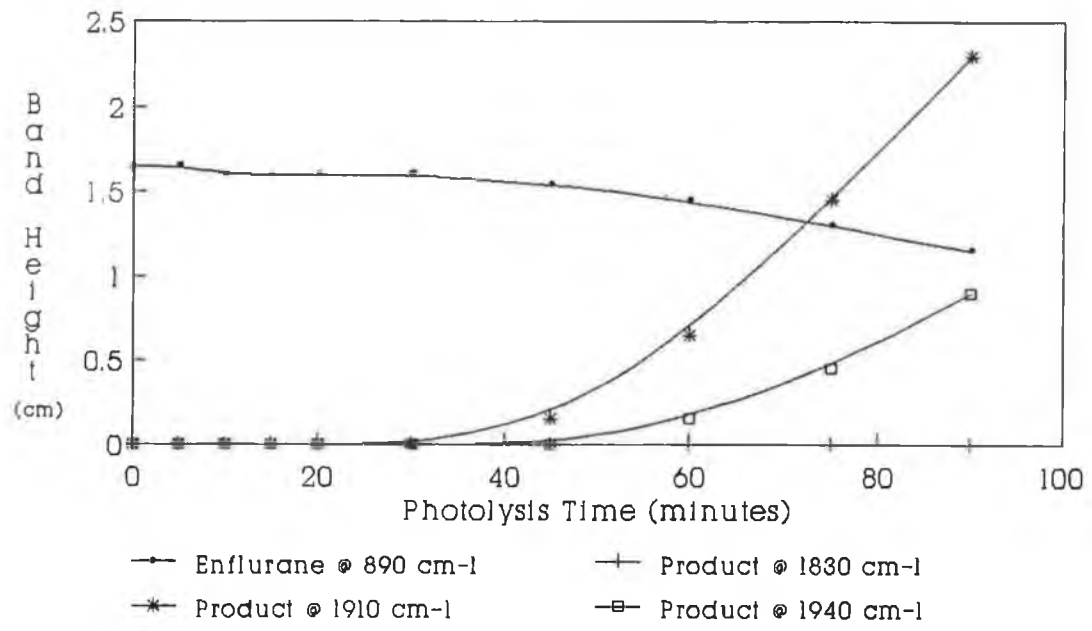

Figure 3.3.4.4
The photooxidation profile for 5 torr enflurane in 194 torr O_2 in the absence of Cl_2 . Reaction was carried out at 47 ± 4 °C using wavelengths above 200 nm .

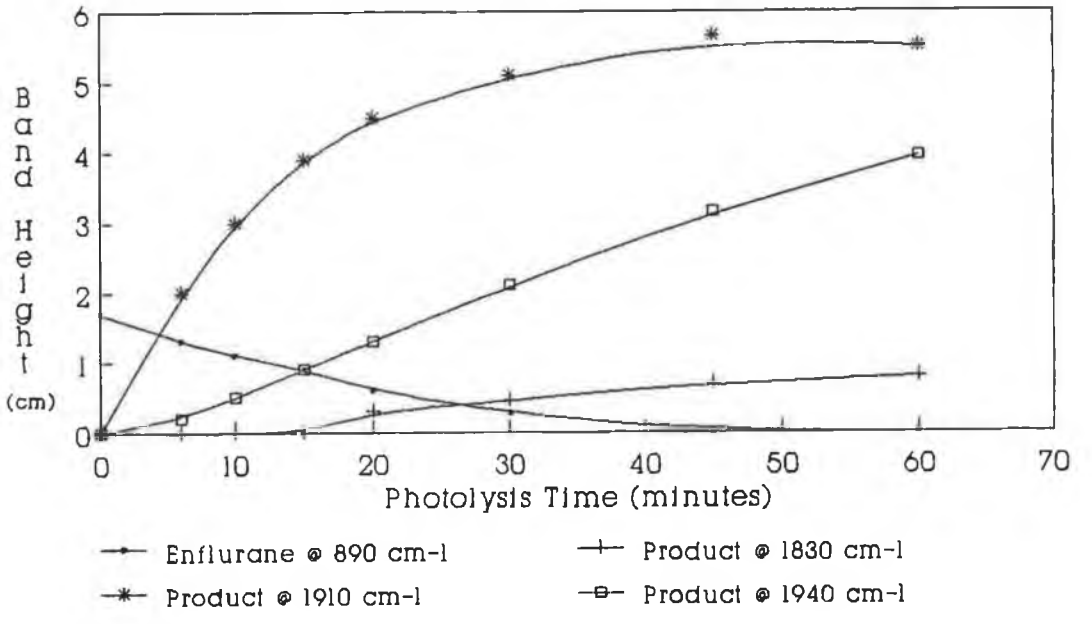

Figure 3.3.4.5
The photooxidation profile for 5 torr enflurane in 1 torr Cl_2 and 194 torr O_2. Reaction was carried out at 47 ± 4 °C using wavelengths above 200 nm.

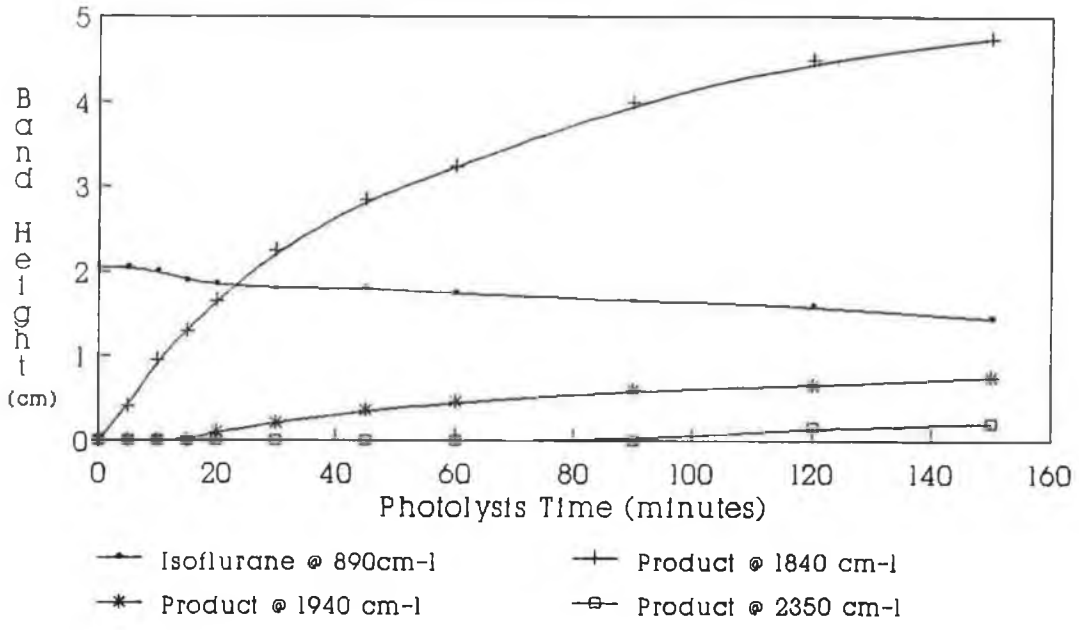

Figure 3.3.4.6
The photooxidation profile obtained for the reaction of 5 torr isoflurane in 1 torr Cl_2 and 194 torr O_2 . Photolysis was carried out using black lamps (λ > 320 nm) at a temperature of 20 ± 1 °C .

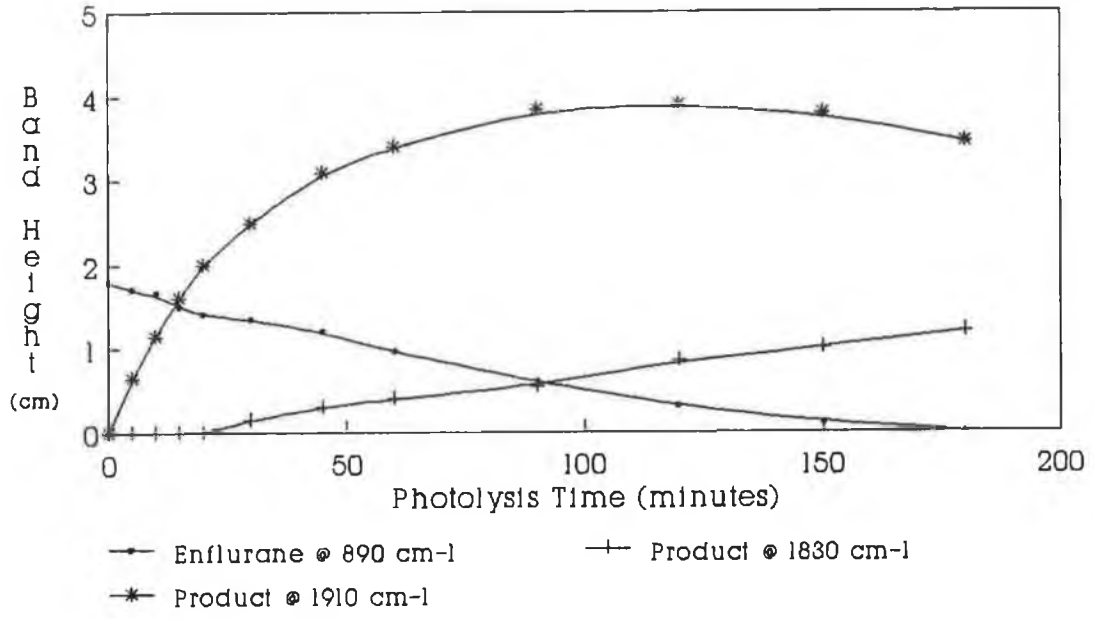

Figure 3.3.4.7
The photooxidation profile obtained for the reaction of 5 torr enflurane in 1 torr Cl_2 and 194 torr O_2 . Photolysis was carried out using black lamps (λ > 320 nm) at a temperature of 20 ± 1 °C .

Prior to establishing the quantum yields, standard curves were determined and these are given in Figure 3.3.4.8 . Figures 3.3.4.9 to 3.3.4.11 demonstrate the effect which light intensity had on the loss of the $CHCl_3$ and the anaesthetics. From the results, it would appear that the rate of reaction of the anaesthetics with oxygen in chlorine (at wavelengths > 300 nm) is essentially linearly dependent on light intensity once the reaction has been initiated. The effect of light intensity on the concentration of the main carbonyl products is also depicted.

Finally , Table 3.3.4.1 illustrates the effect which light intensity exerted on the quantum yield (with respect to the loss of anaesthetics) for the chlorine atom initiated photooxidation of the anaesthetics at λ's > 300 nm .

(a)

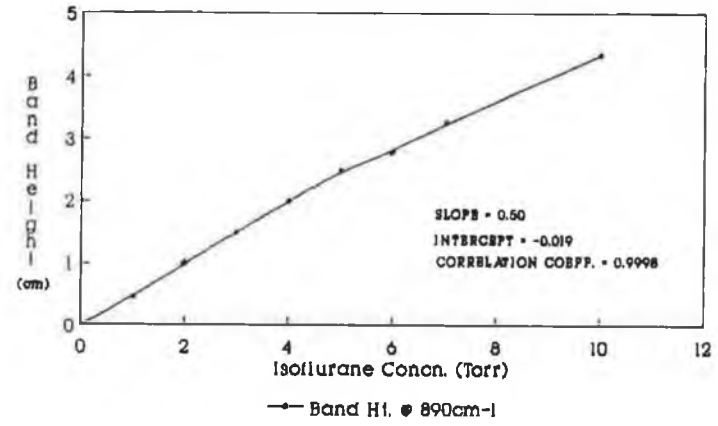

(b)

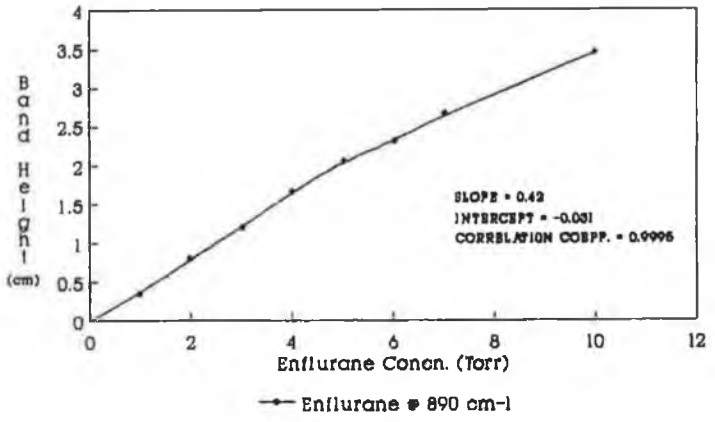

(c)

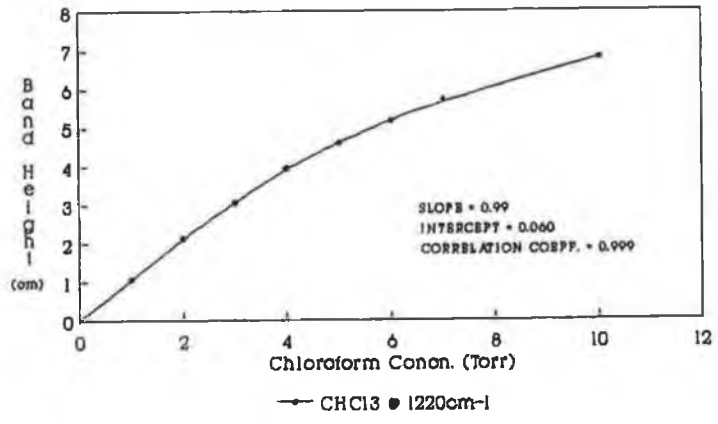

Figure 3.3.4.8
Standard curves for (a) isoflurane @ 890 cm^{-1} ,(b) enflurane @ 890 cm^{-1} and (c) $CHCl_3$ @ 1220 cm^{-1}. Plots were established using IR spectroscopy.

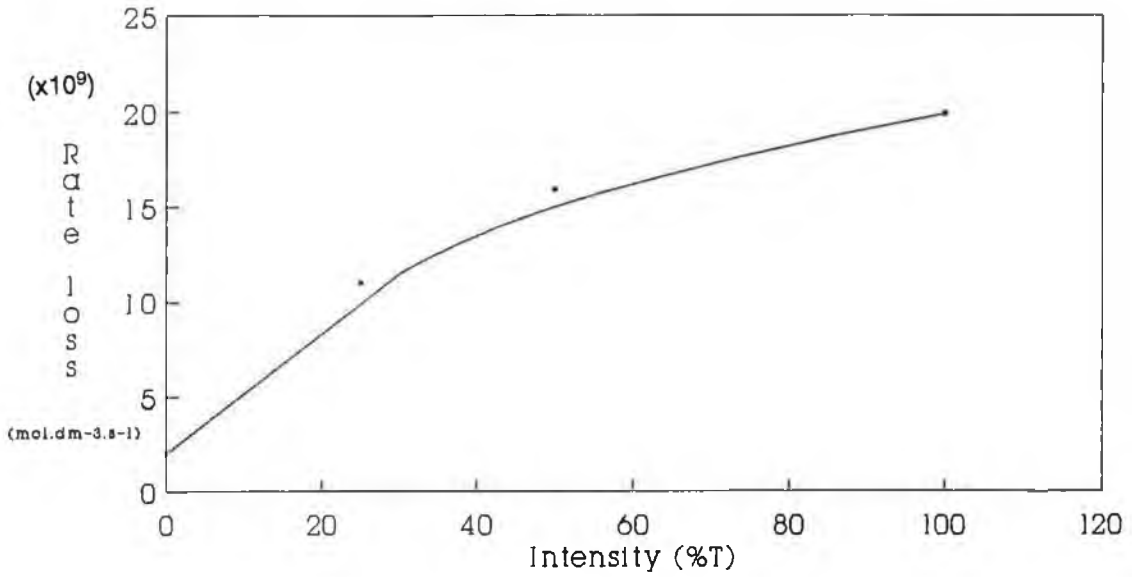

Figure 3.3.4.9
The effect of light intensity on the rate of loss of 5 torr $CHCl_3$ in 1 torr Cl_2 . Reaction was carried out at a temperature of 47 ± 4°C and at wavelengths above 300 nm .

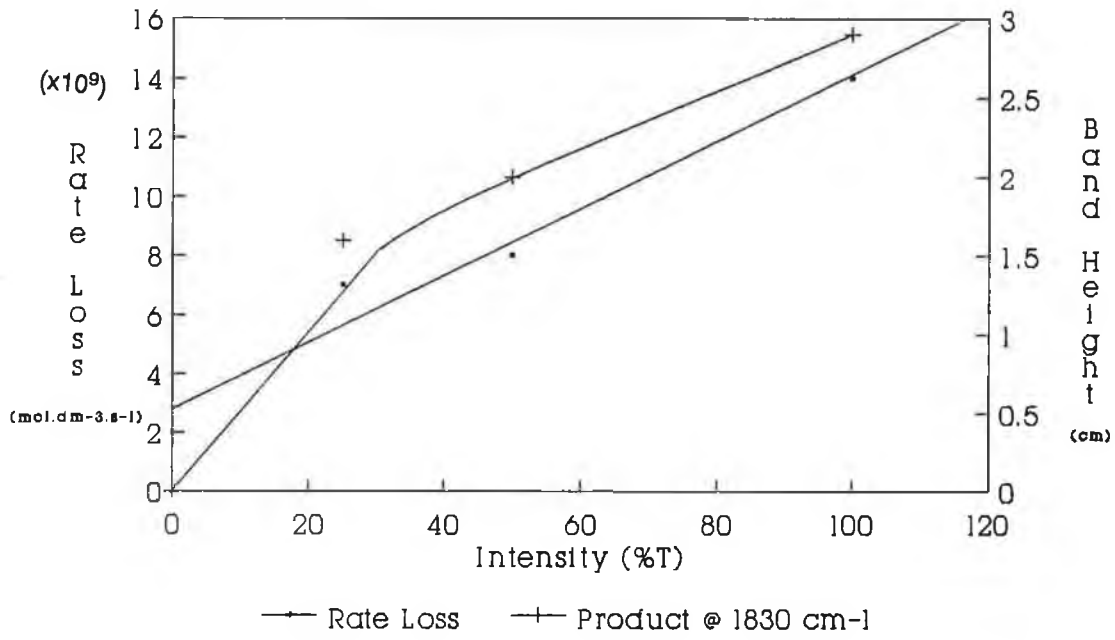

Figure 3.3.4.10
The effect of light intensity on the rate of loss of 5 torr isoflurane in 1 torr Cl_2 and 194 torr O_2 . Reaction was carried out at a temperature of 47 ± 4°C using wavelengths above 300 nm .

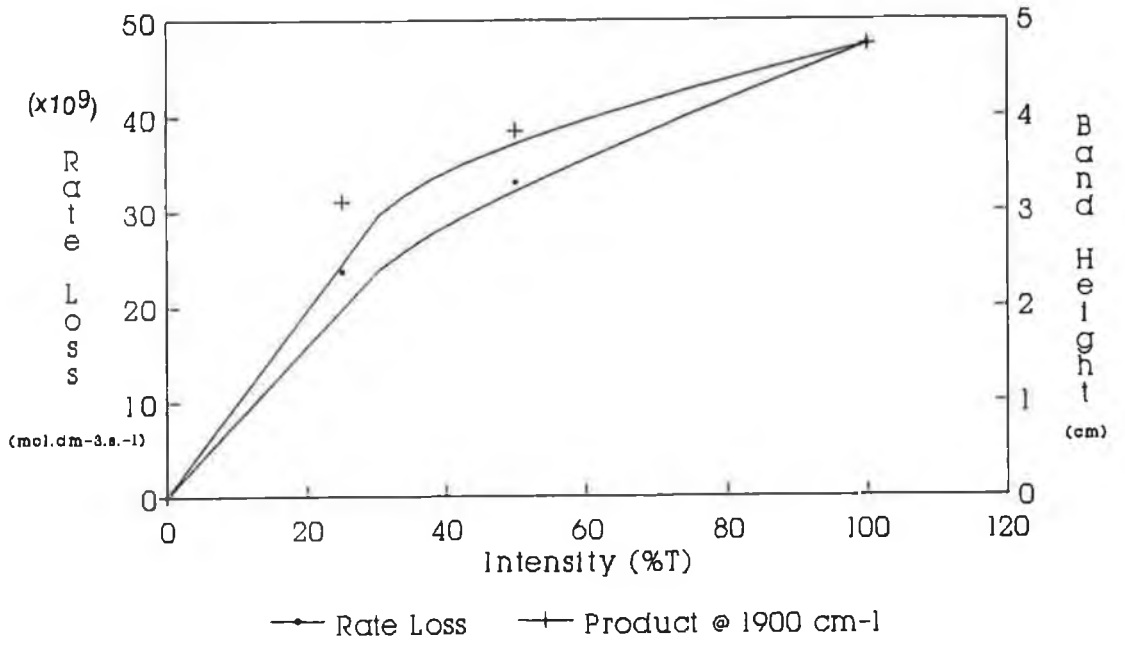

Figure 3.3.4.11
The effect of light intensity on the rate of loss of 5 torr enflurane in 1 torr Cl_2 and 194 torr O_2 . Reaction was carried out at a temperature of 47 ± 4°C using wavelengths above 300 nm .

Intensity %	**Average Rate of Loss** (mol $dm^{-3}s^{-1}$)			Φ loss of anaesthetic	
	$CHCl_3$	**Isofluran e**	**Enflurane**	**Isoflurane**	**Enflurane**
0	0.2×10^{-8}	0.2×10^{-8}	0	1	0
25	1.1×10^{-8}	0.7×10^{-8}	2.4×10^{-8}	0.6	2
50	1.6×10^{-8}	0.8×10^{-8}	3.3×10^{-8}	0.5	2.1
100	2.0×10^{-8}	1.4×10^{-8}	4.8×10^{-8}	0.7	2.4

Table 3.3.4.1
The effect of light intensity on the quantum yield for the chlorine atom initiated photooxidation of the anaesthetics . The chemical actinometer employed was the reaction of $CHCl_3$ with Cl_2 at λ's > 300 nm .

3.3.5 Product studies

(a) *Infrared spectroscopic analyses*

From the IR spectra given in Figure 3.3.2.1 and 3.3.2.2 and from the profiles given in Figure 3.3.2.3 to 3.3.2.8 , it is evident that a number of oxidation products result at different stages during the photolysis of both isoflurane and enflurane. The IR absorption spectra of the products were compared to the standard spectra in Figures 3.3.5.1 to 3.3.5.4 ,for identification. It is also evident that HCl was produced during the photooxidation of both anaesthetics (Figure 3.3.5.4).

During the photolysis of isoflurane, two new bands appeared in the carbonyl stretching region at frequencies of 1840 and 1940 cm^{-1}. By comparison with standard spectra (Figure 3.3.5.1) , the band at 1940 cm^{-1} was assigned to the product CF_2O. During enflurane photooxidation, three new bands appeared at 1830 , 1910 and 1940 cm^{-1}. The band at 1940 cm^{-1} was attributed to CF_2O production . Prolonged photolysis of both anaesthetics resulted in the production of CO_2 , identifiable by its stretching band at 2350 cm^{-1} (Figure 2.3.5.2) .

(b) *Gas Chromatographic analyses*

Very little information was obtained in relation to the identity of the photooxidation products of the anaesthetics using GC / FID . Using the chromatographic conditions outlined in Table 3.2.2.1 , prolonged photolysis resulted in a product peak, visible at approximatley 3 minutes on the GC trace (Figure 3.3.5.5) . To eliminate the pressure surge visible in Figure 3.3.5.5 , GC conditions were switched to those given in Table 3.2.2.2 . Figure 3.3.5.6 shows the chromatogram achieved for the reaction products of isoflurane using these new conditions . Because reaction products were

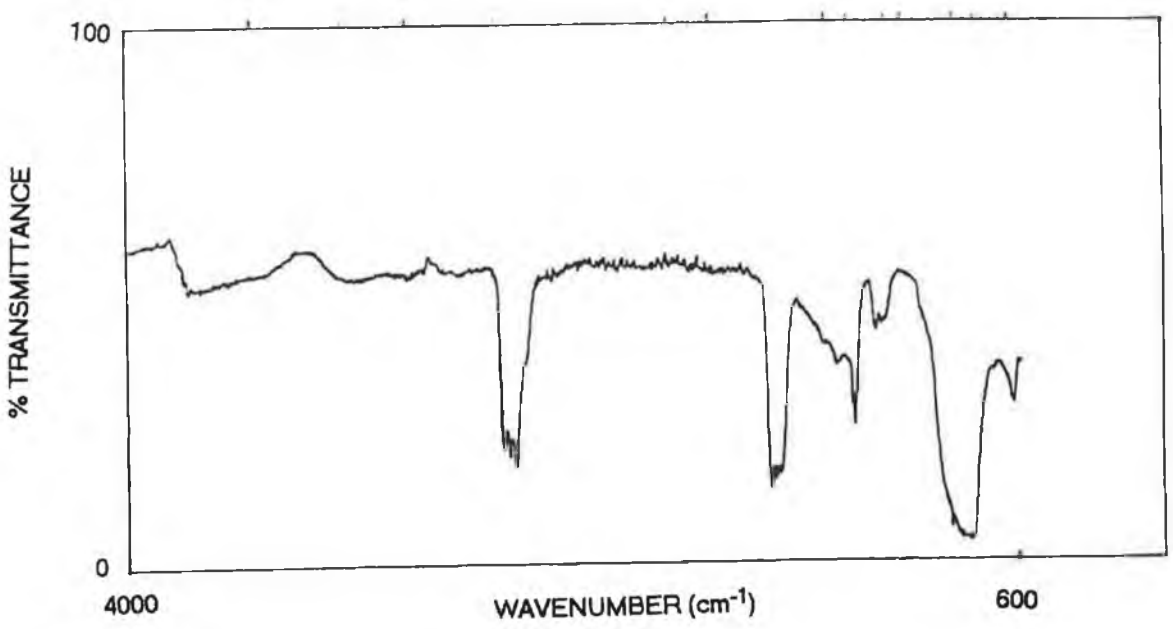

Figure 3.3.5.1

IR spectrum of 4 torr CF_2O in 50 torr O_2 using a pathlength of 10 cm .

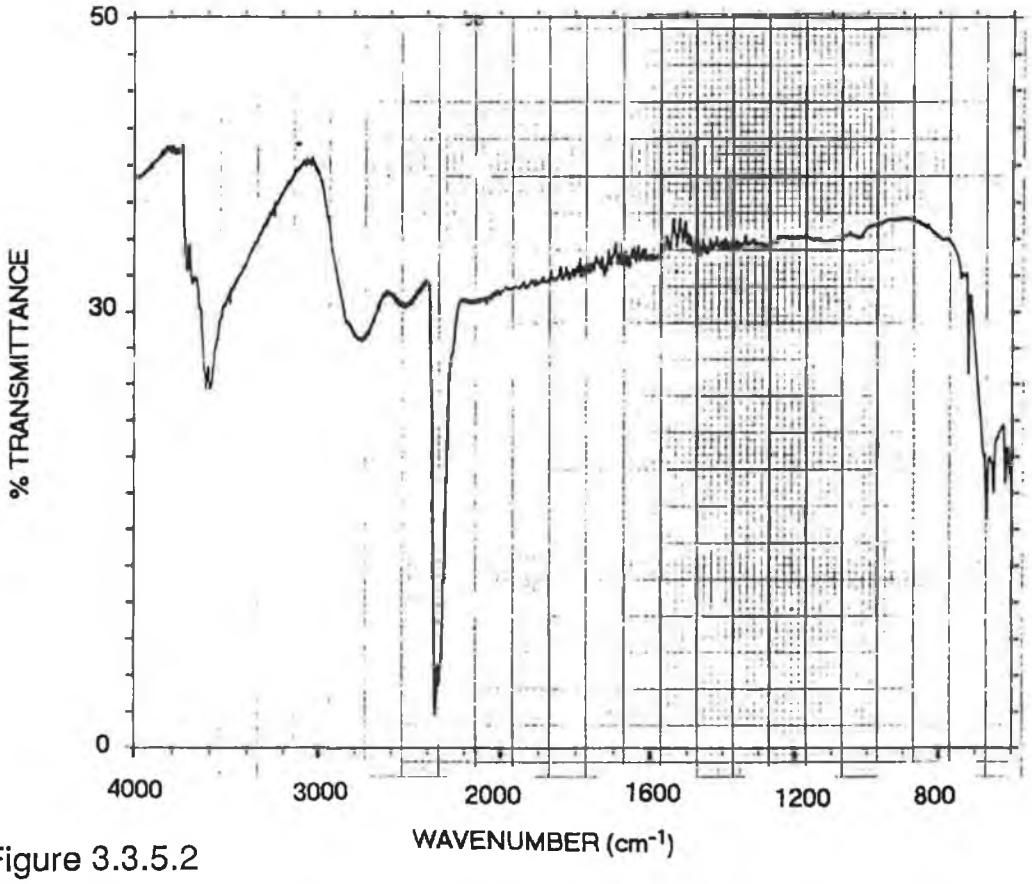

Figure 3.3.5.2

IR spectrum of 10 torr CO_2 using a pathlength of 10 cm .

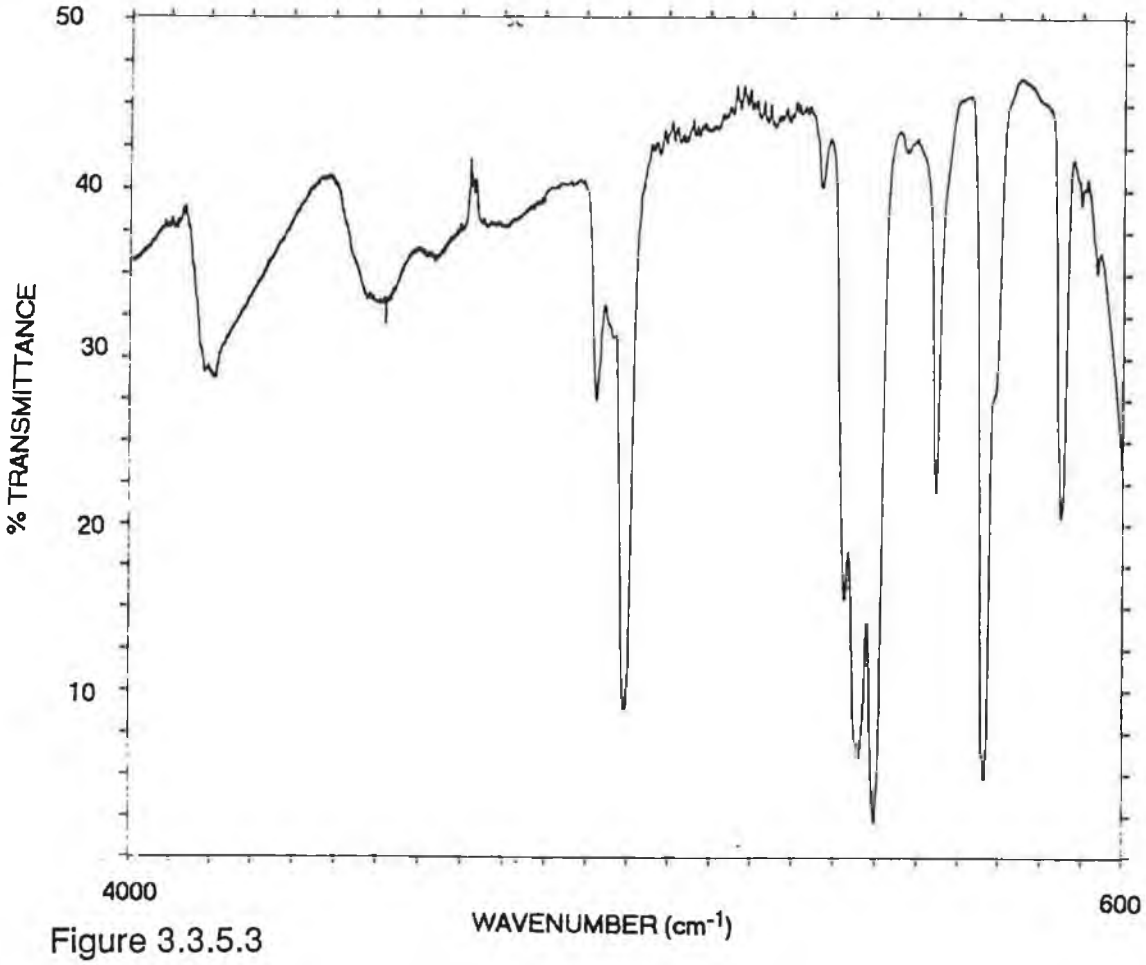

Figure 3.3.5.3

IR spectrum of 4 torr CF_3COCl using a pathlength of 10 cm .

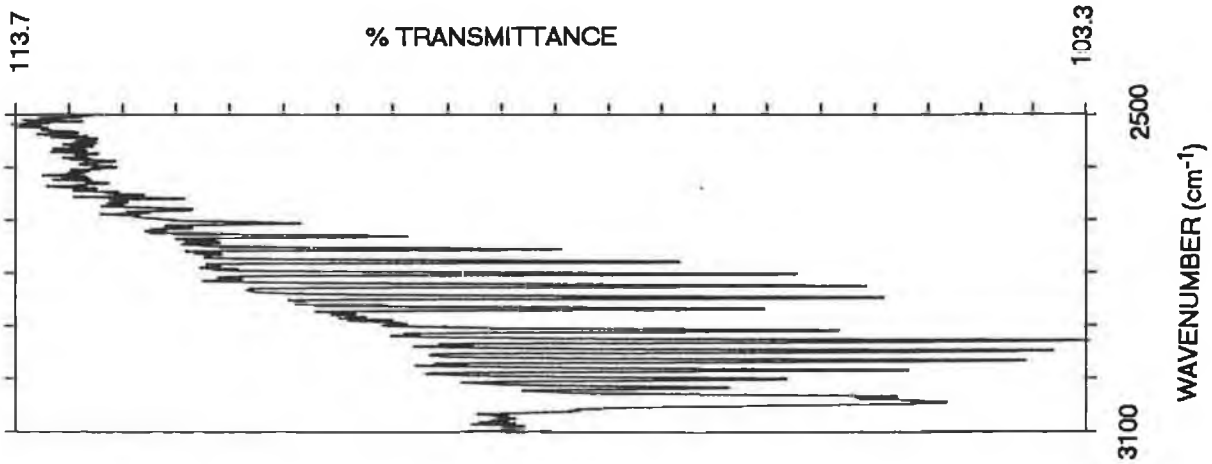

Figure 3.3.5.4

IR spectrum of HCl produced during the reaction of 5 torr isoflurane in 5 torr O_2 and 194 torr N_2 . Reaction was carried out at 47 ± 4 °C for 150 minutes using wavelengths above 200 nm .

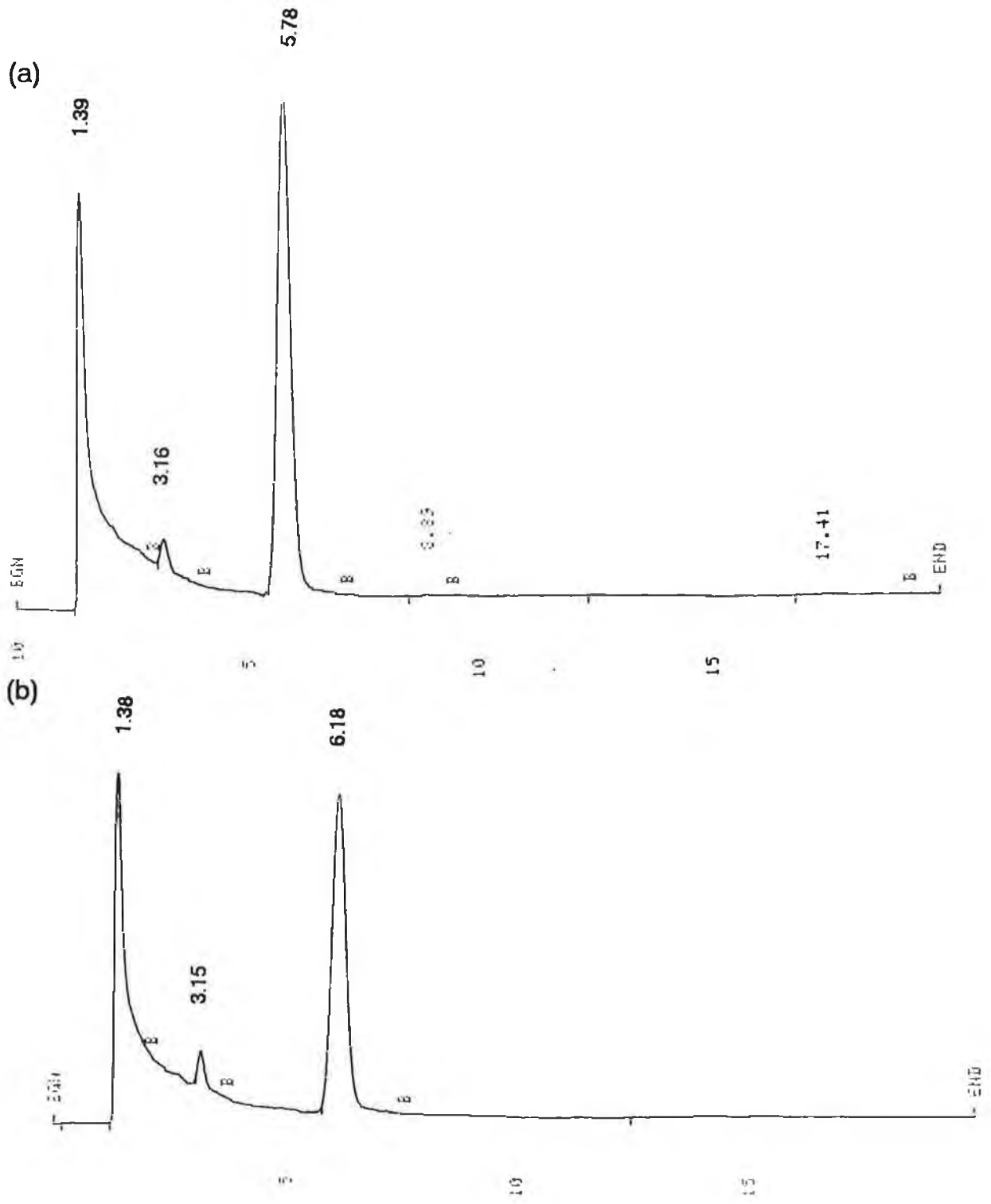

Figure 3.3.5.5
(a) 20 Torr isoflurane plus 300 torr O_2 photolysed for 90 minutes and
(b) 20 Torr enflurane plus 300 torr O_2 photolysed for 75 minutes .
Reaction was carried out at 47 ± 4 °C using wavelengths above 200 nm .
Reaction mixtures were injected onto the GC as outlined in Figure 3.2.2.2 , using the conditions outlined in Table 3.2.2.1 .

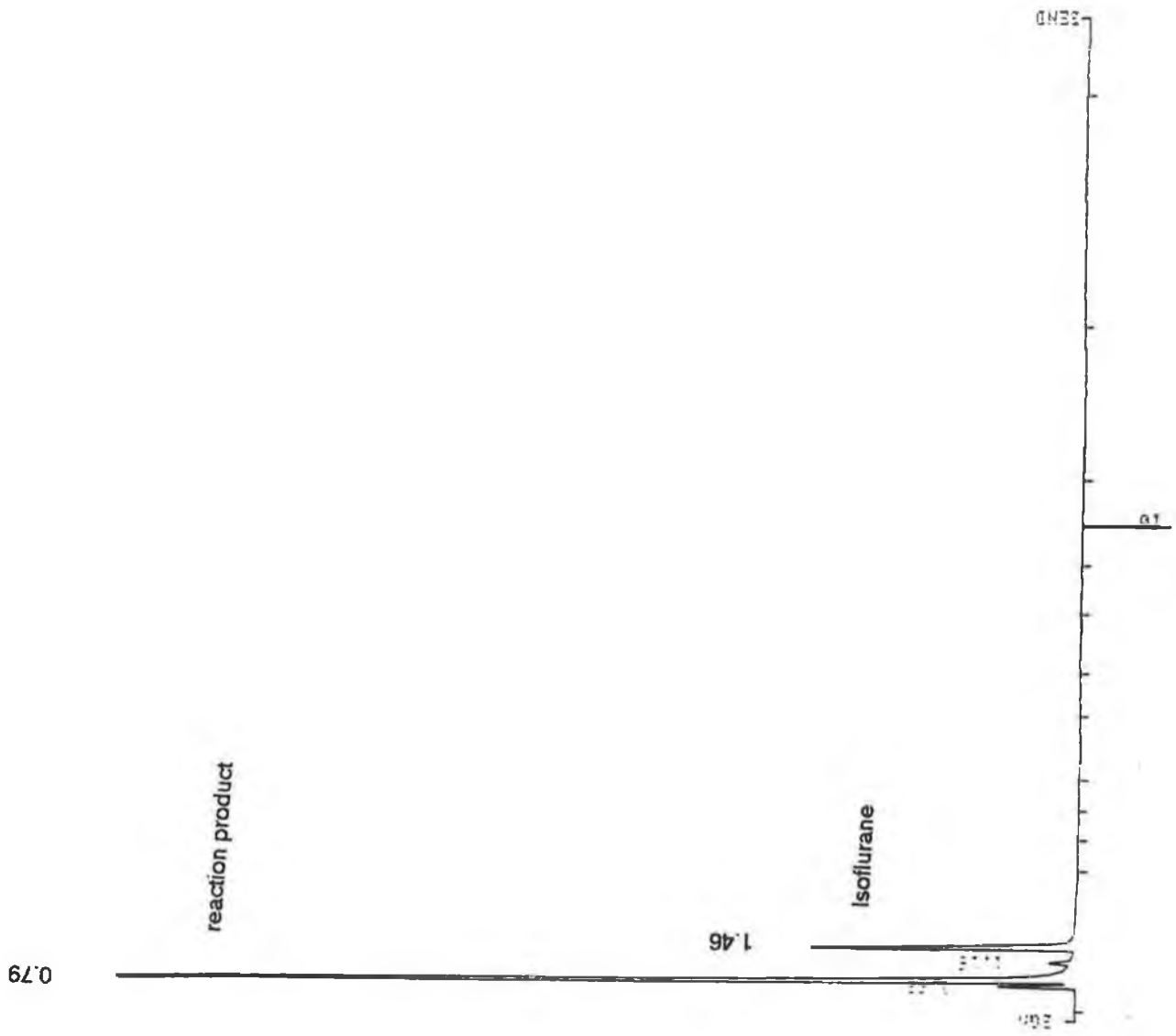

Figure 3.3.5.6
20 Torr isoflurane plus 300 torr O_2 photolysed for 120 minutes and injected onto the GC . Chromatographic conditions used are those outlined in Table 3.2.2.2 . Reaction was carried out at 47 ± 4 °C using wavelengths above 200 nm .

visible using GC / FID samples of the photooxidation products for both anaesthetics were sent for offline GC / MS examination (as outlined in Section 3.2.3.7 (b) of this report), so that possible products might be identified .

The total ion current traces (TIC) obtained for each of the anaesthetic reaction mixtures are given in Figures 3.3.5.7 and 3.3.5.8 . Reaction mixture components visible in the TIC traces were fragmented by electron impact to give the mass spectra in Figures 3.3.5.9 to 3.3.5.12 .

Figure 3.3.5.10 is the mass spectrum obtained from the fragmentation of component two visible in the TIC trace for the isoflurane photooxidation reaction mixture . This spectrum is indicative of unreacted isoflurane in the reaction mixture :

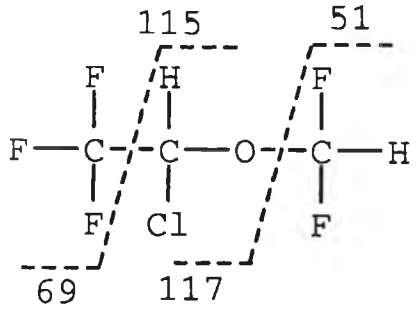

Figure 3.3.5.9 is the mass spectrum resulting from the fragmentation of component one visible in the TIC trace of the isoflurane photooxidation products . This spectrum shows the presence of a CF_3 group ($^m/_z$ = 69) , and a CO_2 moiety ($^m/_z$ = 44) in this reaction mixture component . The mass range covered in this spectrum is too small for definate identification , however , the mass spectrum in Figure 3.3.5.9 may be attributed to the isoflurane photooxidation product :

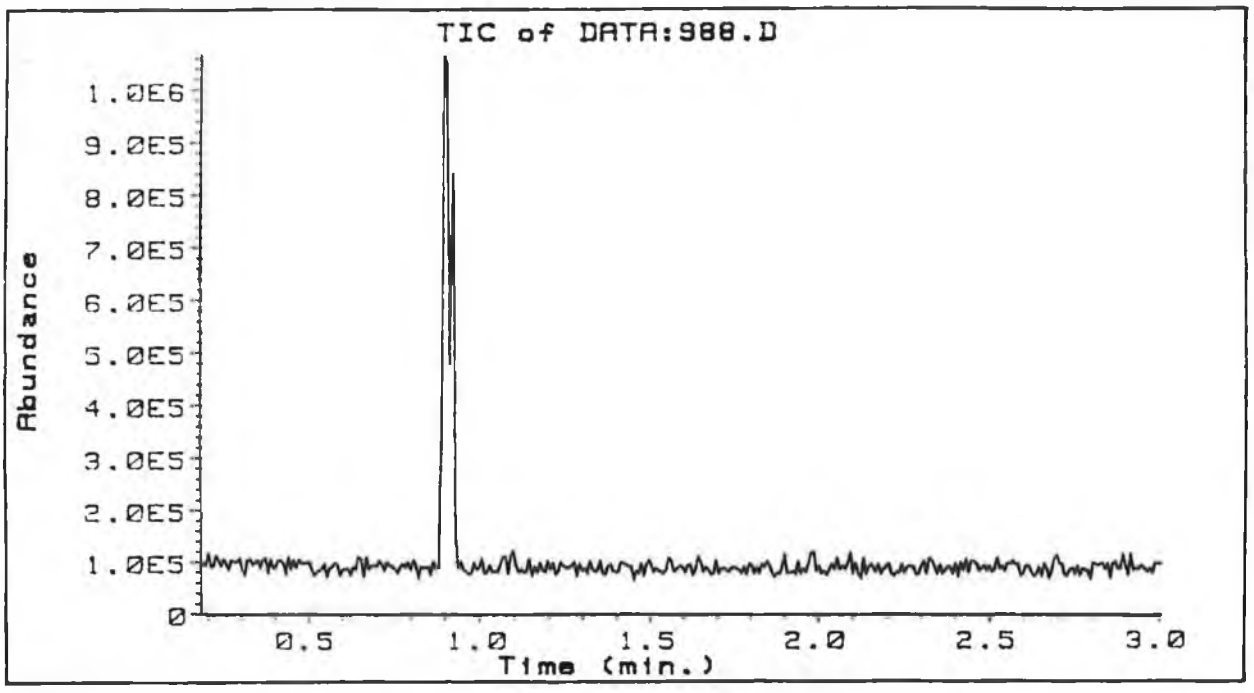

Figure 3.3.5.7
The TIC trace for the isoflurane photooxidation reaction mixture . 20 Torr isoflurane plus 300 torr O_2 was photolysed for 1 hour at 47 ± 4 °C using wavelengths above 200 nm .

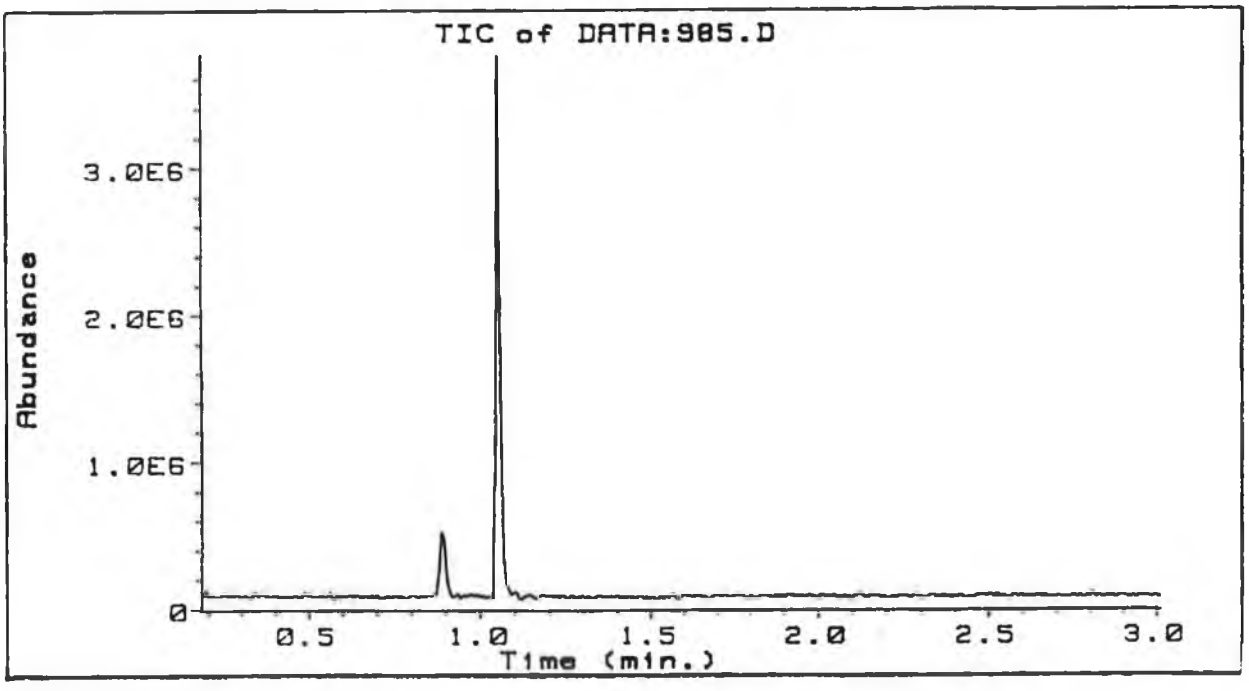

Figure 3.3.5.8
The TIC trace for the enflurane photooxidation mixture . 20 torr enflurane plus 300 Torr O_2 was photolysed for 1.5 hours at 47 ± 4 °C using wavelengths above 200 nm .

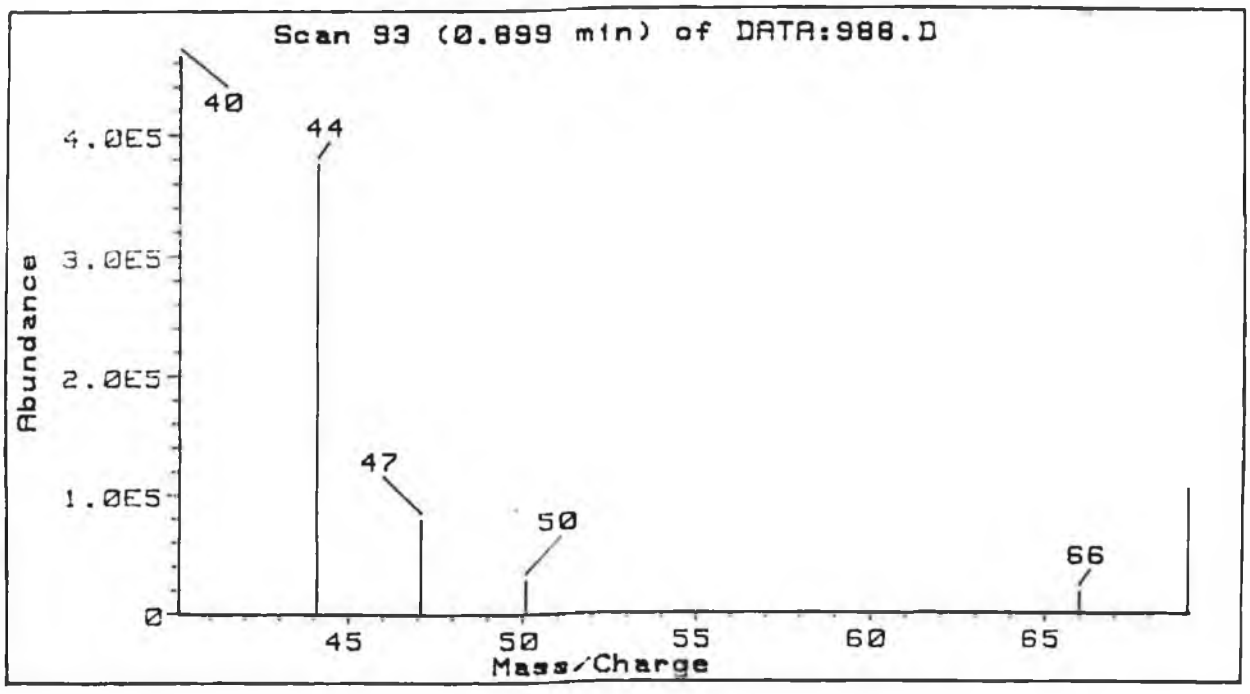

Figure 3.3.5.9
The mass spectrum obtained from the fragmentation of the first eluent visible in Figure 3.3.5.7 .

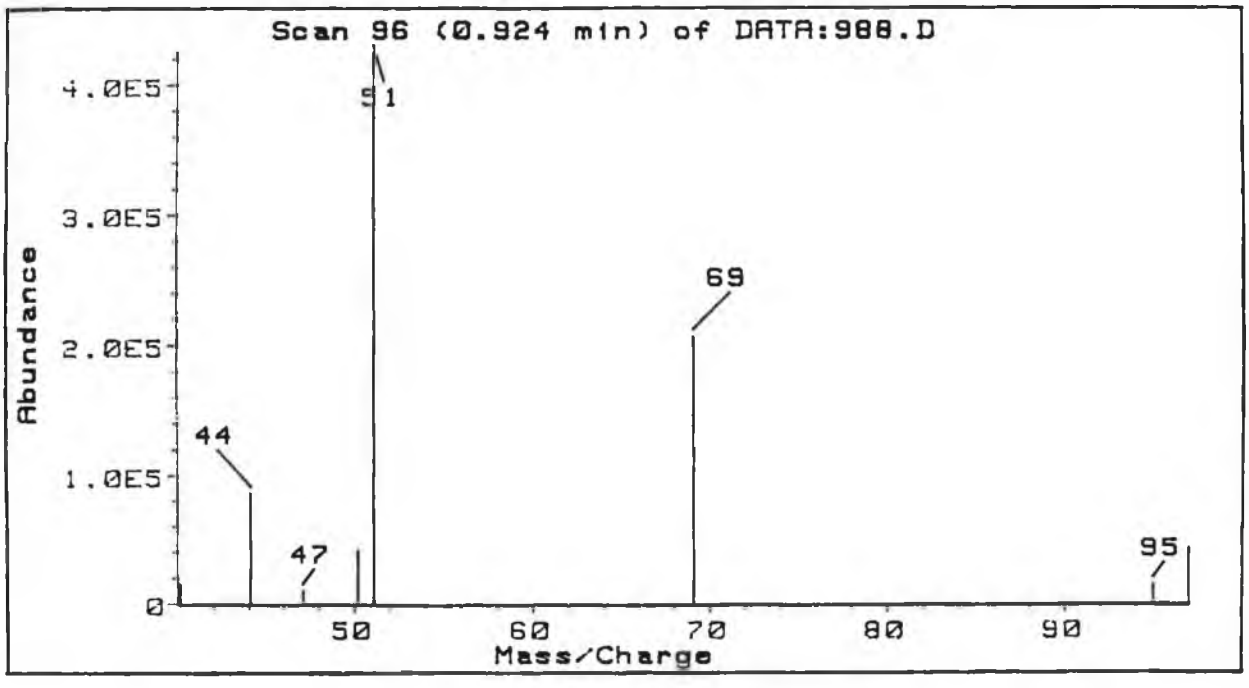

Figure 3.3.5.10
The mass spectrum obtained from the fragmentation of the second eluent visible in Figure 3.3.5.7 .

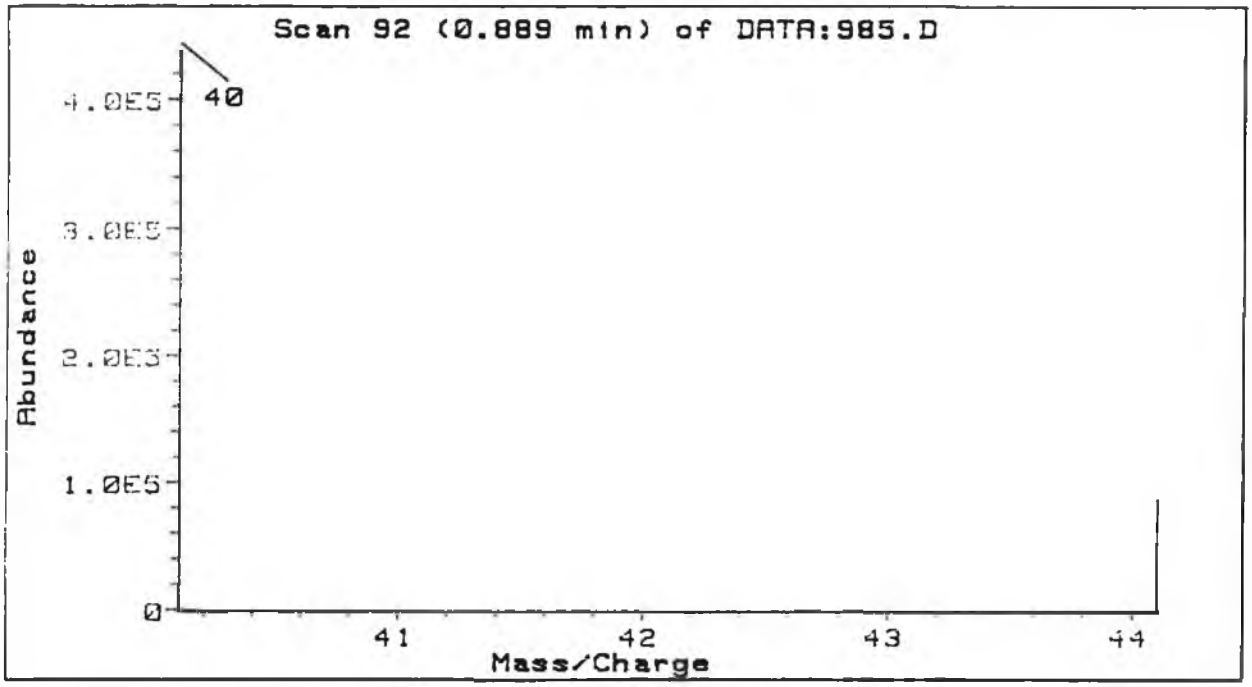

Figure 3.3.5.11
The mass spectrum obtained from the fragmentation of the first eluent visible in Figure 3.3.5.8 .

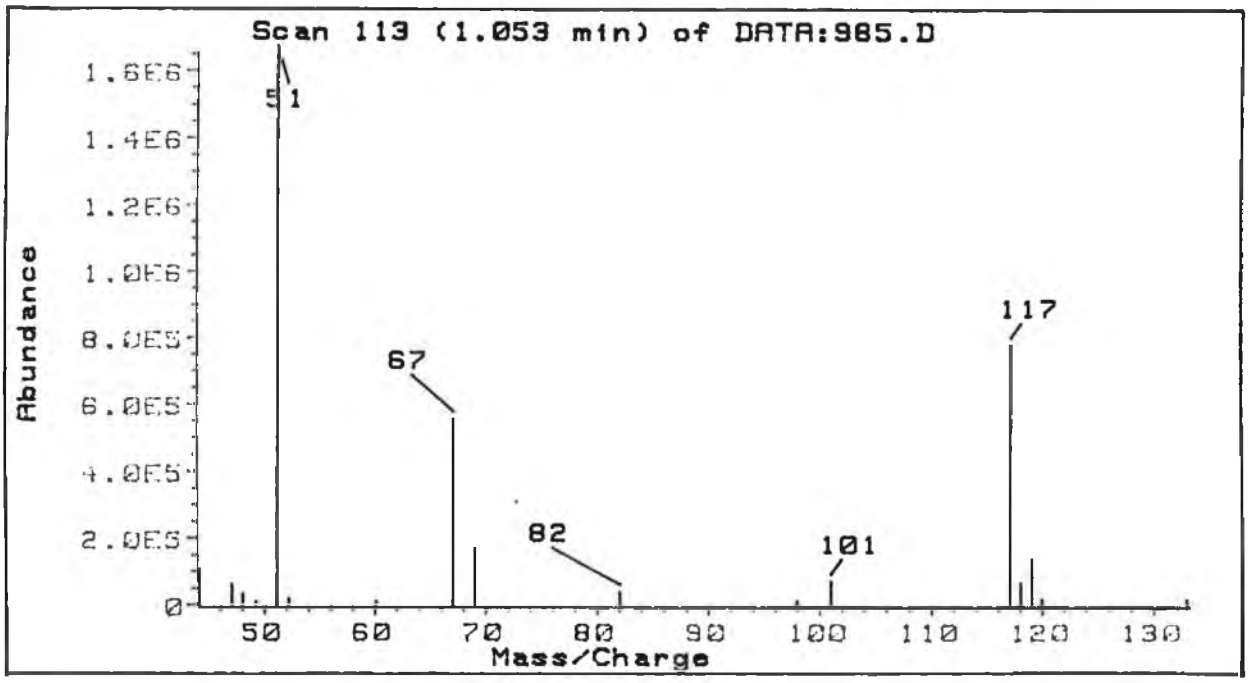

Figure 3.3.5.12
The mass spectrum obtained from the fragmentation of the second eluent visible in Figure 3.3.5.8 .

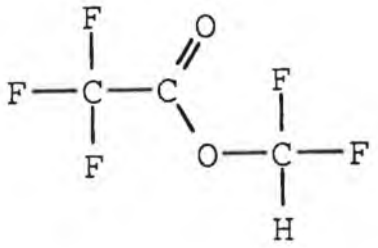

The total ion current trace for the enflurane reaction mixture (Figure 3.3.5.8) also indicated the presence of two components . The mass spectrum of the first eluent (Figure 3.3.5.11) yielded very little information with only two fragments visible at $^{m}/_{z}$ =40 and 44 . The fragment of $^{m}/_{z}$ = 44 may indicate the presence of CO_2 in this reaction mixture component . The fragment of $^{m}/_{z}$ = 40 is also visible in the mass spectra in Figures 3.3.5.9 and 3.3.5.10 and is probably due to the use of argon in the mass spectrometer . The second component visible in the TIC trace for the enflurane reaction mixture (Figure 3.3.5.8) was fragmented to give the mass spectrum visible in Figure 3.3.5.12 . This mass spectrum can be attributed to unreacted enflurane ;

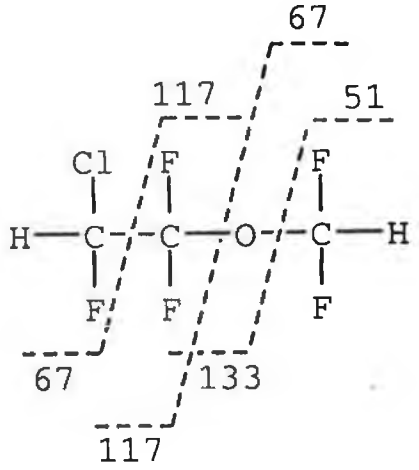

The mass spectrum for enflurane indicates the presence of two sets of isobaric ions (at $^{m}/_{z}$ = 117 and 67) which were not resolved by the mass spectrometer used in these analyses . The presence of chlorine in these two fragments is indicated by it's satelite isotope peaks at 69 and

119 . As the ^{37}Cl isotope occurs in a ratio of 1 : 3 to the main ^{35}Cl atom it is usual to find this ratio preserved in the mass spectrum of chlorine containing compounds unless that is if an isobaric ion is also present as in the above case .

If resolution of the isobaric ions was to be achieved an instrument resolution of 4770 would be required for the 117 fragment and 2740 for the 67 fragment . These resolution figures were calculated from the expression,

$$\text{Resolution} = {}^{m}/_{(m + x) - m}$$

m = Accurate mass of the lower fragment , and

$(m + x)$ = Accurate mass of the higher fragment

(c) *NMR*

Using the procedure outlined in Section 3.2.3.7(d) , NMR spectra were obtained for the anaesthetics and their photooxidation products (Figures 3.3.5.13 to 3.3.5.16) .

The NMR spectrum for isoflurane in d-acetone (Figure 3.3.5.13) is readily interpreted by referring to the structure of the anaesthetic :

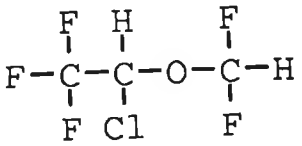

Figure 3.3.5.13 shows that the proton NMR spectrum for isoflurane in d-acetone is composed of a triplet , with a coupling constant of approximately 72 Hz and a quartet with a coupling constant of 4 Hz . The cause of the coupling is the NMR active fluorines . The large coupling constant in the triplet is due to the two fluorines on the same carbon as the hydrogen in the CF_2H group couples with the hydrogen atom on the adjacent carbon.

The NMR for enflurane in d-acetone can also be interpreted from it's structure which appears at the top of this page . Figure 3.3.5.15 shows the NMR consisting of what appears to be 3 sets of triplets. The pair of triplets at 6.6 and 6.7 ppm are due to coupling of the hydrogen in the terminal CFClH group . This hydrogen is coupled by the fluorine on the same carbon giving rise to a doublet with a large coupling constant (46 Hz) .

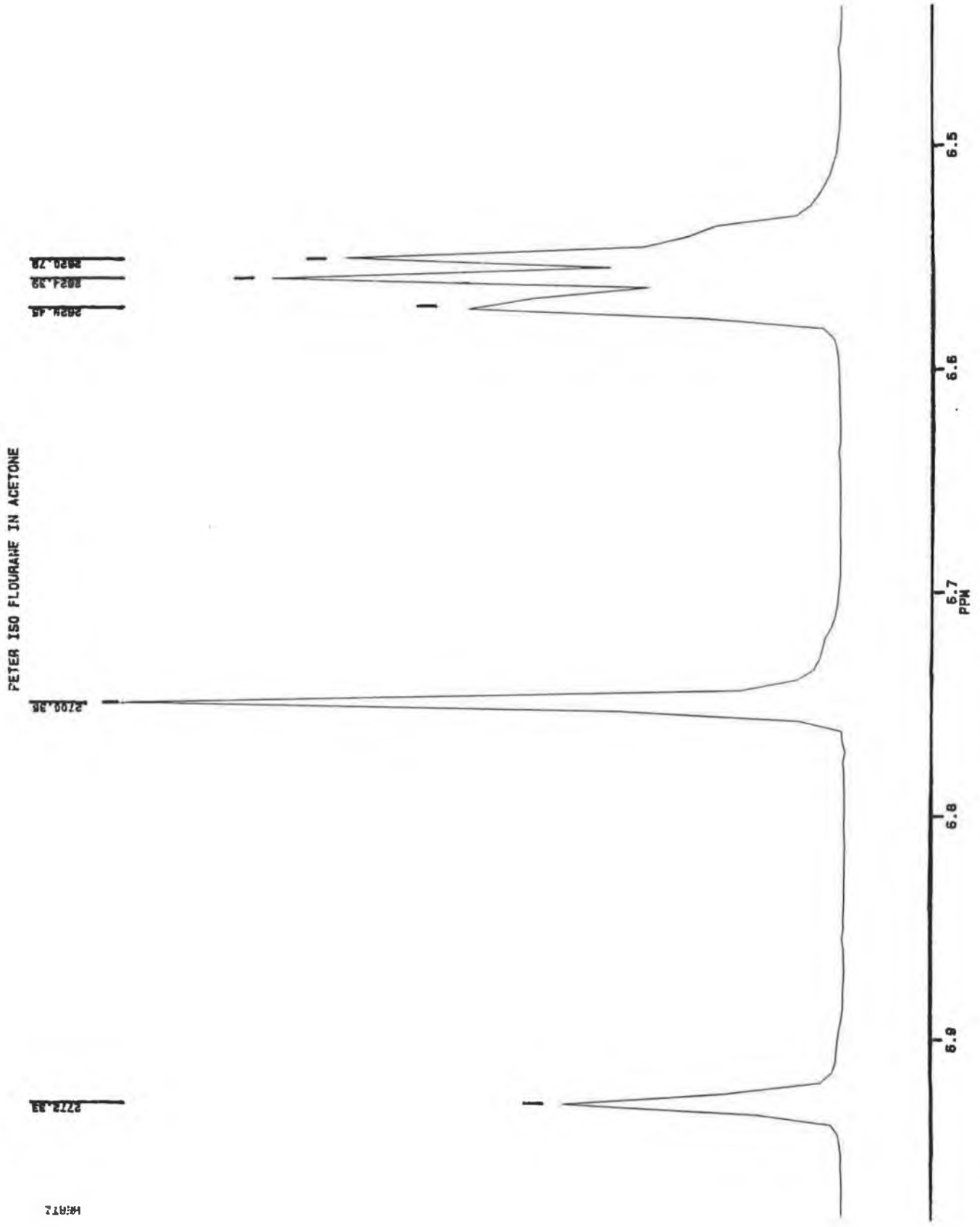

Figure 3.3.5.13
The room temperature proton NMR spectrum for isoflurane in d-acetone .

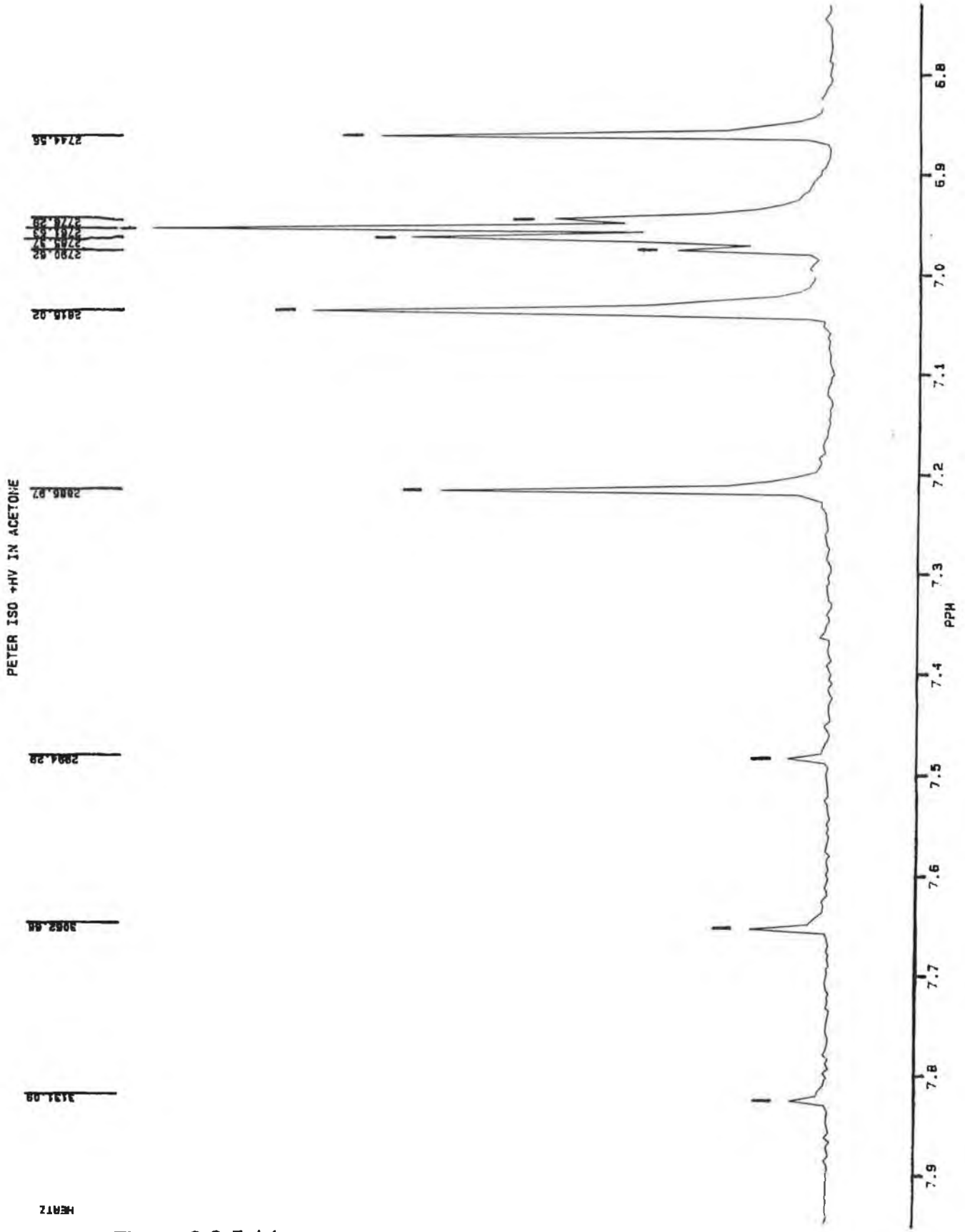

Figure 3.3.5.14
The room temperature proton NMR spectrum for an isoflurane photooxidation mixture in d-acetone . The reaction mixture was obtained by the photolysis of 25 torr isoflurane in 5 torr O_2 for 105 minutes at 47 ± 4 °C using wavelengths above 200 nm .

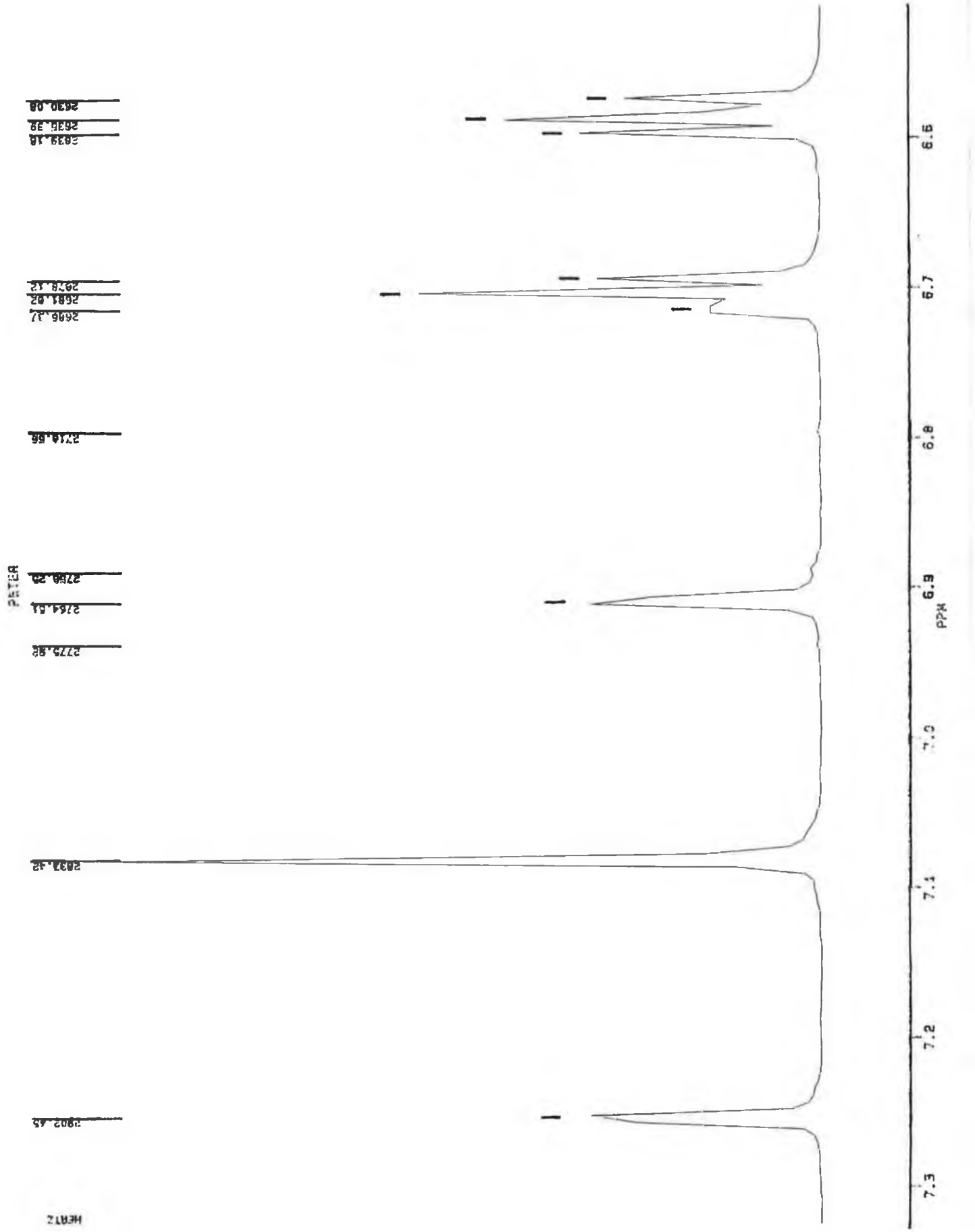

Figure 3.3.5.15

The room temperature proton NMR spectrum of enflurane in d-acetone .

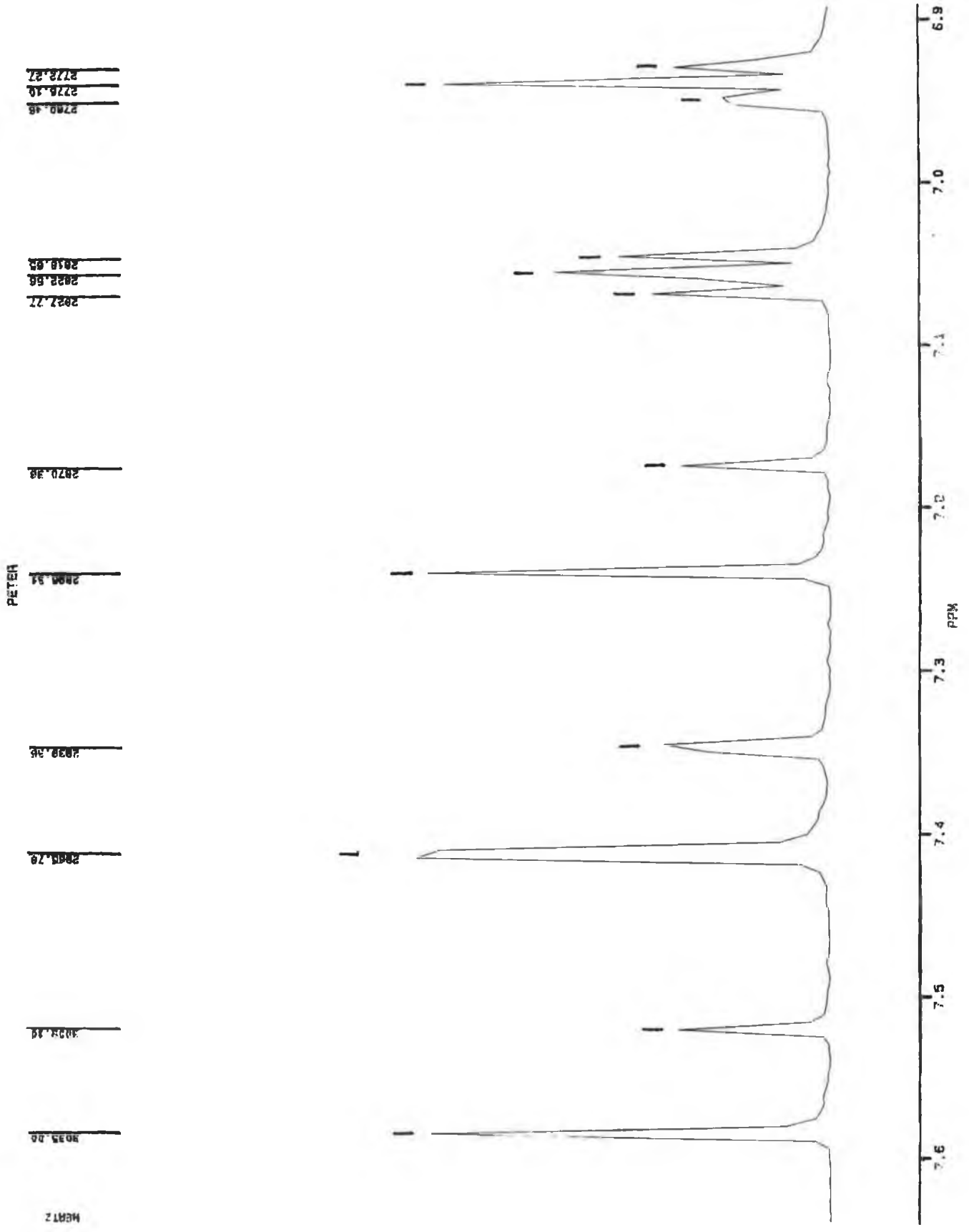

Figure 3.3.5.16
The room temperature proton NMR spectrum for an enflurane photooxidation mixture in d-acetone . The reaction mixture was obtained by the photolysis of 25 torr enflurane in 5 torr O_2 for 90 minutes at 47 ± 4 ^oC using wavelengths above 200 nm .

This doublet is then split to form two triplets by the two fluorine atoms on the adjacent carbon . This coupling is small (4.5 Hz) as the fluorines are one carbon removed from the hydrogen . The remaining triplet with the large coupling constant (69 Hz), is similar to that in isoflurane and is due to the coupling of the hydrogen in the $-CF_2H$ group by the two fluorine atoms .

The NMR spectrum of the photooxidation products of isoflurane given in Figure 3.3.5.14 , shows only one extra feature to the pure spectrum . As with the pure spectrum , unreacted isoflurane is identifiable by the quartet at approximately 6.95 ppm , and the triplet at 7.2, 7.0, and 6.85 ppm . However, an extra triplet is noticeable at higher frequency (*ca.* 7.5 to 7.8 ppm) with the same coupling constant (*ca.* 69 Hz)as that for the CF_2H group in the pure sample of anaesthetic . This triplet can be assigned to an isoflurane photooxidation product containing a $-CF_2H$ group . Furthermore this product may contain a number of oxygen atoms adjacent to this $-CF_2H$ group, resulting in a high degree of shielding thus giving rise to the triplet occuring at a high frequency .

Figure 3.3.5.16 shows the NMR of the products from the photooxidation of enflurane . As with isoflurane an extra triplet is visible, again with a coupling constant corresponding to that of a $-CF_2H$ group (*ca.* 69 Hz) . However , since this triplet is not shifted to a higher frequency , it would appear that the product contains fewer shielding oxygen atoms adjacent to the $-CF_2H$ moiety than in the product formed during the photooxidation of isoflurane .

3.4 Discussion

Photolysis of isoflurane ($CF_3CHClOCF_2H$) in the presence of oxygen at wavelengths above 200 nm yielded HCl (3000 - 2600 cm^{-1}) , CF_2O (1940 cm^{-1}) , CO_2 (2350 cm^{-1}) , and CF_3COOCF_2H (1840 cm^{-1}) . The formation of these products was rationalised in terms of the following reaction mechanism :

$CF_3CHClOCF_2H$	$\xrightarrow[\lambda < 236\ nm]{h\nu}$ $Cl\cdot + CF_3\dot{C}HOCF_2H$	(3.4.1)
$CF_3\dot{C}HOCF_2H + O_2$	----------> $CF_3COOCF_2H + H\dot{O}_2$	(3.4.2)
$CF_3COOCF_2H + O_2$	$\xrightarrow[\lambda > 320\ nm]{h\nu}$ CF_2O	(3.4.3)
CF_3COOCF_2H	$\xrightarrow[\lambda > 320\ nm]{h\nu}$ $CF_3C\dot{O} + \dot{O}CF_2H$	(3.4.4)
$\dot{O}CF_2H + O_2$	----------> CF_2O	(3.4.5)
$CF_3C\dot{O} + O_2$	----------> CF_2O	(3.4.6)
CF_3COOCF_2H	$\xrightarrow[\lambda > 320\ nm]{h\nu}$ $CF_3COO\dot{O} + \dot{C}F_2H$	(3.4.7)
$CF_3COO\dot{O} + O_2$	----------> CF_2O	(3.4.8)
$\dot{C}F_2H + O_2$	----------> CF_2O	(3.4.9)
$CF_2O + O_2$	$\xrightarrow{h\nu}$ CO_2	(3.4.10)
$Cl\cdot + CF_3CHClOCF_2H$	----------> $HCl + CF_3\dot{C}ClOCF_2H$	(3.4.11)
$CF_3\dot{C}ClOCF_2H + O_2$	----------> $CF_3C\dot{O}_2ClOCF_2H$	(3.4.12)
$2CF_3C\dot{O}_2ClOCF_2H$	----------> $2CF_3C\dot{O}ClOCF_2H + O_2$	(3.4.13)
$CF_3C\dot{O}ClOCF_2H$	----------> $CF_3COOCF_2H + Cl\cdot$	(3.4.14)

The reaction summarised by mechanism 3.4.3 is complex and may proceed by one of two routes , 3.4.4 to 3.4.6 or 3.4.7 to 3.4.9 .

Similarly photolysis of enflurane ($CFClHCF_2OCF_2H$) In the presence of oxygen at wavelengths above 200 nm yielded HCl (3000 to 2600 cm^{-1}) , CF_2O (1940 cm^{-1}) , CO_2 (2350 cm^{-1}) and , $CFOCF_2OCF_2H$

(1910 cm^{-1}) . The formation of the products observed can be rationalised in terms of the following reaction mechanism :

$CFClHCF_2OCF_2H \xrightarrow[\lambda<228nm]{h\nu} Cl\cdot + HF\dot{C}CF_2OCF_2H$ (3.4.15)

$HF\dot{C}CF_2OCF_2H + O_2$ ----------> $FOCCF_2OCF_2H + H\dot{O}_2$ (3.4.16)

$OFCCF_2OCF_2H + O_2 \xrightarrow[\lambda<320\ nm]{h\nu} CF_2O$ (3.4.17)

$OFCCF_2OCF_2H \xrightarrow[\lambda<320\ nm]{} OFCF_2\dot{C} + \dot{O}CF_2H$ (3.4.18)

$\dot{O}CF_2H + O_2$ ----------> CF_2O (3.4.19)

$OFCF_2\dot{C} + O_2$ ----------> CF_2O (3.4.20)

$OFCCF_2OCF_2H \xrightarrow[\lambda<320\ nm]{h\nu} OFCCF_2\dot{O} + \dot{C}F_2H$ (3.4.21)

$OFCCF_2\dot{O} + O_2$ ----------> CF_2O (3.4.22)

$\dot{C}F_2H + O_2$ ----------> CF_2O (3.4.23)

$CF_2O + O_2 \xrightarrow{h\nu} CO_2$ (3.4.24)

$Cl\cdot + CFClHCF_2OCF_2H \xrightarrow{(M)} HCl + ClF\dot{C}CF_2OCF_2H$ (3.4.25)

$ClF\dot{C}CF_2OCF_2H + O_2$ ----------> $ClF\dot{O}_2CCF_2OCF_2H$ (3.4.26)

$2ClF\dot{O}_2CCF_2OCF_2H$ ----------> $2ClF\dot{O}CCF_2OCF_2H + O_2$ (3.4.27)

$ClF\dot{O}CCF_2OCF_2H$ ----------> $OFCCF_2OCF_2H + Cl\cdot$ (3.4.28)

The reaction summarised in mechanism 3.4.17 is complex and may proceed by one of two routes , 3.4.18 to 3.4.20 or 3.4.21 to 3.4.23 .

The UV / visible spectra obtained for samples of the degassed liquid anaesthetics are shown in Figures 3.3.1.1 and 3.3.1.3 . Isoflurane absorption takes place at wavelengths less than 236 nm and enflurane below 222 nm . Absorption maxima for both anaesthetics are thought to be due to Cl ----------> Rydberg transitions [24] .

Figures 3.3.1.2 and 3.3.1.4 give the absorption spectra of the oxygen saturated anaesthetics . No difference was observed between the UV / visible spectra for degassed isoflurane and an oxygen saturated sample , i.e. , no absorption was observed above 236 nm . However ,

oxygen saturated enflurane absorbed below 228 nm while the degassed sample absorbed only below 222 nm . This shift in absorption may be due to the formation of a charge - transfer complex between molecular oxygen (O_2) and the oxygen atom in the ether link of enflurane :

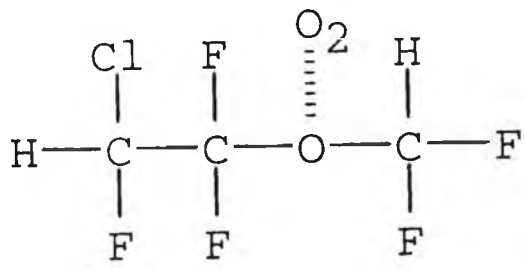

Such a gas phase charge - transfer complex is not without precedent . Wang [22] , discussed the formation of a gas phase charge - transfer mechanism during the photooxidation of tetrahydrofuran . It is possible that the formation of a charge - transfer complex between molecular oxygen and the ether oxygen in isoflurane is hindered due to the presence of the chlorine atom on the α - carbon to the ether link . This chlorine atom may withdraw electron density from the ether oxygen thus reducing it's ability to transfer electron density to molecular oxygen . Alternatively the chlorine atom in isoflurane may sterically hinder the formation of the charge - transfer complex .

Although the intensity of output from the medium pressure mercury lamp is low below 240 nm (in the region where both anaesthetics have maximum absorption) , tail end absorption by ethers has been demonstrated as being an important process in their photooxidation [22] . Preliminary UV experiments showed that the anaesthetics could absorb light of sufficient energy to cause C - Cl bond breakage , and that a charge - transfer mechanism might also occur during enflurane photooxidation .

For mixtures of anaesthetics plus O_2 and N_2 , no dark reactions even at temperatures up to 47 ± 4 ^oC were observed . Furthermore no reaction occurred when gas mixtures were irradiated at wavelengths above 270 nm (radiation was attenuated by use of a Corning 0-53 optical filter) .

Photolysis of the anaesthetics at wavelengths as low as 200 nm in the absence of oxygen led to slow decomposition over the timescales of our experiments (Figures 3.3.15 and 3.3.16) . The slow rate of reaction observed may be due to the low intensity output from the medium pressure mercury lamp below 230 nm , and also due to the lack of oxygen for reaction propagation . A slightly faster loss of isoflurane than enflurane was also indicated in Figure 3.3.15 and 3.3.16 . This may be accounted for by the absorption by isoflurane of longer wavelengths than enflurane .

The results from the initial photooxidation studies followed by IR spectroscopy are given in Figures 3.3.2.1 and 3.3.2.2 . The reaction of isoflurane (Figure 3.3.2.1) resulted in the formation of four products , indicated by the appearance of IR bands at 3000 - 2600 , 2350 , 1940 and 1840 cm^{-1} . The bands from 3000 - 2600 cm^{-1} were assigned to the vibration - rotation spectrum [26] for HCl (Figure 3.3.5.4) . The band at 2350 cm^{-1} was due to the formation of CO_2 and was identified by comparison with a pure spectrum of CO_2 (Figure 3.3.5.2) . The strong band at approximately 1940 cm^{-1} was attributed to CF_2O formation and this was confirmed by comparison with a standard spectrum (Figure 3.3.5.1) . Reaction of isoflurane yielded a product identified by an IR band at approximately 1840 cm^{-1} . This product remained unidentified at this stage but the IR band produced was thought to have been due to a carbonyl group within this product .

The photooxidation of enflurane was also monitored by IR spectroscopy . Typical spectra obtained during photolysis are shown in

Figure 3.3.2.2 . Product bands at 3000 - 2600 , 2350 , 1940 , 1910 , and 1840 cm^{-1} were formed during reaction . As in the photooxidation of isoflurane the bands at 3000 - 2600 , 2350 , and 1940 cm^{-1} were assigned to the products , HCl , CO_2 , CF_2O respectively . The photooxidation products identified by the IR bands at 1910 and 1840 cm^{-1} are indicative of two carbonyl containing compounds .

Therefore at this early stage of analysis , results indicated that the photooxidation of the anaesthetics could be summarised as follows :

(a) *Isoflurane*

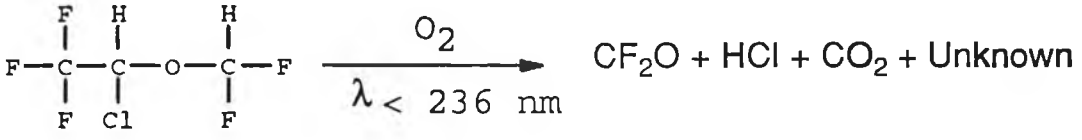

(b) *Enflurane*

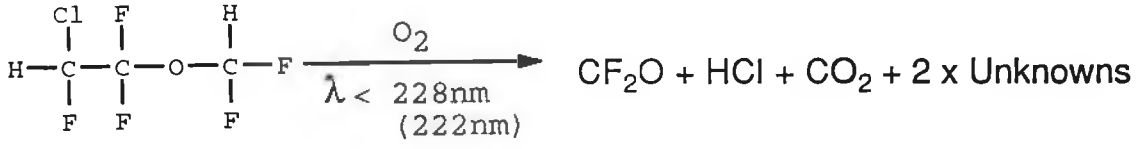

Having completed preliminary product analysis using IR spectroscopy , more detailed photooxidation profiles for the anaesthetics were determined (Figures 3.3.2.3 to 3.3.2.8) . These profiles contain information pertaining to the loss of anaesthetics and the appearance of the various photooxidation products .

Figures 3.3.2.3 and 3.3.2.4 show the profiles obtained during the photooxidation of 5 torr anaesthetic in 195 torr O_2 . A number of observations were made which were helpful in elucidating the photooxidation mechanism for the anaesthetics . Firstly the breakdown of the anaesthetics was preceded by an initiation period , a time during which very little loss of the anaesthetics was observed . As stated earlier [22] , tail end absorption by the anaesthetics may result in Cl - Rydberg

transitions [24] . This absorption process may then result in the breaking of the carbon chlorine bond with the main reaction then following a route whereby the chlorine atoms abstract H - atoms from the parent molecule . In Chapter two , the rate constant for the reaction of chlorine atoms with isoflurane and enflurane was determined to be $< 0.1 \times 10^{-11}$ $cm^3 molecule^{-1} s^{-1}$. This long reaction time results from the few abstractable hydrogens present in these compounds and the high degree of hindrance caused by the halogens in the anaesthetic molecule [3] . This slow reaction rate coupled with the need to first produce Cl atoms for reaction may be responsible for the observed lag time (Figures 3.3.2.3 - 3.3.2.8) . The use of a light source emitting more strongly below 220 nm might reduce this initiation period by increasing the concentration of Cl atoms more rapidly .

During the photolysis of isoflurane the first of the reaction products observed (Figures 3.3.2.3 , 3.3.2.5 , 3.3.2.7) was the unknown carbonyl containing compound identified by it's IR band at 1840 cm^{-1} and CF_2O by it's - C = O stretching frequency at 1940 cm^{-1} . As the photooxidation of isoflurane proceeded , the concentration of the unknown carbonyl reached a maximum while CF_2O levels continued to increase . This may be due to the fact that the unknown carbonyl containing product was a primary product and during the course of the reaction , this product underwent photodecomposition to form CF_2O . Many fluorocarbons undergo photooxidation to CF_2O [27] . Figure 3.3.2.3 also indicates that CO_2 production only commenced after prolonged photolysis . CO_2 is known to be formed from the oxidation of CF_2O [28] and it is therefore probable that the source of CO_2 in these reactions was solely from CF_2O oxidation . As CO_2 was thought to be a secondary reaction product , this would explain it's late appearance in the reaction mixture (Figure 3.3.2.4) .

The photooxidation of enflurane shows a similar induction period at the onset of photolysis . However, unlike isoflurane a single unknown

carbonyl containing product characterised by its IR stretching frequency at 1910 cm^{-1} was formed first . This is also indicated in Figures 3.3.2.6 and 3.3.2.8 . The product formed exhibited a maximum concentration during reaction in a manner similar to the unknown product formed during the reaction of isoflurane . However , CF_2O levels continued to increase . It may be that the unknown carbonyl (at 1910 cm^{-1}) is subsequently broken down to form CF_2O as a secondary reaction product . As in the case of isoflurane , enflurane photooxidation leads to the formation of CO_2 at prolonged photolysis times , (Figure 3.3.2.4 , 3.3.2.6 and 3.3.2.8) . Enflurane photooxidation also resulted in the formation of a seemingly minor reaction product characterised by it's IR stretching frequency at 1840 cm^{-1} . This product is only formed after the appearance of the main carbonyl product and is possibly a secondary reaction product resulting from the breakdown of the unknown primary product .

Oxygen concentration had no visible effect on the photooxidation of the anaesthetics as evidenced by the similarity between the reaction profiles in Figures 3.3.2.3 to 3.3.2.6 (the total initial reaction pressure was the same i.e., 200 torr) . Later experiments detailing the effect of oxygen concentrations on the rate of loss of the anaesthetics (Figures 3.3.3.1 to 3.3.3.2) supported these observations .

The photooxidation profiles in Figures 3.3.2.7 and 3.3.2.8 differ slightly but significantly from those in Figures 3.3.2.3- 3.3.2.6 . In these reaction profiles a large concentration of anaesthetic relative to oxygen was used . This resulted in a levelling off in CF_2O and CO_2 production coupled with incomplete reaction of the anaesthetics . These reactions were helpful in establishing whether other minor products were present and unseen in the previous reactions when smaller concentrations of anaesthetic were reacted .

Having used IR spectroscopy to establish the photooxidation profiles for the anaesthetics , similar work was carried out with gas chromatography used to follow the progress of the reaction . To determine anaesthetic concentrations at each photolysis time , standard curves were prepared and these are shown in Figures 3.3.2.9 and 3.3.2.10 . High correlation coefficients and low intercepts were obtained over the concentration ranges studied . These standard curves also illustrate the accuracy of the procedure used for the preparation of gas mixtures on the vacuum line , and the repeatability of the GC injection apparatus outlined in Figure 3.2.2.2 .

From these standard curves the photooxidation profiles were constructed as shown in Figures 3.3.2.11 and 3.3.2.12 . These profiles are similar to their IR counterparts , with the induction period again indicated at the begining of the reaction . The use of GC with a flame ionisation detector limited the number of reaction products determined . CF_2O was broken down on the column to CO_2 [29] and as CO_2 is completely oxidised it elicited no response from the flame ionisation detector . However a product was observed during the photooxidation of the anaesthetics as is indicated in Figures 3.3.2.11 and 3.3.2.12 . These products may be the unknown carbonyl containing compounds observed in the IR profiles . Complete breakdown of isoflurane was also noticeable by GC unlike the IR study . This difference is most likely due to the differences in sensitivity between the two analytical techniques .

To illustrate the complex nature of these gas phase photooxidation reactions it was decided to demonstrate the non first order conformity of these processes . Plotting the 1^{st} order rate expression gave the non linear plots in Figures 3.3.2.13 and 3.3.2.14 .

To gain more information as to the photooxidation mechanisms involved , the effects of the various reaction parameters on the loss of the

anaesthetics and on the formation of reaction products was investigated , Figures 3.3.3.1 to 3.3.3.6 .

Figures 3.3.3.1 and 3.3.3.2 illustrate the effects of oxygen concentration on the photooxidation of the anaesthetics . Similar trends were observed in the photolysis of both isoflurane and enflurane . At low oxygen concentrations an almost linear relationship existed between the rate of loss of the anaesthetics and oxygen concentration . Above an oxygen concentration of approximately 5 torr the rate of loss of the anaesthetics and the concentration of reaction products stabilised . Since 5 torr anaesthetic was reacted in this study , it would appear that a minimum concentration of oxygen equal to that of the anaesthetic is required for maximum loss of anaesthetic to take place . This observation is not important in the stratosphere where large levels of oxygen are present . Therefore the rate of breakdown of the small levels of these anaesthetics which are expected to reach the stratosphere [3] will not be limited by oxygen concentrations . Figures 3.3.3.1 and 3.3.3.2 when viewed in conjunction with Figures 3.3.2.7 and 3.3.2.8 illustrate the need for oxygen in the photooxidation process , for the breakdown of the anaesthetics and the formation of reaction products .

The effect of anaesthetic concentration on the rate of loss of these compounds and on the concentrations of their main photooxidation products is illustrated in Figures 3.3.3.3. and 3.3.3.4 . As expected , as the concentration of the anaesthetics was increased the rate of loss also increased , as did the levels of the photooxidation products . These observations are consistent with the fundamental rate expression :

$$\frac{-\,d\,[\text{Anaesthetic}]}{dt} = k_r\,[\text{Anaesthetic}]^n$$

where ;

n = order of reaction ,

k_r = rate loss of ananesthetic ,

[anaesthetic] = anaesthetic concentration .

The results presented in Figures 3.3.3.5 and 3.3.3.6 demonstrate the effects which the initial reaction mixture pressure exhibited on the rate of loss of the anaesthetics and on the levels of their main oxidation products . Isoflurane reaction varies little over the pressure range studied in this work (55 to 205 torr) . This would indicate that third body contributions from the nitrogen diluent gas were not significant in the photooxidation of isoflurane. On the other hand , the extent of enflurane photooxidation was affected by the total pressure . Figure 3.3.3.6 demonstrates that at low reaction mixture pressures the rate of loss of enflurane and consequently the levels of it's photooxidation products , were greater than at higher pressures . The nitrogen diluent gas may therefore be acting as a third body in the reaction mechanism , causing a reduction in the energy of reactive intermediates by collision , thus reducing the number of these intermediates which eventually form products . Further work over an extended pressure range , i.e. from 1 to 760 torr would be useful for extending our laboratory data to possible photooxidation processes in the atmosphere .

Figures 3.3.3.7 and 3.3.3.8 demonstrate the linear relationship which was exhibited between the intensity of the light energy incident on the reaction mixtures and the subsequent photooxidation of the anaesthetics . As the intensity of light decreased , so also did the rate of reaction which is consistent with the proposed C - Cl bond breakage mechanism . When the intensity of the light was reduced , the energy supplied to the reaction mixture was also decreased , thus the extent of

photooxidation observed was similarily reduced . The intensity of radiation above 200 nm in the stratosphere is very high [26] and a faster rate of photooxidation for the anaesthetics in this region of the atmosphere would be expected than was observed in this laboratory study .

The data portrayed in Figures 3.3.3.1 to 3.3.3.8 are useful for examining the importance of photooxidation as a loss process for the anaesthetics at different levels within the various regions of the stratosphere .

From experimental observations thus far the following reaction routes were thought to be involved as initial steps in the photooxidation of isoflurane and enflurane :

(a) Isoflurane:

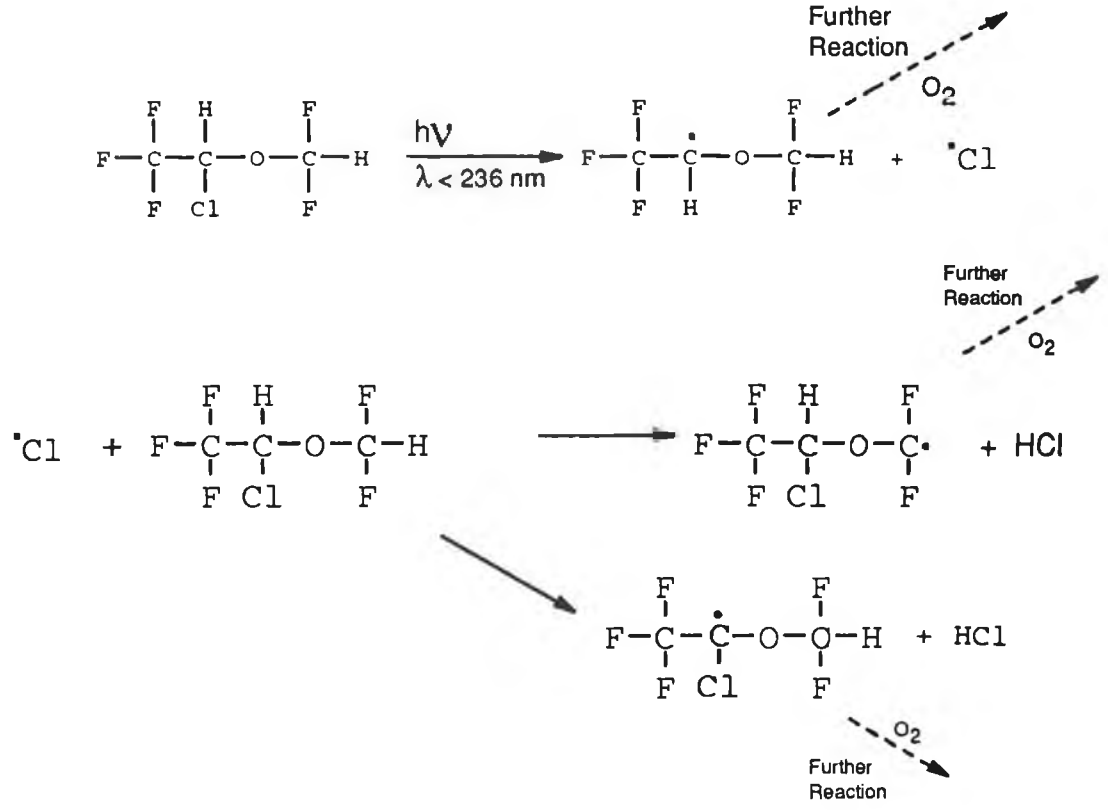

(b) Enflurane

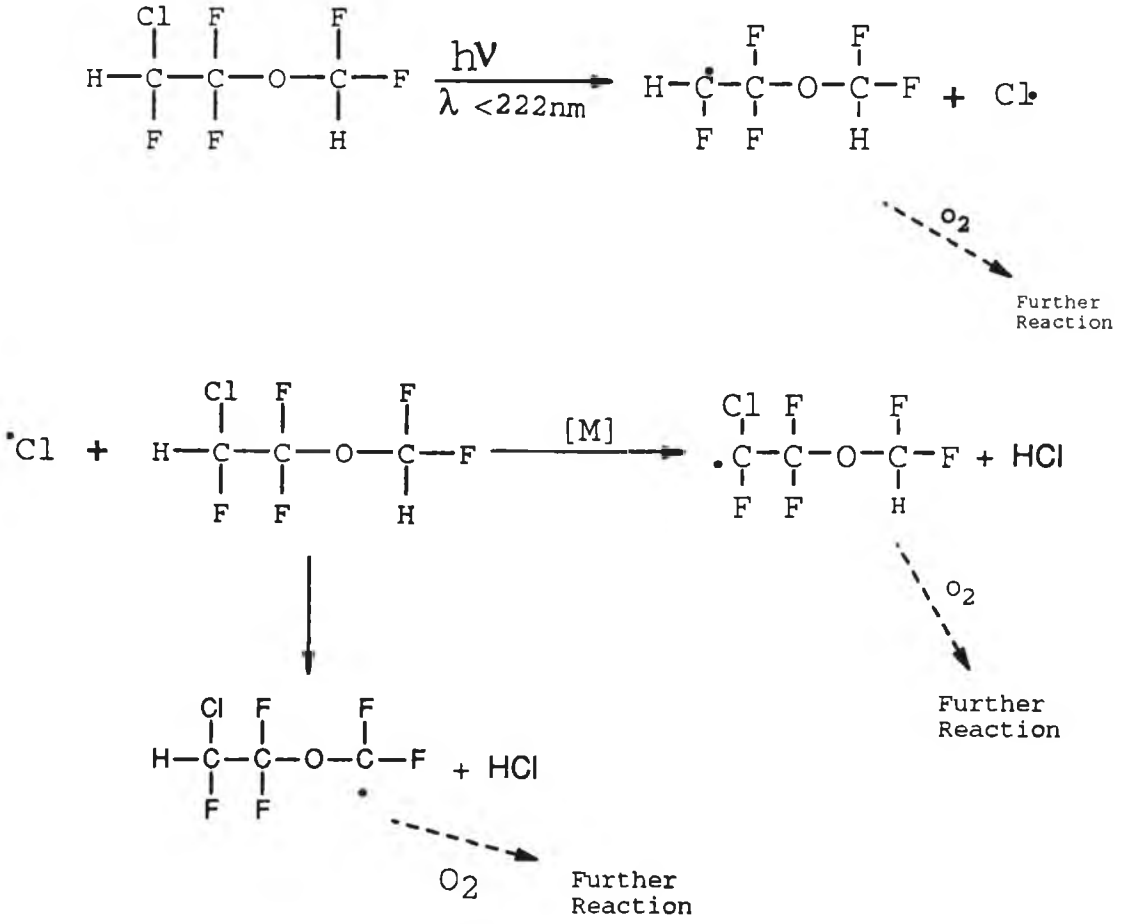

As the reaction of chlorine atoms with the anaesthetics was thought to be important in their photooxidation mechanism , studies were carried out in the presence of chlorine atoms . Initial experimental results shown in Figure 3.3.4.1 reinforced the idea that chlorine was important in the photooxidation mechanism . Similar reaction products were obtained when chlorine atoms were added to the reaction mixture and reaction proceeded more rapidly with no induction period . More detailed profile studies illustrated in Figures 3.3.4.2 - 3.3.4.5 confirmed the importance of chlorine atoms in the photooxidation mechanisms for isoflurane and enflurane . When chlorine atoms were added to the reaction mixture , the induction period at the beginning of photolysis was not evident . Thus it would appear that the initiation time observed in the absence of chlorine atoms is due to a build up of chlorine atoms from the breaking of the C -

Cl bond within the anaesthetics . Therefore , the rate determining step in the photooxidation of the anaesthetics is the initial breaking of the C - Cl bond . Once a certain concentration of chlorine atoms were produced , these atoms can further react , abstracting hydrogen from the parent compound . The formation of similar reaction products with and without Cl atoms added confirmed the importance of these atoms in the overall photooxidation mechanism for the anaesthetics . Such a chlorine - sensitised photooxidation process was observed by Nelson et al [30] in the photooxidation of methylchloroform .

To determine the importance of atomic chlorine in the overall photooxidation mechanism for the anaesthetics , gas mixtures were irradiated using the output from 5 black lamps (Philips TL 20W/08) . As these lamps emit radiation above 320 nm , bond breakage within the anaesthetics was not possible . Therefore the only source of chlorine atoms in these reaction mixtures resulted from the photodecomposition of molecular chlorine added to the reaction mixture . The resulting profiles shown in Figures 3.3.4.6 and 3.3 4.7 show that photooxidation of the anaesthetic commenced immediately after irradiation had begun . Similar fast reaction initiation is illustrated in Figures 3.3.4.3 and 3.3.4.5 . The chlorine - sensitised photooxidation profile for isoflurane shown in Figure 3.3.4.6 was similar to that observed when using the medium pressure mercury lamp for photolysis (Figure 3.3.4.3) . However , when using wavelengths above 320 nm the concentration of CF_2O produced was reduced . The use of the higher wavelength (lower energy) black lamps resulted in no CF_2O production during the photooxidation of enflurane . This would indicate that the CF_2O produced during the photooxidation of enflurane was formed entirely from the photodecomposition of some reaction mixture component. This photodecomposition mechanism would also seem to be an important route for the production of CF_2O during the

photooxidation of isoflurane , however less energetic radiation is required for the decomposition of the parent compound (i.e. CF_3COOCF_2H) .

As a chlorine atom initiated reaction was probably important in the photooxidation mechanism for the anaesthetics , it was decided to study this reaction in more detail . Before any quantum yield work was carried out, standard curves were prepared for the actinometer ($CHCl_3$) and the anaesthetics using IR spectroscopy (Figure 3.3.4.8) . The slopes, intercepts and correlation coefficients presented on the standard curves in Figure 3.3.4.8 cover the linear portion of the curves only .

Figures 3.3.4.9 - 3.3.4.11 demonstrate the effect which light intensity exhibited on the reaction of chlorine atoms with $CHCl_3$ and on the chlorine atom initiated photooxidation of the anaesthetics . The reaction rates and the concentration of the reaction products increase with increasing light intensity . This is probably due to increased concentrations of chlorine atoms being produced at higher intensities (from molecular chlorine) . The rate of loss observed for each of the anaesthetics and the actinometer ($CHCl_3$) shows a levelling off at higher light intensities . This may arise as the concentration of Cl atoms produced reaches a maximum , thus changes in this near excess concentration may have less of an impact on the reaction rate than Cl atom concentrations produced by light intensities below 50% T .

Table 3.3.4.1 illustrates the effect of light intensity on the quantum yield for the chlorine atom initiated photooxidation of the anaesthetics . The values observed are smaller than expected for processes involving chain reaction mechanisms such as Cl atom initiated photooxidation processes . This observation may be accounted for by the wavelength of the light used and hence the possible reactions taking place . The use of filters ensured wavelengths of < 320 nm were not incident on the reaction cell . Previous studies in chlorine at wavelengths less than 320 nm and

summarised in Figures 3.3.4.6 and 3.3.4.7 demonstrate the formation of a number of reaction products , however the number and concentration of these products was less than was observed when unfiltered output from the medium pressure mercury lamp was used , Figures 3.3.2.3 , 3.3.2.4 and 3.3.4.5 and 3.3.4.7 . Obviously certain reaction pathways were hindered when using the lower energy light and it is this limiting process which is probably responsible for the observed low quantum yields .

IR spectroscopy was used extensively in this work to monitor the photooxidation of the anaesthetics . Reaction product bands were identified by comparison with standard spectra , Figures 3.3.5.1 - 3.3.5.4 . As discussed earlier, HCl , CF_2O and CO_2 were identified as reaction products for both anaesthetics (CF_2O is produced in the atmospheric photooxidation of many fluorine containing compounds e.g. CF_2Cl_2 [28]) . Two unknown reaction products identified by their IR bands at 1840 and 1910 cm^{-1} were formed during the photooxidation of enflurane . A single unknown carbonyl containing compound identified by it's IR band at 1840 cm^{-1} was formed during the photooxidation of isoflurane . Based on a chlorine - sensitised photooxidation mechanism it was proposed that CF_3COCl may be formed as a reaction product in the oxidation of isoflurane . However , comparison of the standard spectra for CF_3COCl in Figure 3.3.5.3 with spectra obtained during the photooxidation of isoflurane discounted this .

Three products remained unidentified at this stage of our analyses and it was therefore decided to switch from IR to GC / MS and NMR in order to determine the nature of these photooxidation products .

The possible usefulness of GC / MS was established when reaction products were observed by GC / FID (Figures 3.3.5.5 and 3.3.5.6) . Since these photooxidation products were separated from the parent anaesthetics their identification by mass spectrometry was possible .

The total ion current traces for both reaction mixtures showed the presence of unreacted anaesthetic plus one other reaction product (Figures 3.3.5.7 and 3.3.5.8) . The reaction product formed during the photooxidation of isoflurane was subsequently identified by mass spectrometry as CF_3COOCF_2H (Figure 3.3.5.9) . The enflurane photooxidation product visible as the first eluent in the TIC trace in Figure 3.3.5.8 was fragmented to give the mass spectrum indicated in Figure 3.3.5.11 . Although the electron energy used to fragment this product was too high , it is possible to identify a CO_2 unit in the compound characterised by the $^m/_z$ at 44 . This is indicative of a C = O unit in the reaction product structure .

The final technique employed to help identify the photooxidation products of the anaesthetics was nuclear magnetic resonance (NMR) spectroscopy . Samples of the anaesthetics were reacted in oxygen , the reaction mixtures were trapped in d-acetone and the NMR spectra in Figures 3.3.5.14 and 3.3.5.16 obtained . By comparison of the reaction product spectra with those of the pure anaesthetics (Figures 3.3.5.13 and 3.3.5.15) possible reaction product contributions were identified .

The NMR spectrum for the isoflurane photooxidation mixture indicated the presence of a reaction product containing a - CF_2H moiety . Apart from the product containing this - CF_2H group , no other proton containing compounds except for the parent anaesthetic were indicated (Figure 3.3.5.14) . The position of the - CF_2H in the NMR spectrum indicated a high degree of shielding . This is consistent with the presence of a number of oxygen atoms in the viscinity of this - CF_2H group .It seems likely therefore that the extra triplet in the NMR spectrum for the photooxidation mixture of isoflurane (Figure 3.3.5.14) is due to the proton in the reaction product CF_3COOCF_2H . CF_2O does not appear in Figure 3.3.5.14 as it does not contain any protons .

The NMR spectrum for the enflurane photooxidation mixture (Figure 3.3.5.16) indicated the presence of a reaction product also containing a - CF_2H group . No other proton containing compounds were indicated apart from the unreacted anaesthetic . Thus the NMR spectrum of the enflurane photooxidation mixture identified a - CF_2H group and from the mass and IR spectra a carbonyl group was also identified in the oxidation product structure . Hence the photooxidation product for enflurane was identified as $CFOCF_2OCF_2H$.

Finally , from the results obtained in this work the photooxidation mechanisms which best fit the experimental observations are those summarised in Figures 3.3.5.17 and 3.3.5.18 . All other possible reaction pathways are also included for completeness .

From our observations it was possible to identify the major route for the photooxidation of the anaesthetics . Isoflurane photolysis did yield HCl , CF_2O but no CF_3COCl as reaction products . CF_3COOCF_2H and CO_2 were also identified as major reaction products .The formation of these reaction products is consistent with reaction pathway **I** in Figure 3.3.5.17 . This reaction route is also favoured theoretically . The hydrogen atom closest to the chlorine (the acidic hydrogen [25]) will have the lowest bond dissociation energy of the two protons in the anaesthetic and hence it is this proton which will be preferentially abstracted by chlorine atoms . This arises because the chlorine atom in the anaesthetic structure pulls electron density from it's neighbouring hydrogen and thus decreases the C - H bond strength .

Enflurane photooxidation yielded HCl , CF_2O , CO_2 and $CFOCF_2OCF_2H$. The formation of these products is consistent with reaction pathway **I** indicated in Figure 3.3.5.18 . For reasons similar to those outlined in the photooxidation of isoflurane , abstraction of the proton nearest to the chlorine in the anaesthetic structure is favoured .

Trudeau et al [25] have proposed that the enflurane -CFClH group containing the acidic hydrogen atom undergoes attractive interactions with electron acceptor groups such as Cl atoms and repulsive interactions through it's - CF_2H group . This attractive interaction of the acidic hydrogen atom in both isoflurane and enflurane is consistent with the photooxidation reaction mechanisms outlined in 3.4.1 to 3.4.14 for isoflurane , and 3.4.15 to 3.4.28 for enflurane .

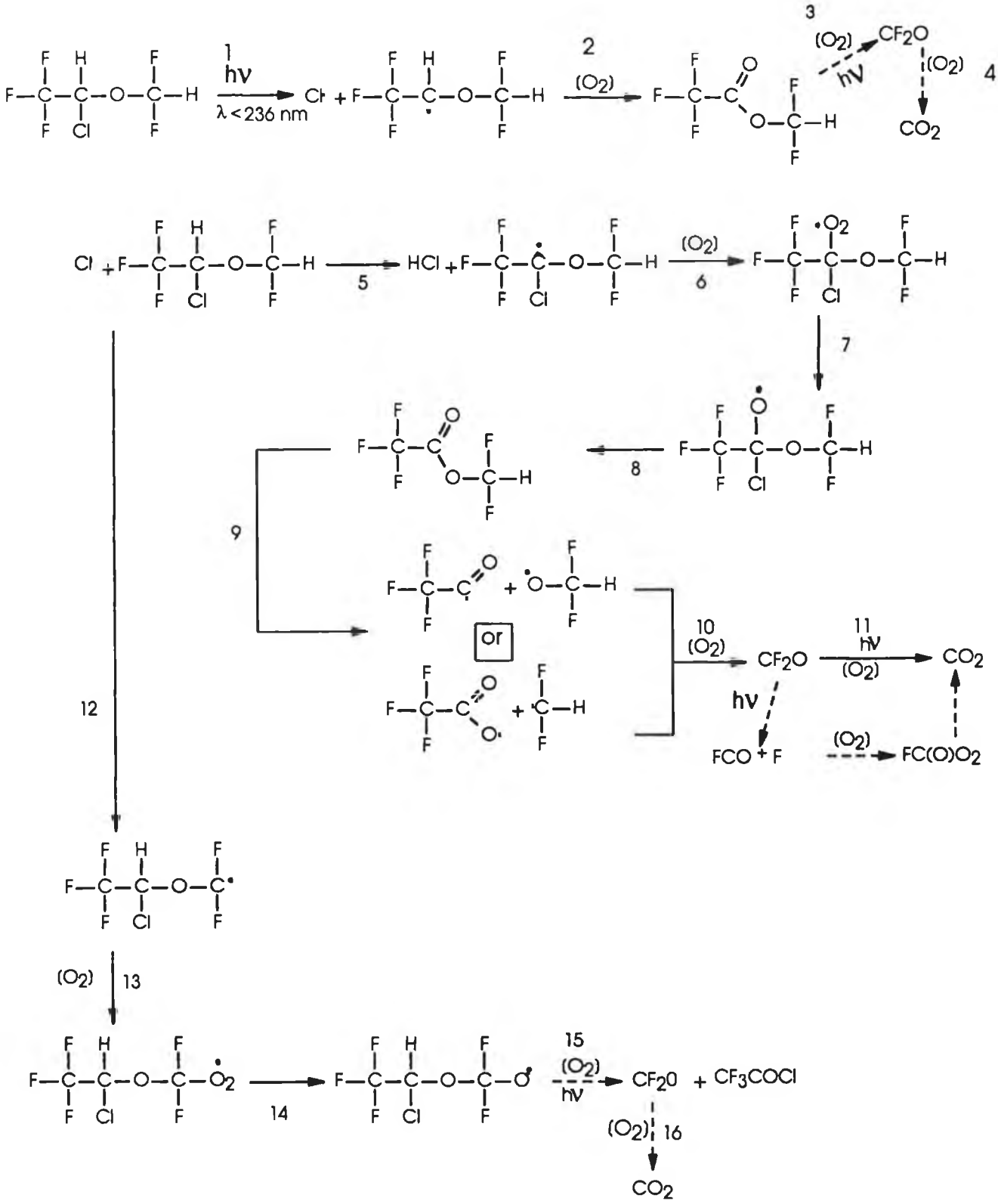

Figure 3.3.5.17
Proposed mechanism for isoflurane photooxidation using wavelengths greater than 200 nm .

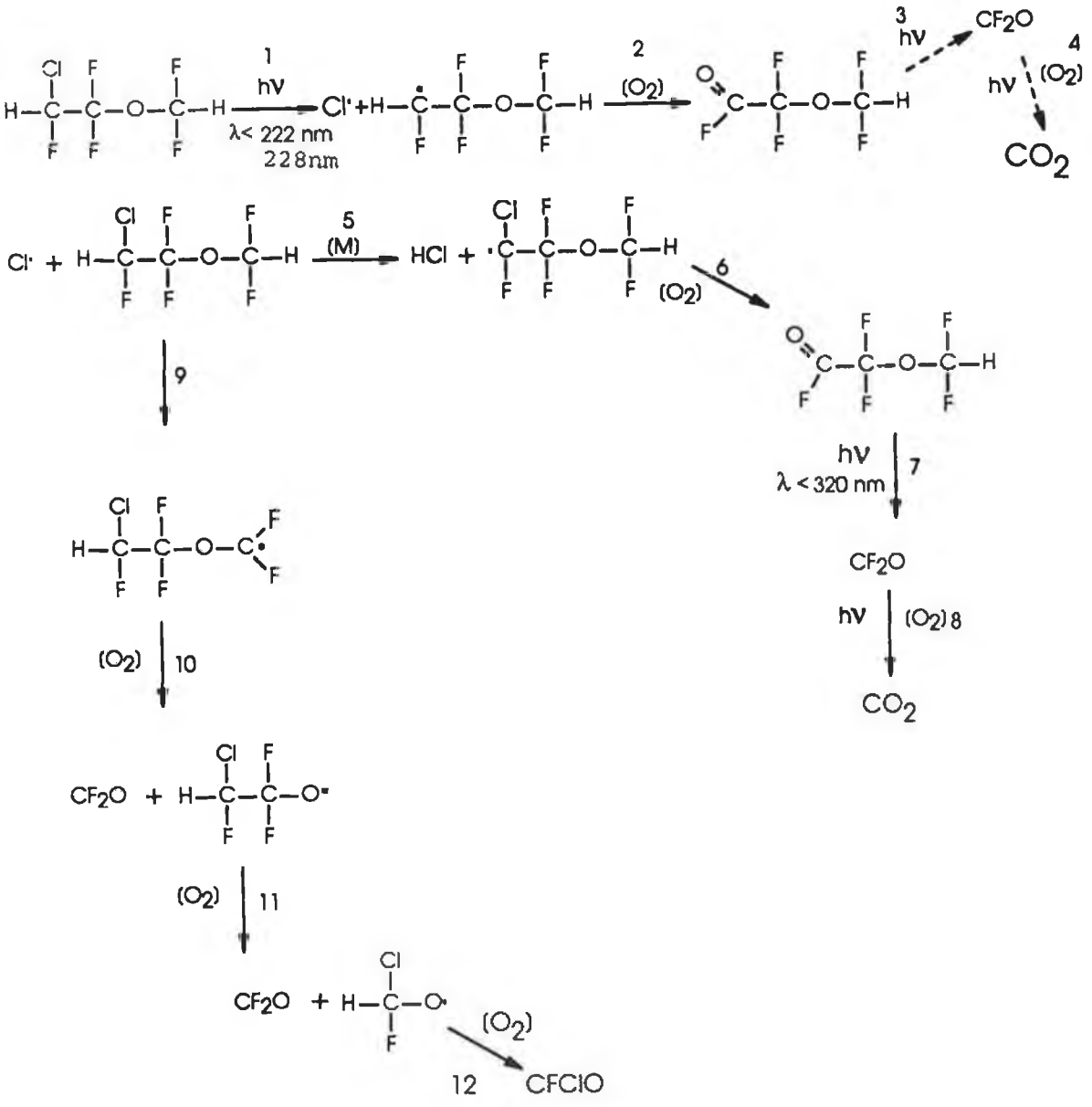

Figure 3.3.5.18
Proposed mechanism for enflurane photooxidation using wavelengths greater than 200 nm .

The photooxidation mechanisms proposed in this thesis for the halogenated anaesthetic ethers , isoflurane and enflurane , are by no means conclusive . Further work in this area needs to be carried out to produce a more comprehensive photooxidation reaction mechanism for these compounds . Techniques such as FTIR and further GC / MS work would be useful in determining reaction products with more certainty than was allowed in this present study . It would also be interesting to further investigate the use of NMR , possible cold temperature and fluorine probe NMR , as a tool for the identification of reaction products .

3.5 Conclusion

From the observations made in this work , the photooxidation of the anaesthetic ethers , isoflurane and enflurane , (using light wavelengths above 200 nm) was found to proceed via a chlorine atom initiated process following C - Cl bond breakage within the anaesthetic molecule . Chapter two of this thesis demonstrated that a small proportion of these anaesthetics may reach the stratosphere . The conditions used in our study of the photooxidation of the ethers are typical of those found in the stratosphere , i.e. low pressures (200 torr) and high energy light ($\lambda > 200$ nm) . Therefore , we can conclude that the anaesthetics which are transported to the stratosphere , will undergo decomposition in a manner similar to that outlined in Figures 3.3.5.17 and 3.3.5.18 .

The effects which these compounds may exhibit on the earth's atmosphere are two - fold . Firstly , the chlorine atom in the anaesthetics will be released by photodecomposition in the stratosphere . These atoms may then participate in reaction pathways , ultimately leading to ozone depletion in a manner similar to all CFC compounds . Secondly , the major reaction products from the photooxidation of the anaesthetics were found to ultimately oxidise to CO_2 , a greenhouse gas .

Although the levels of the anaesthetics released are low compared to other CFC emissions , and even smaller amounts of these compounds reach the stratosphere , this study does serve to illustrate the fact that it is not only the parent compound released to the troposphere which must be assessed . To establish the total impact a compound may exhibit on the environment , the tropospheric and stratospheric reactions of the released compound and it's reaction products must be studied .

3.6 References

[1] A.C. Brown , C.E. Canosa - Mas , A.D. Parr , and R.P. Wayne , *Atmospheric Environment* , **24A** , 2499 , (1990) .

[2] N. Baggett , *Comp. Org. Chem.* , **1** , 799 , (1979) .

[3] P. McLoughlin , R. Kane , and I. Shanahan , *Int. J. Chem. Kinet.* , In press .

[4] L. Nelson , O. Rattigan , R. Neavyn , H. Sidebottom , J. Treacy , and O.J. Nielsen , *Int. J. Chem. Kinet.* , **22** , 1111 , (1990) .

[5] R.V. Morris , and S.V. Filseth , *Can. J. Chem.* , **48** , 6 , **924** , (1970) .

[6] S.V Filseth , *J. Phys. Chem.* , **73** , 4 , 793 , (1969) .

[7] C. von Sonntag , and H-P. Schuchmann , *Adv. Photochem.* , **10** , 59 , (1977) .

[8] S. Patai , "Chemistry of Ethers , hydroxyl groups and their Sulphur analogues" , John Wiley and Sons , 2 , (1980) .

[9] H. Mikuni , and M. Takahasi , *J. Photochem.* , **16** , 179 , (1981) .

[10] H-P. Schuchmann , C. von Sonntag , and G. Schomburg , *Tetrahedron* , **28** , 4333 , (1972) .

[11] C. von Sonntag , and H-P. Schuchmann , *Stud. Phys. Theor. Chem.* , **35** , 563 , (1985) .

[12] C. von Sonntag , Photophysics and Photochemistry in the vacuum ultraviolet , S.P. McGlynn et al (eds) , **142** , 913 , (1985)

[13] A.J. Harrison , and J.S. Lake , *J. Phys. Chem.* , **63** , 1489 , (1959) .

[14] J.F. Meagher , and R.B. Timmons , *J. Chem. Phys.* , **57** , 1 , (1972) .

[15] C. Johnson , and W. Lawson , *J. Chem. Soc. Perkin Trans.* II , 353 , (1974) .

[16] H. Mikuni , M. Takahasi , and S. Tsuchiya , *J. Photochem.* , **9** , 481 , (1978) .

[17] C. von Sonntag , K. Newald , H-P. Schuchmann , F. Weeke , and E. Janssen , *J. Chem. Soc. Perkin Trans.* II , 171 , (1975) .

[18] K. Maeda , A. Nakane , and H. Tsubomura , *Bull. Chem. Soc. Japan* , **48** , 2448 , (1975) .

[19] J. Chien , *J. Phys. Chem* , **69** , 4317 , (1965) .

[20] N. Kulevsky , C. Wang , and V. Stenberg , *J. Org. Chem.* , **34** , 5 , 1345 , (1969) .
[21] V. Stenberg , R. Olson , C. Wang , and N. Nulevsky , *J. Org. Chem.* , **32** , 3227 , (1967) .
[22] C. Wang , taken from a Ph.D thesis , University of North Dakota , (1969) .
[23] G.E. Hall , and F. Ubertini , *J. Org. Chem.* , **15** , 715 , (1950) .
[24] J-M. Dumas , P. Dupuis , G. Pfister - Guillouzo , and C. Sandorfy , *Can. J. Spectroscopy* , **26** , 3 , 102 , (1981) .
[25] G. Trudeau , J-M. Dumas , P. Dupuis , M. Guerin , and C. Sandorfy , "Topics in Current Chemistry" , Springer , Berlin . **93** , 91 , (1980) .
[26] B.J. Finlayson - Pitts , and J.N. Pitts Jr. , "Atmospheric Chemistry" , Wiley & Sons publishers , (1986) .
[27] J.A. Kaye , A.R. Douglas , C.H. Jackman , R.S. Stolarski , R. Zander , and G. Roland , *J. Geophys. Res.* , **96** , D7 , 12865 , (1991) .
[28] W.C. Francis , and R.N. Haszeldine , *J. Chem. Soc.* , 2151 , (1955) .
[29] V.I. Vedeneev , M.A. Teitel'boim , and A.A. Shoikhet , *Izv. Akad. Nauk SSSR , Ser. Khim.* , **9** , 1968 , (1976) .
[30] L. Nelson , J.J. Treacy , and H.W. Sidebottom , *Proc. 3rd Eur. Symp. Physio. Chem. Behav. Atmos. Pollut.* , 258 , (1983) .

CHAPTER 4.0

Appendix

A RELATIVE RATE STUDY OF THE REACTION OF CHLORINE ATOMS (Cl) AND HYDROXYL RADICALS (OH) WITH A SERIES OF ETHERS.

*Peter McLoughlin ; Rosaleen Kane and Imelda Shanahan

*To whom correspondence should be addressed .

School of Chemical Sciences , Dublin City University , Glasnevin , Dublin 9 , Ireland.

ABSTRACT:

Rate constants for the gas phase reactions of hydroxyl radicals and chlorine atoms with a number of ethers have been determined at 300 ± 3 K and at a total pressure of 1 atmosphere. Both OH radical and chlorine atom rate constants were determined using a relative rate technique. Values for the rate constants obtained are as follows.

Compound	k_{OH} x 10^{12} ($cm^3molecule^{-1}s^{-1}$)	k_{Cl} x 10^{11} ($cm^3molecule^{-1}s^{-1}$)
Hexane	5.53 ± 1.55	----
2-Chloro ethyl methyl ether	4.92 ± 1.09	14.4 ± 5.0
2,2-Dichloro ethyl methyl ether	2.37 ± 0.50	4.4 ± 1.6
2-Bromo ethyl methyl ether	6.94 ± 1.38	16.3 ± 5.4
2-Chloro,1,1,1-trifluoro ethyl ethyl ether	< 0.3	0.30 ± 0.10
Isoflurane	< 0.3	< 0.1
Enflurane	< 0.3	< 0.1
Di -*i* -propyl ether	11.08 ± 2.26	16.3 ± 5.4
Diethyl ether	----	25.8 ± 4.4

The above relative rate constants are based on the values of k(OH + pentane) = [3.94 ± 0.98] x 10^{-12} and k(OH + diethyl ether) = [13.6 ± 2.26] x 10^{-12} $cm^3molecule^{-1}s^{-1}$ in the case of the hydroxyl reactions . In the case of the chlorine atom reactions, the above rate constants are based on values of k(Cl + ethane) = [5.84 ± 0.88] x 10^{-11} and k(Cl + diethyl ether) = [25.4 ± 8.05] x 10^{-11} $cm^3molecule^{-1}s^{-1}$. The quoted errors

include ±2σ from a least squares analysis of our slopes plus the uncertainty associated with the reference rate constants.

Atmospheric lifetimes calculated with respect to reaction with OH radicals are based on a tropospheric OH radical concentration of (7.7 ± 1.4) x 10^5 radicals cm^{-3} , and lifetimes with respect to reaction with Cl atoms are based on a tropospheric Cl atom concentration of 1 x 10^3 atoms cm^{-3} . Observed trends in the relative rates of reaction of hydroxyl radicals and chlorine atoms with the ethers studied is discussed . The significance of the calculated tropospheric lifetimes is also reviewed .

INTRODUCTION :

Recent years have seen a marked increase in awareness of environmental issues in general , and particularly in issues relating to air quality . Large quantities of chemicals are emitted into the atmosphere each year from natural as well as man-made sources ; the potential atmospheric significance of such pollutants is dependent on the transformations which they undergo in the atmosphere , the nature of the products of these transformations , and the atmospheric lifetimes of each species .

It is now well established that the nitrate radical (NO_3) and ozone both contribute to the atmospheric chemistry of tropospheric pollutants and that the dominant day-time loss process for most organic pollutants in the troposphere is reaction with the hydroxyl radical [1 - 7] . Thus the tropospheric lifetime of a given pollutant is determined mainly by its reaction with OH radicals .

Until recently , the importance of chlorine chemistry in the troposphere had received little attention because Cl atoms were thought to be sufficiently scarce as not to compete with OH radicals . Singh et al. [8] have reviewed the sources of chlorine atoms in the troposphere and calculate marine tropospheric concentrations of approximately 10^3 atoms cm^{-3} , or roughly 1000 times lower than that of OH radicals . The primary source of Cl atoms in the troposphere is the reaction of OH radicals with HCl derived from sea salt [8] . It has been predicted that the greater reactivity of Cl atoms with non-methane hydrocarbons (N.M.H.C.'s) could mean that between 20 to 40% of N.M.H.C. oxidation in the troposphere and 40 to 90% in the stratosphere could be caused by reaction with Cl atoms [8] .

Recognition of the importance of the reaction of Cl atoms with organic species has led to a number of kinetic studies of the reaction of Cl atoms with hydrocarbons ,

chloroalkanes and aromatic species . However , despite the growing kinetic data base for the reaction of Cl atoms with volatile organic compounds , few studies on the reaction of chlorine atoms with oxygenated organic species have been carried out [9 - 16] .

The reactions of OH radicals and Cl atoms are both important processes in the chemistry of the natural and polluted atmosphere . The possible atmospheric significance of ethers is thus considered in terms of their reactions with both OH radicals and Cl atoms .

Oxygenated hydrocarbons especially ethers are being released in increasing quantities into the atmosphere because of their use as solvents and fuel additives [16 - 17]. For example , methyl *tert* butyl ether (M.T.B.E.) is being widely used as a gasoline additive to increase octane number and reduce CO emissions . In fact M.T.B.E. production in the United States has risen annually by approximately 27% from 1985 - 1990 thus making it the 24th most abundantly produced chemical in the U.S. [18] . Besides fuel additives , ethers are also released into the troposphere as intermediates in hydrocarbon combustion [19] . Cyclic ethers such as furan and thiophene are also released into the troposphere from fuel conversion facilites [20] .

One of the reasons for our interest in the ethers, specifically the methyl ethyl ethers, has been to assess the possible importance of the increased usage of halogenated anaesthetic agents such as isoflurane (1-Chloro-2,2,2,-trifluoro ethyl difluoro methyl ether) , $CF_3CHClOCF_2H$ and enflurane (2-Chloro-1,1,2-trifluoro ethyl difluoro methyl ether) , $CHClFCF_2OCF_2H$. These anaesthetics are the most widely used general anaesthetics in the western world and their use has led to some concern about their possible adverse effects on ozone concentrations [21 - 28] . Because of this concern work has been carried out in our laboratory to estimate the

emission rates of these compounds into the atmosphere . The results of this work will appear in a separate publication .

This work was undertaken to determine the rate constants for reaction of Cl atoms and OH radicals with a series of ethers (mostly halogenated) . This work is of fundamental importance in gaining kinetic information about ethers in general and increasing the existing data base in relation to such compounds . We have also completed a detailed mechanistic study of the gas-phase photochemical reactions of these species with oxygen under simulated stratospheric conditions , the results of which will be published at a future date [29]. .

EXPERIMENTAL:

The technique and apparatus employed in this study have been described in detail in other publications [30] , [31] , so only a brief summary is given here .

In the determination of both chlorine atom and hydroxyl radical rate constants , reaction mixtures consisting of the reference and test organic were prepared in a collapsible Teflon bag (86 dm^3) . Hydroxyl radicals were generated by the photolysis of methyl nitrite (CH_3ONO) in the presence of synthetic air and an excess of nitric oxide (NO) . Photolysis was achieved by irradiating gas mixtures with 10 black lamps (Philips TLD 18W/08) and 10 sun lamps (Philips TL 20W/09N) placed on either side of the bag . Chlorine atoms were generated by photolysis of molecular chlorine using 5 black lamps .

In the presence of OH radicals or Cl atoms , the test and reference organics decay via the reactions :

$$Cl \text{ (or OH)} + \text{Test Organic} \xrightarrow{k_1 \text{ (or } k_2)} \text{Products} \qquad (1) , (2)$$

$$Cl \text{ (or OH)} + \text{Reference Organic} \xrightarrow{k_3 \text{ (or } k_4)} \text{Products} \qquad (3) , (4)$$

To ensure no loss of reference or test organic occurred due to photodecomposition or due to reactions in the absence of light , samples were first analysed in the absence of either CH_3ONO or Cl_2 and secondly , in the dark with all constituents present . Once satisfied that both test and reference were lost solely due to reaction with hydroxyl radicals and chlorine atoms , we then used the following equation to calculate rate constants for reaction of the test organic with either Cl atoms or OH radicals (k_{Test}) :

$$\ln([Test]_o / [Test]_t) = k_{Test} / k_{Ref.} \times \ln([Ref.]_o / [Ref.]_t) \qquad (5)$$

$[Test]_o$ and $[Ref.]_o$, and $[Test]_t$ and $[Ref.]_t$ are the concentrations of the test and reference organics at time 0 and time t respectively .

The concentrations of test and reference were determined by periodically sampling from the Teflon bag through a Valco 10-port automatic gas sampling valve and analyzing on a Perkin Elmer , model 8500 gas chromatograph (G.C.) , equipped with a flame ionization detector (F.I.D.) .

As a test for interferences caused by secondary reaction products in our system , separate experiments were carried out in which mixtures of methyl nitrite (or Cl_2) and either the test or reference organic were irradiated and analyses performed to check for the formation of potentially interfering products . For all of the rate constants determined , no such interferences were observed over irradiation times typical of our experiments .

Initial concentrations of test and reference were typically in the range 5 to 20 ppm , with fixed concentrations of 50 ppm Cl_2 (in our chlorine reactions) , 50 ppm CH_3ONO and 25 ppm NO (in our hydroxyl radical work) . Each reaction mixture was prepared to a total volume of 50 dm^3 with zero grade air (B.O.C.) .

All experiments were carried out at atmospheric pressure of synthetic air , ensuring that the Teflon bag was cleaned thoroughly between experiments . Chlorine atom rate constants in this work were determined at 300 ± 1 K , and the hydroxyl radical rate constants at 301 ± 2 K . The test and reference organics used had stated purities of at least 99% , and were thoroughly degassed prior to use .

A summary of the test compounds studied , their corresponding reference , and the analytical conditions used for their quantitation is given in Table 1 .

TEST	REFERENCE	COLUMN	G.C. CONDITIONS
Hexane	Pentane	10% SE 30 on Chromosorb WHP (80-100µm) 2M	Column Temp. = 44°C Flow = 31cm³/min.
Diethyl ether	Ethane	10% SE30 on Chromosorb WHP (80-100µm) 2M	Column Temp. = 55°C Flow = 45cm³/min.
2,2-Dichloro ethyl methyl ether	Diethyl ether	10% SE 30 on Chromosorb WHP (80-100µm) 2M	Column Temp. = 65°C Flow = 35cm³/min.
Isopropyl ether	Diethyl ether	10% SE 30 on Chromosorb WHP (80-100µm) 2M	Column Temp. = 50°C Flow = 35cm³/min.
2-Chloro ethyl methyl ether	Diethyl ether	10% P.E.G. on Chromosorb WHP (80-100µm) 2M	Column Temp. = 65°C Flow = 35cm³/min.
2-Bromo ethyl methyl ether	Diethyl ether	10% SE 30 on Chromosorb WHP (80-100µm) 2M	Column Temp. = 65°C Flow = 40cm³/min.
2-Chloro,1,1,1,-trifluoro ethyl ethyl ether	Ethane	10% SE 30 on Chromosorb WHP (80-100µm) 2M	Column Temp. = 75°C Flow = 31.5cm³/min.
Isoflurane	Diethyl ether	10% SE 30 on Chromosorb WHP (80-100µm) 2M	Column Temp. = 40°C Flow = 28cm³/min.
Enflurane	Diethyl ether	10% SE 30 on Chromosorb WHP (80-100µm) 2M	Column Temp. = 40°C Flow = 28cm³/min.

Table 1

Summary of the analytical conditions used in our experiments .

RESULTS

The kinetic data reported in this work represent the first measurements of this type using our present apparatus . To test our system , therefore , a series of experiments were carried out on compounds for which reliable rates of reaction have already been determined and published , i.e., OH + hexane and Cl + diethyl ether .

Table 2 lists the Cl atom and OH radical rate constants for reactions of ethers measured in our laboratory together with the corresponding tropospheric lifetimes of these compounds . A comparison is made between our results and those in the literature . Table 2 demonstrates that our results are within the quoted error limits established for these compounds. Each of the quoted slopes in Table 2 represent an average value calculated from repeat determinations.

Reaction mixtures for both OH radical and Cl atom rate studies were stable in the dark over time scales typical of the experimental runs . Similarly , no photodecomposition of either test or reference compounds was observed over the time scales used in our experiments .

Hence, we concluded that for our OH radical work loss of test and reference was due to reaction with OH radicals alone, and in the case of our chlorine work, loss of test and reference was due to reaction with Cl atoms alone.

A high degree of precision in the results was obtained using our system of analysis . For example, three repeat runs for the reaction of OH radicals with 2-Chloro ethyl methyl ether yielded slopes of, 0.358 ± 0.004 . Similar reproducibility was obtained for each of the compounds studied for both OH radical and Cl atom determinations.

In both our OH radical and Cl atom work the slopes given in Table 2 were obtained from lines with correlation coefficients > 0.995 and having minimal intercepts. Typical line plots are given in Figures 1 and 2.

Test Organic	k_1 / k_2	$k_{Cl} \times 10^{11}$ ($cm^3 molecule^{-1} s^{-1}$)	k_2 / k_4	$k_{OH} \times 10^{12}$ ($cm^3 molecule^{-1} s^{-1}$)	Temp. (K)	τ_{Cl} (Days)	τ_{OH} (Days)	Reference
Hexane	---	---	1.39 ± 0.05	5.53 ±1.55	301 ± 2	----	2.7	This Work
	---	---	---	5.61 ± 1.40	298	---	---	[32]
Diethyl ether	4.40 ± 0.09	25.8 ± 4.4	---	---	298 ± 1	45	---	This work
	---	25.4 ± 1.7	---	---	298 ± 2	---	---	[9]
		35.6 ± 2.8	---	---	295 ± 2	---	---	[16]
2 - Chloro ethyl methyl ether	0.56 ± 0.02	14.4 ± 5.0	0.358 ± 0.021	4.92 ± 1.09	300 ± 3	80	3.1	This Work
2,2 - Dichloro ethyl methyl ether	0.17 ±0.01	4.4 ± 1.6	0.173 ± 0.008	2.37 ± 0.50	300 ± 3	263	6.3	This Work
2 - Bromo ethyl methyl ether	0.64 ± 0.01	16.3 ± 5.4	0.507 ± 0.017	6.94 ± 1.38	300 ± 3	71	2.1	This Work
2 - Chloro , 1,1,1,- trifluoro ethyl ethyl ether	0.05 ± 0.01	0.30 ± 0.10	n.d.	< 0.3[a]	300 ± 3	10.6 years	> 50	This Work
Di -*i* - propyl ether	0.64 ± 0.01	16.3 ± 5.4	0.809 ± 0.032	11.08 ± 2.26	300 ± 3	71	1.4	This Work
	---	15.1 ± 0.7		10.7 ± 2.0	298 ± 2	---	---	[9]
	---	---	---	11.3 ± 0.7	298 ± 2	---	---	[9]

Isoflurane	n.d.	< 0.1[b]	n.d.	< 0.3[a]	300 ± 3	> 32	> 50	This Work!
	---	---	---	0.021 ± 0.005	300	---	2.0 years	[27] , [28]
Enflurane	n.d.	< 0.1[b]	n.d.	< 0.3[a]	300 ± 3	> 32	> 50	This Work
	---	---	---	0.017 ± 0.005	300	---	2.4 years	[27] , [28]

Table 2

Summary of reported room temperature rate constants for the reaction of Cl atoms and OH radicals with a series of ethers . The error bars on our slope values represent ± 2σ from a least squares analysis of our data . Rate constants calculated from our slopes also include errors inherent in the reference rate constant used to place our results on an absolute basis .

[a] and [b] Limits based on the sensitivity of the analytical procedures .

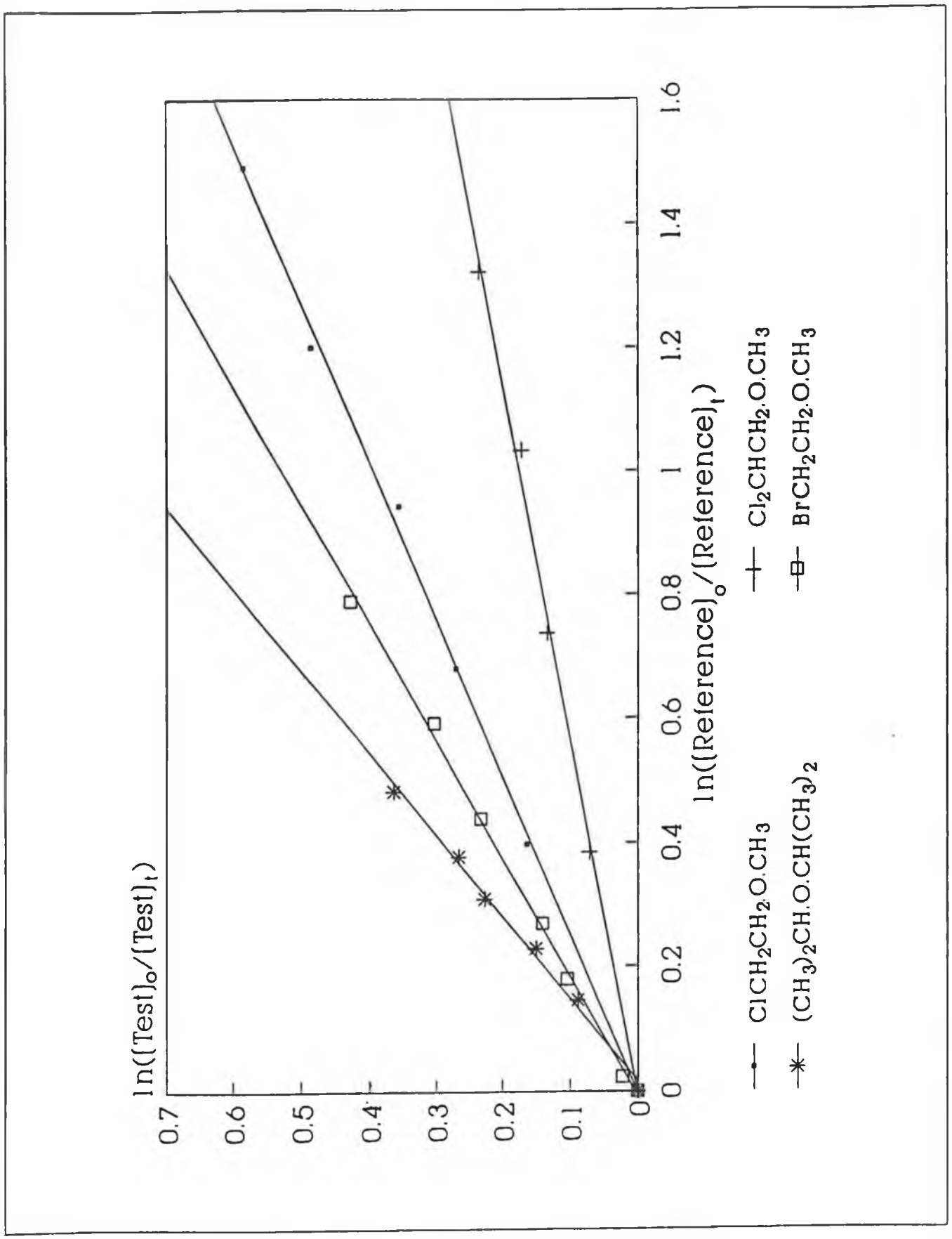

Figure 1

Typical plots obtained for the reaction of OH radicals with a series of ethers .

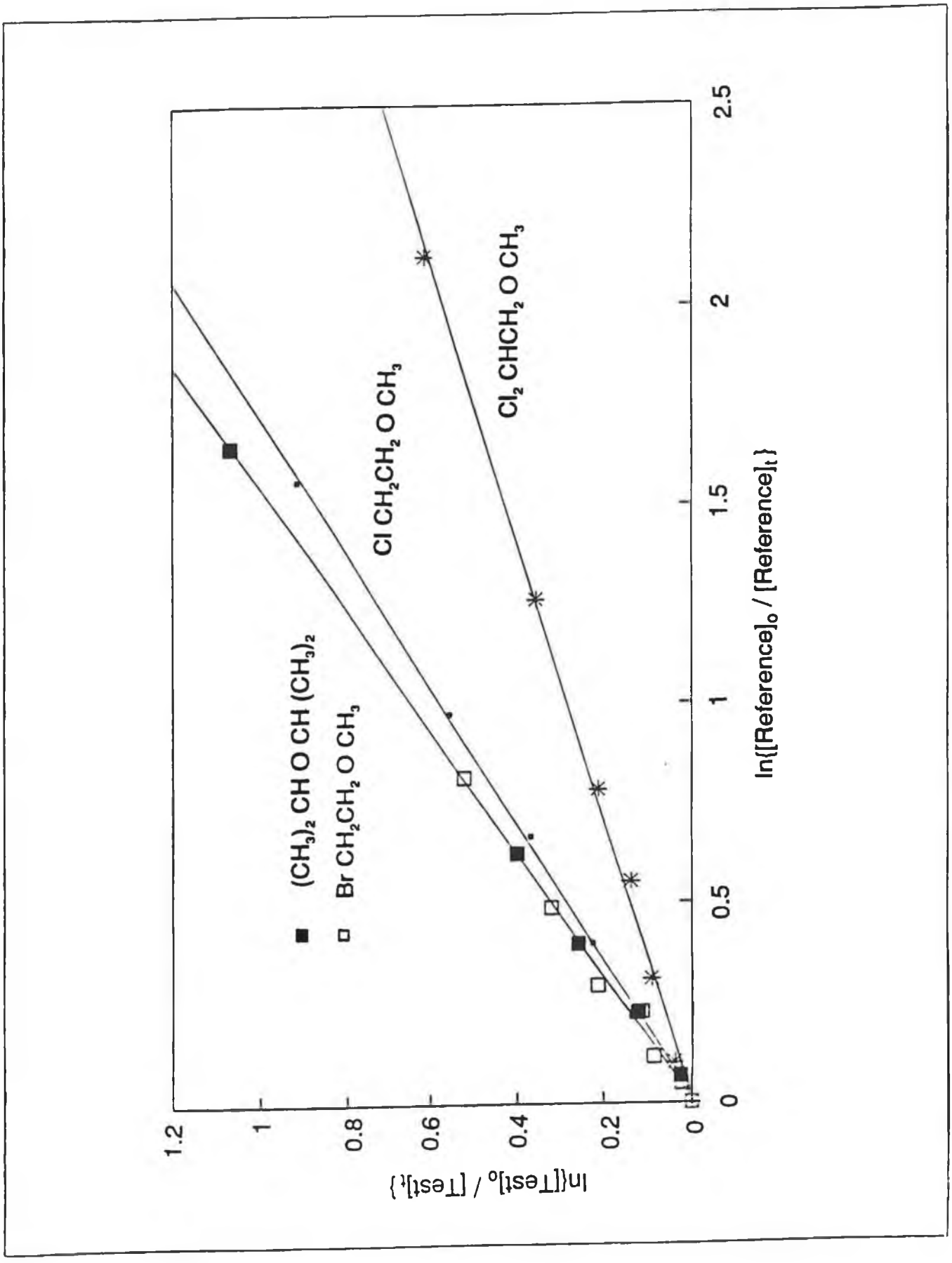

Figure 2

Typical plots obtained for the reaction of Cl atoms with a series of ethers .

As stated in the experimental section , potential interferences from reaction products were investigated. Any such interferences were overcome by tailoring our analytical conditions and therefore reaction products did not introduce errors in our results.

Figures 1 and 2 show representative plots of our data for both our OH radical and chlorine atom work. The expression used to plot our data is given in equation 5. The concentration of test and reference at time, 0, and time, t, corresponded to the peak heights of each compound prior to irradiation and at some time, t, during photolysis. The slopes of the lines thus obtained correspond to $k_{reference} / k_{test}$. Knowing $k_{reference}$ allowed us to place the results on an absolute basis.

In the case of our OH radical work, two reference compounds were used. Pentane was used as the reference compound for the determination of hexane, and diethyl ether for each of the other compounds studied . A value of k (OH + pentane) = 3.94 ± 0.98 x 10^{-12} $cm^3molecule^{-1}s^{-1}$ [32] was used , and included total errors associated with its determination . Although the OH radical rate constant for pentane was obtained using a relative rate technique , our only reason for examining the reaction of OH radicals with hexane was purely as a system check . We wished to determine whether our new experimental set - up could be used to obtain rate constant values similar (within experimental error) to those recommended by Atkinson [32]. A value of k (OH + diethyl ether) = 13.6 ± 2.26 x 10^{-12} $cm^3molecule^{-1}s^{-1}$ was obtained from Wallington et al [33] . This figure was calculated using an absolute technique and includes all of the errors incurred in its calculation (i.e., $\pm 2\sigma$ plus a maximum possible experimental error of 10%) . These reference rates were chosen as they were calculated at similar temperatures to those of our experiments and are representative of reported rate data for these compounds.

Two reference compounds were used in the determination of the chlorine atom rate constants . Ethane was used as the reference for diethyl

ether and 2 - Chloro,1,1,1-trifluoro ethyl ethyl ether and diethyl ethyl was used as the reference for the remaining compounds . A value for k (Cl + Ethane) = (5.84 ± 0.88) x 10^{-11} $cm^3molecule^{-1}s^{-1}$ [34] was used (average of 4 absolute values) and includes all errors associated with it's determination (i.e., ± 15%) . A value of k (Cl + diethyl ether) = (25.4 ± 8.05) x $10^{-11}cm^3molecule^{-1}s^{-1}$ [9] used is traceable to an absolute value and includes all experimental errors associated with its determination (i.e., 2σ + 25% error on $k_{reference}$) . The value for k_{Cl} diethyl ether [9] referred to in Table 2 includes errors corresponding to ±2σ and does not include the possible additional experimental error of 25% suggested as being present in the rate constant [9] . Both reference rates were determined at similar temperatures to those in our experiments.

In Table 2, limits of reactivity are quoted for isoflurane, enflurane and 2-Chloro,1,1,1-trifluoro ethyl ethyl ether. The limits quoted for the OH radical rate constants are those recommended by Bufalini et al. [31] for the relative rate technique employed in our laboratory. The chlorine atom rate limits were established using a technique employed by Bufalini et al. [31] to set OH radical rate constant limits for the relative rate technique.

Table 2 lists the tropospheric lifetimes of each of our test compounds with respect to both OH radicals and Cl atoms. A value for the OH radical concentration of (7.7 ± 1.4) x 10^5 radicals cm^{-3} was used to determine the tropospheric lifetimes of our test compounds with respect to OH radicals. This value was calculated by Prinn et al. [35] and represents a globally averaged tropospheric value, calculated over a seven year period .

A value for the Cl atom concentration of 1 x 10^3 atoms cm^{-3} was used to determine the tropospheric lifetimes of our test compounds with respect to Cl atoms [8] .

DISCUSSION

The kinetic data reported in this work are among the first to be reported for the reaction of OH radicals and Cl atoms with halogenated ethers . Table 2 lists the OH radical and Cl atom rate constants plus the corresponding atmospheric lifetimes calculated from these rate constants for all of the compounds studied in this work . The slopes obtained indicate the precision of our results . The large error bars quoted for the rate constants is due to the inclusion of the total uncertainty associated with the reference rate constants used to place our results on an absolute basis .

Aliphatic ethers are expected to react with OH radicals and Cl atoms via a H-atom abstraction mechanism in a similar manner to the alkanes [32] :

i.e.,

$$\dot{O}H + CH_3OCH_3 \longrightarrow H_2O + \dot{C}H_2OCH_3 \qquad (6)$$

In the atmosphere the radicals produced in the abstraction reaction further react to give stable oxygenates :

$$\dot{C}H_2OCH_3 \xrightarrow[NO_2]{O_2,\ N_2} \dot{O}CH_2OCH_3 \xrightarrow{O_2} HOCCH_3 + \dot{O}_2H \qquad (7)$$

As expected from the bond energy of 93 ± 1 kcal mol^{-1} for the primary C - H bonds in CH_3OCH_3 compared with the primary C - H bond energy of 98 ± 1 kcal mol^{-1} for the alkanes [9] , the ethers are much more reactive than the corresponding alkanes (k_{OH} CH_3OCH_3 = 2.98 x 10^{-12} , k_{OH} CH_3CH_3 = 0.268 x 10^{-12} cm^{-3}molecule-

$^{1}s^{-1}$ [32]) . This difference in bond dissociation energies is attributable to the activating effect of the oxygen . This activating effect has been shown to operate up to 5 carbons away from the ether link [9] .

The presence of chlorine in the ethers is expected to lower the C - H bond dissociation energy due to its electron withdrawing effect, and thus give rise to an increase in the observed hydroxyl radical and chlorine atom rate constants for the abstraction process .

Almost all of the ethers studied in this work were ethyl methyl ethers. Experimentally determined rate constants were not obtained for ethyl methyl ether, however a value for the OH radical rate constant was calculated using Wallingtons group reactivity technique [36]. A value of 8.0×10^{-12} $cm^3molecule^{-1}s^{-1}$ was obtained thus indicating a drop in reactivity with respect to OH radicals on going from the unhalogenated to the dichlorinated ethyl methyl ether . This drop in reactivity was not expected based on observed trends in reactivity of the alkanes (Table 3) and needs to be confirmed by further laboratory study . However this decrease in reactivity is consistent with an increase in steric hindrance with chlorination .

Very little information is currently available on the effects of halogenation on the rate of reaction of ethers with OH radicals and Cl atoms. However , as a similar H-atom abstraction mechanism is expected for both ethers and ethanes (mechanisms (6) and (7)) , it is useful to compare the effect of halogenation on the rates of reaction of ethanes and ethers. Table 3 shows the effect of chlorine substitution on the OH radical rate constants for a series of chloroalkanes .

Compound	Temperature (K)	k x 10^{12} $cm^3molecule^{-1}s^{-1}$	Estimated uncertainty	Reference
CH_3CH_3	298	0.268	± 20%	[32]
CH_3CH_2Cl	298	0.390	± 35%	[32]
CH_3CHCl_2	296	0.260	± 23%	[37]
CH_3CCl_3	298	0.0119	± 30%	[32]

Table 3:
The Influence of Cl substitution on the rate constant for the reaction of OH radicals with substituted ethanes.

Table 3 shows that OH radicals react quicker with the monosubstituted ethane than with ethane, suggesting that the Cl atom lowers the C - H bond dissociation energy causing a corresponding increase in the rate of H-atom abstraction, as expected. However, it is of interest to note that the OH radical rate constant for the disubstitued ethane is lower than that of the monosubstitued compound. A similar trend in reactivity was observed with regard to the mono- and di-chloro ethyl methyl ethers studied in our laboratory (Table 2). This apparent decrease in the rate of reactivity cannot be explained by bond dissociation energies alone. One possible reason for this deactivating effect of the chlorine substituent may be attributed to steric considerations .

Another reason for the observed rate decrease may be due to polarity changes associated with the incorporation of an extra Cl atom into the ether structure . It is possible that the inductive effect of an extra Cl atom may result in a partial positive charge on the β - hydrogen :

i.e.,

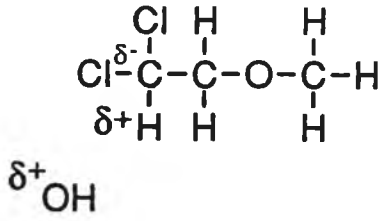

This may then reduce the stability of the transition state for H - atom abstraction by introducing repulsive forces between the OH radical and the H - atom . This argument is not without precedent [38 , 39] for an electrophilic radical such as OH . This hypothesis is supported by Taylor et al [38] who pointed to the similarity in bond dissociation energies of the α - hydrogens in CH_2ClCH_2Cl and CH_3CH_2Cl (96.5 ± 1

and 96.7 ± 3 kcal mol^{-1} respectively) while the reaction of OH radicals with CH_2ClCH_2Cl is much smaller than CH_3CH_2Cl .

The above decrease in reaction rate , noted for the reaction of OH radicals with the chlorinated ethyl methyl ethers, was also found in the reaction of Cl atoms with these compounds, although the observed decrease was more significant. As both OH radicals and Cl atoms react via a similar H-atom abstraction mechanism (mechanisms (6) and (7)) , and due to the relatively larger size of the Cl atom compared to the OH radical, it would appear that steric effects may significantly influence the speed of the reaction. To gain further knowledge as to possible steric contributions , further work on the reaction of Cl atoms and OH radicals with other halogenated ethers is needed.

The OH radical and Cl atom rate constants quoted in Table 2 for bromo ethyl methyl ether are both slightly larger than those for chloro ethyl methyl ether. This slight increase in reactivity of the bromo-substituted relative to the chlorine substituted compound has also been observed by a colleague in our laboratory studying halogenated alkanes. However, the difference in reactivities between the compounds may not be significant, as the reaction rates for both compounds lie within the error limits quoted for each rate constant. This similarity in reactivity between chlorinated and brominated compounds is consistent with data published by Atkinson [32] for CH_3Br and CH_3Cl.

The order of reactivity of the compounds studied is similar in both our OH radical and Cl atom data, reflecting the similarity of the reaction mechanisms involved. One surprising result was the unexpected similarity between the rates of reaction of bromo ethyl methyl ether and di- *iso* -propyl ether. From the trends in the OH radical rate constant data, we would have expected a greater Cl atom reaction rate for di- *iso* -propyl ether. One possible reason for this could be due to the

activating effect of the oxygen atom having less of an effect on distant carbons in the case of Cl atom reactions [9], thus the H-atoms on the branched methyl groups are relatively more difficult to remove than in the corresponding OH radical reaction.

One of the drawbacks of the relative rate technique employed in our laboratory is the difficulty in monitoring slow reactions . In fact compounds with OH radical rate constants < 0.3 x 10^{-12} $cm^3molecule^{-1}s^{-1}$ and Cl atom rate constants of < 0.1 x 10^{-11} $cm^3molecule^{-1}s^{-1}$ were not determined over the time scales employed in our laboratory (30 minutes) . These limits (also quoted in Table 2) were determined using a procedure outlined by Bufalini et al [31] . Both of these limits are defined by the sensitivty of the analytical technique used to measure the concentrations of the test and reference compounds . By modifying the concentration of Cl_2 and the nature of the reference compound it may be possible to determine Cl atom rate constants below 0.1 x 10^{-11} $cm^3molecule^{-1}s^{-1}$ using our present experimental design . This was not carried out in the case of the anaesthetics as no loss of these species was observed after photolysis for 30 minutes in the presence of Cl atoms .

Atmospheric lifetimes in Table 2 were calculated using the relationships

$$\tau_{Cl} = 1/ k_{Cl}[Cl] \quad \text{and} \quad \tau_{OH} = 1/k_{OH}[OH] \qquad (8), (9)$$

where k_{Cl} and k_{OH} are the chlorine atom and hydroxyl radical rate constants respectively and [Cl] and [OH] are the concentration of chlorine atoms and hydroxyl radicals respectively. The concentration of OH radicals of (7.7 ± 1.4) x 10^5 radicals cm^{-3} [35] used to calculate the atmospheric lifetimes of the ethers with respect to OH radicals approximates that of a relatively clean troposphere. The concentration of Cl atoms of 1 x 10^3 cm^{-3} used to calculate the atmospheric lifetimes with respect to Cl atoms is typical of a clean marine troposphere [8].

The long reaction times of isoflurane, enflurane and 2-Chloro,1,1,1-trifluoro ethyl ethyl ether, given in Table 2 are consistent with the small number of

abstractable hydrogens present in these compounds, and also the high degree of hindrance associated with these compounds. A limit of > 50 days was established for our OH radical tropospheric lifetime. Using an absolute technique, Brown et al [27,28] calculated the tropospheric lifetimes of isoflurane and enflurane to be 2 and 2.4 years respectively (relative to a tropospheric OH radical concentration of 7.7 x 10^5 radicals cm^{-3}) , which is consistent with our data. From the results obtained by Brown et al and from the release figures for isoflurane and enflurane calculated in our laboratory and soon to be published, it is evident that only a small quantity of these anaesthetics will firstly be emitted to the atmosphere and secondly an even smaller quantity will reach the stratosphere .It has been calculated by Logan et al [40] that by appropriate use of absorption breathing systems with fresh gas flow rates of perhaps 1 litre min^{-1} , the total emissions of these anaesthetics might further be reduced immediately by 50 - 75% . Although the extent to which isoflurane and enflurane presently effect stratospheric ozone levels is minimal compared to compounds such as CFC - 11 and 12, the role of such trace compounds in atmospheric chemistry can not be overlooked and must be considered in conjunction with all such minor contributors .

To gain mechanistic information on OH radical and Cl atom reactions with haloethers , further work is required on compounds containing different halogens at different carbon sites. Product studies should also be carried out so that a complete environmental assessment can be made regarding the release of such haloether compounds.

ACKNOWLEDGEMENTS :

The authors wish to thank the technical staff and post - graduates at Dublin City University for their friendship and help throughout this work , and the School of Chemical Sciences at Dublin City University for research funding .

BIBLIOGRAPHY

[1] R.A. Cox , R.G. Derwent , A.E.J. Eggleton , and J.E. Lovelock , *Atmospheric Environment* , **10** , 305 , (1976) .

[2] D. Rhasa , and R. Zellner , *Free Rad. Res. Comms.* , **3** , No. 1-5 , 199 ,(1987).

[3] J.A. Logan , M.J. Prather , S.C. Wofsy , and M.B. McElroy , *J. Geophys. Res.* , **86** , 7210 , (1981) .

[4] R. Atkinson , *Atmospheric Environment* , **24A** , No. 1 , 1 , (1990) .

[5] R.A. Cox , *J. Photochem. and Photobiol.* , **51** , 29 , (1990) .

[6] D.A. Fisher , C.H. Hales , W-C. Wang , M.K.W. Ko , and N.D. Sze , *Nature* , **344** , 513 , (1990) .

[7] R.G. Prinn , and A. Golombek , *Nature* , **344** , 47 , (1990) .

[8] H.B. Singh , and J.F. Kasting , *J. Atmos. Chem.* , **7** , 261 , (1988) .

[9] L. Nelson , O. Rattigan , R. Neavyn , H. Sidebottom , J. Treacy , and O.J. Nielsen , *Int. J. Chem. Kinet.* , **22** , 1111 , (1990) .

[10] W.A. Payne , D.F. Nava , F.L. Nesbitt , and L.J. Stief , *J. Phys. Chem.* , **94** , 7190 , (1990) .

[11] H.B. Libuda , F. Zabel , E.H. Fink , and K.H. Becker , *J. Phys. Chem.* , **94** , 5860 , (1990) .

[12] G. Poulet , G. Laverdet , and G. Le Bras , *J. Phys. Chem.* , **85** , 1892 , (1981).

[13] W.A. Payne , J. Brunning , M.B. Mitchell , and L.J. Stief , *Int. J. Chem. Kinet.* , **20** , 63 , (1988) .

[14] T. Khatoon , J. Edelbuttel-Einhaus , K. Hoyermann , and H. Gg. Wagner , *Ber. Bunsenges. Phys. Chem.* , **93** , 626 , (1989) .

[15] M. Bartels , K. Hoyermann , and U. Lange , *Ber. Bunsenges. Phys. Chem.* , **93** , 423 , (1989) .

[16] T.J. Wallington , L.M. Skewes , W.O. Siegl , C-H. Wu , and S.M. Japar , *Int. J. Chem. Kinet.* , **20** , 867 , (1988) .

[17] T.J. Wallington , P. Dagaut , R. Liu , and M.J. Kurylo , *Environ. Sci. Technol.* , **22** , 842 , (1988) .

[18] M.S. Reisch , *C & EN* , **13** , 8 April , (1991) .

[19] J.H. Lee , and N. Tang , *J. Chem. Phys.* , **77** , 4459 , (1982) .

[20] P.H. Wine , and R.J. Thompson , *Int. J. Chem. Kinet.* , **16** , 867 , (1984) .

[21] J. Norreslet ,S. Friberg ,T.M. Nielsen , and U. Romer , *The Lancet* , 719 , (1989).

[22] P. Hutton , J.A. Kerr , J.M.T. Pierce , and S.P.K. Linter , *The Lancet* , 1011 , (1989) .

[23] K.J. Hopkins , and R. Albanese , *The Lancet* , 1209 , (1989) .

[24] B.D. Joyner , The *Lancet* , 1209 , (1989) .

[25] R.C. Rodgers , and J.A.S. Ross , *The Lancet* , 1209 , (1989) .

[26] A.C. Brown , C.E. Canosa-Mas , A.D. Parr , R.P. Wayne , and J.M.T. Pierce , *The Lancet* , 279 , (1989) .

[27] A.C. Brown , C.E. Canosa-Mas , A.D. Parr , J.M.T. Pierce , and R.P. Wayne , *Nature* , **341** , 635 , (1989) .

[28] A.C. Brown , C.E. Canosa-Mas , A.D. Parr , and R.P. Wayne , *Atmospheric Environment* , **24A** , 2499 , (1990) .

[29] P. McLoughlin , B. Murphy , and I. Shanahan , document in preparation .

[30] R. Atkinson , W.P.L. Carter , A.M. Winer and J.N. Pitts , Jr. , *J. Air Pollut. Cont. Assoc.* , **31** , 1090 , (1981) .

[31] J.J. Bufalini , and R.R. Arnts , **E.P.A. / 600/3-87/046** , (1987) .

[32] R.Atkinson , *J. Phys. Chem. Ref. Data , Monograph No. 1* , (1989) .

[33] T.J. Wallington , R. L iu , P. Dagaut , *Int. J. Chem. Kinet.* , **20** , **41** , (1988) .

[34] R. Atkinson , and S.M. Aschmann , *Int. J. Chem. Kinet.* , **17** , 33 , (1985).

[35] R. Prinn , D. Cunnold , R. Rasmussen , P. Simmonds , F. Alyea , A. Crawford , P. Fraser and R. Rosen , *Science* , **238** , 945 , (1987) .

[36] T.J. Wallington , P. Dagaut , R. Liu , and M.J. Kurylo , *Int. J. Chem. Kinet.* , **20**, 541 , (1988) .

[37] C.J. Howard , and K.M. Evenson , *J. Chem. Phys.* , **64** , 4303 , (1976) .

[38] P.H. Taylor , S. McCarron , and B. Dellinger , *Chem. Phys. Lett.* , **177** , 1 , 27 , (1991) .

[39] L. Nelson , I. Shanahan , H.W. Sidebottom , J. Treacy , and O.J. Nielson , *Int. J. Chem. Kinet.* , **22** , 577 , (1990) .

[40] M. Logan and J.G. Farmer , *Br. J. Anaes.* , **63** , 6 , 645 , (1989) .